Observational Climatology of Dust Activity in the Atacama Desert

Inaugural-Dissertation
zur
Erlangung des Doktorgrades
der Mathematisch-Naturwissenschaften Fakultät
der Universität zu Köln

vorgelegt von

Rovina Janis Pinto
aus Bangalore, Indien

Köln, 11. März 2024

UNIVERSITÄT
ZU KÖLN

BERICHTERSTATTENDE:

Prof.in Dr.in Stephanie Fiedler
Prof. Dr. Ulrich Löhnert

TAG DER MÜNDLICHEN PRÜFUNG:

04.06.2024

Diese Arbeit wurde von der Mathematisch-Naturwissenschaftlichen Fakultät der Universität zu Köln im Jahr 2024 als Dissertation angenommenen.

IMPRINT

Observational Climatology of Dust Activity in the Atacama Desert

COLOPHON

This thesis was typeset using LaTeX and the `memoir` document class. It is based on Aaron Turon's thesis *Understanding and expressing scalable concurrency*[1], itself a mixture of `classicthesis`[2] by André Miede and `tufte-latex`[3], based on Edward Tufte's *Beautiful Evidence*.

The LaTeX template is adapted from *Security Arguments and Tool-based Design of Block Ciphers*[4] by Friedrich Wiemer.

The thesis was written using `Overleaf` and the bibliography was processed by `biblatex`.

The body text is set 10/14pt (long primer) on a 26pc measure. The margin text is set 8/9pt (brevier) on a 7pc measure. Matthew Carter's Charter acts as both the text and display typeface. Monospaced text uses Jim Lyles's `Bitstream Vera Mono` ("Bera Mono").

[1] https://people.mpi-sws.org/~turon/turon-thesis.pdf

[2] https://bitbucket.org/amiede/classicthesis/

[3] https://github.com/Tufte-LaTeX/tufte-latex

[4] https://github.com/pfasante/phd_thesis

For those of us who live at the shoreline
standing upon the constant edges of decision
crucial and alone
for those of us who cannot indulge
the passing dreams of choice
who love in doorways coming and going
in the hours between dawns
looking inward and outward
at once before and after
seeking a now that can breed
futures
like bread in our children's mouths
so their dreams will not reflect
the death of ours;

For those of us
who were imprinted with fear
like a faint line in the center of our foreheads
learning to be afraid with our mother's milk
for by this weapon
this illusion of some safety to be found
the heavy-footed hoped to silence us
For all of us
this instant and this triumph
We were never meant to survive.

—Audre Lorde, A Litany for Survival

"The spirits say you have all the data.
Just do something."

Pat Byrnes / CartoonStock.com

Abstract

Arid and semi-arid regions are sources of mineral-dust aerosols, but very little is known about dust activity in the arid Atacama Desert. These dust aerosols have implications for human life and the climate system. By absorbing and scattering radiation, they affect the Earth's radiation budget. The dust aerosols act as cloud condensation nuclei and ice nucleating particles for clouds and, fertilise terrestrial and marine ecosystems. In the Atacama Desert, the dust aerosols have the potential to influence the formation, lifetime and composition of the prominent stratocumulus clouds and fog, and, on deposition, they can impact the biogeochemical cycle of the upwelling waters offshore. However, despite its importance, only global studies of the dust cycle in the Atacama Desert exist with significant uncertainties regarding the dust emission rates. This thesis provides the first quantitative assessment of the dust activity in the Atacama. Dust reports and meteorological data from ground-based observations spanning 72 years (1950-2021) were analysed. 1920 dust days were recorded, with less than 10% dust storms. The mean threshold wind speed for at least 5% of dust event-occurrence is $10.9 \pm 1.6\,\mathrm{ms}^{-1}$ which is twice as large as the values in the Taklamakan, Western Sahel, and Sudan, and consistent with the perceived infrequent dust activity despite the exceptional aridity.

The threshold wind speed depends on the soil properties such as particle size distribution, soil composition and soil moisture and, surface characteristics such as surface roughness and vegetation. Therefore, using the Portable in situ Wind Erosion Lab (PI-SWERL), the dependence of the threshold wind speed given soil surface conditions in the Atacama was analysed. It is found that the mean threshold wind speeds required for dust emission over crusted surfaces are nearly twice that of disturbed surfaces where crusts were removed, indicating the role of surface crusts in controlling the dust emission potential. The maximum dust concentration measured at the lowest friction velocity is almost an order of magnitude higher from disturbed surfaces than crusted surfaces. The thresholds from the ground-based observations were validated against the in-situ measurements from the undisturbed crusted surfaces. An agreement between the station estimates and the in-situ values at Chuculay is found, but the station estimates are higher than those measured at Pisagua. This is because the surfaces are very heterogeneous, even locally, making it difficult to constrain the threshold wind speeds. Nevertheless, these results show that very high wind speeds are required to trigger dust emission from the crusted desert surfaces in the Atacama.

On investigating the meteorological processes that drive dust activity, the study that the dust activity is connected to the thermal wind circulation in the Atacama. The dust activity peaks just before the wind maximum, suggesting the possibility of dry convection driving the diurnal cycle of dust. The dustiest station, Chañaral, recorded most dust events in the summer (DJF) in agreement with several global aerosol models. However, a winter-spring maxima was found at other stations. This was also observed for dust storms, as 70% of the dust storms were recorded in the winter and spring. 42% of the dust storms were recorded in Calama. Dust storms usually require sufficiently large pressure gradients to generate high wind speeds for dust emission and transport. Hence, ERA5 reanalysis data was visually inspected to identify the synoptic weather patterns associated with dust storms. The analysis revealed that more than half of the dust storms in the Atacama were associated with mid-tropospheric troughs and their surface lows (54.6%), 22.3% with cut-off lows, 8.5% each with intense anticyclones and coastal lows and 6.1% with ridges. Composite analysis of the wind speeds

during dust storms shows that these synoptic weather patterns induce wind speeds that are well above the climatological mean at the station, and at times, it is the uncharacteristic direction that the wind blows from that triggers dust storms in the Atacama.

Zusammenfassung

Aride und semiaride Gebiete sind als Quellen von aus Mineralstaub bestehenden Aerosolen bekannt, doch über die Staubaktivität in der ariden Atacama-Wüste weiß man wenig. Solche mineralstaubhaltigen Aerosole haben Auswirkungen sowohl auf den Menschen als auch das Klimasystem. Durch Absorption und Streuung von Strahlung beeinflussen sie die globale Strahlungsbilanz. Sie fungieren als wolkenbildende Kondensations- bzw. Kristallationskeime und düngen terrestrische und marine Ökosysteme. In der Atacama-Wüste haben Staubaerosole das Potenzial, die Bildung, Lebensdauer und Zusammensetzung der dort häufig auftretenden Stratokumuli und Nebelbänke zu beeinflussen. Bei Ablagerung können sie sich auf den biogeochemischen Kreislauf der der Atacama vorgelagerten Küstenauftriebsgebiete auswirken. Doch trotz seiner Bedeutung gibt es nur Studien, die den Staubkreislauf der Atacama-Wüste im globalen Kontext betrachten, mit großen Unsicherheiten hinsichtlich der Staubemissionsraten. Diese Studie stellt die erste quantitative Erhebung und Analyse der Staubaktivitäten in der Atacama-Wüste dar. Dafür wurden Augenbeobachtungen und meteorologische Daten aus Bodenbeobachtungen über einen Zeitraum von 72 Jahren (1950-2021) ausgewertet. Es wurden insgesamt 1920 Staubtage gezählt, wovon an weniger als 10% der Tage Staubstürme registriert wurden. Die mittlere Mindestwindgeschwindigkeit für das Auftreten von mind. 5% Staubereignissen liegt bei $10{,}9 \pm 1{,}6\,\mathrm{ms}^{-1}$ und ist damit doppelt so hoch wie die Werte in der Taklamakan-Wüste, der westlichen Sahelzone und im Sudan. Dies deckt sich mit der trotz der außergewöhnlichen Trockenheit als selten wahrgenommenen Staubaktivität.

Die Mindestwindgeschwindigkeit hängt sowohl von Bodeneigenschaften wie Partikelgrößenverteilung, Bodenzusammensetzung und -feuchtigkeit als auch von Oberflächenmerkmalen wie Rauigkeit und Vegetation ab. Daher wurde mittels des Portable in situ Wind Erosion Lab (PI-SWERL) die Mindestwindgeschwindigkeit in Abhängigkeit von den Beschaffenheiten der Bodenoberflächen in der Atacama untersucht. Es konnte ermittelt werden, dass die für die Staubemissionen verkrusteter Oberflächen notwendigen mittleren Mindestwindgeschwindigkeiten fast doppelt so hoch sind wie die gestörter Oberflächen deren Krusten entfernt wurden. Dies weist auf die entscheidende Rolle der Oberflächenkrusten bei der Regulierung des Staubemissionspotenzials hin. Die maximale Staubkonzentration, die bei der niedrigsten Schubspannungsgeschwindigkeit gemessen wurde, ist auf gestörten Oberflächen fast eine Größenordnung höher als auf verkrusteten Oberflächen. Die Mindestwindgeschwindigkeiten aus den Bodenbeobachtungen konnten im Abgleich mit den an unbeschädigten, verkrusteten Oberflächen vorgenommenen in situ-Messwerten bestätigt werden. In Chuculay stimmen die kalkulierten Mindestgeschwindigkeiten mit den gemessenen überein, wohingegen in Pisagua die kalkulierten Werte über den gemessenen liegen. Das liegt an der großen Heterogenität der Oberflächen, auch lokal, was es schwierig macht, die Mindestwindgeschwindigkeiten präzise einzugrenzen. Dennoch zeigen die Ergebnisse, dass es sehr hoher Windgeschwindigkeiten bedarf, um Staubemissionen von den Wüstenflächen der Atacama freizusetzen.

Bei der Untersuchung von den meteorologischen Prozessen, die Staubaktivität bedingen, konnte festgestellt werden, dass die Staubaktivitäten in der Atacama mit thermischer Windzirkulation in Verbindung stehen. Die Staubaktivität erreicht ihren Höhepunkt kurz vor dem Windmaximum, was auf die Möglichkeit trockener Konvektion als Antrieb für den täglichen Staubzyklus hindeutet. Die staubreichste Station, Chanaral, verzeichnete in Übere-

instimmung mit mehreren globalen Aerosolmodellen die meisten Staubereignisse im Sommer (DJF). An anderen Stationen wurde jedoch ein Winter-/Frühjahrsmaximum festgestellt. Dies gilt auch für Staubstürme, von denen 70% im Winter und Frühjahr registriert wurden. 42% aller Staubstürme wurden in Calama registriert. Da Staubstürme in der Regel ausreichend große Druckgefälle benötigen, um hohe Windgeschwindigkeiten für Staubemission und -transport zu erzeugen, wurden ERA5-Reanalysedaten einer visuellen Prüfung unterzogen, um die mit den Staubstürmen verbundenen synoptischen Wettermuster zu identifizieren. Die Analyse ergab, dass mehr als die Hälfte der Staubstürme in der Atacama mit mitteltroposphärischen Trögen und deren Bodentiefs (54,6%), 22,3% mit Cut-Off Lows, jeweils 8,5% mit intensiven Antizyklonen und Küstentiefs und 6,1% mit Höhenrücken verbunden waren. Die Gesamtanalyse der Windgeschwindigkeiten während der Staubstürme zeigt, dass diese synoptischen Wettermuster Windgeschwindigkeiten hervorrufen, die weit über dem klimatologischen Mittelwert an der Station liegen. Zuweilen ist es die untypische Windrichtung, die die Staubstürme in der Atacama auslöst.

Acknowledgements

To Stephanie Fiedler, my supervisor, and Yaping Shao, Nicolas Huneeus and Mark Reyers, my thesis advisory committee, thank you for taking the time to discuss my work and giving me feedback. Your expertise has been valuable in shaping my research. I thank Ulrich Löhnert for agreeing to be one of the examiners, Peter Schilke for being the chair and Christoph Böhm for taking notes during the defence.

To José, who has taught me pretty much everything I know about the Atacama Desert. Thank you for sharing your invaluable expertise, for using your connections to get me the data even before it was publicly accessible, for teaching me how to read weather charts, and for being a good friend. I'm also very grateful to Christoph for putting up with my impromptu office visits with so many questions about the Atacama and for creating the topography map of the Atacama Desert for me. Thank you both, and Nicolas, for your feedback on Chapter 5. It helped me develop it further. I am indebted to Vic Etyemezian and George Nikolich from the Desert Research Institute, Nevada for all their help with the instrument and data used in Chapter 4.

To Federica, my brilliant office-mate and even more brilliant friend. Thank you for painstakingly reading my thesis in its entirety and teaching me how to bake a pizza. Before you came, I was alone crying in the office. Now I cry, but with you in it.

To my old office-mate Robert and our old research group: Linh, Feifei, Eduardo, Vidya, Franz and Lisa. Thank you for having been a good work-support group. I miss all our group dinners and the breakout rooms. Doing a PhD during the pandemic would have been extra difficult if I didn't have a kind and supportive group to share my experiences with. The same goes for my peers at the CRC: Rosa, Fatima and Barbara. Thanks for the mental and physical health support. I will miss our camaraderie and not understanding much of German in our yoga and spinning classes. I disliked sports until I met a fun group who motivated me to care for myself.

I was lucky enough to take a trip to Chile to see the breathtaking Atacama Desert. Despite an exhausting trip, being there helped me get a lot of perspective on my research and gave me insights that otherwise would not have been possible. I thank Benedikt Ritter for allowing me to join his expedition and the team members for helping me with my fieldwork. Feifei and Franko, thank you for helping me with the instrument and the paperwork in Chile. I had a wonderful time with you both in Antofagasta while running from one office to another, trying to get a permit to visit again. A massive thanks to Barbara and Juan for packing the instrument in Chile so I didn't have to make a trip halfway around the world. None of my work in Chapter 4 would have been possible without Dagmar, who saved me from a lot of bureaucracy with the instrument and helped me with all the administrative work. Thanks to Robert, Eduardo, Rainer and Pavel for assisting me with the instrument and instrument-related queries.

I am indebted to the financial support I received from the institute during the last months of my PhD; without it, I would have been stressed and upset. I'm very grateful to Karin and Hannah and the Graduate School for the support you gave me, especially during the difficult

times. Thank you to my lovely colleagues for giving me a good environment to work in.

I feel privileged to have a group of wonderful friends who have cheered me on through the roller-coaster ride that was this PhD. Adeesh, Meenal, Kopal, Jenieve, Joel and Joanne for always keeping home close; to Ziad, Fatima, Tracy and Dini for making me feel at home here. I hope I am a halfway friend, at least.

To sweet Lennart, come rain or sun, you have been there for me through it all. Thank you for caring and loving, cooking and cleaning and, for taking charge of all the chores in the last weeks of my PhD. I would have gone hungry, tired and grumpy without you. Thank you for helping me with the Zusammenfassung. I'm so happy that we have Savvas, Moe and Bouboulina to wash away all our worries by being heart-breakingly cute!

To my sister, Fiona, who has always been encouraging and supportive of me through all the different phases of my life.

To my mother who raised me to be fierce, and fiercely independent. I wouldn't be who I am without the sacrifices you made, I wouldn't be where I am without the sacrifices you made. I know you'd be proud of me even if I didn't have this PhD. I dedicate this to you.

Contents

List of Figures

List of Tables

Part I

INTRODUCTION

1

Motivation and Objectives

1.1 WHY STUDY DUST ACTIVITY IN THE ATACAMA DESERT?

"The storm took place at sundown, it lasted through the night, When we looked out next morning, we saw a terrible sight. We saw outside our window where wheat fields they had grown Was now a rippling ocean of dust the wind had blown."

—Great Dust Storm Disaster, Woody Guthrie

On 8 July 2016, a rare dust outbreak off the coast of the Atacama Desert, Chile, was captured by the Moderate Resolution Imaging Spectroradiometer (MODIS) on the TERRA satellite (MODIS Science Team 2017). This dust storm in the Atacama Desert is rare for present-day conditions (Reyers et al. 2019). It reduced visibility to 200 m, affected air quality, and caused power outages and damage to roofs and vehicles. In the city of Iquique, 10 m wind speeds of 19.5 ms^{-1} and wind gusts of 26 ms^{-1} blowing from the east were measured (Dirección Meteorológica de Chile - Servicios Climáticos 2016). In another instance, on 17 March 2022, a dust storm engulfed the town of Diego de Almagro in the southern part of the Atacama, along with strong winds, hail and heavy precipitation, affecting much of the infrastructure and leaving thousands without electricity (Figure 1.1).

FIGURE 1.1: (*Left*) True colour image of airborne dust off the coast of the Atacama Desert on 8 July 2016 as taken by the MODIS/TERRA instrument (source: `https://modis.gsfc.nasa.gov/gallery/individual.php?db_date=2016-07-14`) and (*Right*) an image of a dust storm in Diego de Almagro, southern Atacama from 17-03-2022. Photo courtesy: Arica Libre.

The Atacama Desert is the driest non-polar desert on Earth (McKay et al. 2003; Houston & Hartley 2003). Bounded by the South Pacific to the west and the Andes to the east, the Atacama occupies a long but narrow extent along the subtropical south-west coast of South America from 16°S to about 28°S. The desert rests between steep coastal cliffs, "the Coastal Cordillera", a narrow mountain range that is 1000–2000 m above sea level (as), rising along the shoreline and the mountain ranges of the Andes that are as high as 5000 m asl and about 300 km inland from the coastline. Despite annual average precipitation ranging from 1 mm in the north to 20 mm in the southern fringes of the desert (Houston 2006c), it is home to 1.5 million people.

Large dust outbreaks can substantially affect the people in the arid Atacama Desert. Not only do such events compromise air quality and health (Goudie 2014; Kwon et al. 2002; Chen et al. 2004), but they also adversely impact visibility and transport (Middleton et al. 2021) and lead to agriculture and infrastructure damage (Shao 2008; Ravi et al. 2011; Glotter & Elliott 2016). The impact of mineral dust on the climate systems is manifold [1], by scattering and absorbing radiation, dust aerosols affect the Earth's radiation budget (Highwood & Ryder 2014). Dust aerosols can act as cloud condensation nuclei and as ice nucleating particles for clouds (Nenes et al. 2014), hence influencing cloud properties such as cloud lifetime, the liquid water path and cloud thickness to name a few (Seinfeld et al. 2016). Dust deposition can fertilise terrestrial ecosystems such as the Amazon rainforest (Swap et al. 1992; Yu et al. 2015) and marine ecosystems (Schulz et al. 2012a). Dust aerosols from the Atacama can potentially influence the chemical composition and formation of stratocumulus clouds and fog (Chand et al. 2010) in the region and impact the productivity of upwelling waters offshore.

[1] An extensive study on the effects of mineral dust on global climate and climate change can be found in Kok et al. (2023)

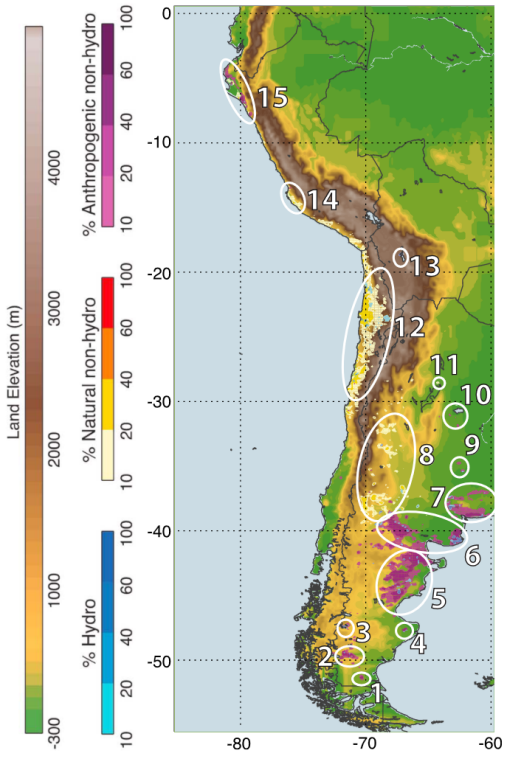

FIGURE 1.2: Distribution of the percentage number of days per year where dust optical depth (DOD) > 0.2 for the summer (DJF) estimated from MODIS Deep Blue from 2003–2009. The Atacama Desert is marked as 12. The frequencies associated with (hydro) and without (nonhydro) ephemeral water bodies are marked in blue and increasing shades of yellow–red, respectively. Anthropogenic sources (more than 30% land use) are shaded in magenta. Figure adapted from Ginoux et al. (2012a)

Despite large-scale dust outbreaks in the Atacama and severe implications for humans and the climate system, dust activity in this region has only been explored in the context of global studies. Global studies have found that the Atacama Desert, while being a potential

dust source (Goudie 2013b; Ginoux et al. 2012b), contributes marginally less than the deserts in the northern hemisphere (Kok et al. 2021; Schepanski 2018). Figure 1.2 shows the frequency of occurrence of dust optical depth[2] (DOD) > 0.2 per year for the summer (DJF) estimated from MODIS Deep Blue DOD with information on land use. Only about 10% of the days per year have DOD > 0.2 for the summer when dust activity is estimated to be the highest for the region. Furthermore, Kok et al. (2021) found that South America contributes approximately 3% (0.4–1.1 Tg) of the global dust emissions (Figure 1.3) across different global aerosol models from the Aerosol Comparisons between Observations and Models (AeroCom) Phase I (Huneeus et al. 2011), the authors' model ensembles and an inverse model. The inverse model integrated simulations from the model ensembles with constraints on dust properties obtained from observational datasets. The contribution of the Atacama Desert to the annual total dust emission fluxes is absent in the data from the European Centre for Medium-Range Weather Forecasts (ECMWF) MACC (Monitoring Atmospheric Composition and Climate) reanalysis dataset for 2003–2012 by Schepanski (2018). Another modelling study (Li et al. 2008) found an annual dust emission rate of 13 Tg yr^{-1} from the Atacama Desert, which is higher than Kok et al. (2021) but still low given other dust sources in the Southern Hemisphere. However, dust deposition rates from Jickells et al. (2005) show that the Atacama receives the same order of magnitude dust deposits as other prolific dust sources in the world (Figure 1.4), but the authors do not discuss the source of this high dust flux in the region. Although there are significant uncertainties in the dust emission flux, the results point towards the Atacama being a non-prolific dust source compared to primary sources like the Sahara and Sahel and East Asian Deserts like the Gobi and Taklamakan.

[2]DOD is the proportion of aerosol optical depth (AOD) attributed to mineral dust particles usually derived by validating against ground-based observations of AOD.

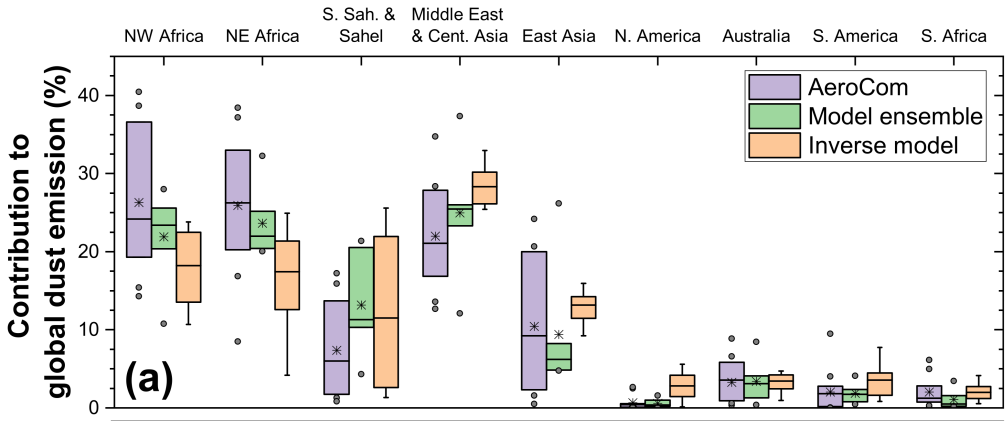

FIGURE 1.3: This figure from Kok et al. (2021) shows the fractional contribution of different source regions to the annual global dust emission and deposition flux for the AeroCom ensemble, the authors' model ensemble and inverse model.

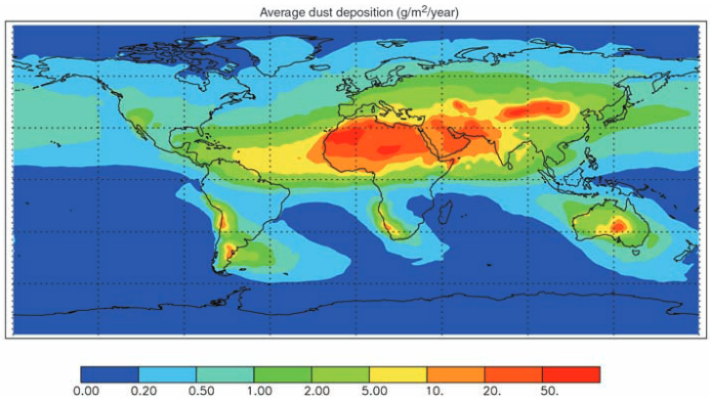

FIGURE 1.4: Average dust deposition from different sources based on a composite of three modelling studies that used the aerosol optical depth (AOD) from satellites, in-situ dust concentration data and dust deposition observations. Figure from Jickells et al. (2005).

There have been a few regional studies covering different aspects of the dust cycle in the

Atacama. One study analysed the dust devil activity driven by strong dry convective episodes in the desert (Kurgansky et al. 2011) and the wind erosion transport of sediments along the coast of the Atacama by southerly, southwesterly winds (Flores-Aqueveque et al. 2010; Flores-Aqueveque et al. 2012). Other studies have emphasised the role of mid-tropospheric troughs and strong easterly winds triggering the dust storm aforementioned (Reyers et al. 2019) and retrieved the aerosol optical depth (AOD) [3] from satellites to understand the connection between natural dust emissions and air quality in the Atacama (Oyarzún 2021). However, no climatology of dust activity exists in the region. This leads us to the overarching questions of this PhD thesis.

[3] AOD is the total content of aerosols in the atmospheric column calculated by computing the light extinction due to particle scattering or absorption.

Central questions of the thesis

Given the limited moisture supply and barren landscape,
the Atacama Desert should be a region prone to dust emission.

Why, then, is the dust activity low in the Atacama Desert?

If the dust activity is low,
then, what drives the rare yet intense dust storms in the Atacama?

The results from Kok et al. (2021) show a biased ranking of the dust sources. Emission estimates between different models diverge widely for significant source regions, not just in the AeroCom models (Huneeus et al. 2011) but also for the Coupled Model Intercomparison Project (CMIP)5 models (Wu et al. 2020; Kok et al. 2021). This is also true for emission and deposition rates estimated via satellites and reanalysis data, as seen in the studies above. The most recent CMIP6 models also suffer from significant uncertainties, with global dust emissions varying by a factor of five across models, with the model ensemble mean being twice that of reanalysis datasets (Zhao et al. 2022). Furthermore, it has been suggested that the dust processes in the models are becoming more uncertain as they become more sophisticated (Zhao et al. 2022). One of the main reasons for disagreement between the contribution of each dust source to the global dust cycle comes from the lack of constraints from observational data on regional dust loading (Kok et al. 2021). To better represent the global dust cycle, understanding the dust emission potential from various landforms at a local scale is necessary (Kohfeld et al. 2005).

Dust emission occurs when the wind stress acting on soil particles is higher than a threshold value (Gillette 1978; Morales 1979; Helgren & Prospero 1987). The threshold wind speed depends on the soil properties, surface roughness and vegetation (Shao 2001; Okin 2008; King et al. 2005; Menut et al. 2013). Furthermore, complex topography and coarse resolution of the grid boxes result in poorly represented near-surface winds in models and reanalysis datasets. This would then imply that dust emission in models occurs at inaccurate threshold wind speeds (Lunt & Valdes 2002; Cakmur et al. 2004; Ridley et al. 2013). To compensate for the lack of high-resolution data on soil properties and emission environment, many models employ static dust source functions [4] (Ginoux et al. 2001; Zender et al. 2003b) to simulate dust emission further contributing to uncertainties (Lunt & Valdes 2002). These uncertainties in the global dust cycle then translate to uncertainties in the impact of mineral dust aerosols on the climate system, for example, poor confidence in the net dust radiative effect and inadequate representation of the historical increase in dust mass loading (Kok et al. 2023).

[4] Static dust source function is a probability of dust uplifting with a value between 0 and 1 for a given region.

The results from this work contribute to a better understanding of the dust emission potential in the Atacama. The spatiotemporal distribution of dust events in the region and the climatology of dust activity estimated from long-term ground-based observations will not only help validate the magnitude of dust activity from satellites and global climate models, but the threshold wind speeds computed can be combined with regional and global dust models to better constrain the regional dust emission flux for the present-day Atacama Desert. These thresholds also circumvent the need for empirical dust source functions. Furthermore, meteorological processes that generate high winds required for dust emission have been identified, which can help reproduce historical dust emissions in the region and ascertain changes in dust activity with changing climate.

In the very arid Atacama Desert, where water is limited and vegetation scarce, wind erosion plays a pivotal role in shaping the land surfaces. Addressing uncertainties in dust emission and deposition rates is crucial to understanding how the atmosphere and land surface interactions affect the soil formation and land surface evolution of hyper-arid areas such as the Atacama Desert. Surface crusts are ubiquitous in the region (Ewing et al. 2006; Michalski et al. 2004; Wang et al. 2014; Li et al. 2019) and have been studied to attenuate the dust emission potential of the soil surface (Gillette et al. 1982; McKenna Neuman et al. 1996; Zobeck 1991; Rice & McEwan 2001). These crusts are also known to host microbial life (Wang et al. 2017; CRC1211-Proposal 2024), which suggests that a biogenic aspect is also present in the atmosphere-land surface interaction, with all of these processes being influenced by climatic conditions (CRC1211-Proposal 2020).

This work provides the first in-situ measurements of threshold wind speeds required for dust emission from crusted surfaces and disturbed surfaces in the Atacama Desert, providing a proxy measurement for the stability of the surface crusts under present-day conditions. The meteorological processes driving strong winds identified in this work can be used to inform paleo dust archives (Albani et al. 2015), understand the variability of dust concentration in these records to changes in the wind and weather patterns (Clemens 1998; Kohfeld & Tegen 2007; Maher et al. 2010; Stuut et al. 2002) and, calculate dust deposition rates based on the frequency of occurrence of these meteorological processes (Mahowald et al. 1999; Albani et al. 2015). This proxy-based reconstruction of atmospheric changes can provide vital hints for understanding the past changes in the atmosphere-ocean dynamics, more specifically, the changes in the El Niño Southern Oscillation and Pacific Decadal Oscillation (of great importance to the biogeochemical cycle in the (south) East Pacific) and the changes in aridity and humidity on the continent (Prospero & Bonatti 1969; Saukel et al. 2011; Martínez 2013; Stuut & Lamy 2004; Flores-Aqueveque et al. 2015).

1.2 SCOPE OF THIS THESIS

This work aims to understand why the dust activity in the Atacama Desert is low despite its aridity. To investigate this, first, the frequency of dust activity is quantified using long-term ground-based observations (Surface Synoptic Observations) spanning nine stations across the extent of the Atacama. This dataset includes weather codes that state the prevalent atmospheric phenomena at the time of recording, with several codes dedicated to recording dust activity such as dust devils, blowing dust and dust storms. The wind speeds from dust observations are then used to compute the threshold wind speed required for dust emission. Second, the thresholds are validated using in-situ measurements with the Portable in-situ Wind Erosion Lab (PI-SWERL). This fieldwork was done from September to October 2022 at two test sites in Central Atacama. The threshold wind speeds were computed for crusted and disturbed surfaces (crust removed) to estimate the differences in the thresholds over the two

surface types. Soil samples were also analysed, but the effect of the soil properties on the thresholds is only briefly explored and not quantified in this work. Third, by combining the ground-based observations with the ECMWF ERA5 reanalysis dataset, the work investigates the meteorological processes that generate winds that trigger the rare yet intense dust activity in the region. The entire study is laid out in two main parts:

1. Thresholds for dust emission (Part I) and
2. Meteorological drivers of dust activity (Part II)

Part I contains two chapters: Chapter 3 and Chapter 4. In Chapter 3, the dust activity is quantified, and threshold wind speeds are computed for the nine different stations. The inter-annual variability between the dust activity is also discussed. Large parts of this chapter are from: **Pinto, R.** & Fiedler, S. (2024, JGR: Atmospheres). **Why is the dust activity in the Atacama Desert low despite its aridity?**. In Chapter 4, the threshold wind speeds required for dust emission are computed for two test sites in central Atacama. The tests are conducted using the PI-SWERL on crusted and disturbed surfaces to mimic anthropogenic land use in the region. The differences between the two test sites and the two surface types are analysed and the implications of these findings for dust activity in the region are discussed. Part II contains one chapter, Chapter 5. This chapter combines dust storms recorded in the ground-based observations with reanalysis data to identify synoptic-scale weather patterns that trigger dust storms in the region. A composite analysis of the wind speed is performed to understand how these dust storms are associated with the weather patterns. Preceding the two parts is a concise background (Chapter 2) to help the reader acquaint themselves with the topics of the thesis. The entire work is summarised in Chapter 6. The objectives of the individual chapters are as follows:

- CHAPTER 3: WHY IS THE DUST ACTIVITY IN THE ATACAMA DESERT LOW DESPITE ITS ARIDITY?
  1. What is the frequency of dust activity?
  2. Is the dust activity low, as the models, satellites, and reanalysis data suggest?
  3. What is the threshold wind speed required for dust emission?

- CHAPTER 4: THE SOIL SURFACE OF THE ATACAMA DESERT: A CONTROL FOR DUST EMISSION
  1. How different are the threshold wind speeds from crusted and disturbed surfaces?
  2. How different are the in-situ threshold measurements from station observation estimates?
  3. Is there local-scale heterogeneity in the thresholds and dust concentrations from the two sites?

- CHAPTER 5: WHAT DRIVES THE RARE DUST ACTIVITY IN THE ATACAMA DESERT?
  1. Is there a diurnal and seasonal dust cycle in the Atacama?
  2. Which weather patterns can be associated with dust storms?
  3. Why do these weather patterns identify trigger dust storms?

2

On Desert Dust and the Atacama Desert

"I lived three years in the Sahara. I also, like so many others, have been gripped by its spell. Anyone who has known life in the Sahara, its appearance of solitude and desolation, still mourns those years as the happiest of his life. The words "nostalgia for sand, nostalgia for solitude, nostalgia for space" are only figures of speech, and explain nothing. But for the first time, on board a ship seething with people crowded upon one another, I seemed to understand the desert. "

—Letter to a Hostage, Antoine de Saint-Exupéry

2.1 DESERT DUST

2.1.1 *Importance of desert dust*

Mineral dust is emitted in large quantities from arid and semi-arid regions of the world (Kohfeld & Tegen 2007) and is the most abundant aerosol type in the atmosphere in terms of aerosol mass (Kinne et al. 2006), with global emission estimates ranging from 1000–3000 $\mathrm{Tg\,yr^{-1}}$ (Cakmur et al. 2006; Zender et al. 2004). They significantly impact multiple facets of the Earth's climate directly and indirectly. Deposited dust particles can fertilise both terrestrial ecosystems such as the Amazon rainforest (Swap et al. 1992; Yu et al. 2015) and marine ecosystems (Schulz et al. 2012a) when it contains iron, an essential micro-nutrient for ecosystems in the oceans thus affecting the global carbon cycle (Jickells et al. 2014). Mineral dust can change cloud properties via several processes (Nenes et al. 2014). They act as efficient ice nucleating particles facilitating the formation of ice crystals in high clouds (Targino et al. 2006). When coated with soluble material such as sea spray or anthropogenic pollutants, they can become effective giant cloud condensation nuclei (Wurzler et al. 2000; Levin et al. 1996). Dust aerosols within clouds also absorb radiation, enhancing cloud evaporation (Ackerman et al. 2000). Dust aerosols have a more direct effect on the radiative energy balance by scattering and absorbing incoming and re-emitting outgoing radiation (Claquin et al. 1998; Tegen et al. 1996). However, recent studies have shown that the magnitude of the radiative forcing due to mineral dust is small (Ryder et al. 2018; Kok et al. 2017). Whether the dust aerosols scatter or absorb radiation depends on the optical properties of the particle, such as the size, mineral composition, and shape (Sokolik & Toon 1996; Liao & Seinfeld 1998; Highwood & Ryder 2014). These properties vary according to the dust source region (Tegen 2003).

Severe dust episodes can adversely affect the habitability of dust-affected regions. For example, the Dust Bowl, a series of severe dust storms in the 1930s, extensively damaged the ecology of the Prairies, adversely impacted agriculture and resulted in the migration of 3.5 million people outside the Great Plains in the US (Worster 2004). More recently, the same is seen in Sistan, Iran, where a present-day 'dust bowl' is unfolding over the region (Lee 2023; Esfandiari & Zarghami 2023; Schwartzstein 2019). Dust storms can remove nutrient-rich topsoils affecting agricultural yields (Shao 2008; Ravi et al. 2011; Glotter & Elliott 2016). Intense dust outbreaks contribute to poor air quality, adversely affecting human health, particularly the respiratory system (Goudie 2014; Kwon et al. 2002; Chen et al. 2004). In the sub-Saharan and Sahel regions, the meningitis epidemic season is said to coincide with dust storms where bacterial spores travel on dust aerosols (Goudie 2014). The negative impact of dust on visibility and transport has also been well documented.

2.1.2 *Dust emission*

Dust is emitted when the wind stress acting on a surface is higher than the threshold. This threshold is dictated by surface characteristics and soil properties, which determine the minimum wind velocity required to transfer momentum from the wind to set the soil particle in motion (Gillette 1978; Morales 1979; Helgren & Prospero 1987). The wind shear stress τ is given by:

$$\tau = \mu \frac{\delta U}{\delta z} \tag{2.1}$$

where U is the wind velocity at height z and μ is the dynamical viscosity of air. It can also be expressed as a function of friction wind velocity, U_*:

$$\tau = \rho U_*^2 \tag{2.2}$$

where ρ is the air density. Under neutral stratification, the wind velocity U at height z can be given by a logarithmic wind profile:

$$U(z) = \frac{U_*}{\kappa} \ln \frac{z}{z_0} \tag{2.3}$$

where $z > z_0$, and z_0 is the aerodynamic surface roughness length and, κ is the von Karman constant (0.4). Once the particle is in motion, its movement depends on size, shape and density. For smaller particles ($< 20\,\mu$m), the inter-particle cohesive forces, composed of Van der Waals force, electrostatic forces, chemical binding forces, etc., dominate, while for larger particles ($> 500\,\mu$m) gravitational force dominates.

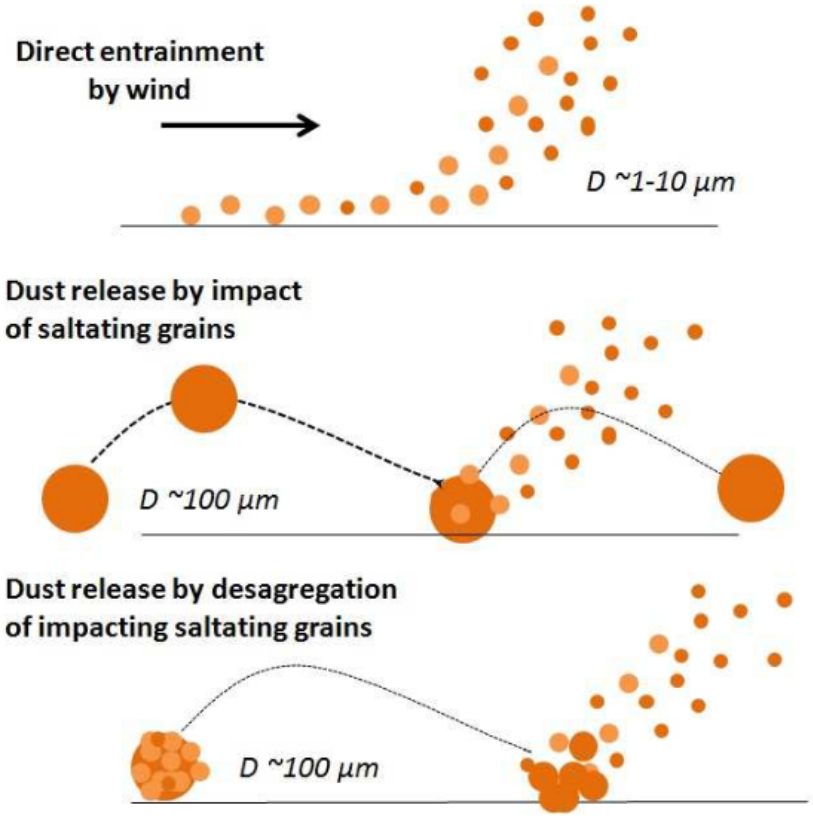

FIGURE 2.1: Dust emitted via a) aerodynamic lift, b) by saltation bombardment and c) by disaggregation. Figure from Marticorena (2014); adapted from Shao (2008)

There are three main mechanisms by which dust is emitted (Figure 2.1): aerodynamic entrainment, saltation and aggregate disintegration (Bagnold 1974; Shao 2008). Aerodynamic

or direct entrainment occurs when particles, usually smaller than 60 μm, are set into motion when the wind stress acting upon a surface overcomes the inter-particle cohesion forces and the gravitational force holding the particles on the surface. However, very high friction wind velocities are required to overcome the cohesive forces, as determined by wind tunnel experiments (Shao et al. 1993). Hence, the mechanism of aerodynamic dust entrainment is considered negligible. The inter-particle cohesion, however, varies for particles of the same size as the cohesive force depends on the particle shape, the mineralogy, the surface roughness, etc., (Zimon 2012).

Particles of diameters between 70–100 μm, lifted from the ground by aerodynamic forces but are too heavy to be suspended into the atmosphere, follow a ballistic trajectory because of the aerodynamic drag force and fall onto the surface after a distance potentially impacting other particles (Marticorena 2014). If sufficient momentum is transferred upon impact, then the other particles also become suspended. This hopping motion is called saltation. When the impact leads to the ejection of smaller particles, it is called sandblasting or saltation bombardment. Another mechanism for dust emission is when soil aggregates are transported in saltation, and upon impact with the surface, the aggregates disintegrate, releasing smaller particles. This mechanism is called aggregates disintegration or auto-abrasion (Shao 2008). Saltation and auto-abrasion account for most likely dust emission mechanisms. Large particles that cannot be suspended from the surface roll along the surface in a creeping motion (Bagnold 1974). These creeping particles can dislodge other particles as they abrade the surface.

To allow the transfer of momentum to the particles, the wind speed must exceed a threshold, U_{t*}. This threshold can be expressed as a function of particle diameter, D_p and air and particle density, ρ_a and ρ_p, respectively. The threshold, based on Shao and Lu (2000) is given by:

$$U_{t*}(D_p) = [A_N(\frac{\rho_p\, g\, D_p}{\rho_a} + \frac{\gamma}{\rho_a\, D_p})]^{0.5} \tag{2.4}$$

where A_N is a dimensionless threshold parameter which depends on the friction Reynolds number, the term $\frac{\gamma}{\rho_a D_p}$ accounts for the inter-particle forces with γ adjusted to wind-tunnel measurements (Marticorena 2014). The relationship between U_{t*} and particle size D_p can be seen in Figure 2.2 where small particles ($< 60\,\mu$m) require high threshold friction velocities. As this relationship between the threshold friction wind speed and particle diameter is non-linear, an exact particle size distribution of the dust source is required to estimate the threshold wind speed. Furthermore, surface roughness characteristics such as the presence of vegetation, gravel, and surface crusts (Gillette et al. 1980a; Gillette & Passi 1988; Zender & Kwon 2005; Mahowald et al. 2005; Mahowald et al. 2003; Ginoux et al. 2012b; Shao et al. 2020; Fécan et al. 1998; Raupach et al. 1993) influence the threshold.

The surface roughness, z_0, influences the erosive capacities of the wind. Surface roughness elements such as vegetation and gravel absorb a fraction of the wind momentum, increasing the threshold for dust emission (Raupach et al. 1993). Roughness heights over 1 mm can suppress dust emission rates (Gillette 1999) while vegetation greater than 16% limits erosion by wind (Wolfe & Nickling 1993). Soil moisture increases the threshold due to the capillary effect of moisture, which leads to cohesive particles (Chepil 1956; Fécan et al. 1998; McKenna-Neuman & Nickling 1989). However, vegetation and soil moisture mostly play a small role in influencing the dust emission potential in the Atacama Desert.

The defining roughness feature in the Atacama is the ubiquitous surface crust. Crusted surfaces protect the surface from wind erosion and decrease the dust emission potential (Gillette et al. 1982; Goossens 2004; Klose et al. 2019). These crusted surfaces limit wind erosion as long as the crust is not broken (Gillette et al. 1982). Once the crust is broken, it

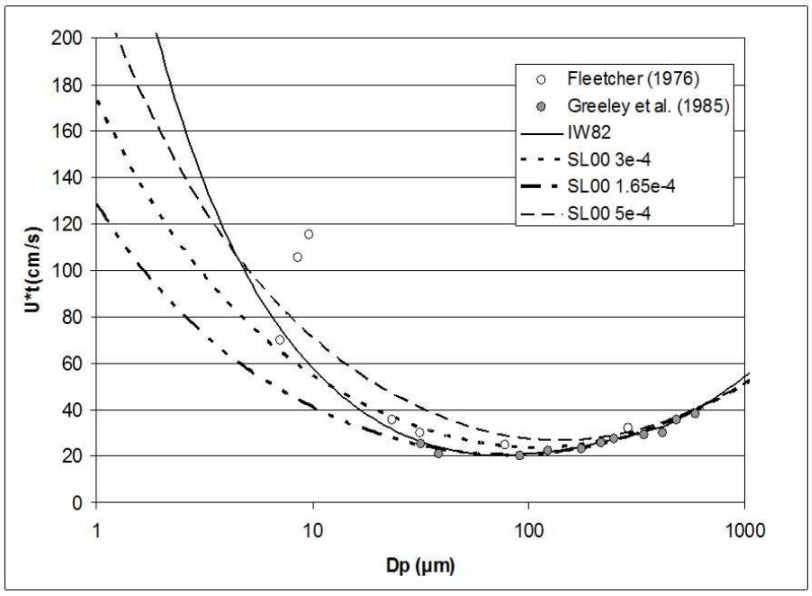

FIGURE 2.2: Threshold wind friction velocity, U_{t*} as a function of particle diameter, D_p on based IVERSEN and WHITE (1982) ((IW82) and Shao and Lu (2000)) for different values of inter-particle forces, (SLOO). White dots are experimental data from Fletcher (1976) and grey dots from Greeley and Iversen (1985). Figure from Marticorena (2014); adapted from Shao (2008)

depends on the availability of eroding material between the gaps and underneath the crust to supply and support continuous dust emission (Houser & Nickling 2001). Surface crusts formed by rain events, for example, tend to be weak and crack as soon as they start to dry (Gillette et al. 2001). Weak bonds between the grains in the crust can also be broken by the bombardment of saltating particles (Rice et al. 1999; Goossens 2004), which after repeated impact may make the surface more prone to erosion (Rice & McEwan 2001). Therefore, regionally specific information on the soil properties and surface characteristics is required to accurately represent the dust emission in regional and global aerosol models.

2.2 THE ATACAMA DESERT

2.2.1 *Climatic setting*

The Atacama Desert is the driest non-polar desert on Earth (McKay et al. 2003; Houston & Hartley 2003). Nestled between the South Pacific Ocean to the west and the Andes to the east, it stretches along the subtropical southwest coast of South America from 16°S to about 28°S. The hyper-aridity[5] of the desert is attributed to its location in the subtropics at the descending branch of the Hadley cell and, consequently, the presence of the semi-permanent anticyclone over the southeast Pacific (Houston & Hartley 2003; Rodwell & Hoskins 2001). The anticyclone typically blocks the passage of mid-latitude disturbances, drives southerly winds along the coast and forces the coastal upwelling of deep cold waters (Shaffer et al. 1999; Rutllant & Montecino 2002).

[5]Regions, where precipitation is less than 5% of the potential evapotranspiration rate, are called hyper-arid (UNEP 2011).

Along the coast, the cold Humboldt Current transports cold water from higher latitudes towards the Tropics (Montecino & Lange 2009). The temperature contrast between the cold sea surface temperatures and the warm subsiding air above inhibits deep convection over the ocean and land (Strub 1998). Furthermore, the strong temperature inversion separates the relatively cold and humid marine boundary layer (MBL) from the relatively warmer air mass subsiding above, leading to a dry and stably stratified lower troposphere (Rutllant et al. 2003). It is below this warm subsiding air mass that the largest stratocumulus deck on Earth forms (Klein & Hartmann 1993).

Additionally, the unique orography of the region further facilitates the aridity of the Atacama. The presence of steep coastal cliffs as high as 1000–2000 m above sea level (asl)

on the western flanks of the Atacama Desert prevents the moist marine air from penetrating inland, inhibiting inland moisture transport from the Pacific (Rutllant et al. 2003). And, on the eastern flanks of the desert, the rain-shadow effect of the Andes (Houston & Hartley 2003; Garreaud et al. 2010) effectively blocks the moisture transport from the Amazon Basin (Houston & Hartley 2003). All these factors, in concert, result in a region nearly devoid of rain (Houston 2006c).

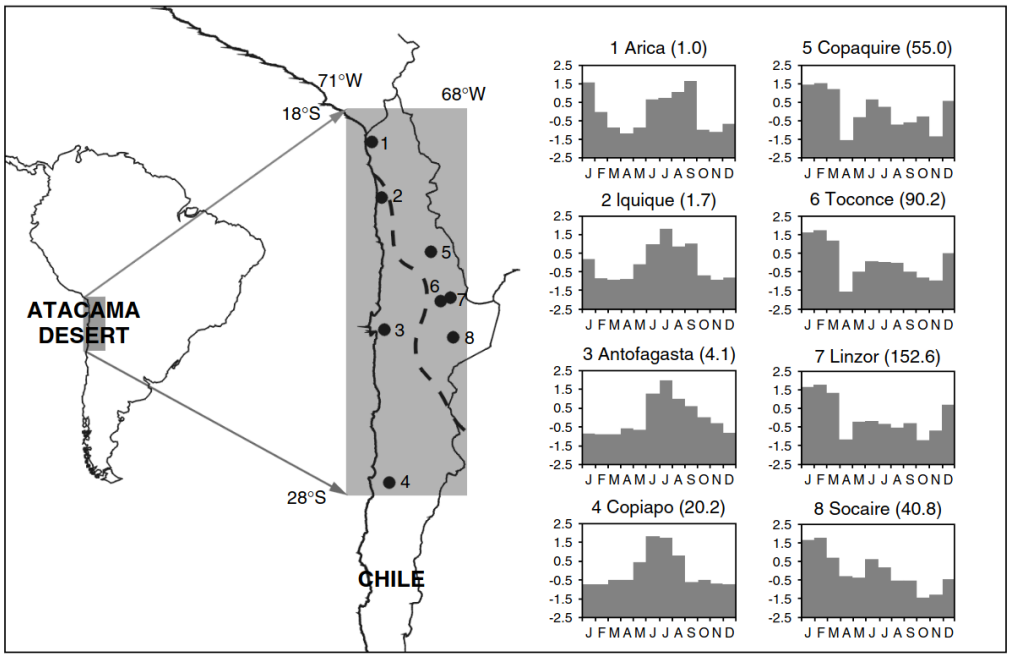

FIGURE 2.3: Monthly rainfall frequency (from data between 1900–2000) with winter-dominated rainfall along the coast and summer-dominated along the interior (Andean) stations. Mean annual rainfall in mm is given in brackets with increasing rainfall with increasing latitude. The dashed line divides stations based on the seasonality of rainfall. Figure from Houston (2006c).

In the dry Atacama, the rare precipitation events are controlled by different meteorological sources (Houston 2006c; Aceituno et al. 2021). Between 23°S and 27°S, frontal systems and cut-off lows originating in the extra-tropical storm track bring precipitation to the southern fringes of the Atacama during the southern hemisphere winter (Vuille & Ammann 1997; Vargas et al. 2006). Summer precipitation is mainly limited to the northeastern part of the Atacama (Houston 2006c). Here, moist easterly winds of the South American Monsoon System bring rainfall to the Andean Range and the Altiplano and also further across toward the west coast but with sharply decreasing magnitudes (Figure 2.3). Böhm et al. (2021a) found that nearly 40–80% of the precipitation between the coast and the Andean foothills is associated with atmospheric rivers. Additionally, dense fog along the coast, locally known as *camanchaca*, is another significant moisture source (Ericksen 1981). This fog, which is predominant in the winter (Böhm et al. 2021b), forms when marine stratocumulus clouds advect inland at nighttime and intercept the coastal cliffs (Cereceda et al. 2008; Cáceres et al. 2007). The fog zone fosters the growth of plant communities called *lomas* (Rundel et al. 1991), which follow a north-south gradient with increasing *loma* communities towards the south of the Atacama (Figure 2.4). Apart from increasing surface roughness and dust emission threshold, these *lomas* also potentially trap windblown sand (Latorre et al. 2011).

2.2.2 *Synoptic circulation patterns*

Dust storms, in particular, require intense wind speeds to lift dust particles off the surface and transport them over long distances (Prospero 1996; Shao 2008; Schepanski 2018). These strong winds that initiate dust emission and support long-range transport are driven by sufficiently large surface pressure gradients. For example, cyclones and cold fronts are

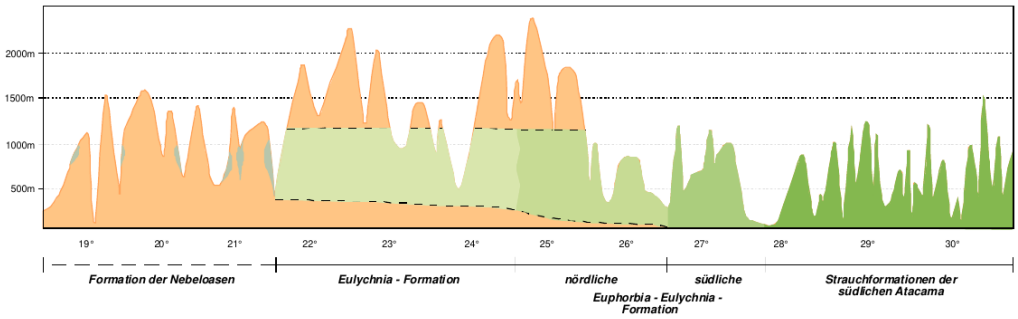

FIGURE 2.4: Latitude and approximate elevations of the *loma* along the anterior of the coastal cliffs. Figure from Schulz (2009).

major synoptic systems driving dust storms in China (Qian et al. 2002; Takemi & Seino 2005; Huang et al. 2008), non-precipitating cold fronts over southern and central Australia (Ekström et al. 2004; Leslie & Speer 2006), convective systems in North Africa (Heinold et al. 2013) and the Middle East (Francis et al. 2023). Strong anticyclones can also drive strong winds, as observed over the Sistan, where a pronounced increase of an anticyclonic disturbance over the Caspian Sea enhances the west-to-east pressure gradient and results in dust storms over the Sistan (Kaskaoutis et al. 2015). In East Asia, the intense Siberian and Mongolian highs bring strong winds and cold air outbreaks, inducing dust storms in Mongolian and Northern China and transporting the dust aerosols to central Korea (Chung et al. 2014). In the Pisco-Ica Desert in southern Peru, *Parcas* winds that initiate dust storms are associated with the strengthening of the anticyclone in northern Chile (Briceño-Zuluaga et al. 2017). Here, a few of the synoptic patterns that could influence dust activity in the Atacama are discussed.

Over the Atacama, the synoptic weather patterns are highly influenced by the semi-permanent SEPA located below the subsidence branch of the Hadley cell (Mechoso et al. 2014; Klein & Hartmann 1993; Ma et al. 1996; Muñoz & Garreaud 2005; Rodwell & Hoskins 2001; Grotjahn 2004). The changes in the intensity of the SEPA are driven by synoptic variability and large-scale atmospheric circulation like the Madden-Julian Oscillation, ENSO and the Antarctic Oscillation (or the Southern Hemisphere Annular Mode). These result in inter-annual and decadal changes in the intensity of the SEPA (Rahn 2012). However, rare cut-off lows from the storm track in the higher latitudes move towards the coastal region (Vuille & Ammann 1997; Vargas et al. 2006). These disturbances can enhance northwesterly winds and result in calmer nocturnal winds compared to the usual diurnal mean values (Jacques-Coper et al. 2015).

Mid-tropospheric cut-off lows (CoLs) are segregated low-pressure systems that are detached from the mid-latitude westerly jet (Palmén & Newton 1969; Ndarana & Waugh 2010) enclosing cold air from high latitudes (Palmén 1949; Hoskins et al. 1985). Generally, the cold air enclosed by a CoL in the upper and mid-troposphere leads to statically unstable conditions closer to the surface before the CoL dissipates or merges with the main flow (Hoskins et al. 1985; McInnes et al. 1992; Barnes et al. 2021). There have been several studies focusing on CoLs in Chile and the southern hemisphere, specifically on the role of the Andes in dissipating CoLs (Garreaud & Fuenzalida 2007), the impacts on precipitation in Southern Chile as well as in the Atacama (Pizarro & Montecinos 2000; Bozkurt et al. 2016; Aceituno et al. 2021) and, CoL climatology (Pizarro & Montecinos 2000; Fuenzalida et al. 2005; Campetella & Possia 2007; Reboita et al. 2010; Muñoz et al. 2020; Reyers & Shao 2019). These studies show that CoLs along the Chilean coast are not infrequent. However, there has been no consensus on the yearly mean CoL frequency and the seasonality due to differences in datasets, period of analyses and the level of geopotential height used in the identification schemes (Pinheiro

et al. 2017; Ndarana et al. 2012).

Fuenzalida et al. (2005) found 17 CoLs per year for the South American region with a standard deviation of 6.2 CoLs/year and a summer minimum. This seasonality is also in agreement with Reboita et al. (2010). For the same region, Campetella and Possia (2007) also found 17 CoLs/year with an autumn and winter maxima and a summer minimum. Along the subtropical coast of Chile, they found most events in spring. Of the 171 CoLs, only 25% had a surface cyclonic circulation with high-frequency south of 40°S. The seasonality of non-surface CoLs was different insofar as there was still an autumn maximum but a winter minimum. Muñoz et al. (2020) found 26 CoLs/year with the highest frequency of 500 hPa cut-off lows over South America between late autumn and early spring. Using NCEP-NCAR reanalysis data over Chile, Pizarro and Montecinos (2000) found seven CoLs per year. Still, the occurrences had significant inter-annual variability ranging from 2 to 16 events, with a winter and spring maximum. They also found that of the 130 CoLs during the analysis period, only 17 did not produce precipitation. For the Atacama Desert, Reyers and Shao (2019) found 4 CoLs/winter with a strong inter-annual variability ranging from one to eleven CoLs per winter, using 500 hPa geopotential height fields of ERA-Interim for the period 1979–2015, which are responsible for wet conditions in the Atacama and also reported a change in the thermally driven wind system with different stations recording either an increase or decrease in mean wind speed during a CoL.

In addition to the SEPA, southern Atacama can also be influenced by the eastward migrating anticyclone (Demortier et al. 2021; Aguirre et al. 2021). With the passage of the migratory anticyclone across south Chile, strong southerly winds over 8–10 ms^{-1} are found with high probability. These strong winds are characteristic of a coastal low-level jet, which is driven by the alongshore surface pressure gradient between a coastal low in north-central Chile and the migratory anticyclone (Aguirre et al. 2021; Garreaud & Muñoz 2005; Muñoz & Garreaud 2005). These coastal low-level jets are more intense during winter and early spring around the region 28–30° (Aguirre et al. 2021; Garreaud & Muñoz 2005).

Coastal lows are thermal sub-synoptic systems propagating pole-ward along the coast of Chile, on the eastern flank of the SEPA and the west Andes (Figure 5.23) (Garreaud et al. 2002; Rutllant 1994; Rutllant & Garreaud 2004). These coastal lows tend to develop with the approach of a cold, migratory anticyclone drifting east from the southern Pacific towards southern Chile at about 40°S (Garreaud et al. 2002). As the anticyclone moves northeastward into the continent, it reverses the alongshore pressure gradient, which prompts low-level easterly winds offshore of coastal central Chile. However, the presence of the coastal cliffs inhibits the generation of this easterly flow at low levels. Therefore, this easterly flux is compensated by descending winds from the western side of the Andes (Rutllant 1994; Garreaud et al. 2002). These down-slope winds are called *Terral* by local communities in north-central Chile (30°S, also La Serena) (Rutllant & Garreaud 2004; Montes et al. 2016). The winds blow from the east for stations south of the coastal low (e.g. La Serena) and from the north, northwesterly directions for stations north of the coastal low. The hourly surface wind speed can reach intensities up to 14 ms^{-1} at any moment of the day as the coastal low moves southward (Pinto 2019), leading to strong wind gusts, which may allow the lifting of dust. Coastal lows can occur in all seasons at the rate of once a week, are prominent between fall and spring and are mainly concentrated around 27°S to 37°S (Rutllant & Garreaud 1995; Garreaud et al. 2002; Gallardo et al. 2002). They are of great relevance as they are connected to poor air quality with occasional episodes of intense air pollution (Rutllant & Garreaud 1995; Gallardo et al. 2002; Pozo et al. 2019; Huneeus et al. 2006).

2.2.3 *Wind systems*

The diurnal differences in the mesoscale circulation in the Atacama Desert are driven by strong differential heating of land and ocean coupled with the steep terrain in the region. The coastal cliffs prevent the incursion of most of the maritime air masses inland (Schween et al. 2020), which results in the formation of two mainly independent circulation cells (Rutllant et al. 2003). The lower cell is contained within the coastal MBL, within which the land-sea breezes are superimposed on the prevailing southerlies driven by the SEPA. This results in strong near-surface south-westerlies during the afternoon with an offshore return flow below the MBL top and light northeasterly winds during nighttime and early morning. Above the MBL, an upper cell is driven by the strong heating of the Andean slopes (Andean pumping, Rutllant et al. (2003)), which results in strong near-surface westerlies and south-westerlies and a weak return flow at higher altitudes (Rutllant et al. 2003; Rutllant et al. 2013). During nighttime and early morning, regions inland observe a return drainage flow or easterly winds down-slope of the Andes (Rutllant et al. 2003; Jacques-Coper et al. 2015; Muñoz et al. 2018; Muñoz et al. 2013; Schween et al. 2020).

The nocturnal flow over the Atacama Desert is characterised by strong low-level jets (Muñoz et al. 2013). The strongest down-valley jets are found extending down the slope of the Andes into the Atacama Desert (Muñoz et al. 2018). Using 80 m high towers, located up and down-valley from Calama, Muñoz et al. (2013) analysed 0–80 m wind flow and found that the vertical profiles of the nocturnal flows have nose-shaped wind profiles with maximum speeds occurring between 20 and 60 m above ground. The intensity had a marked seasonality, with stronger flows occurring between May and October. These low-level jets are of great interest not only because of their wind energy potential but also because of the transport of pollutants from mining activities in the region.

Other important down-slope winds in the region are the *terral* winds in La Serena (southern edge of the Atacama Desert). These winds are warm and dry, mostly blowing between nighttime and dawn during winter, with wind speeds periodically reaching 8–10 ms^{-1} in 2-hour intervals (Montes et al. 2016). These winds are associated with a high-pressure system crossing the Andes in southern Chile, reversing the typical equatorward pressure gradient. This forces a low-level easterly offshore flow, which is compensated by descending winds (*terral*) from the western side of the Andes (Rutllant 1994; Garreaud et al. 2002).

2.2.4 *Soil surfaces*

Given the lack of vegetation in most regions of the Atacama (especially the hyper-arid core), the surface geomorphology dictates the extent to which the soil surface is prone to erosion. Soil surfaces in Central Atacama usually are a combination of a thin fragile surface crust that ranges from a few to tens of millimetres thick, sitting on top of fine-sand rich soil layers called *chuca* consisting of gypsum/anhydrite that is 10–30 cm thick (Ewing et al. 2006; Michalski et al. 2004; Wang et al. 2014; Li et al. 2019). Apart from the surface crusts, the Atacama has diverse soil surfaces (Figure 2.5) ranging from desert pavements, which are layers of closely packed gravel, to loess, gypsum, and salt-crusted soils (Arenas-Díaz et al. 2022). Alluvial fans, dry lake beds, and salt-crusted playas (*salars*) are also found in the desert (Finstad et al. 2014). Biological crusts have also been identified in some areas of the Atacama (Wang et al. 2017), with increased fine-sediment present underneath the crusts that the study has attributed to the ability of biological crust trapping more dust than areas without the biological crust by inhibiting wind erosion. Vegetation, as mentioned in the previous section, is limited to the fog regions of the desert. Additionally, the desert's geomorphology spans from relict land-forms such as sand dunes in Iquique (Paskoff 2005) to Chuquicamata, one

of the largest open pit mines in the world just outside of Calama, to the Mejillones Pampa near Antofagasta (Flores-Aqueveque et al. 2010) to mega-yardangs in Chañaral (de Silva et al. 2010; Goudie 2013a) and, to the barchan in Copiap 'o (Goudie 2013a).

FIGURE 2.5: Photos from the fieldwork in Sep–Oct 2022 in the Atacama Desert (see Chapter 4). The last photo with the snow-peaked Andes is credited to B. Ritter, while the others are the author's.

2.2.5 *Mining activity*

An overview of the Atacama Desert is incomplete without mentioning its long history with mining. A unique combination of extreme aridity and tectonic activity has facilitated the abundance of minerals in the region. It hosts Chuquicamata, near the city of Calama, the largest open-pit copper mine in the world with dimensions over 12 sq. km and 850 m deep. With the world's largest nitrate deposits (Ericksen 1981), essential for fertilisers and the manufacture of saltpetre (used in gunpowder), Chile was the world's leading supplier of sodium nitrate until the invention of the Haber-Bosch process in 1909 (Gross 2014). Today, it is the world's largest producer of copper (USGS 2024a) and the second largest producer of lithium and molybdenum (USGS 2024b; USGS 2024c), with mineral extraction contributing to 10.1% of the Chilean Gross Domestic Product in 2018 (USGS 2018). Environmental conditions of mineral extraction were poorly regulated until 1994 with the enactment of law No. 19.300 and an amendment in 2002, which requires an environmental impact assessment for new mineral exploration or extraction processes (USGS 2018).

Despite the regulations, several issues persist, from improper closing of mines to problematic handling and storage of large deposits of mine tailings (López-Berenguer et al. 2021). These tailings are a mixture of crushed rocks from mineral ores and other effluents involved in the extraction process. They are considered major pollutants as they can lead to severe water contamination, air pollution and land degradation (Araya et al. 2020; López-Berenguer et al. 2021). Several studies in the Atacama already document the dangerously poor air quality (Mesías Monsalve et al. 2018; Tapia et al. 2018) and contaminated water in towns

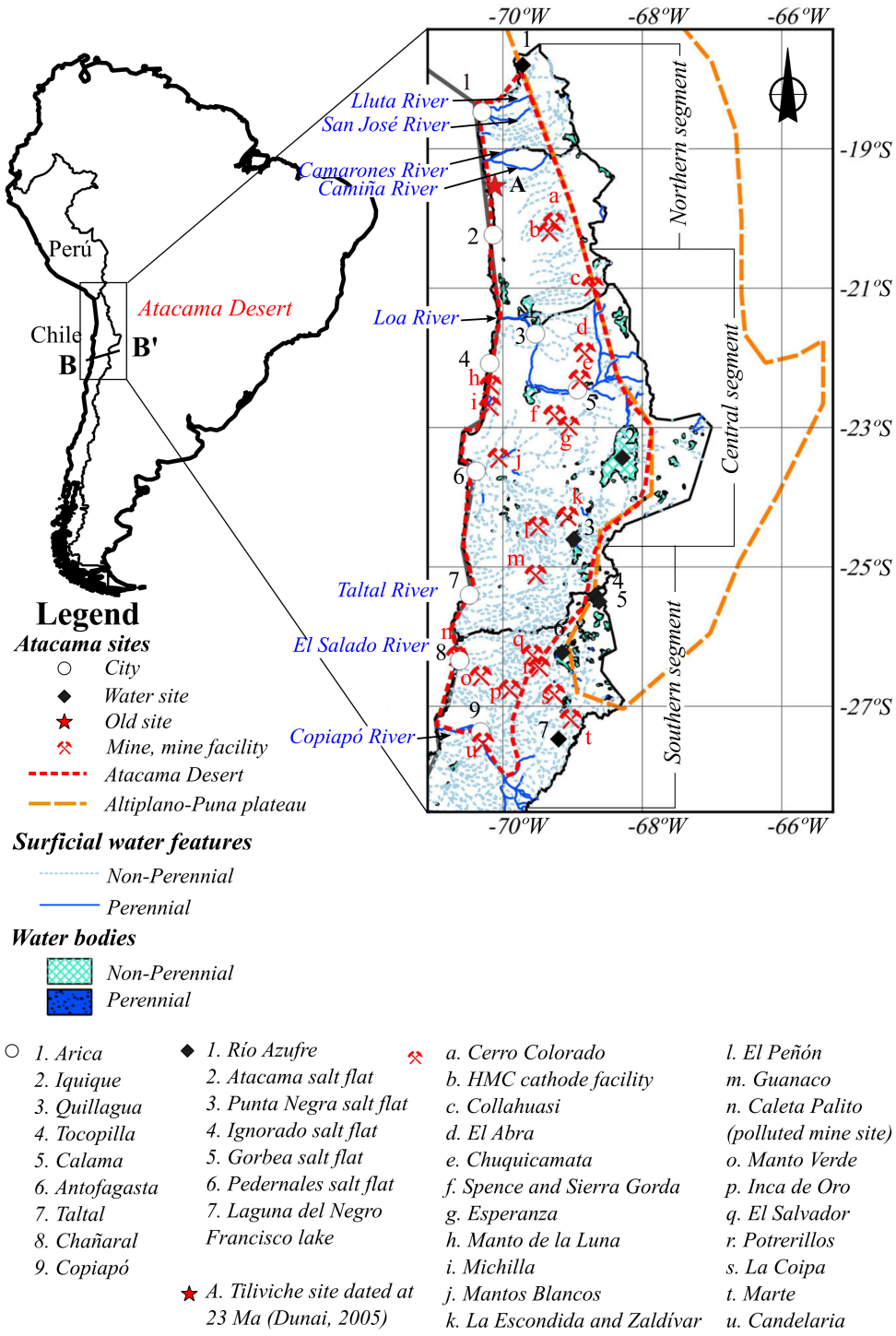

FIGURE 2.6: Location of mines in the Atacama Desert. These mines are only some of the 150-plus mines, quarries and mining facilities recorded in mindata.org for the Atacama Desert. Figure adapted from Tapia et al. (2018).

around the mines and tailing deposits (Orihuela 2014; Jorquera 2009; Castro & Sánchez 2003). Many mine tailings dot the Atacama Desert (Cacciuttolo & Valenzuela 2022; Aguilar et al. 2021; Dold 2006; Kidder et al. 2020; López-Berenguer et al. 2021; Araya et al. 2020). In 2018, the Geological Survey of Chile estimated that Chile produces 1,400,000 tons of mine tailings daily, and 696 of these tailing deposits exist, with a majority in the Antofagasta region (Araya et al. 2020).

This knowledge of mining activity is of particular interest while studying dust activity as the different stages of mineral extraction, such as blasting, crushing, drilling, transporting and storing material involve land degradation (Figure 2.7) that results in soil surfaces, which depending on the local meteorological conditions, can be prone to wind erosion and increased dust emission potential (Grange 1973; Chaulya 2003; Kahraman & Erkayaoglu 2021).

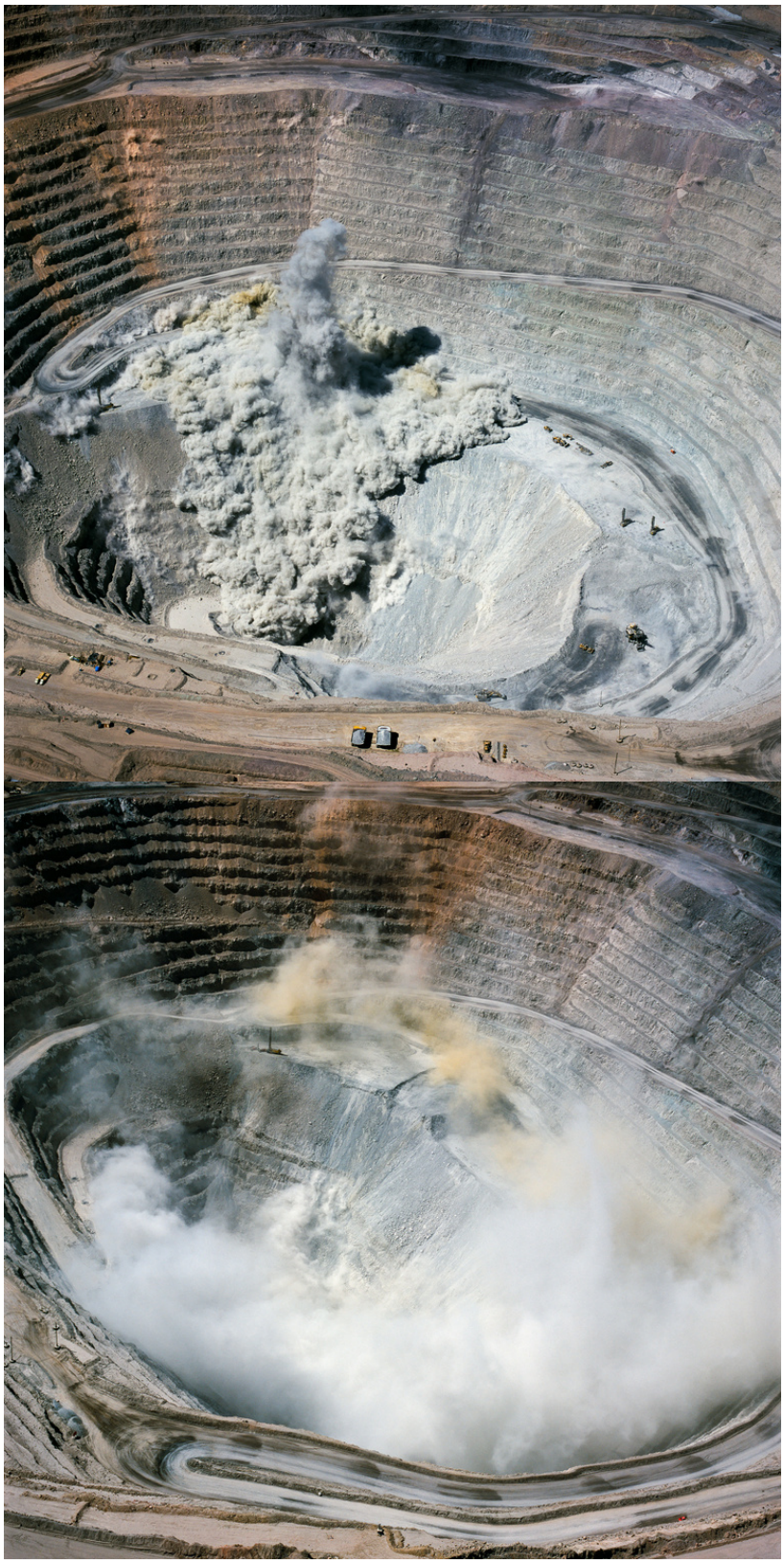

FIGURE 2.7: Minera Centinela, Copper Mine, Antofagasta Region, Atacama Desert, Chile, 2018. Photographs from 'Desert Desolation' by David Maisel (Maisel 2019).

2.3 DUST IN THE ATACAMA

2.3.1 *Literature review*

There have been some studies on dust activity in the Atacama Desert. Kurgansky et al. (2011) and Metzger et al. (2010) conducted the first dust devils campaign in January 2009 for 12 days, outside Huara (80 km northeast of Iquique). The study region was adjacent to a dry lakebed composed of clay and silt. They found 3622 dust devils between 1130 LT and 1630 LT. They also deduced from their fieldwork that the dust devil activity ceases for wind speeds beyond 8 ms^{-1}. However, they could not conclude on the minimum wind speed required for dust devils to occur. They did conclude that wind gusts drive the dust devil activity with gustiness sourced from the strong convective activity during the early afternoon when the wind speeds begin to increase and, from the surface inhomogeneities, facilitating turbulence during the late afternoon after peak convection.

Another study by Reyers et al. (2019) studied the synoptic conditions of an unusually large dust storm in the Atacama Desert on 8 July 2016. The dust plume from this event travelled hundreds of kilometres west and southwestwards. Using reanalysis data and models, they found that a horizontal convergence band over the north Atacama due to the zonalisation of a mid-tropospheric trough over the southeast Pacific resulted in strong down-valley easterly winds. During this event, wind speeds greater than 12 ms^{-1} were observed at a coastal station, while the authors note that the average wind speed is less than 3 ms^{-1} at this station. Because of the intensity of this event, the authors concluded that the Atacama Desert has the potential to be a major dust source.

The wind erosion along the coast of the Atacama Desert around the Mejillones Peninsula Bay (23°S) north of Antofagasta was studied by Flores-Aqueveque et al. (2010) and Flores-Aqueveque et al. (2012). For the study, Flores-Aqueveque et al. (2010) analysed data from sediment traps, wind speed observations from ground-based stations and a dust emission model (Marticorena & Bergametti 1995) to estimate the threshold friction velocity of 0.31 ms^{-1} required for dust emission. They observed that this threshold was exceeded only for a small duration of the fieldwork and almost always in the afternoon when the southerly, southwesterly winds peaked. Flores-Aqueveque et al. (2012) used 14 years of wind speed observations to analyse the inter-annual variability of surface winds in the Mejillones Peninsula Bay and study its impact on the transport and deposition of dust aerosols. Using an emission, transport and deposition model (Alfaro et al. 2011), they concluded that for wind speeds 10–12 ms^{-1} at 10 m height, there is increased transport of coarse dust particles ($>100\,mu$m) towards the sea.

As part of their PhD thesis, Oyarzún (2021) used the MODIS instrument on Terra and Aqua satellites (NASA), along with the only AERONET data (Holben et al. 1998) available for the Atacama Desert in Arica from 2010–2019, to compute the aerosol load and the number of dust days in the Atacama Desert. Terra passes over the Atacama Desert between 1100 to 1200 LT, while Aqua is between 1400 to 1600 LT. They found mean AOD values between 0.10–0.22 between the two satellites and seasons (0.17–0.39 is the range for mean AOD values for desert regions, Dubovik et al. (2002)). They found that the decadal mean AOD was highest along the coast 18°S and 20°S and the central desert region between 21°S and 23°S. They also found a noticeable summer and spring seasonality in high AOD values and spatial extent of high AODs. Using a threshold for AOD across the four seasons, they estimated the number of dust events, with approximately 500 dust events spanning an entire decade with a standard deviation of 18 events. Furthermore, they found that coarse aerosols were associated with intense easterlies and southerly winds, and the high aerosol load retrieved

from Terra was associated with winds between southwesterly and northwesterly, with some easterly components. From the Aqua satellite, the high aerosol load was associated with the westerly flow with a few instances of southerly flow.

Cordero et al. (2018b) also analysed satellite data to obtain the average AOD values over the Atacama Desert to study dust accumulation on photovoltaic panels (soiling). Their results showed that the satellite estimates have consistently low climatological AOD values (Figure 2.8) over the Atacama Desert (ranging from 0.25 in the northern coastal part of the desert to 0.05 over the Andean plateau). The study found that the changes in wind speed did not significantly change the soiling rate[6]. They also reported that the soiling rate in northern Atacama is comparable to that measured in North Africa and the Middle East. It is important to note that satellite retrievals of AOD can be prone to inaccuracies, especially close to the Atacama because of the contributions of other aerosol species such as sea spray and anthropogenic aerosols (Ridley et al. 2016). In another study (Cordero et al. 2018a) found that the AOD values over the Atacama showed significant differences between different instruments (MISR and MODIS), especially over the coastal northern part of the Atacama and highlighted the need for more ground-based AOD measurements.

[6]Soiling is the deposition and accumulation of snow, dust aerosols, etc, onto the surface of photovoltaic modules.

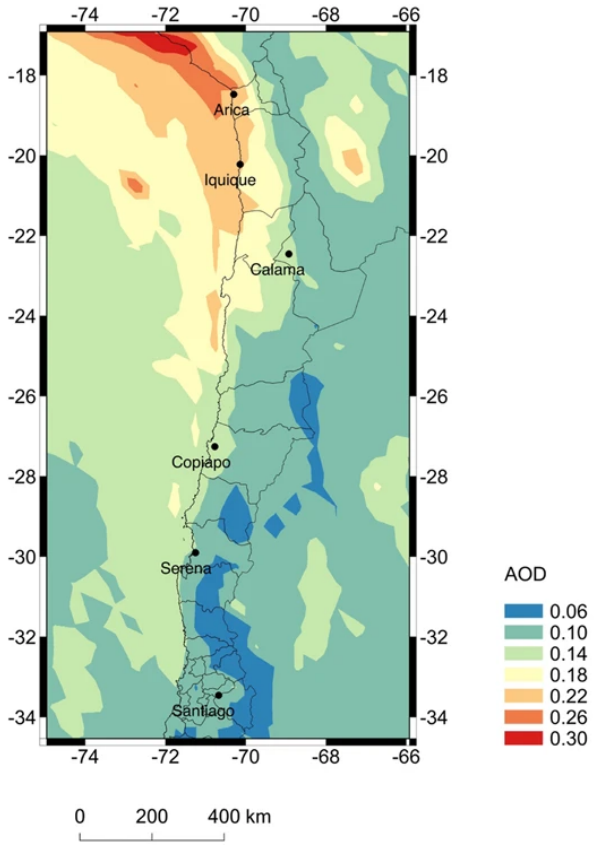

FIGURE 2.8: Annual average of AOD at 555 nm computed from retrievals of the Multi-angle Imaging Spectro-Radiometer (MISR) instrument on TERRA for the period 2006–2016. For Santiago and Arica, ground-based measurements of the AOD are used from AERONET. Figure from Cordero et al. (2018b)

An extensive review summarising the current knowledge on the evolution of the landscape in the Atacama was performed by Arenas-Díaz et al. (2022) to understand the spatial and temporal dynamics of atmospheric dust deposition. They reviewed several studies on soil surfaces and wind erosion and analysed the processes of aerosol emission and transport. Based on the review, they concluded that local and remote aerosols deposited in the Atacama are essential in forming soil and salt deposits. They also suggested that the low dust storm activity in the Atacama could be due to the low erodibility of the soil surfaces in the Atacama, the presence of boulders and large stones and the occurrence of desert pavements and surface

crusts that reduce mobilisation of dust aerosols and require a strong threshold wind speed for entrainment of dust. Additionally, they hypothesise that the prevailing present climate of the Atacama is unsuitable for generating sufficiently strong enough winds for dust emission and that the topography of the Atacama, with its high mountain ranges on the east and west, acts as natural traps for dust aerosols that are emitted, thereby allowing only a local reach.

Studies focusing on soil formation and landscape evolution in the Atacama have long used dust traps in the desert to understand atmospheric dust and salt deposition (Wang et al. 2014; Wang et al. 2015; Li et al. 2019). Using a series of dust traps set up along an east-west transect from the Pacific coast to the Andean Plateau, the authors analysed the sediments collected in these traps to find that insoluble dust mainly originated from local sources and weathered rocks, the salt deposits found in the traps closest to the coast were sourced from the ocean. That inland, erosion from salars and salt lakes played an important role. They also conclude that wind speed and precipitation changes can affect the insoluble dust and salt fluxes collected. However, these meteorological factors more easily influenced dust fluxes than salt fluxes. They also found that dust traps close to open-pit mines had increased dust flux (Li et al. 2019). A corresponding study that aimed to study soil formation in the Atacama (Wang et al. 2017) found thicker loose soil profiles and higher fractions of fine particles underneath biological crusts than physical crust sites. This, they hypothesised, could be due to past geological processes and the ability of biological crusts to protect the soil beneath them from wind erosion and allow for the trapping of fine dust.

Saukel et al. (2011) analysed deep-sea sediments in the eastern equatorial and subtropical Pacific (10°N to 25°S) to investigate the relationship between the southeast trade winds and dust transport from the Peruvian and Atacama Desert, the two dust sources in the region. They found that the sediments were fine-grained (4–8 μm) and that wind is the leading transport agent of this dust in the deep-sea sediments. They hypothesise that dust distributed over the ocean is lifted into the upper levels of the atmosphere and carried by the southeast trade winds. They also note that the feldspar and illite, a clay-mineral component of the sediments, point towards dust transport from the Atacama Desert than the Peruvian desert.

2.3.2 *Ground-based dust observations*

Observations of dust activity were extracted from ground-based weather stations as part of the Surface Synoptic Observations (SYNOP) dataset maintained by the Meteorological Service of Chile (Dirección Meteorológica de Chile- Servicios Climáticos 2019) and with standardised measurements prescribed by the WMO (World Meteorological Organization 1995). SYNOP data has been used to compute the threshold wind speed required for dust emission in East Asia (Kurosaki & Mikami 2007) and North Africa (Morales 1979; Helgren & Prospero 1987; Cowie et al. 2014). It has also been used to identify global trends in dust activity (Shao et al. 2013) and visibility (Mahowald et al. 2007).

The variables of interest from the SYNOP dataset are the records for present weather and wind velocity. The wind speed is measured at 10 m height, averaged over 10 min using a cup and vane wind measurement system as seen in the photos by the Meteorological Service of Chile. Wind gusts were not available at the time of accessing this dataset. However, as of 2020, most stations in the Atacama have 2 min average wind speed available.

The present weather is the qualitative description of the significant weather phenomenon present at the time of observation, as determined by a station observer, out of a possible 100 different atmospheric states prescribed (WMO code table 4677). These 100 codes describe states of the atmosphere that impact human activity and transport and their significance for forecasting synoptic weather systems (World Meteorological Organization 1995). Only

All of the present weather codes and their descriptions from WMO code table 4677 can be found here: https://www.nodc.noaa.gov/archive/arc0021/0002199/1.1/data/0-data/HTML/WMO-CODE/WMO4677.HTM and the past weather codes from WMO code table 4561 here: https://www.nodc.noaa.gov/archive/arc0021/0002199/1.1/data/0-data/HTML/WMO-CODE/WMO4561.HTM.

present weather codes 06, 07, 08, 09, 30-35 and 98 describing dust activity are used from human-observer stations for this work. Also, past weather codes (WMO code table 4561), which record significant weather events of the previous hour but do not occur at the time of observation, are used. Only weather code 03 for a sand storm, dust storm, or blowing dust is used in this thesis. Information on accessing this data can be found in Section 6.3 and more on dust codes used in Section 3.2.

The observations are always recorded at the main synoptic hours: 0000, 0600, 1200 and 1800 Coordinated Universal Time (UTC), as regulated by the WMO. However, observations may also be recorded at 0300, 0900, 1500 and 2100. At some stations, only daytime observations are available. For the Atacama (18° S–30° S and 68.9° W–71.2° W), nine SYNOP stations are available with different operational periods (Figure 2.9). Only three stations are inland, and only four have daytime and nocturnal observations (Figure 2.10).

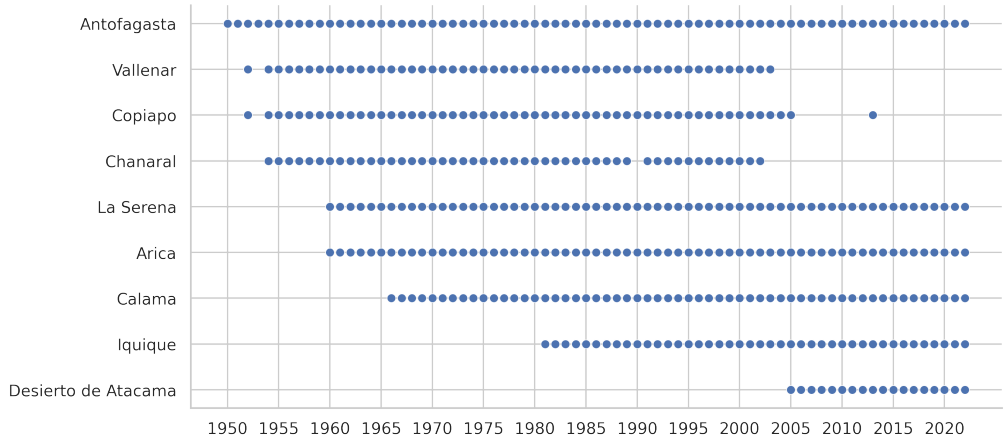

FIGURE 2.9: Operational periods of the nine stations in the Atacama Desert.

As noticed, the SYNOP station network is very sparse and restricted to the coastal areas of the Atacama and not the uninhabited central regions of the desert. This means that the dust events do not entirely represent the 'true' dust activity of the Atacama Desert. Regardless, this dataset is of immense value for understanding dust activity as it is a long-term dataset with direct observations of dust events. There are very few gaps in the observations, and the observation periods during the day remain consistent over the decades. However, there may be inconsistencies due to human error in categorising the present weather codes. As such, the station observers are trained personnel, and it is highly improbable that an entirely different code is used (or not used). Regardless, this error, even if it exists, cannot be quantified without additional data that can be used for verification. An accuracy check could have been performed with satellite data for dust storms, but this was not completed in the interest of time.

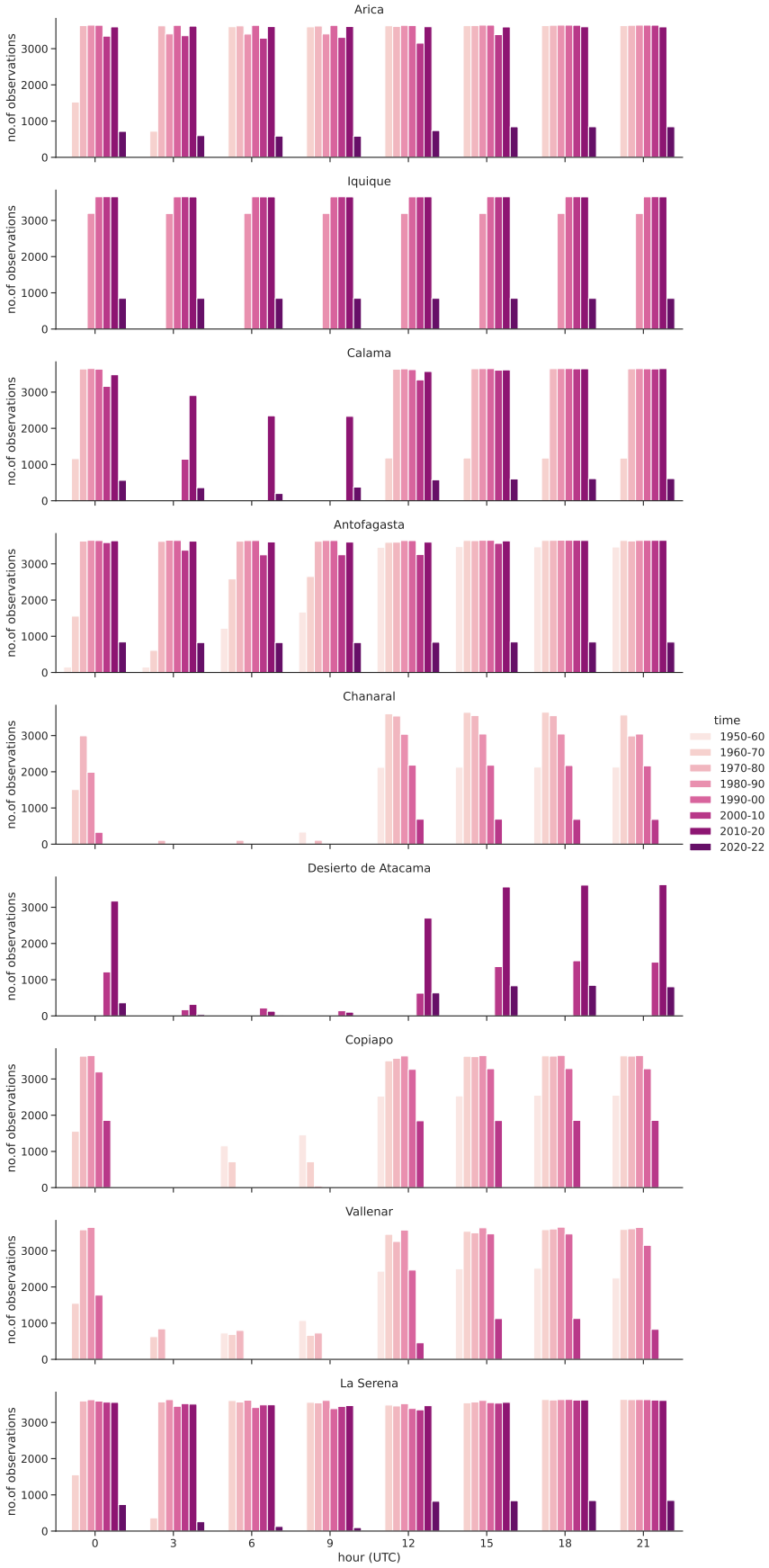

FIGURE 2.10: Temporal resolution of SYNOP records across the stations and decades.

Part II

THRESHOLDS FOR DUST EMISSION

3

Why is the dust activity in the Atacama Desert low despite its aridity?

"The desert could not be claimed or owned–it was a piece of cloth carried by winds, never held down by stones, and given a hundred shifting names..."

—Michael Ondaatje, The English Patient

3.1 MOTIVATION

There are very few studies that examine dust activity in the Atacama Desert (see Section 2.3.1 on page 21), but there has been no systematic observation-based analysis of dust activity in the Atacama extending several decades into the past. This chapter uses long-term observations from ground-based weather stations across the Atacama Desert, reporting the prevalent atmospheric phenomena at 3–6-hour intervals. Despite the lack of strong network coverage across the Atacama, these station data can give us insight into the climatology, seasonality and diurnality of dust emission in the region and also an estimate of the wind speeds required for dust emission.

In this study, the first detailed assessment of the frequency of dust events in the Atacama Desert is compiled based on station observations over the past 72 years. The focus is on (1) the threshold wind speeds for dust emission in the Atacama to assess the influence of spatial differences in soil properties on dust activity and (2) the long-term trends in dust activity. This chapter is structured as follows: Section 3.2 introduces the dataset and methods used in this study, followed by the results for the mean dust activity and the threshold wind speeds in Section 3.3. In Section 3.4 and Section 3.5, the main findings are discussed and summarised.

3.2 DATA AND METHODOLOGY

3.2.1 *Surface Synoptic Observations*

The data comprises of surface synoptic observations (SYNOP) spanning 72 years (1950–2021) from the Dirección Meteorológica de Chile (Dirección Meteorológica de Chile- Servicios Climáticos 2019). Station observations have been used in the past to study dust activity in other deserts (Ackerman & Cox 1989; Dagsson-Waldhauserova et al. 2014; McTainsh & Pitblado 1987; Kurosaki & Mikami 2007; Cowie et al. 2014; Shao et al. 2013; O'Loingsigh et al. 2010; Klose et al. 2010). The dataset for the Atacama Desert covers latitudes from 18° S to 30° S and longitudes 68.9° W to 71.2° W, with nine stations (Figure 3.1). Surface observations are sparse in uninhabited parts of desert regions, limiting the spatial coverage of the data, and the Atacama is no exception. Stations are mostly along the coast with three inland stations, Calama, Copiapó and Vallenar. The SYNOP observations were recorded at manned weather stations. The stations in Calama, Chañaral, Desierto de Atacama (also

called Caldera), Copiapó and Vallenar provide daytime observations, and the other stations have additional nocturnal observations. Each station has a different operational period and is listed in Figure 3.1. The manned weather station in Chañaral, for instance, closed in 2002 followed by Vallenar in 2003 and Copiapó in 2005.

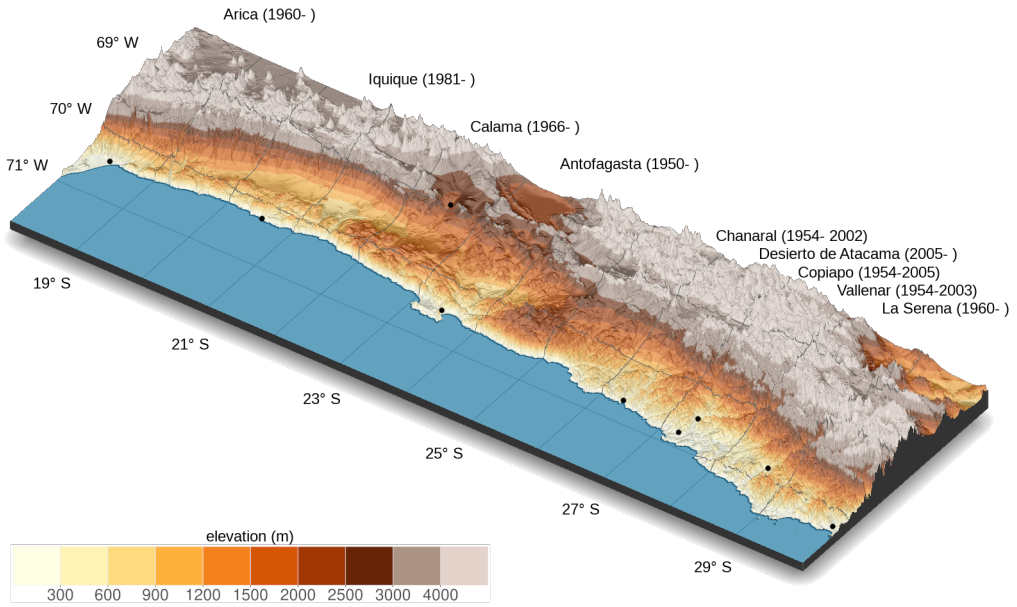

FIGURE 3.1: Topography of the Atacama Desert along with the location of the weather stations and their period of operation.

Observations of 10 min mean wind speed and direction at 10 m above ground level (agl), horizontal visibility and, present and past weather codes were used. The observations are at a 3-hourly resolution for stations that provide daytime and nighttime observations (Figure 2.10). Six-hourly accumulated precipitation was also included in the dataset. The World Meteorological Organisation (WMO) weather codes qualitatively describe weather phenomena as seen by the observer at the station. Present weather codes (ww): 06–09, 30–35, and 98 describe different types of dust events (World Meteorological Organization 1995). Past weather codes (past_ww) record significant weather events of the previous hour, e.g., weather code 03 for a sand storm, dust storm, or blowing dust. Following Shao et al. (2013) and Cowie et al. (2014), different dust codes were grouped for the analysis of dust events, where a dust event corresponds to any of the weather codes listed in Table 3.1. A dust day is a day with at least one recorded dust event. Codes with low values are superseded by those with high values when two or more significant weather phenomena occur (O'Loingsigh et al. 2010). This implies that if fog, rain, or thunderstorms, which have a higher code, occur in the same period as a dust event, a weather code for dust is not recorded. The number of dust events in this study is, therefore, a conservative estimate.

3.2.2 *Determining the Dust Emission Threshold*

There is little information on the soil conditions in the Atacama that would allow us to infer observation-based estimates of dust emission fluxes. To overcome this limitation, the threshold wind speeds for dust activity are computed to indicate the influence of different soils across the desert. The threshold wind speeds are statistically computed using the SYNOP data following studies for other deserts (Kurosaki & Mikami 2007; Cowie et al. 2014; Morales 1979; Helgren & Prospero 1987). The frequency of a dust event at a given wind speed is computed as:

TABLE 3.1: SYNOP weather codes used for the definition of dust events in this study

dust type	code	description
transported dust	06	widespread dust in suspension, not raised at or near the station at the time of observation
suspended dust	07	dust or sand raised by wind at the time of observation, but no sand or dust storm
dust devil	08	well-developed dust devils, but no sand or dust storm at or near the station during the preceding hour or at the time of observation
dust storm	09, 30-32	slight or moderate dust storm or sandstorm at the time of observation, at the station or has begun/changed during the preceding hour
severe dust storm	33-35	severe dust storm or sandstorm at the time of observation, at the station or has begun/changed during the preceding hour
other dust events	98, 03[a]	thunderstorm combined with a sand or dust storm at the time of observation; From past weather: sand storm, dust storm, or blowing snow

[a] Past weather code = 03 with air temperature lower than 3°C was removed to exclude blowing snow events.

$$f = N_{dust}/N_{obs} \cdot 100$$

where f is the occurrence of dust events in %, N_{dust} is the count of dust events, and N_{obs} is the total number of observations all within a bin size of $1 \dot{m} s^{-1}$. Figure 3.2 illustrates the calculation of the threshold wind speeds in Chañaral in 1997. The first dust events are seen around $5\,ms^{-1}$, and the number of dust events increases gradually up to $10\,ms^{-1}$, after which almost all wind observations temporally coincide with dust event reports. The thresholds are then calculated by linearly interpolating the wind speeds at the recorded dust event occurrence frequency, f. The wind speed thresholds t_5, t_{25}, and t_{50} mark the wind speed at the occurrence of 5%, 25%, and 50% of all dust events at the station. In other words, the three thresholds quantify at which wind speed how many dust events have been observed, e.g. 5% of all or 50% of all dust events. These thresholds are indicators of the winds required for dust emission and transport.

The threshold wind speed can differ spatially and temporally due to soil properties (Helgren & Prospero 1987). Spatial differences in wind thresholds for dust events are linked to the land surface conditions such as soil moisture, soil composition, natural surface cover and land use. Snow cover and vegetation also impact seasonal and multi-year differences. Dust transported to the weather station is included in the analysis (dust code: 06) to retain a sufficient number of observations and to account for the fact that many of the stations are located close to the margin of the desert. The results are not sensitive to removing transported events from the analysis. The only notable exception is the wind speed threshold for 50% of dust event occurrence in Antofagasta that increased from 13 to $16\,ms^{-1}$ when dust transport was removed, suggesting that dust sources affecting the station are located mostly upwind from the coastal city.

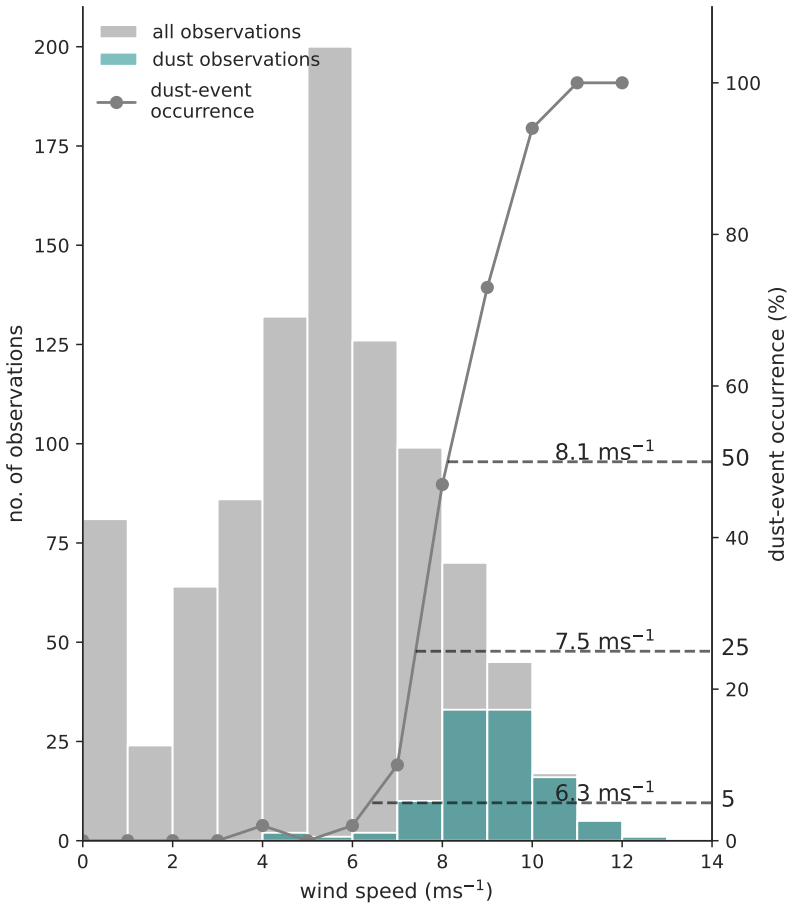

FIGURE 3.2: Frequency distribution of 3-hourly surface wind speeds in Chañaral in 1997. Grey bars indicate the frequency distribution of wind speed for all observations, while green bars indicate the frequency distribution for dust observations. Each point on the grey line marks the dust event at that bin. Horizontal dashed lines mark the threshold wind speeds for different percentages of dust event occurrence.

3.3 RESULTS

3.3.1 *Mean Dust Activity*

1920 dust days with high inter-annual variation were recorded in the Atacama Desert for the past 72 years (Figure 3.3). Of all the dust days, 72 days had a visibility of less than a kilometre and 12 of these were on days with a reported dust storm (codes: 09, 30-35). Dust storms do occur in the Atacama but are less frequent and weaker when compared to the visibility and mean statistics of other deserts (Engelstaedter et al. 2003). In total, 130 dust storms were recorded in 72 years, i.e., on average less than two dust storms occur per year across the entire desert. The number of dust days across the Atacama differs from region to region, with station differences varying by an order of magnitude. Chañaral recorded by far the most dust days, with a mean of 19.6 dust days per year. Calama had 4.5 days/year, Vallenar 3.7 days/year, Antofagasta 2.7 days/year, Desierto de Atacama and Copiapó each 1.8 days/year, and Arica, Iquique and La Serena each 1.4 days/year. Suspended dust dominated throughout the observation period, and almost 78% of these events were recorded in Chañaral.

There is no long-term trend in dust activity. In total, three periods of increased dust activity are observed compared to the present day, with at least 25 dust days per year, which are: 1966–1978, 1984–1988 and 1992–2002. Most dust days per year were observed in the 1990s, with up to 100 dust days in 1993 (Figure 3.3a). Few stations (four) and coarse temporal sampling (6-hourly), for instance, may have contributed to fewer reports of dust in the 1950s as compared to the 1960s and onward. Post 2002, three stations ceased operations, which may have contributed to few reports of dust activity, although we see a period of

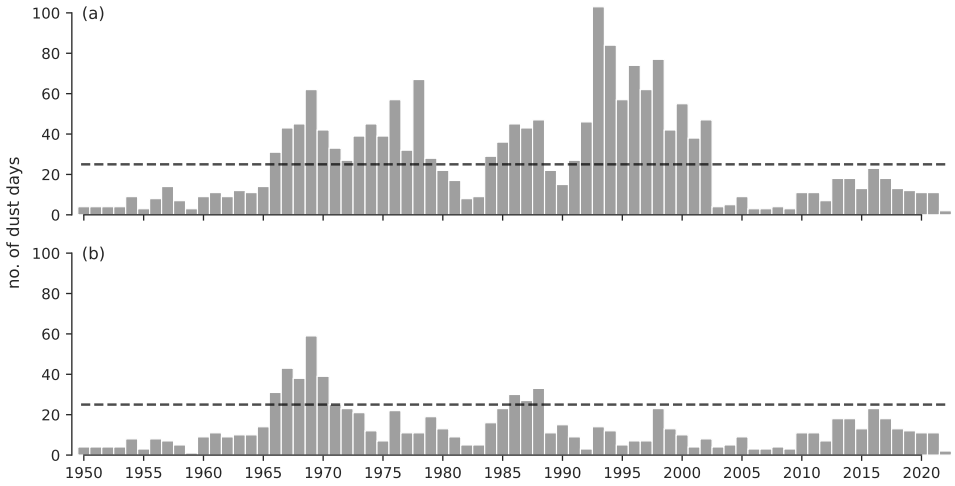

FIGURE 3.3: Annual count of dust days in the Atacama from 1950 to 2021 for (a) 9 stations (b) 8 stations without Chañaral. Three periods of enhanced dust activity are visible in (a): 1966–1978, 1984–1988 and 1992–2002 with at least 25 days of dust activity a year (dashed line).

moderate dust activity from 2010 with 10–20 dust days per year. Moreover, dust activity observed through the decades is dominated only by some stations. Almost all recorded dust between 1991–2002 is in Chañaral (Figure 3.3b). These periods of increased activity can be caused by changing meteorological processes leading to more frequent above-threshold winds for dust emission or changes in the threshold for dust emission, e.g., due to changes in precipitation or land use, or can be a combination of both.

3.3.2 *Threshold Wind Speed for Dust Emission*

To better understand the regional differences in dust activity, the threshold wind speeds for dust events were evaluated. Averaged across all stations, the threshold wind speed for 5% (t_5), 25% (t_{25}) and 50% (t_{50}) of dust event occurrence are $10.9 \pm 1.6\,ms^{-1}$, $13.2 \pm 1.9\,ms^{-1}$ and $15.6 \pm 2.3\,ms^{-1}$ respectively. In analysing these thresholds at each station, it is found that $t_5 > 9\,ms^{-1}$ at all stations except in Chañaral (t_5=$7.3\,ms^{-1}$, Figure 3.4). This could imply that the soil conditions and surroundings of Chañaral are more conducive for dust emission than other stations in the dataset. Threshold values for t_{50} cannot be computed in Calama and La Serena due to less than 50% reported dust events with simultaneously strong winds. Moreover, the t_{25} value in La Serena is $13.7\,ms^{-1}$ and even higher in Calama with $16\,ms^{-1}$, and wind speed observations above these thresholds are too few for robust calculations. Nonetheless, to investigate why despite strong winds, dust events were not recorded, changes in the direction of dust-emitting winds (local topography potentially inhibiting emission and observation) and strong winds driven by deep moist convection via the precipitation codes (as increased soil moisture would increase the threshold for emission) were investigated. No changes in the wind direction (Figure 3.5) were found, but there were two records of precipitation (out of 18 observations) in La Serena.

The largest t_5 values are seen in Calama ($13\,ms^{-1}$) and one of the driest northern stations, Arica ($12\,ms^{-1}$). This is surprising as one would expect that given the minimal precipitation rates and the lack of vegetation, the soil particles are not held together by moisture, and the land surface is bare and exposed, thus making it more prone to wind erosion. However, the high thresholds indicate that the surface offers resistance to the winds. Such surfaces could be desert pavements, or salt or gypsum-crusted playas, for instance (Finstad et al. 2014).

Interestingly, t_5=$9.5\,ms^{-1}$ in Desierto de Atacama is in contrast to t_5=$12.5\,ms^{-1}$ in Copiapó although both stations are only 50 km away from each other (Figure 3.1). The mean annual precipitation is 12.5 mm in Copiapó and 15 mm in Desierto de Atacama, and the mean daytime

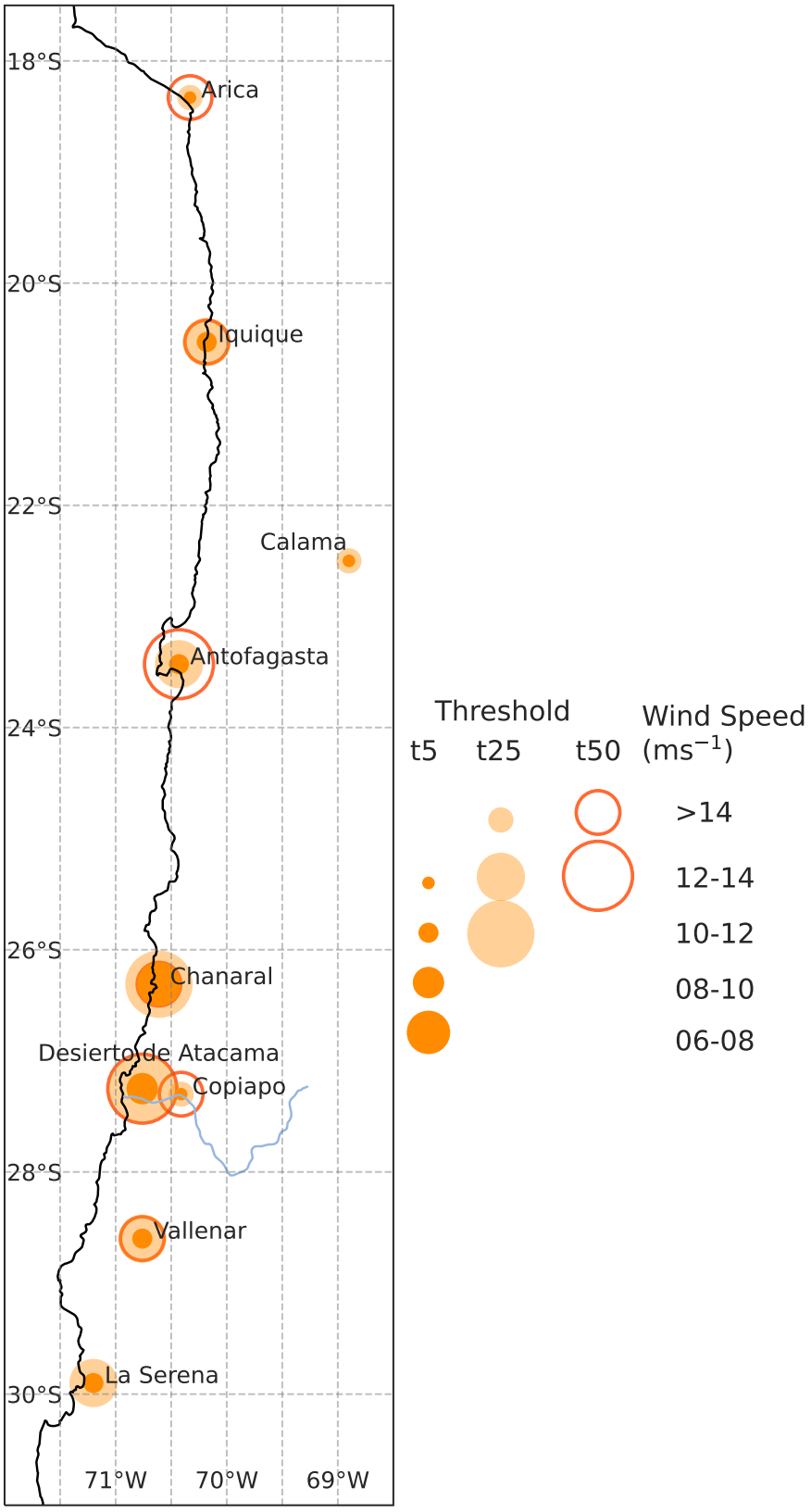

FIGURE 3.4: Mean threshold wind speeds for 1950–2021. The size of each circle corresponds to a range of threshold wind speeds. The solid orange circle represents t_5, light orange t_{25} and an unfilled orange circle represents t_{50}. Large circles indicate low threshold wind speeds hence more potential for dust emission. Note that not all stations have all three thresholds.

(15 UTC) wind speed in Copiapó is 6 ms^{-1} and in Desierto de Atacama is 5 ms^{-1}. The different t_5 at these two stations could be due to the combined result of different measurement periods (Copiapó: 1954–2005; Desierto de Atacama: 2005–) and different land surfaces. Desierto de Atacama is situated 16 km inland from the Pacific Ocean with playas along the coastline, while Copiapó is on the Copiapó river surrounded by coastal cliffs and vegetation. The direction of dust-emitting winds is also very different at the two stations, with westerly winds triggering dust activity in Copiapó and northerly and northwesterly winds in Desierto de Atacama (Figure 3.5). Local effects of different land surfaces and wind channelling, thus influence the different thresholds for these stations.

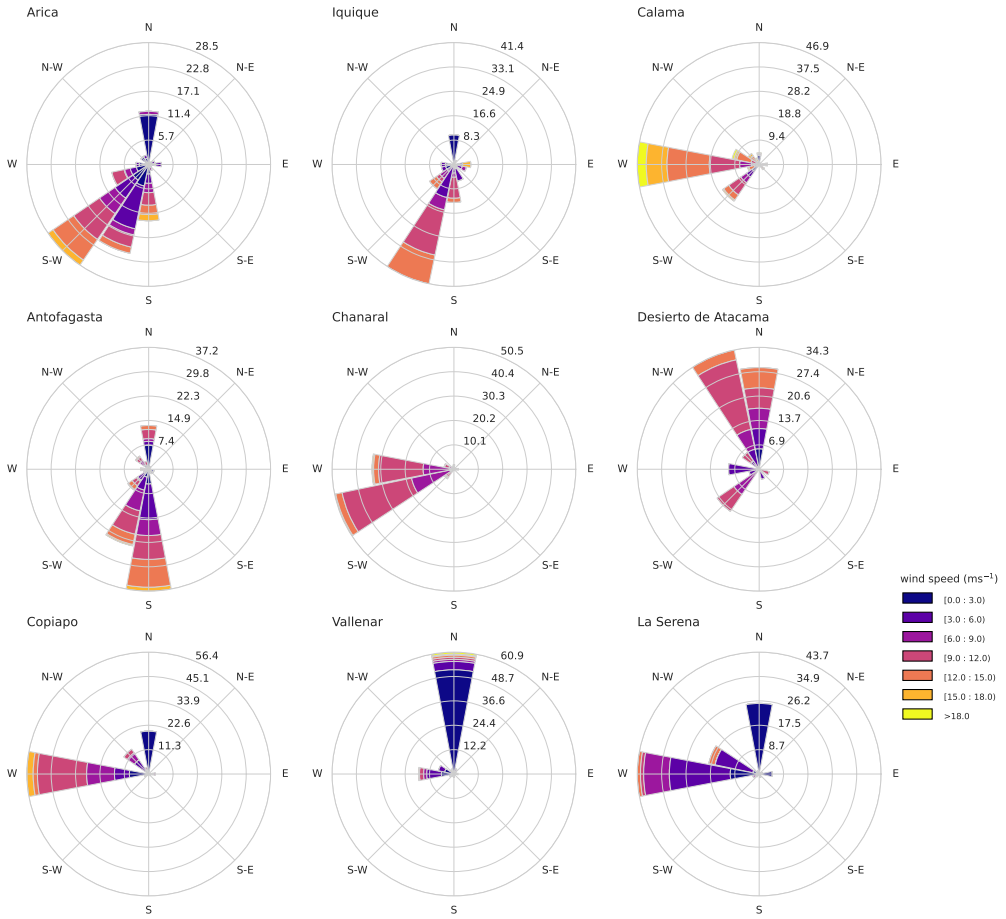

FIGURE 3.5: Wind roses at each station during dust events. Shown is the frequency of 3-hourly mean winds per direction.

3.3.3 *Variability in Dust Activity*

The range of thresholds indicates how susceptible a soil surface is to wind erosion. Small differences between the threshold t_{50} and t_5 can be an indicator for small changes in the surface conditions (Kurosaki & Mikami 2007). The difference between t_{50} and t_5 was smallest for Desierto de Atacama (2 ms^{-1}), Antofagasta (2.3 ms^{-1}) and Copiapó (3 ms^{-1}), and largest in Chañaral (11.7 ms^{-1}). This suggests that the surface conditions at and upwind of the stations with small differences changed little throughout time, but in Chañaral, the soil surface might have undergone changes that influenced the frequency of dust events. Such changes could be due to annual rainfall anomalies or anthropogenic changes in land use.

In the south of the Atacama (stations south of 26°S), increased precipitation coincides with a low number of dust days, with exceptions, as increased soil moisture results in soil aggregation. In the north of the Atacama (stations north of 26°S), however, despite decreased

precipitation large number of dust days are not observed. On further investigating the role of precipitation in enhancing and attenuating the dust activity in the Atacama, it was found that most dust days are associated with close to zero precipitation, with some exceptions. In Vallenar, in the 1980s, increased precipitation is accompanied by increased dust activity. While rainfall is not uncommon in Vallenar, in 1984 and 1987, it recorded over 100 mm. Between 1966–1978, most dust events were recorded in either Calama or Chañaral. For the first half of the period, Calama recorded the highest dust count, during which it also received less than 10 mm of rainfall. And for the second half, Chañaral recorded an increase in dust activity (40 dust days per year) while receiving less than 10 mm of precipitation. Similarly, during 1993–1996 most of the dust activity (60–90 days per year) was observed at Chañaral with no recorded rainfall. But a year later (1997), along with high precipitation amounts (> 100 mm), over 50 dust days were recorded at Chañaral (Figure 3.6). This is because, while soil moisture decreases the dust emission potential, above-average precipitation that leads to river runoffs and flash floods can increase the supply of erodible material (Haug et al. 2010; Walk et al. 2020; Houston 2006b; Sepúlveda et al. 2006). The surface runoffs loosen and displace fine soil particles. After the water has evaporated, the now deposited fine particles at the surface can be eroded by sufficiently strong winds.

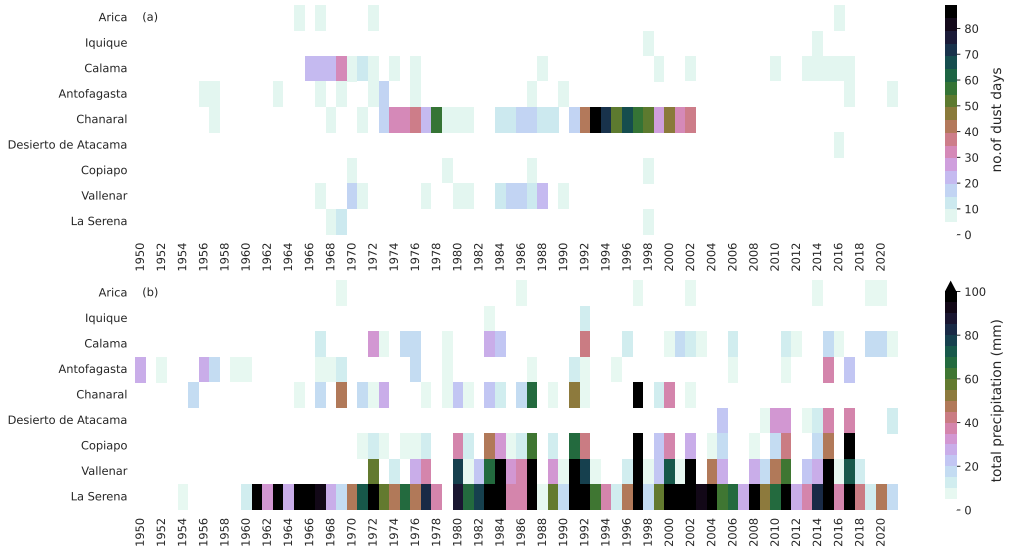

FIGURE 3.6: Distribution of (a) number of dust days across the years and (b) the total precipitation (mm) received at each station. Note that precipitation was still recorded at stations that ceased operation except in Chañaral.

The above-threshold wind speeds (here, defined by the average t_5) over all stations (Figure 3.7 and Figure 3.8) were also analysed. Between 1970–1974 and 1986–1991, more above-threshold winds occurred than in other periods when all stations were in operation. In Chañaral, the average number of observations with wind speed above the threshold has remained nearly constant since the 1960s, with only 1971 being an outlier. Still, the number of dust reports does not coincide with the frequency of above-threshold winds. This is also true for all other stations, where a correlation between the winds and dust days is absent. However, this is expected as dust emission is not a function of wind speed alone but also of soil conditions which affects the dust emission potential of the region.

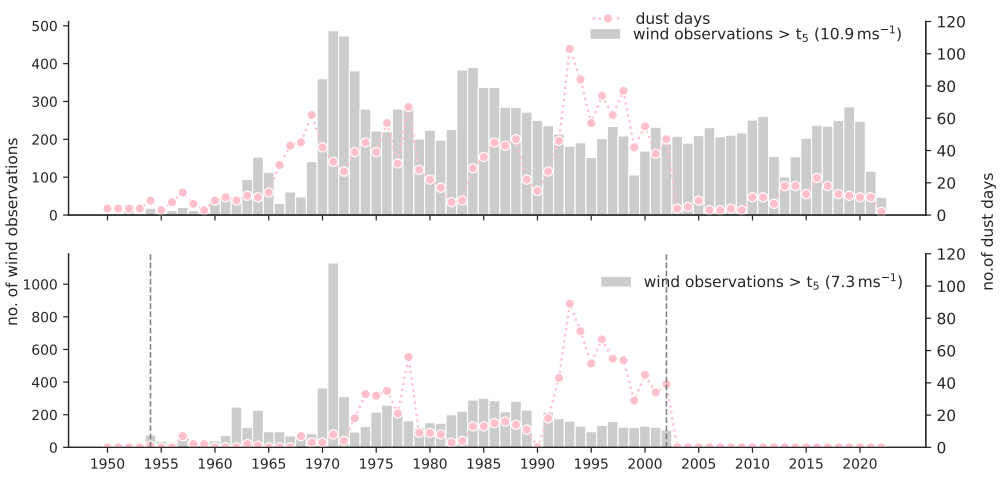

FIGURE 3.7: Total annual count of dust days (pink line) in the Atacama from 1950 to 2021 for (a) all 9 stations and (b) only Chañaral with the number of 3-hourly wind observations above their regional average t_5 threshold (grey bars). The vertical dashed lines indicate the beginning and the end of observation at that station. Note the different limits on the y-axis of both plots.

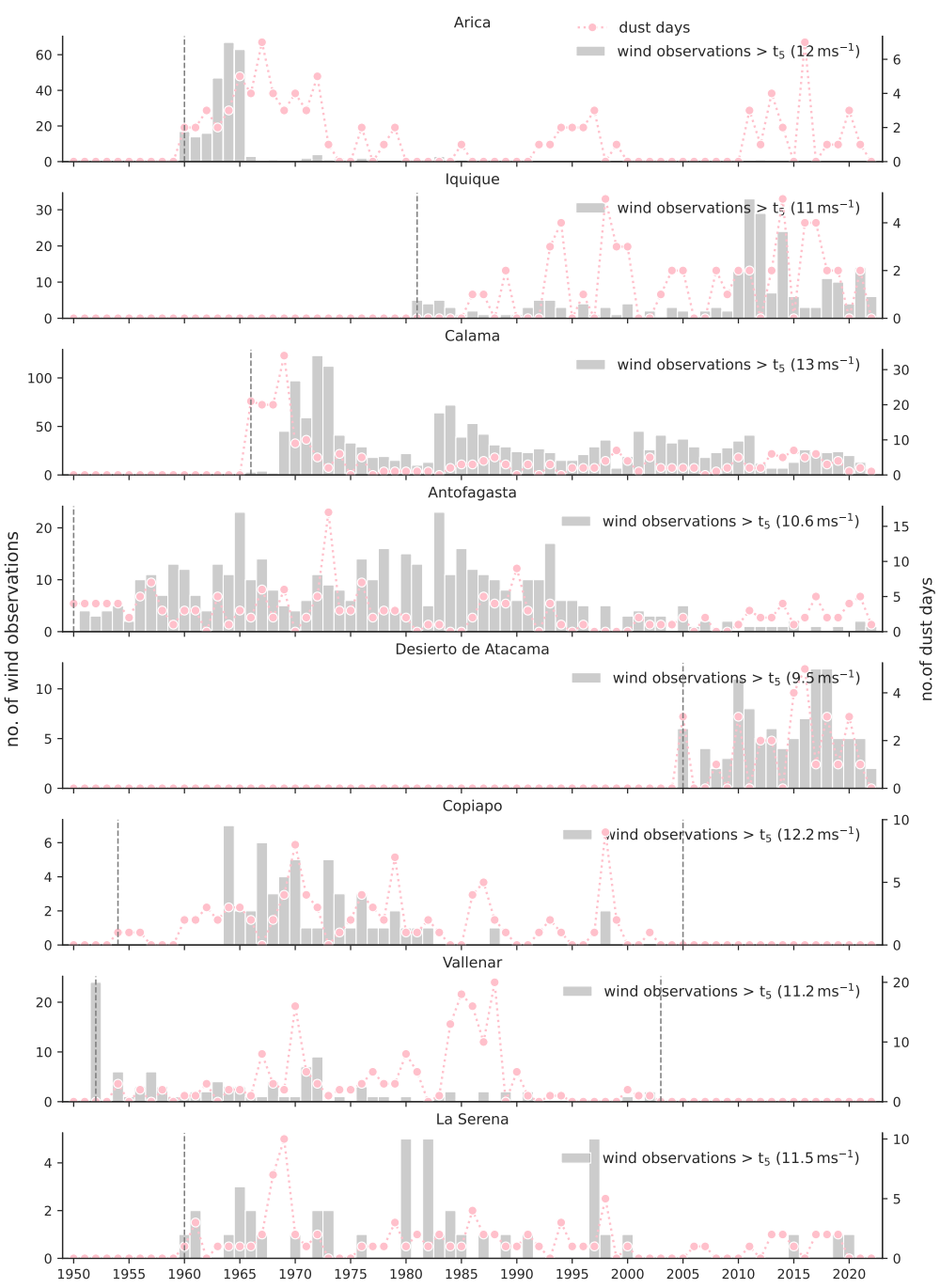

FIGURE 3.8: Total annual number of dust days (pink line) and the number of 3-hourly wind observations above their respective annual mean t_5 thresholds (grey bars) for each station except Chañaral. The vertical dashed lines indicate the beginning and the end of observation at that station. Note the different limits on both y axes.

3.4 DISCUSSION

The dust activity in Chañaral dominates the overall activity recorded in the Atacama. From 1991–2002, almost all recorded dust is in Chañaral, but above-threshold winds cannot explain the enhanced dust activity. No correlation was also found at other stations. Precipitation anomalies are present in some years and might explain the observed dust activity during some periods, such as 1966–1978, when Calama and Chañaral recorded increased dust activity while no precipitation was recorded. However, no overall connection between increased or decreased precipitation anomalies and the annual count of dust days is apparent. Detailed analysis of diurnal and seasonal dust activity is required to understand the drivers of dust activity. It is plausible that the relatively high dust activity in Chañaral is favoured by the estimated 200–300 Mt mine tailings deposited at the Chañaral Bay between 1930–1990 (Ramirez et al. 2005; Dold 2006; Castilla 1983; Martínez et al. 2016; Lee & Correa 2005; Neary & Garcia-Chevesich 2008; Wisskirchen & Dold 2006). The tailings covering an area of about 4 km^2 have resulted in a 1 km displacement of the shoreline towards the Pacific Ocean and an accumulation of a 10-15 m thick layer of contaminants along the shore (Dold 2006). Therefore, the signal from anthropogenic activity is possibly embedded in the dust record. The absence of strong dust activity in the decades before the 1990s, given that the station began recording in 1954, might have to do with the degree of accumulation and drying of the waste material before it can be deflated.

The estimate of dust storms in this dataset (130 in 72 years) is five times less than the estimate by Engelstaedter et al. (2003) of 10–50 days per year for the Atacama. Using a climatological average of observations from the International Station Meteorological Climate Summary (ISMCS) version 4.0 for 1970–1990, the authors computed the annual average dust storm frequency as a fraction of days with visibility less than 1 km. They found a dust storm frequency of greater than 50 days per year in northern Africa, the Middle East, and the Iberian Peninsula, 2–50 days per year in Australia, eastern China, southern South America, and the southwestern USA and, 10–50 days per year for the Atacama region. But this large difference in the estimate of dust storm frequency between this dataset and Engelstaedter et al. (2003), as discussed in Mahowald et al. (2007), is because Engelstaedter et al. (2003) do not use the visibility to constrain dust storm frequency but rather use the number of days with blowing dust or sand (ww=06,07) per year. The estimate of blowing dust per year by the authors is within the estimates for the average number of dust days per year.

The threshold velocities for Antofagasta (t_5=10.6 ms^{-1}) are similar to estimates from station observations. Flores-Aqueveque et al. (2012) analysed hourly winds from two automated weather stations in Antofagasta over 14 years to derive friction velocities and horizontal saltation fluxes. Their results showed two saltation modes: a 'low saltation mode' with the saltation threshold centred around 0.35 ms^{-1} and 0.38 ms^{-1} and, a 'high saltation mode' centred around 0.49 ms^{-1} and 0.52 ms^{-1} on the surface. They associated the low mode erosion events to wind speeds of 6–8 ms^{-1} and the high mode erosion events to wind speeds of 12 ms^{-1} at 10 m above the ground. In another study, Flores-Aqueveque et al. (2010) characterised the wind erosion process at the Mejillones Peninsula (23°S) just north of Antofagasta. Using the dust emission scheme proposed by Marticorena and Bergametti (1995), along with particle size distribution and mineral composition from field measurements and sediment traps, they computed the average threshold wind speed of 0.31 ms^{-1} at the surface or 7.95 ms^{-1} at 10 m height for surface roughness length of 0.35 mm. They compared this model output with measurements from station data. They found that a small fraction exceeded the threshold during the measurement period (October-November 2006) and always during the afternoon at the peak of the south and southwest winds.

The station-based estimates for threshold velocities are larger compared to results from combining satellite and reanalysis data. Using the global velocity threshold data for dust emission (Pu & Ginoux 2019; Pu et al. 2020), annual threshold wind speeds of $6.5 \pm 1.0\,ms^{-1}$ and $8.2 \pm 1.2\,ms^{-1}$ for the Atacama for dust optical depth (DOD) 0.02 and 0.05 respectively were obtained. These thresholds are lower than the mean threshold value (t_5=$10.9 \pm 1.6\,ms^{-1}$) averaged across all stations from this analysis. This difference in thresholds could result from the different measurement periods (2003–2015), with more dust activity expected in recent times due to land use change and water sequestration (Babidge 2019). Moreover, the cumulative DOD frequency used could overestimate dust emission in regions with significant transported dust events and hence possibly lead to underestimated thresholds (Pu et al. 2020). The NCEP1 reanalysis dataset in which surface winds are computed at one grid point and not from observations from land stations could also explain the difference due to the coarse spatial grid for simulating winds, especially over areas with a complex orography where local influences are strong (Ramon et al. 2019). On the flip side, results can differ due to different temporal resolutions and the location of the stations. Specifically, most of the nine stations are confined to settlements along the coast.

The annual mean threshold wind speeds t_5, t_{25}, t_{50} for 5%, 25% and 50% dust event occurrence were $10.9 \pm 1.6\,ms^{-1}$, $13.2 \pm 1.9\,ms^{-1}$ and $15.6 \pm 2.3\,ms^{-1}$ respectively. These threshold wind speeds are higher than the values from the same method reported by Kurosaki and Mikami (2007) for the Taklamakan Desert ($t_5 = 4 \pm 0.6\,ms^{-1}$, $t_{50} = 6.7 \pm 1.5\,ms^{-1}$), for the Gobi Desert ($t_5 = 8.9 \pm 2.2\,ms^{-1}$, $t_{50} = 13.8 \pm 2.0\,ms^{-1}$) and for the Loess Plateau ($t_5 = 6.9 \pm 1.2\,ms^{-1}$, $t_{50} = 9.4 \pm 1.5\,ms^{-1}$). In the Sahel and Saharan regions, stations above 22°N ($t_{50} = 10$–$15\,ms^{-1}$), Egypt and West Sahel ($t_{50} = 7$–$10\,ms^{-1}$) and stations between 16-20°N ($t_{50} = 5$–$6\,ms^{-1}$) thresholds were reported by Cowie et al. (2014).

3.5 CONCLUSIONS

This study presents an assessment of the observed dust reports and threshold wind speeds for dust activity from station observations for the Atacama dating back to 1950. Arid and semi-arid regions are sources of mineral-dust aerosols (Kohfeld & Tegen 2007), but very little is known about the dust activity in the hyper-arid Atacama Desert. The limited moisture supply and barren landscape should promote dust emission through wind erosion, but the Atacama rarely sees strong dust outbreaks. Therefore, this study set out to build a climatology of dust activity and estimate the required threshold wind speeds in the Atacama Desert. The Atacama saw 1920 days of dust events in the past 72 years, with less than 10% of them reported as dust storms. There is no long-term trend in dust activity but a high inter-annual variability with three periods of increased dust activity: 1966–1978, 1984–1988, and 1992–2002. The 1990s was the dustiest decade, with most of this activity recorded at Chañaral with a signal from the anthropogenic activity possibly linked with the natural dust activity.

The annual mean threshold wind speeds t_5, t_{25}, t_{50} for 5, 25 and 50% dust event occurrence were $10.9 \pm 1.6\,ms^{-1}$, $13.2 \pm 1.9\,ms^{-1}$ and $15.6 \pm 2.3\,ms^{-1}$ respectively, are higher than the mean wind speeds at the stations and higher than the thresholds found in the Sahara, Sahel (Cowie et al. 2014), Gobi and the Taklamakan deserts (Kurosaki & Mikami 2007). Therefore, despite the aridity of the Atacama Desert, wind speeds are often insufficient to activate dust sources due to the sub-optimal soil conditions for wind erosion. Measurements of the soil conditions, such as the roughness length, particle distribution and soil moisture, would allow for a more complete picture of dust activity in the Atacama.

4

The soil surface of the Atacama Desert: A control for dust emission

"I know
you won't
believe me,
but
it sings,
salt sings, the skin
of the salt mines
sings
with a mouth smothered
by the earth.
I shivered in those
solitudes
when I heard
the voice
of
the salt
in the desert.
Near Antofagasta
the nitrous
pampa
resounds:
a
broken
voice,
a mournful
song."

—Pablo Neruda, Ode To Salt

4.1 MOTIVATION

In the previous chapter, the threshold wind speeds required for dust events across nine stations in the Atacama were characterised. It was found that the thresholds in the Atacama are much higher than the previously determined values for North African (Cowie et al. 2014) and East Asian Deserts (Kurosaki & Mikami 2007). This is unexpected, given the exceptional aridity in the region. It is hypothesised that this high threshold value is due to the soil properties, namely the surface crust that acts as a control mechanism for dust emission. Using the Portable in situ Wind Erosion Lab (PI-SWERL) (Etyemezian et al. 2007), this hypothesis that deflatable material that otherwise can be entrained is fixated in the soil by thin friable crusts in the desert is tested.

This desert surface is also subject to extensive land degradation via mining activities. The Atacama Desert is a vital economic zone with centuries of mining history (Méndez 2021; Salazar et al. 2011; Graffam et al. 1996). It is a hotbed of mineral extraction, especially for metals such as copper and lithium. Mining activities not only contribute to dramatic land and water degradation but also to anthropogenic dust-aerosols in the atmosphere (Jung et al. 2020a; Li et al. 2019; Zanetta-Colombo et al. 2022; Carkovic et al. 2016). The Geological Survey of Chile estimates that 696 mine tailings (waste deposits from mineral extraction) exist in the Antofagasta region alone, with 1,400,000 tons of mine tailings produced daily in Chile (Araya et al. 2020). To assess the different dust emission potential from these regions of extensive anthropogenic activity, the top crust was mechanically removed to disturb the soil surface and to estimate the threshold for dust emission from these disturbed surfaces.

With this study, the aim is to analyse the dependence of dust emission threshold given the specific soil surface conditions in the Atacama and to compare the thresholds from the station data (see Chapter 3) with those from remote regions in the Atacama where SYNOP observations do not exist. Such local measurements currently do not exist but are essential to fully understand regional dust activity and effectively constrain complex model simulations. This is the first study to provide in situ measurements of the threshold wind speed required for dust emission in the Atacama. In this chapter, you will find an introduction to the instrument (Section 4.2.2) and the measurement techniques (Section 4.2.3). Section 4.3 presents the results, and in Section 4.4 and Section 4.5, a detailed discussion and summary of the main results can be found.

4.2 METHODOLOGY

4.2.1 *Test Sites*

The fieldwork was carried out with a team of geologists and microbiologists between 24.09.2022 to 07.10.2022 (Southern Hemisphere spring) in two test sites: Chuculay Fault System (21.03°S 69.78°W) on the east of the Salar Grande, a dry salt lake and Pisagua (19.73°S 70.07°W) which is north of Iquique (Figure 4.1). Ideally, the test sites would have represented the varied soil surfaces present in the Atacama, namely the crusted surfaces, salt and clay pans, Tillandsia dunes and regions close to the SYNOP stations from where thresholds have been computed using station data (see Chapter 3). Nonetheless, the test sites in this study are equally exciting and sufficient to test the hypothesis for surface crusts and measure the threshold wind speeds.

The soils in the Central Depression (between the Coastal Cordillera and the Precordillera) of the Atacama Desert are often found with thin, solid, fragile crusts (ranging from a few to tens of mm in thickness) on the top with a fine sand-rich layer of dust, called *chuca* underneath it (about 10–30 cm in thickness). This layer of *chuca* is formed by powdery to poorly cemented gypsum and anhydrite (gypsum without the water component) and atmospherically deposited dust (Ewing et al. 2006; Michalski et al. 2004; Wang et al. 2014; Li et al. 2019). Below the *chuca* is 0.5–2 m thick layer of firmly cemented gypsum and anhydrite called *costra* (Ericksen 1981). The surface crust, while intact, protects the soil layers underneath it from wind erosion (Gillette et al. 1982; Goossens 2004; Klose et al. 2019).

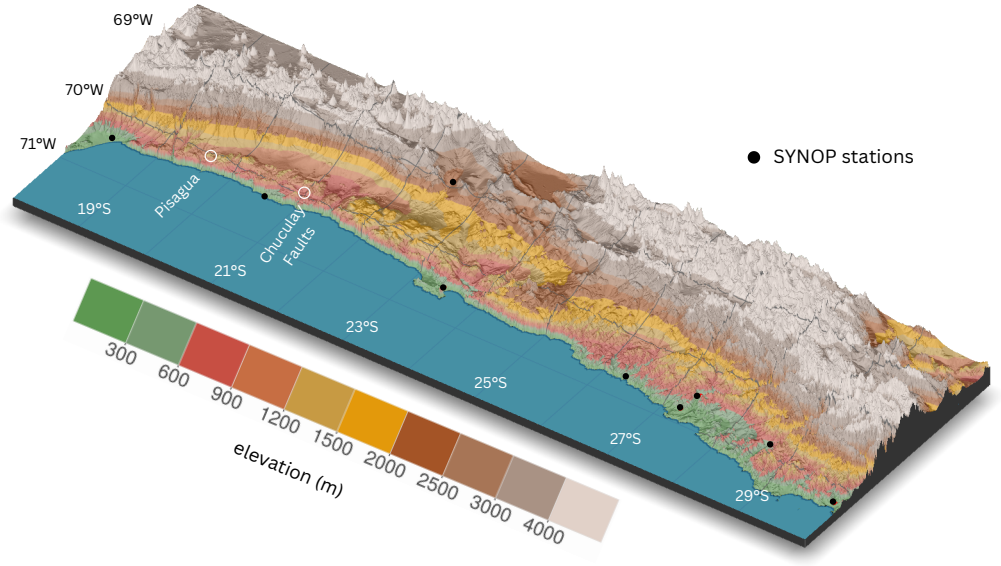

FIGURE 4.1: The two test sites (white circles) where the measurements were taken along with the locations of the SYNOP stations used in Chapter 3

The first test site in the Chuculay Faults is approximately 37 km from the coast and at approximately 1030 m asl (CRC1211-Proposal 2024). It is located in the eastern margin of the Salar Grande with five prominent 20-300 m high escarpments (Figure 4.2) that were formed due to fault displacement (May et al. 2020). The Coastal Cordillera west of the site is about 1165 m asl. The site is dotted with gravel and small boulders. The surface has a thin crust with white specks of gypsum visible on it. The second site of Pisagua is located approximately 14 km from the coast at a height of 1200 m asl. A single mountain ridge of approx. 1230 m asl separates the test site from the coast.

Using the weather station network established by the CRC 1211 (Schween et al. 2020; Hoffmeister 2018), the diurnal and seasonal winds at these sites were analysed. The wind speed and direction are measured at 2.5 m height. The data is available with a 10 min resolution taken as an average of winds recorded every 10 s. Data from three stations is used: station 22 (operational between 2018-10.2023), 13.7 km north and station 40 (since 03.2022, but continuous measurement only from Oct 2023) 19.5 km east of Pisagua and station 42 (since 03.2022, but continuous measurement only from Oct 2023) 14.5 km west of Chuculay. The winds at station 42 are strong with wind speeds above 6 ms^{-1} becoming frequent in the evening (18–22 LT) until night and blowing from the southwest to northwest directions during these hours. This diurnality in wind speeds is also observed in station 40, except that the winds blow from the south to west during the evening and are weaker during the day compared to station 42. Median daytime wind speed at station 40 is 1 ms^{-1}, while at station 42 it is above 2.5 ms^{-1}. Higher median wind speeds between 2–4 ms^{-1} are observed at station 22 during the evenings, but frequent winds above 6 ms^{-1} are observed between 8–14 LT from the southwest, westerly directions than other hours. The highest wind speeds are observed across all stations in summer, while the lowest are in winter. From CRC1211-Proposal (2024), the relative humidity close in the region of Pisagua and Chuculay are similar. May et al. (2020) found that the soils in Chuculay showed no significant changes in soil moisture during fog events, which was opposed to that in Pisagua, where increased soil moisture was observed a few days after several-day long periods with relative humidity >60–70% (CRC1211-Proposal 2024).

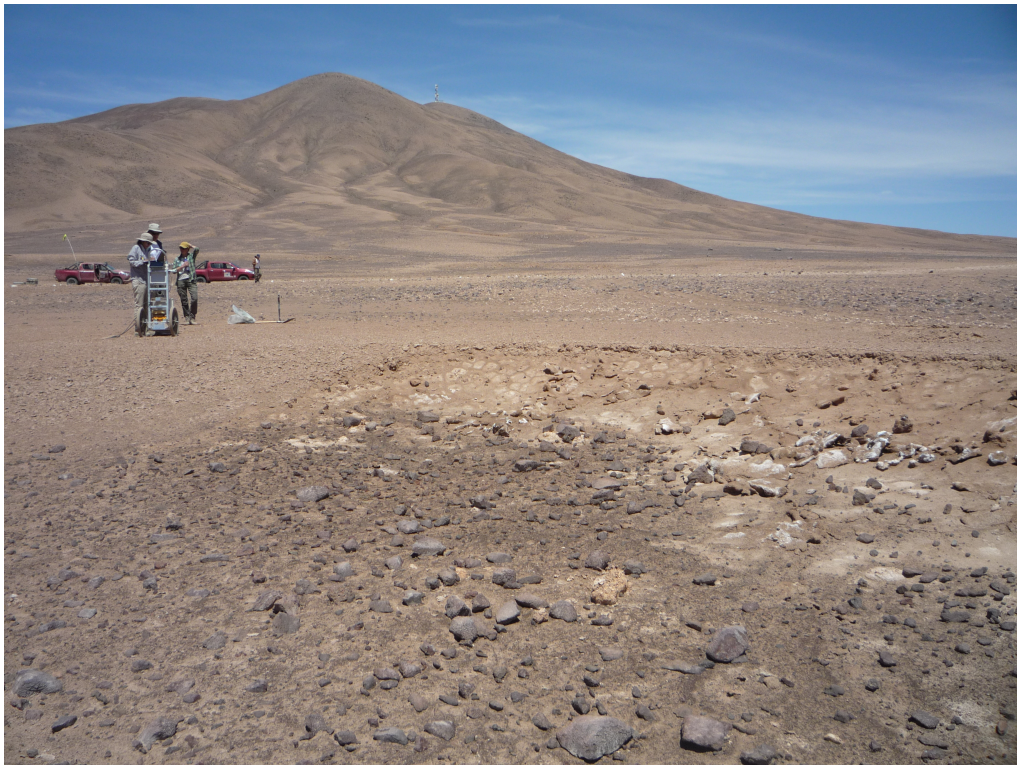

FIGURE 4.2: A series of faults have formed five prominent 20–300 m high north facing scarps.

4.2.2 *The Instrument*

The Portable in situ Wind Erosion Lab (PI-SWERL) (Etyemezian et al. 2007) by the Desert Research Institute (DRI), Nevada, is designed keeping in mind that wind tangential to the surface drives dust emission and transport (Bagnold 1974; Sweeney et al. 2008) and has

FIGURE 4.3: PI-SWERL model MPS-2b – Chamber with mounted DustTrak II monitor and the battery cart.

been successfully used in several studies (Macpherson et al. 2008; Sweeney et al. 2011; Vos et al. 2021; Sweeney & Mason 2013; King et al. 2011; Vos et al. 2021; Dickey et al. 2023). The miniature PI-SWERL model MPS-2b (Figure 4.3) includes a flat annular blade enclosed in a cylindrical chamber (D = 30 cm, H = 20 cm) that rotates for a predefined number of rotations per minute (RPM) that is adjusted to the desired friction wind velocity u_*. A foam seal of approximately 6 cm height separates the chamber from the soil surface of interest. The rotations are computer-controlled by a 24-volt DC motor attached to the chamber's top and monitored by a magnetic sensor every 15 revolutions per minute (RPM). The rotation of the blade generates a velocity gradient between the blade and the surface, producing a shear stress on the surface. This flow inside the PI-SWERL is turbulent and axial symmetric. The shear stress entrains particles at a certain threshold that depends on the surface properties.

A dust monitor measures particles entrained inside the chamber every second (DustTrak TSI Model 8530). This dust monitor can be equipped with the PM10 or PM2.5[7] inlet (two provided by the DRI), but the measurements are not mass-based. The PM (the PM10 inlet was used in this fieldwork) dust concentration is measured by a 90° scattering of 750 nm laser light. Additionally, four optical gate sensors mounted on the sides of the chamber detect sand movement within the chamber by counting the large particles (100μm) that can initiate saltation. Two are located about 1 cm above the annular blade and two more are located 5 cm higher and, measure the movement of large particles every second with an infrared light sensor. Data from the optical gate sensors (OGS) used to measure saltation is not used in the

[7]Particles with an aerodynamic diameter equal to or less than 2.5 μm are known as particulate matter 2.5 or PM2.5 particles smaller than 10 μm are called PM10.

study as preliminary analysis shows that the entrained particles at both sites are less than 100μm in size and cannot be effectively detected by the sensors. More information on the instrument can be found in the User Manual.

4.2.3 *Measurements*

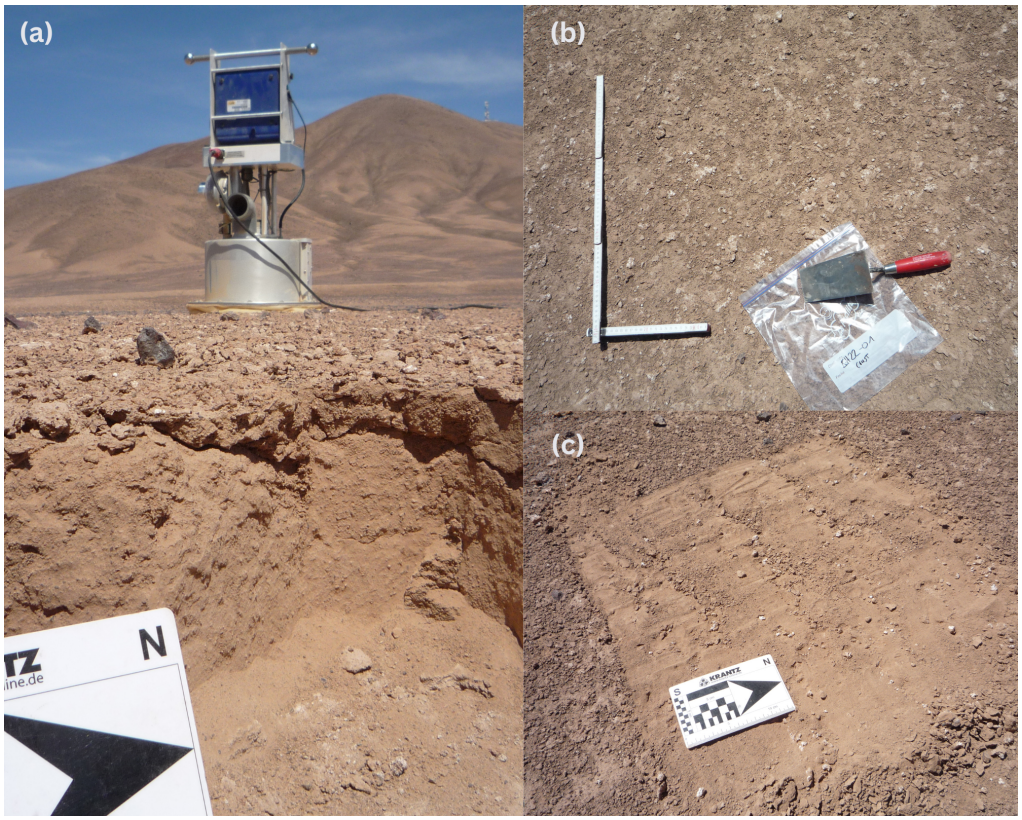

FIGURE 4.4: Measurements at Chuculay: (a) A vertical cross-section of the soil with the PI-SWERL and scarps in the background. A thick crust is visible, with a few large stones on the surface. Underneath the crust, deflatable soil material is present. (b) The surface was prepped before measurements by removing large stones. White flecks of gypsum are also visible in the image. (c) The top surface crust is removed for 'disturbed surface type' measurements. Here, some gypsum nodules can also be seen.

To test the main hypothesis of this study, the measurements were conducted on two surface types: undisturbed soil surface and disturbed surface. The surface was disturbed by removing the crust present on the top, as seen in Figure 4.4 and Figure 4.5. At both these sites, 11 replicate tests with the PI-SWERL were completed, with at least 5 replicate tests for each surface type. As we are primarily interested in the threshold friction velocity, u_*, ramp tests (n=16) were conducted with only very few step tests (n=6).

Ramp and step tests are two of the three distinct programmed tests available. These tests begin with an initial clean air flush of 40 seconds with 0 RPM and flow rate 100 L min^{-1} to flush out any PM10 in the chamber. Clean air is blown by a DC blower with a sponge filter at the inlet to ventilate the chamber and is exhausted through a port at the top of the chamber. This ensures that the air in the chamber is particle-free compared to the dust concentrations when the instrument is used during a measurement cycle. During a ramp test, the RPM is linearly increased to the target value to simulate the effects of increasing wind speeds. This ramp test can be supplemented before and after with a constant phase where the RPM is kept constant for different intervals, making it a step test. Towards the last 10 seconds of the measurement, the RPM is reduced to zero, bringing the test to a halt. The choice of the number of RPMs and the duration of the constant RPM phase is primarily based on how emissive the test surface is.

The target values for the ramp and step tests were conducted with RPMs from 2000 for 120 s on disturbed surfaces to 6000 on undisturbed surfaces for 220 s. This range of RPMs

FIGURE 4.5: Measurements at Pisagua: (a) Undisturbed soil surface with large nodules of gypsum present. (b) The test site also had large stones. (c) Disturbed surface after removing the surface crust. More gypsum nodules are present at the test site than at Chuculay.

was chosen based on the PM10 values observed in the field. For example, in Pisagua, the RPMs varied from 2000 on disturbed surfaces to 4000 on undisturbed, while in Chuculay, 3000 RPM was used for disturbed surfaces and 6000 on undisturbed surfaces. This difference in observed PM10 already highlights the differences in soil conditions at the two sites. Each replicate test was done 1.5 m apart on a transect line. These replicate tests not only help increase the statistical significance of the results but also capture the heterogeneity of the surfaces on a local and high-resolution scale. The chamber was cleaned with a soft cloth to prevent cross-contamination between the tests.

The friction velocity, u_* can be obtained from the RPM using

$$u_* = C_1 \alpha^4 \, \mathrm{RPM}^{\frac{C_2}{\alpha}} \tag{4.1}$$

where u_* is the friction velocity (ms^{-1}), C_1 and C_2 are constants that have a value of 0.000683 and 0.832 respectively, and α is a calibration parameter that depends on the surface roughness with an α of 1 being perfectly smooth with decreasing values as the surface roughness increases. Etyemezian et al. (2014) proposed four roughness categories: the highest α value (0.98) is associated with silt-clay-crusted playa or lake bed with cracks and sparse gravel (< 2.5% cover), and the lowest value (0.86) is associated with a gravel-covered surface (10%–35% cover). Here, an α value of 0.98 for disturbed surfaces is used, which is the same as the value used by Cui et al. (2019) also for disturbed surfaces and 0.88 for undisturbed surfaces based on the Visual Surface Roughness Look-up Table for PI-SWERL Measurements database (Hartshorn et al. 2023). The look-up table comprises a collection of α values of various desert landforms calculated from a 'high-resolution micro-topographic Digital Elevation Model' along with high-resolution images. The potential error in choosing an incorrect α ($\Delta\alpha$=0.04) increases with increasing RPM and decreasing values of α (Etyemezian et al. 2014).

The threshold friction velocity, u_t, required for the direct entrainment of dust particles,

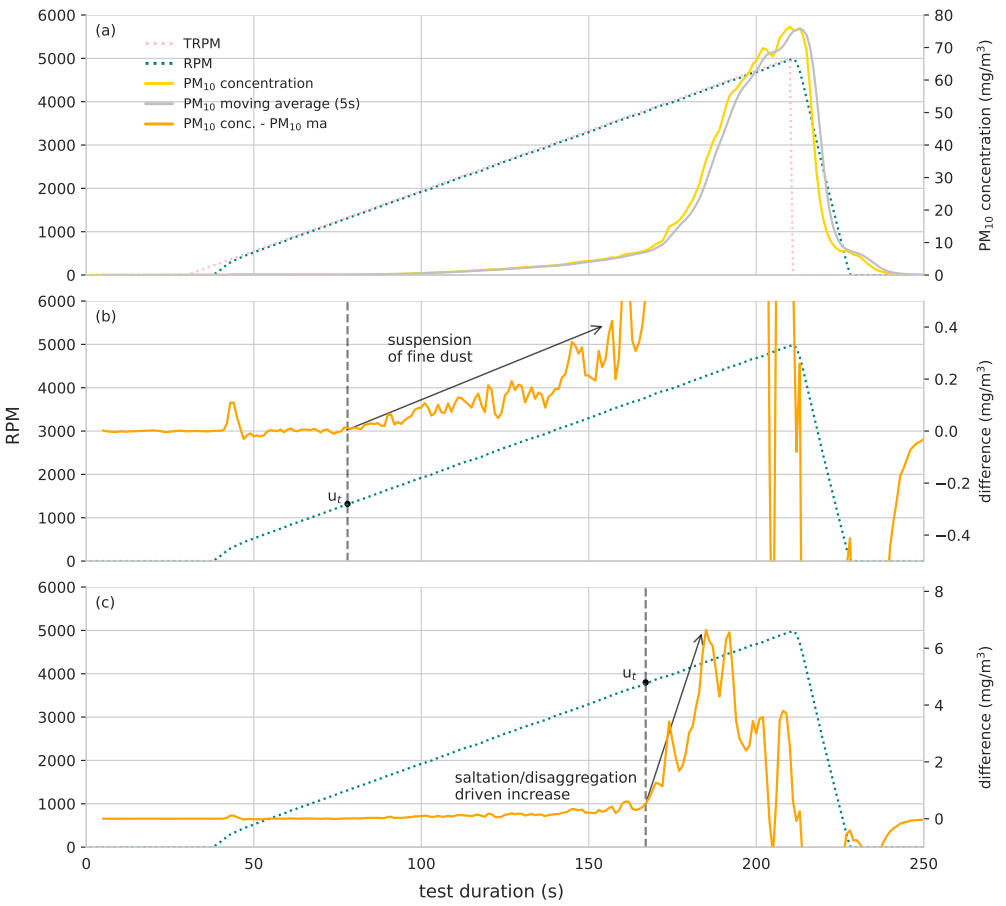

FIGURE 4.6: The PM_{10} dust concentration (conc., yellow line) and the revolutions per minute (RPM, green) of the PI-SWERL blade versus test duration. Panel a shows the target RPM (TRPM, pink) converging with the RPM and the 10 s moving average (ma, grey) PM_{10}. Panels b and c show the difference between the noisy PM_{10} and the averaged value. Two PM10 thresholds, u_t, can be identified, where the lower threshold is the wind speed required to suspend fine dust particles on the surface (panel b), and the higher threshold is the wind speed at which saltation drives an increase in dust emissions (panel c).

can be identified in several ways. In Figure 4.6, a ten-second moving average is computed to smooth over the background noise, and the difference between the measured PM10 concentration and the moving average is used to visually locate the point of increase in concentration (Figure 4.6b). For this study, u_{t1} is identified as the first data point which is continually above a fluctuating background noise of 0.1 mg m^{-3} with steadily increasing PM10 concentrations. Also observed in Figure 4.6c is another rapid increase in the PM10 concentrations. This inflection point, after which there is an exponential increase in the measured flux, can be attributed to a different emission mechanism where dust aggregates are abrading the surface and possibly also exploding into smaller dust-sized particles (called saltation and disaggregation respectively, see Section 2.1.2 for an introduction into the topic). In this study, the second threshold, u_{t2} or the elbow of the curve is identified as the first data point exhibiting an exponential increase of 10 mg m^{-3} PM10 concentrations in at least 10 s. This second threshold is identified only for some tests, as not all soil surfaces exhibit this behaviour.

Assuming neutral stability conditions, the vertical profile of the threshold wind velocity can be obtained using the logarithmic wind profile:

$$\frac{u_z}{u_*} = \frac{1}{\kappa} \ln \frac{z}{z_0} \tag{4.2}$$

where u_z is the wind speed(ms^{-1}) at height z metres, κ is von Karman's constant(0.4), and z_0 is the aerodynamic surface roughness length (m). As the PI-SWERL does not simulate the atmospheric boundary layer and therefore does not allow measurement of the wind speed profile and calculation of z_0 (Etyemezian et al. 2007), a z_0 value of 0.35 mm is used for

disturbed surfaces as obtained by Flores-Aqueveque et al. (2010) in the Mejillones Pampa in the coastal Atacama, north of Antofagasta. This surface roughness value was calculated from wind profiles measured by a sonic anemometer for a soil surface characterised by abundant coarse gravel and partial crust coverage. For undisturbed surfaces, a z_0 of 3 mm is used as estimated from the thickness of the surface crust in Pisagua (Figure 4.7). While these values are not exact, they are a good approximation for the surface conditions at the test sites.

FIGURE 4.7: Thin friable crust removed from the test site in Pisagua. The crust measures 3 mm in height.

Additionally, the emission flux can be calculated using (Etyemezian et al. 2007)

$$\mathrm{E}_i = \frac{\sum_{\text{begin},i}^{\text{end},i} C \times F \times 1s}{(t_{\text{end},i} - t_{\text{begin},i}) \times A_{\text{eff}}} \tag{4.3}$$

where E_i is the emission flux mg $\mathrm{m}^{-2}\mathrm{s}^{-1}$ or amount of PM_{10} per area per second, at a specific RPM level i, C is the dust concentration mg m^{-3}, F is the blower flow rate for fresh air entering the PI-SWERL chamber ($\mathrm{m}^3\mathrm{s}^{-1}$), A_{eff} is the effective test area underneath the PI-SWERL annular ring with value 0.035 (m^2), and t is the time (s) at the beginning ($\mathrm{t}_{\text{begin}}, i$) and ending ($\mathrm{t}_{\text{end}}, i$) of each RPM step level, i (Sweeney & Mason 2013).

4.3 RESULTS

Figure 4.8 shows the two stages of dust emission for disturbed surfaces in Chuculay. The first stage is a slow and steady increase in PM10 concentration, followed by a second stage with a rapid increase (peak) in dust concentration over a relatively short time compared to the first stage of emissions. But this behaviour is not exhibited by Test ID 3747489990 and hence does not meet the criteria for the computation of u_{t2}. The maximum PM10 concentrations from these surfaces also vary. Test IDs 3747489475 and 3747489990 have a maximum RPM set to 4000, while the others are set to 5000. However, even for surfaces with the same maximum RPM, the maximum PM10 differs by a factor of two. The disturbed surfaces exhibit appreciable PM10 emissions at 4000 RPM, while the undisturbed sites do not.

For undisturbed sites in Chuculay (Figure 4.9), the maximum PM10 concentration measured is low. A step test was conducted on one of the five undisturbed fields in Chuculay. In Test ID 3747493099, emissions initially rise at the beginning of the step test but fall to a low but non-zero value as the RPM is maintained. This quickly increases again as the friction velocity also increases. The target RPM set in the case of the step tests is 6000, which also explains why the maximum PM10 is higher than with the ramp test. Interestingly, despite Test IDs 3747493597 and 3747494021 targeting an RPM of 6000, the maximum PM10 concentrations are not much higher than Test IDs 3747490699 and 3747491839 with a target RPM of 4000 (the maximum PM10 concentration during ramp tests despite the RPM

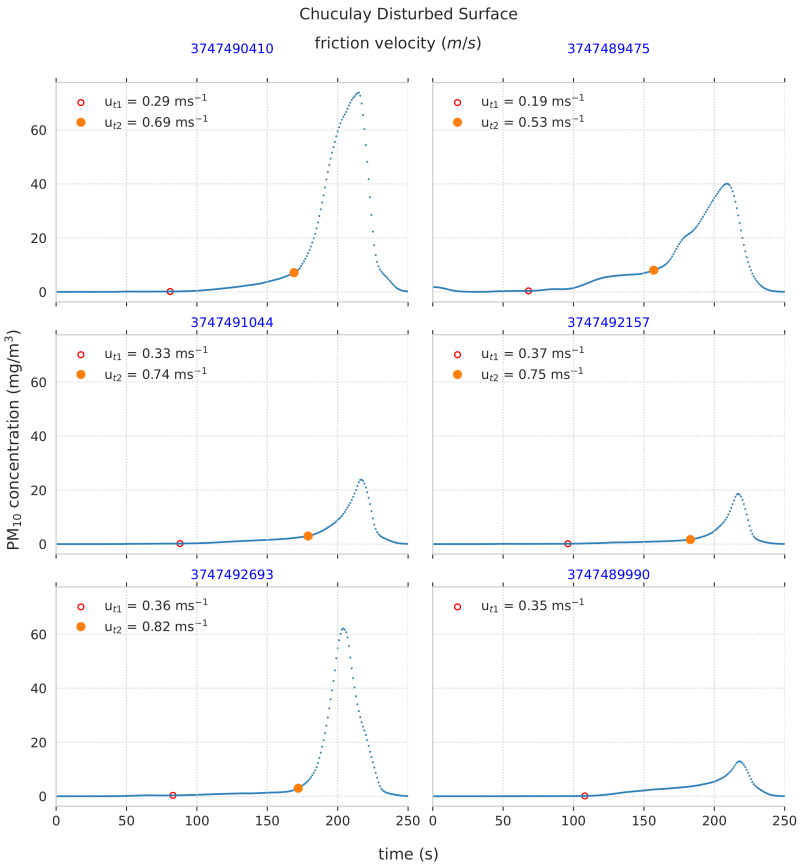

FIGURE 4.8: The 10 s moving average of PM_{10} dust concentration along the time axis for the disturbed surfaces in Chuculay. The threshold friction velocity, u_{t1} for the direct entrainment of dust, along with the second threshold, u_{t2}, associated with different dust emission mechanisms is shown for all but one test sites that exhibit an exponential increase in PM10 concentrations.

does not increase more than 6 mg m^{-3}). The general 'peaked' temporal behaviour of PM10 concentrations is also seen in Pisagua for disturbed and undisturbed surfaces (Figure S4.1 and Figure S4.2).

To identify which sites and surfaces are more emissive than the others, their target RPM and the corresponding maximum PM10 concentration are summarised in Table 4.1. The disturbed sites are generally more emissive than the crusted, undisturbed surfaces. The PM10 concentrations from crusted and disturbed surfaces in Pisagua are higher than in Chuculay. The maximum PM10 concentration from an undisturbed surface in Pisagua can be an order of magnitude higher than the disturbed surface in Chuculay at RPM 4000. Interestingly, the range of PM10 concentrations in Pisagua, from both disturbed and undisturbed surfaces, overlap at RPM 4000 for one replicate surface test. Furthermore, the maximum PM10 concentration does not linearly increase with increased RPM at either site. Curiously, the step tests (denoted by H) in Pisagua result in lower maximum PM10 concentrations than a ramp test with the same RPM. For perspective, RPM 2000 for a disturbed surface using the roughness height from the study is close to 10 ms^{-1}. However, on a crusted surface, this is nearly 14 ms^{-1}.

The threshold u_{t1} for direct entrainment and u_{t2} for saltation in Chuculay and Pisagua for disturbed and undisturbed sites are summarised in Figure 4.10. For undisturbed surfaces in Chuculay, the thresholds, u_{t1} range from 0.37–0.62 ms^{-1} and for disturbed surfaces 0.19–0.37 ms^{-1}. Similarly, in Pisagua, undisturbed surfaces have thresholds ranging from 0.27–0.39 ms^{-1} while the disturbed surfaces range from 0.21–0.29 ms^{-1}. As expected, the threshold u_{t1} for direct entrainment of fine dust is higher for undisturbed crusted surfaces than disturbed surfaces at both sites. The values of u_{t1} are much higher in Chuculay and show

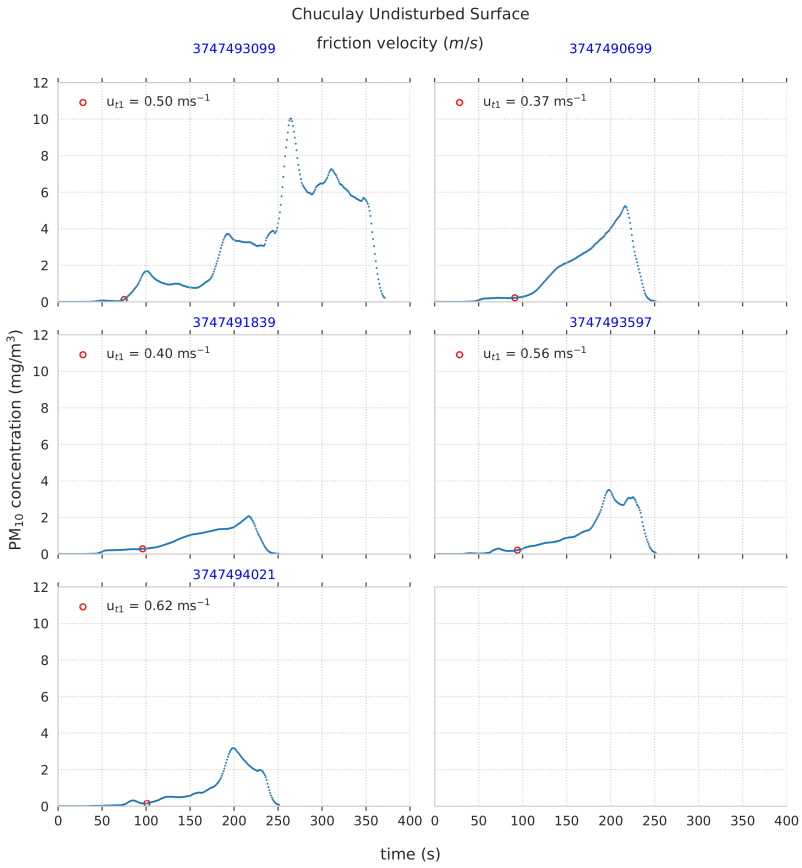

FIGURE 4.9: The 10 s moving average of PM_{10} dust concentration along the time axis for undisturbed surfaces at the Chuculay Fault. The threshold friction velocity, u_{t1} for the direct entrainment of dust is also shown.

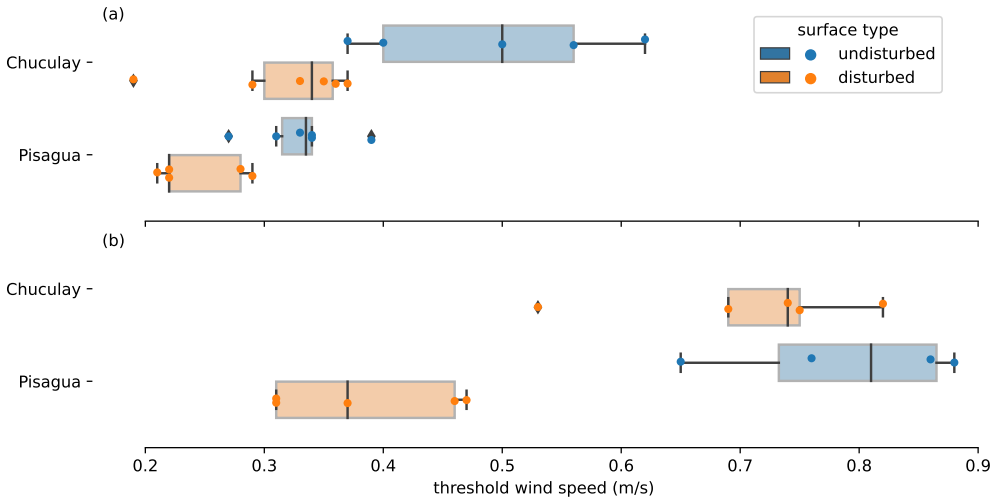

FIGURE 4.10: Panels a and b show the threshold wind velocities u_{t1} and u_{t2} respectively, at both test sites for disturbed and undisturbed surfaces. No u_{t2} could be computed for undisturbed surfaces in Chuculay.

significant variance per surface than in Pisagua (Figure 4.10a). Interestingly, the threshold values for the disturbed sites in Chuculay are similar to the undisturbed sites in Pisagua. The thresholds u_{t2}, shown in Figure 4.10b for saltation cannot be computed for undisturbed surfaces in Chuculay. On the other hand, the saltation threshold values for the disturbed surfaces are close to undisturbed surfaces in Pisagua (as with u_{t1}).

Using the roughness height for undisturbed surfaces ($z_0 = 3$ mm) along with the minimum threshold wind speed of 11 ms^{-1} for dust emission in Iquique (see Chapter 3), the near-surface threshold wind speed of 0.43 ms^{-1} was obtained in Iquique. Iquique being the closest

TABLE 4.1: The maximum PM10 concentration (mg m^{-3}) measured at each surface for each surface type along with the target RPM used for that test. The H before the RPM denotes a step test.

site	surface type	Test ID	target RPM	max. PM10
Chuculay	undisturbed	3747491839	4000	2.3
		3747490699	4000	5.8
		3747493597	6000	3.8
		3747494021	6000	3.4
		3747493099	H6000	10.8
	disturbed	3747489990	4000	15.6
		3747489475	4000	47.4
		3747492157	5000	23.0
		3747491044	5000	30.1
		3747490410	5000	76.3
		3747492693	6000	57.4
Pisagua	undisturbed	3747829995	2000	13.2
		3747831184	3000	25.3
		3747832093	H3000	12.1
		3747826595	4000	68.7
		3747827127	4000	400
		3747827571	H4000	119
	disturbed	3747828503	2000	115
		3747828978	2000	130
		3747830328	3000	400
		3747828121	4000	400
		3747831663	H4000	137

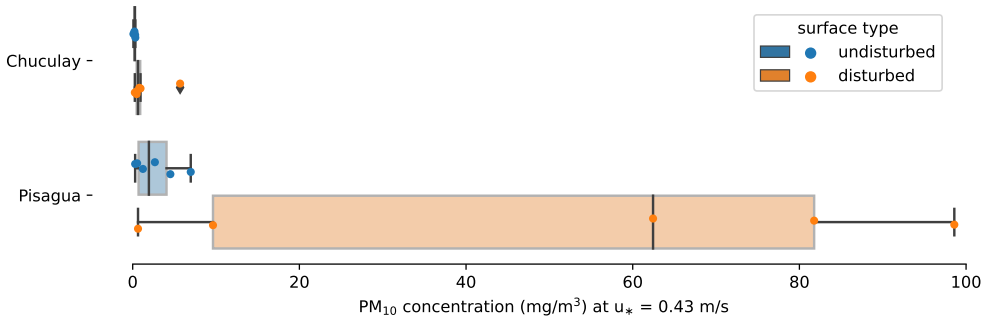

FIGURE 4.11: The PM10 dust concentration in Chuculay and Pisagua for disturbed and undisturbed surfaces for a near-surface threshold friction velocity of 0.43 ms^{-1} derived from the minimum 10 m threshold wind speed required for dust emission in Iquique.

SYNOP station for which we have threshold values computed is chosen. Pisagua is roughly 25 km north of Iquique, while the Chuculay Fault is at least 90 km away south of Iquique. At this threshold wind speed ($u_* = 0.43\,ms^{-1}$), the PM10 concentration at both sites shows very large differences (Figure 4.11). Almost no dust emission is present in Chuculay, while in Pisagua, the undisturbed surfaces show low PM10 concentrations. However, the disturbed surfaces in Pisagua show a high variance in PM10 concentration ranging from close to zero to nearly 100 mg m^{-3}. The 10 m threshold wind speed was also calculated for the sites (Figure 4.12). To compare with the SYNOP stations and other studies using PI-SWERL in various desert regions, only the threshold u_{t1} is used. The threshold wind speeds in Chuculay range from 9.5–15 ms^{-1} for undisturbed surfaces and 5–9.5 ms^{-1} for disturbed surfaces. In Pisagua, the thresholds range from 7–10 ms^{-1} for undisturbed surfaces and 5–7.5 ms^{-1} for disturbed surfaces. The lower threshold range over undisturbed surfaces in Chuculay and the upper range in Pisagua is closest to the minimum threshold wind speed of 11 ms^{-1} as

estimated for Iquique.

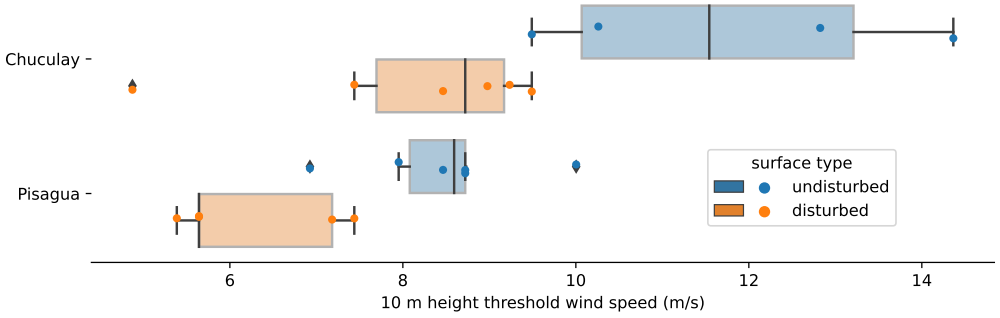

FIGURE 4.12: The threshold wind speed at 10 m that is required for the direct entrainment of dust in Chuculay and Pisagua for disturbed and undisturbed surfaces.

4.4 DISCUSSION

The PI-SWERL does not simulate the vertical motions in the atmospheric boundary layer (Sweeney et al. 2008). Instead, it is based on the relationship between friction velocity and dust emission. Therefore, only surface interactions of the wind are investigated. The blade height is limited and close to the outer casing of the chamber, which might result in sand particles ricocheting off the surface, thereby altering the measured saltation flux (Sweeney et al. 2008). This study does not use the saltation flux as the particle size is smaller than the required size for effective measurements. However, several past studies (Sweeney et al. 2011; Sweeney et al. 2008; Leeuwen et al. 2021; Cui et al. 2019; Macpherson et al. 2008; Bacon et al. 2011) have shown that the PI-SWERL provides a decent measure of dust emission potential for different surfaces and its compact size, minimal setup and ease of transport makes it ideal for measuring the emission potential over a large number of surfaces within a reasonable amount of time.

The differences in threshold wind speed and maximum PM10 concentrations in both crusted and disturbed surfaces in Pisagua as compared to Chuculay reflect the local variability in soil texture between surfaces of the same type. The low threshold wind speed and the high maximum PM10 concentration at RPM 4000 from the crusted surfaces in Pisagua, as compared to Chuculay, could indicate that the binding strength of the crust can be weakened with sufficiently high friction velocity, generating maximum PM10 concentrations of over 100 mg m^{-3}. The weak crust strength would also explain why the saltating threshold u_{t2} could be determined and the overlap between the maximum PM10 concentrations between crusted and disturbed surfaces in Pisagua at RPM 4000. Along with a weak crust, the presence of more erodible material underneath the crust would explain why the maximum PM10 concentrations are high.

The local-scale heterogeneity of surfaces is further enhanced in crusted surfaces in Chuculay, where a large range of threshold wind speeds was determined for dust entrainment. This is also seen with the measured maximum PM10 concentration, which does not scale linearly with the friction velocity. The degree of crusting can vary over a small area, and the presence of small stones and gravel can influence the dust emission potential of the test surface (Flores-Aqueveque et al. 2010). Furthermore, Brown (2007) showed that the variation in crust strength in centimetre scale is enough to influence the dust emission potential of surfaces. In the field, it was also observed that the presence of gypsum differed between the sites. While gypsum nodules were present underneath the crust in both sites, in Pisagua, they were more abundant than in Chuculay and white specks of gypsum more visible on the surface crust in Chuculay than in Pisagua. The disaggregation of soil particles

by saltating grains may also play a role in the increase in dust emission flux, especially with the presence of gypsum (Vos et al. 2021) in these test surfaces. Several studies have shown that the gypsum aggregates can shatter easily upon impact by saltating particles can lead to large emission fluxes (Reynolds et al. 2007; Sweeney et al. 2021; Jerolmack et al. 2011; Buck et al. 2011).

Peaked emission behaviour is observed in the temporal behaviour of the PM10 concentrations across both test sites, suggesting supply-limited environments for dust emission (Sweeney et al. 2011; Cui et al. 2019). This is typical of crusted surfaces that lack availability of erodible material (Macpherson et al. 2008). The lag between the initial slow increase in PM10 and the sharp increase could be driven by increased friction velocity required to lift saltators that might be embedded in the surface but become mobile only when the threshold is reached (Sweeney & Mason 2013). The lack of signal detected by the OGS sensors (measuring saltation counts) might have to do with the gravitational settling of large saltators below the sensors that detect them or that they disaggregate easily into fine particles (like gypsum) upon impact with other particles and hence only particles $<100\mu$m are picked up by the sensors. Figure S4.3 shows a preliminary grain size distribution of samples from Chuculay and Pisagua where it is evident that large particles $>100\,\mu$m are present in the sample but are not picked up by the instrument. Either these particles do not participate in the emission process, or they disaggregate into finer particles that the instrument cannot effectively categorise as saltators.

Crusted surfaces require a higher threshold wind speed to initiate dust emission than disturbed surfaces where the crust has been removed. This is consistent with other studies (Sweeney et al. 2011; Gillette et al. 1980b; Gillette et al. 1982). The undisturbed surfaces in Chuculay exhibit very high thresholds (9.5–15 ms^{-1}) for dust entrainment and are consistent with the estimates for threshold wind speed (9.5–13 ms^{-1}) computed from long-term SYNOP stations barring Chañaral. However, the undisturbed surfaces in Pisagua have a lower threshold than Chuculay and almost all SYNOP stations except Chañaral. The median threshold in Pisagua is 8.5 ms^{-1}, which is still slightly higher than the mean threshold wind speed of 7.3 ms^{-1} in Chañaral. These results indicate that the Atacama soil surfaces are heterogeneous even if surface crusts are ubiquitous. More field measurements are necessary to identify regions with higher dust emission potential. In Chapter 3, it was suspected that the comparatively low wind speed threshold measured in Chañaral is due to the 200–300 Mt tailing deposits (deposits from mines dumped between 1930–1990) present along the shores of the region. This estimate is within the 10 m threshold wind speeds from disturbed surfaces in Chuculay (7.5–9.5 ms^{-1}) and Pisagua (5–7.5 ms^{-1}), indicating that if anthropogenic activities can damage the surface crust in the Atacama, then the potential for dust emission may increase.

Wind speeds above 6 ms^{-1} were measured by the CRC weather stations at 2.5 m height close to the test sites. These winds are close to the threshold winds estimated from the field if neutral boundary layer conditions and the same roughness length (z_0=3 mm) are assumed. So, in theory, dust events should be as frequent as the threshold wind speeds at these sites. However, the median wind speed is far too low at these stations during daytime and the frequency of occurrence and atmospheric conditions under which wind speeds $>6\,ms^{-1}$ occur is yet to be determined. As is with SYNOP thresholds, the PI-SWERL thresholds are higher than the threshold values estimated by Pu et al. (2020), of $6.5 \pm 1.0\,ms^{-1}$ using satellite and reanalysis data and assuming a dust optical depth threshold of 0.02. As already discussed in Section 3.4, this could be because in the NCEP1 reanalysis dataset, the surface winds are computed at one grid point and not from observations from ground-based stations, and the grids are too coarse to accurately capture the surface winds, especially in a region with

complex terrain.

A good agreement with the thresholds (0.27–0.39 ms^{-1}) obtained for undisturbed surfaces in Pisagua and with those from Flores-Aqueveque et al. (2010) and Flores-Aqueveque et al. (2012) for the Mejillones Peninsula Bay (23°S) north of Antofagasta was found. Flores-Aqueveque et al. (2010) estimated a threshold wind speed of 0.31 ms^{-1} using a dust emission model (Marticorena & Bergametti 1995) calibrated using wind speed observations and dust traps in the field. Meanwhile, Flores-Aqueveque et al. (2012) used wind speed observations from two weather stations in Antofagasta, one operating from 1991–2003 and the other from 2000-2004 and von Karman's equation (see Equation (4.2)) using roughness length, z_0=0.03 mm, to obtain the near-surface winds. Then, using the same calibrated model (Marticorena & Bergametti 1995) and the equation for horizontal emission flux, they simulated the wind erosion events, including their magnitude and variability (White 1979). With this, they estimated that all wind speeds between the threshold of 0.31 ms^{-1} and a maximum of 0.58 ms^{-1} drive erosion, but that around 0.45 ms^{-1} contributed statistically less to the erosion flux than the other winds. They used this value to mark two "saltation modes": low and high. The low saltation mode centred around 0.35 ms^{-1} and 0.38 ms^{-1} and, the high saltation mode centred around 0.49 ms^{-1} and 0.52 ms^{-1}. Both these modes are significantly lower than the saltation threshold (0.65–0.86 ms^{-1}) determined in this study. Two glaring reasons for this are that their roughness length is similar to ours for disturbed surfaces but not for crusted surfaces (this study uses z_0=3 mm). Two, the increase in erosion flux for wind speeds greater than 0.45 ms^{-1} (used to mark the two modes) is only observed in 2004.

4.5 CONCLUSION

This study used the Portable in situ Wind Erosion Lab (PI-SWERL) to determine the threshold wind speed required for dust emission from two test sites in the Atacama. The measurements were conducted on undisturbed and disturbed surfaces where the top crust was removed. The estimated threshold wind speed and the maximum PM10 concentrations measured indicate the role of surface crusts in controlling the dust emission flux observed in Pisagua and the Chuculay. Without the crust, the average threshold wind speed is twice less than crusted surfaces in Chuculay and 1.3 times less in Pisagua. The maximum PM10 concentrations for the lowest friction velocity used at the sites are almost an order of magnitude higher from disturbed surfaces than crusted surfaces.

The high dust emissions are a function of saltation from possibly gypsum particles in and underneath the crust. They are likely to influence the threshold and concentration rates for a given surface, reflecting the local variability in soil texture. The thresholds estimated using the SYNOP station are within those calculated on the crusted surfaces in Chuculay. Still, they are higher (except in Chañaral) than those in Pisagua. However, to fully understand the differences within and between the sites and the SYNOP stations, soil surface analyses and more field measurements (at least n=30 for a given surface type) are needed to constrain the field thresholds better. Additionally, several more step tests from PI-SWERL are required to test the saltation theory of gypsum particles in the test sites and if the emissions can be sustained with constant friction velocity. We also need to consider if seasonality has a role in the heterogeneity of dust emissions.

This study shows that high friction wind speeds alone are insufficient for dust emission. The right soil conditions are required to trigger dust emission from desert surfaces in the Atacama. However, the results raised more questions, as seen in the discussion. While we do not have answers to all of them, these results have set the ground for future research in the Atacama in the context of dust emission mechanisms, local heterogeneity of surfaces, and

the potential for dust events given the right conditions. The crust preserves the surface from wind erosion if the friction wind velocity does not exceed the threshold. With increasing anthropogenic activities in the Atacama disturbing the topsoil, there is potential for more dust activity. Future work should identify surfaces prone to dust emission using the PI-SWERL and satellite data. Furthermore, the crust strength should be quantified, and the factors affecting it should be identified. This would give us insight into the degree of change in the dust emission potential that anthropogenic activities could have in the region. Regardless, the crust and large particles in the soil surface efficiently control dust emission in the Atacama.

▸ SUPPORTING INFORMATION

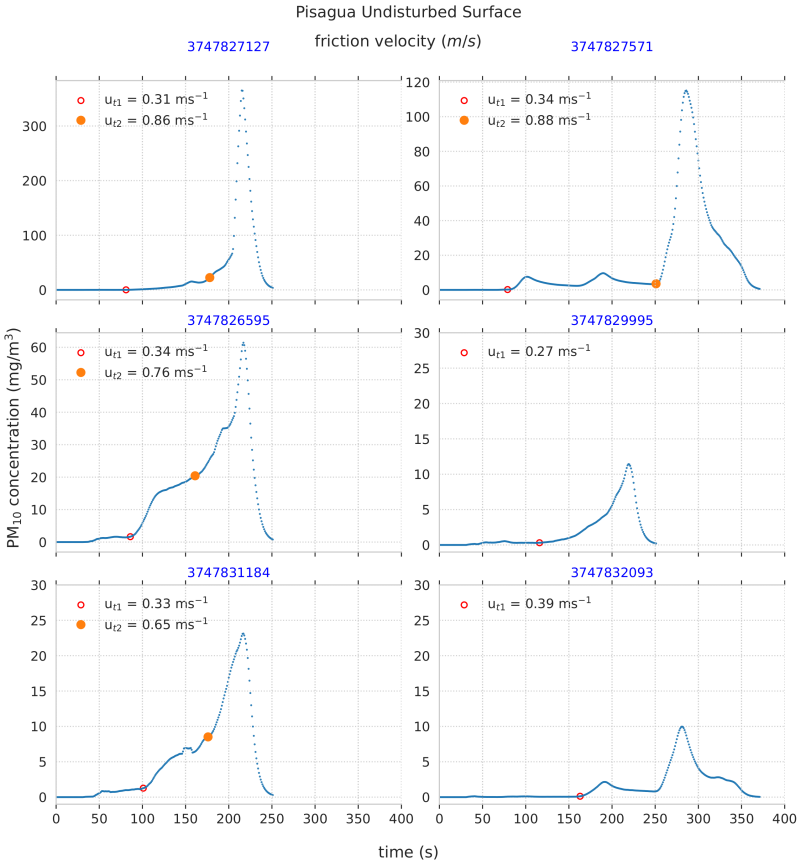

FIGURE S4.1: The 10 s moving average of PM_{10} dust concentration along the time axis for the undisturbed surfaces in Pisagua. The threshold friction velocity, u_{t1} for the direct entrainment of dust, along with the second threshold, u_{t2} associated with a different dust emission mechanism, is shown for some of the test sites that exhibit an exponential increase in PM10 concentrations. The PM10 concentrations in Pisagua for undisturbed surfaces are much higher than in Chuculay.

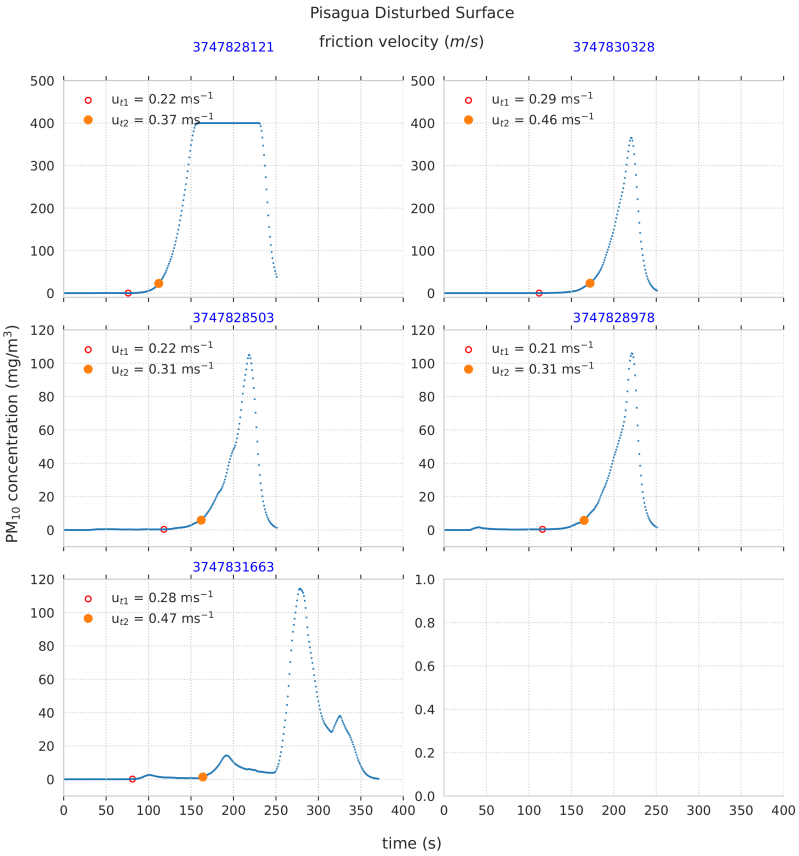

FIGURE S4.2: The 10 s moving average of PM_{10} dust concentration along the time axis for the undisturbed surfaces in Pisagua. The threshold friction velocity, u_{t1} for the direct entrainment of dust, along with the second threshold, u_{t2} is shown for all the test sites. The disturbed surfaces in Pisagua emit twice the PM10 concentration than in Chuculay.

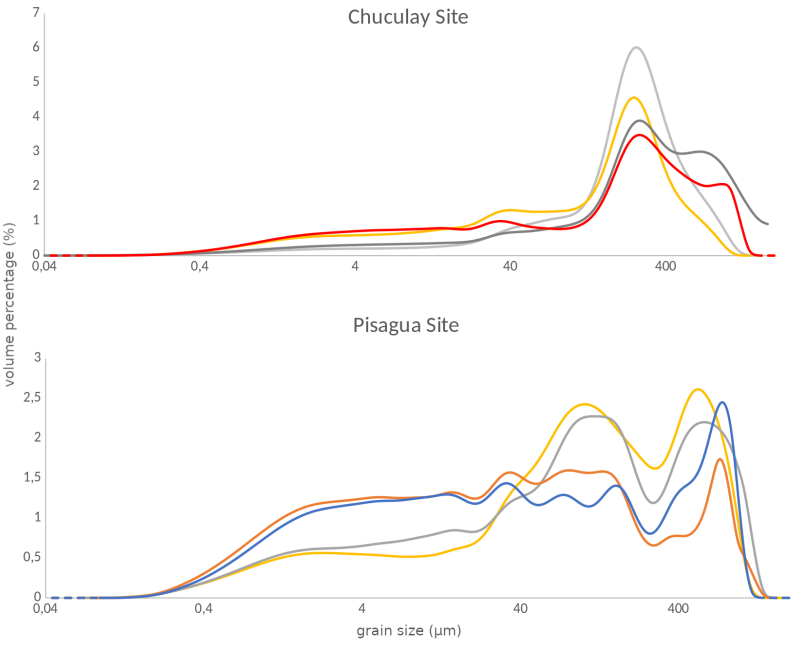

FIGURE S4.3: Grain size distribution of soil surface from Chuculay and Pisagua determined with a sieve analysis.

Part III

METEOROLOGICAL DRIVERS OF DUST ACTIVITY

5

What drives the rare dust activity in the Atacama Desert?

"The shifting sands!
Slowly they move,
wave upon wave,
drift upon drift;
but by day and by night
they gather, gather, gather.
They overwhelm,
they bury,
they destroy,
and then a spirit of
restlessness
seizes them,
and they move off
elsewhere,
swirl upon swirl,
line upon line,
in serpentine windings
that enfold some new
growth
or fill in some
new valley
in the waste.
So, it happens
that the surface
of the desert
is far
from being
a permanent affair. "

—John C. Van Dyke, The Desert

5.1 MOTIVATION

In Chapter 3, the SYNOP observations were analysed to find that of all the observations from 1950–2021, only 0.25% belonged to dust activity. There have been 1920 dust days in 72 years, but the inter-annual variability is very high. It was also found that most activity is recorded at one station (Chañaral: 19.6 dust days per year and other stations: 2.7 days per year). In Chapter 4, the thresholds estimated from the observations with in-situ measurements were validated, confirming the role of the surface crust as a control for dust emission potential. Nevertheless, intense dust outbreaks occur in the Atacama Desert (see Figure 5.1) with 130 dust storms recorded in the SYNOP dataset which may impact multiple socio-economic sectors (Middleton et al. 2021).

Almost 30–70% of the dust emissions in the major dust source regions are associated with diurnal variability (Luo et al. 2004). In the Atacama Desert, the daytime heating of the land forces near-surface westerly winds from the coast to the Andes, and at night, a return flux is observed but with weaker wind speeds (Rutllant et al. 2003; Rutllant et al. 2013). This thermal wind circulation most likely influences the dust activity. The winds in the Atacama are strongly affected by the position and intensity of the southeast Pacific anticyclone (SEPA), which might lead to enhanced dust activity in the spring and summer when the SEPA is at its northernmost position, producing stronger southerly winds. To test this hypothesis, the diurnal and seasonal cycle of dust activity is analysed.

Dust storms, in particular, require intense wind speeds to lift dust particles off the surface and transport them over long distances (Prospero 1996; Shao 2008; Schepanski 2018). These strong winds that initiate dust emission and support long-range transport are driven by sufficiently large surface pressure gradients. Following up on Chapter 4, where it is found that dust activity is controlled by the surface crust and from Chapter 3 that the climatological mean winds in the Atacama are insufficient to drive frequent dust activity, we, therefore, hypothesise that changes in circulation at synoptic and local scales likely drive intense dust activity in the Atacama Desert. Except for a study by Reyers and Shao (2019), where they found a dust storm triggered by a mid-tropospheric trough and strong easterly winds, there are no other studies discussing dust activity in the light of synoptic scale mechanisms.

In this last chapter, the precursors or drivers of dust activity are explored and an analysis of the synoptic weather patterns associated with dust storms. Section 5.2 introduces the datasets and classification methods used in this study and, in Section Section 5.3, the seasonal

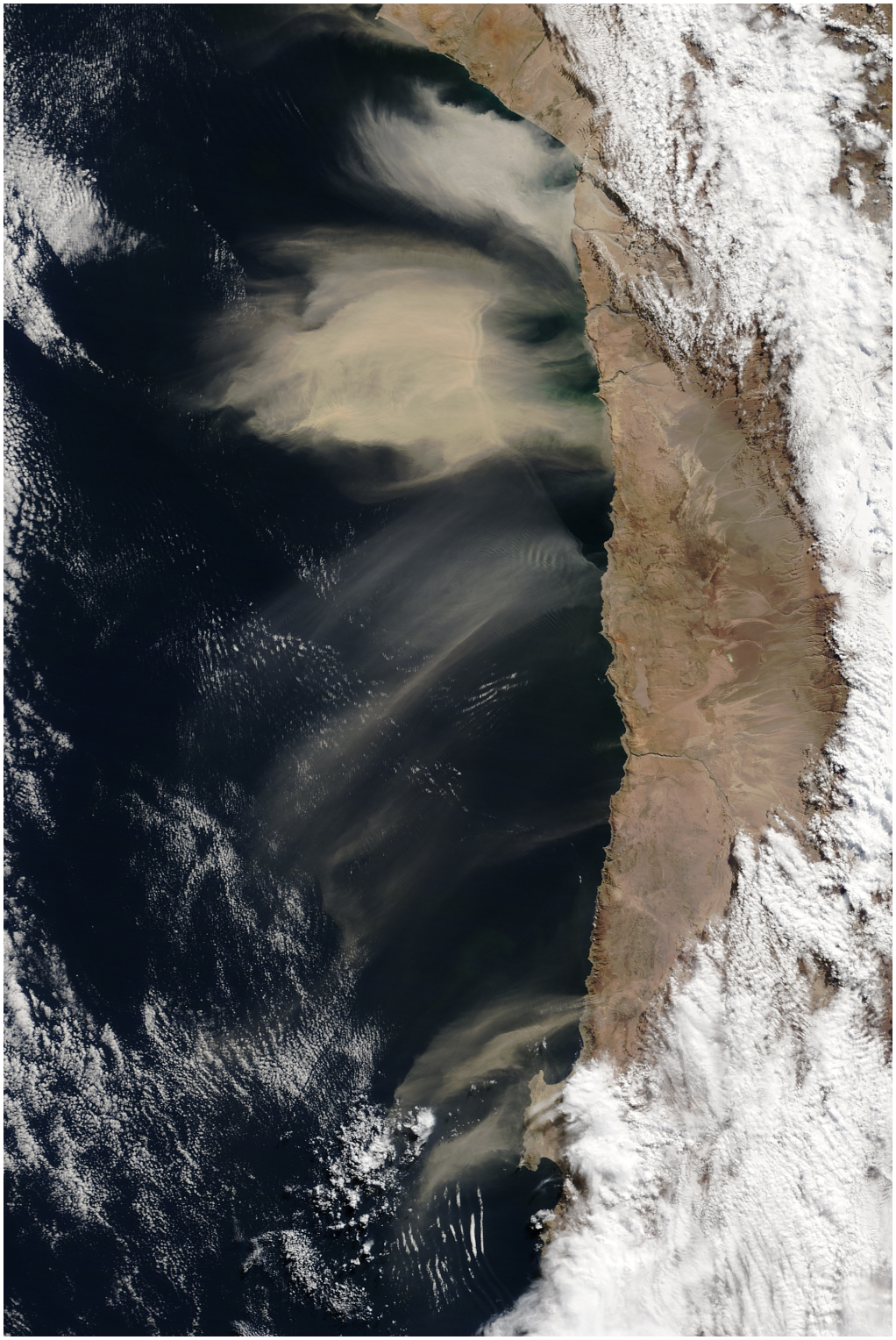

FIGURE 5.1: True colour image of airborne dust off the coast of the Atacama Desert on 8 July 2016 as taken by the MODIS/TERRA instrument (source: https://modis.gsfc.nasa.gov/gallery/individual.php?db_date=2016-07-14)

and diurnal differences in dust activity are presented, followed by the different synoptic patterns that are associated with dust storms. In Section 5.5 and Section 5.6, it is discussed as to how these results contribute to a better understanding of the meteorological drivers of dust activity in the Atacama.

5.2 DATA AND METHODOLOGY

5.2.1 *Data*

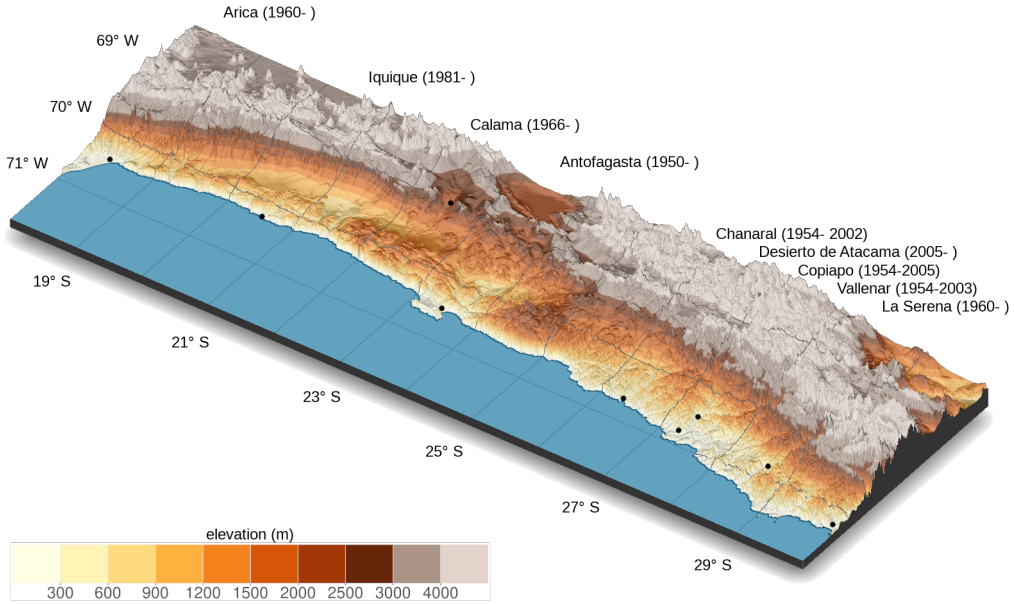

FIGURE 5.2: Topography of the Atacama Desert along with the location of the weather stations and their period of operation. The elevation of the stations, above sea level, from the SYNOP dataset are as follows:
Arica: 55 m
Iquique: 48 m
Calama: 2320 m
Antofagasta: 135 m
Chañaral: 30 m
Desierto de Atacama: 204 m
Copiapó: 290 m
Vallenar: 526 m
La Serena: 146 m

Surface synoptic observations (SYNOP, Dirección Meteorológica de Chile- Servicios Climáticos (2019)) from 1950 to 2021 from nine stations in the Atacama Desert (Figure 5.2) are used. The observational dataset includes pre-defined present and past weather codes from the World Meteorological Organisation (World Meteorological Organization 1995). The present (ww) and past weather codes provide a qualitative description of the state of the atmosphere as observed by an observer every three hours. Along with these codes, the 10 min mean wind speed and direction at 10 m above ground level (agl) and horizontal visibility is analysed. For the seasonal analysis, the 3-hourly 10 min wind speed is averaged, and for the diurnal analysis, hourly 10 min wind speed is used. Nocturnal observations of the present weather exist only for the stations Arica, Iquique, Antofagasta and La Serena. Therefore, for some stations, the diurnal and seasonal cycle only represents daytime conditions (9–21 LT). The weather codes for dust events were grouped following Shao et al. (2013) and Cowie et al. (2014), and include transported dust (ww=06), suspended dust (ww=07), dust devils (ww=08), dust storms (ww=09,30–32), severe dust storms (ww=33–35) and, other dust events (ww=98) along with the past weather code 03 with air temperature higher than 3°C to exclude blowing snow events (Table 5.1). More information on the codes and their limitations can be found in Chapter 3.

For synoptic weather conditions associated with dust storms in the Atacama, dust storms and severe dust storms (ww = 09, 30–35) (hereafter, dust storms) in the SYNOP dataset at all stations were selected. For the times of the recorded dust storms, the mean sea level pressure (MSLP) and geopotential heights at 700 hPa and 500 hPa pressure levels was obtained, along with 10 m zonal (u) and meridional (v) wind components from the European Centre for Medium-Range Weather Forecast (ECMWF) ERA5 Reanalysis (Hersbach et al. 2020). The ERA5 data covers the time of the entire SYNOP dataset with an hourly resolution and a horizontal resolution of 0.25° × 0.25°. The domain size of ERA5 data encompasses 10°S–40°S and 60°W–90°W. This ensures that all the SYNOP stations are within the domain size.

TABLE 5.1: SYNOP weather codes used for the definition of dust events in this study

dust type	code	description
transported dust	06	widespread dust in suspension, not raised at or near the station at the time of observation
suspended dust	07	dust or sand raised by wind at the time of observation, but no sand or dust storm
dust devil	08	well-developed dust devils, but no sand or dust storm at or near the station during the preceding hour or at the time of observation
dust storm	09, 30-32	slight or moderate dust storm or sandstorm at the time of observation, at the station or has begun/changed during the preceding hour
severe dust storm	33-35	severe dust storm or sandstorm at the time of observation, at the station or has begun/changed during the preceding hour
other dust events	98, 03[a]	thunderstorm combined with a sand or dust storm at the time of observation; From past weather: sand storm, dust storm, or blowing snow

[a] Past weather code = 03 with air temperature lower than 3°C was removed to exclude blowing snow events.

It is important to note that ERA5 data is shown to have a bias in sea level pressure with lower values of sea level pressure in the southern hemisphere before the 1980s when no assimilation of satellite data was possible (Hersbach 2023).

5.2.2 *Analysis strategy*

For stations located <500 m asl (Arica, Iquique, Antofagasta, Desierto de Atacama, and La Serena. Elevation of each station is available in Figure 3.1), the MSLP, surface horizontal wind speed, and 500 hPa geopotential height at the time of a dust storm record were analysed. Only for Calama, located at 2200 m asl, an additional pressure level in the analysis (700 hPa geopotential height) corresponding to the station altitude is included. This also takes into account that the topography of the Andes strongly influences the MSLP. From the climatological perspective, the typical subsidence above the cool and moist marine boundary layer (MBL) leads to an inversion at the top of the MBL, suppressing the development of deep convection and precipitation. The inversion height changes diurnally and seasonally but is approximately 800–1000 m asl (Schulz et al. 2012b; Muñoz et al. 2011). Therefore, the coastal stations are at altitudes within the height of the MBL and are influenced by the variability in the location and strength of the Southeast Pacific Anticyclone (SEPA, see Section 2.2.1). To account for the diurnal and seasonal differences in the SEPA (Fuenzalida 1996), the hourly MSLP and 10 m wind speeds are subtracted from their respective hourly climatological mean (1991–2021) for that given month. The MSLP, 700 hPa, 500 hPa and surface winds maps were then visually inspected and grouped to identify weather patterns associated with the dust storms at coastal stations.

The weather patterns were systematically studied and visually categorised into groups according to their main synoptic characteristics. Five independent groups: cut-off lows, mid-tropospheric troughs and surface lows, intense anticyclones, mid-tropospheric ridges, and coastal lows were identified. This classification can be found in a tabular format (Table S1) and the images of the weather patterns at the different geopotential heights for each

dust storms are presented (Folder S1).

In the case of cut-off lows, past studies have identified 'cut-off lows' (CoLs) using techniques such as first and second derivatives of a continuous 500 hPa geopotential height (Fuenzalida et al. 2005), closed cyclonic geopotential contour in 200 hPa, a geopotential minimum in either 500, 300 or 200 hPa or through the potential vorticity framework (Muñoz et al. 2020). Here, a simple approach following Bell and Bosart (1989) is used and Reyers and Shao (2019), where a CoL is identified when a local minimum is detected in the geopotential height at 500 hPa. Tear-off lows or closed lows embedded in a mid-level trough (Pinheiro et al. 2021; Favre et al. 2012) were also included as 'cut-off lows'. Mid-tropospheric troughs are identified in the 500 hPa by the decreasing heights along isobars on an equator-ward elongated region (in the southern hemisphere, in the northern hemisphere, it is pole-ward elongated) without a closed contour. The increasing heights of isobars help identify mid-tropospheric ridges along a poleward elongated region. Surface projections of the troughs are identified via the negative contours in the surface anomaly map and classified as 'surface lows'. In contrast, mid-tropospheric troughs without a surface projection are classified as 'UL troughs' (UL: upper-level, 500 hPa troughs).

Dust storms associated with 'intense anticyclones' have been defined as cases with a positive anomaly in MSLP of at least +4 hPa paired with an anomaly in the 10 m wind speed of at least +3 ms^{-1} offshore Atacama. As the study domain is small, positive surface pressure anomalies, not explicitly attributed to either the SEPA or a migrating anticyclone, were classified as 'intense anticyclone'. The extension of the regional domain up to 30°S further allows the identification of coastally trapped disturbances. Such coastal lows vary in their characteristics (Rutllant & Garreaud 1995; Rutllant 1994). A more lenient criteria than in the method by Garreaud et al. (2002) is used. A coastal low is defined when a mid-tropospheric ridge in the 500 hPa geopotential height, paired with an anomalously strong anticyclone in the southeast Pacific and an anomalously weak mean sea level pressure oriented poleward along the north-central coast, are observed.

Large-scale oscillations such as the El Niño-Southern Oscillation (ENSO) are known to affect the circulation in the vicinity of the Atacama, leading to changes in precipitation (Houston 2006c; Reyers et al. 2021; Vargas et al. 2006; Ortega et al. 2019; Bozkurt et al. 2016) and alongshore winds (Rahn 2012; Rahn & Garreaud 2014), which could enhance dust activity. However, signatures of anthropogenic activities (especially those related to mining) may be present in the dataset (see Section 3.3.2 on page 33), making it challenging to infer possible trends and drivers at the interannual and decadal scale.

5.3 RESULTS

5.3.1 *Diurnal Cycle*

The direction of the daytime winds (Figure 5.3) informs us of the effects of the local topography and solar insolation on the wind system. For stations along the coast, during nighttime, wind speeds are low (mean ranging 1–3 ms^{-1}), and the direction scatters but is mainly from the land. During the daytime, wind along the coast mostly blows from the southwest and west with increased speeds (mean 5 ms^{-1}, Figure 5.4), except in Desierto de Atacama and Vallenar, where winds also blow from the northern and northwesterly directions. Both these stations are less than 50 km inland from the coast, surrounded by the coastal cliffs that channel the winds. Meanwhile, during the day, winds farther into the desert (in Calama, for example) blow from the west (mean 8 ms^{-1}) with northwesterly up-slope flow during the afternoon and the nighttime winds are easterly down-slope winds (Muñoz et al. 2020;

Muñoz et al. 2013; Muñoz et al. 2018) and can be stronger than in the coastal regions (mean around 6 ms^{-1}).

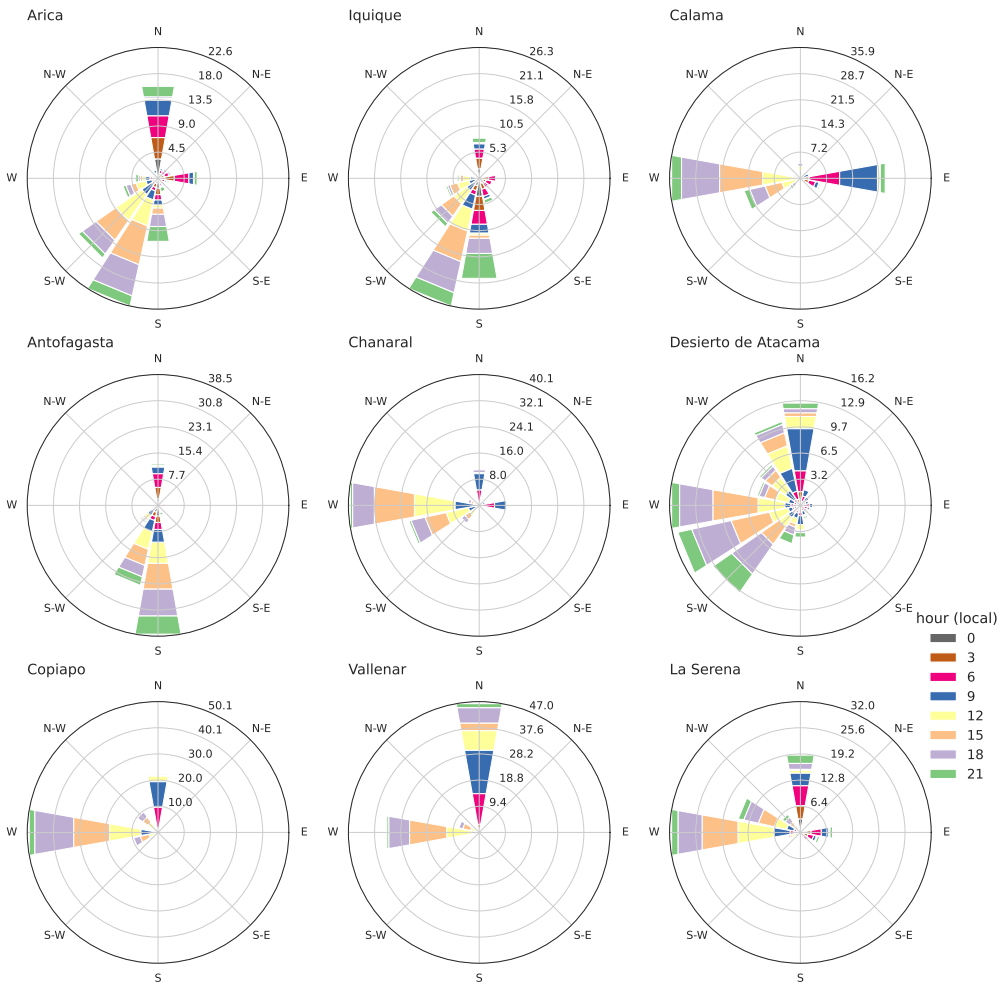

FIGURE 5.3: Wind roses at each station for all observations. The frequency of 3-hourly winds per direction with a colour-coded time of occurrence in local time, based on SYNOP data for 1950–2021.

A strong diurnal variability in dust activity is observed at all stations (Figure 5.4) with dust activity recorded between 9–15 local time (LT), and the peak activity is at 1200 LT just before the wind speed maxima (all hours in Chile Standard Time: UTC-4). The four stations in Arica, Iquique, Antofagasta and La Serena have weather codes for daytime and nighttime, while other stations have weather reports only for the daytime. Despite the lack of weather codes at night at about half of the stations, the strength of the winds suggests that these stations may also have increased dust activity during the day compared to at night when the average surface wind speeds are low. Optimal wind stress and surface heating occur just before the wind maxima, enhancing the conditions for dust emission. However, the lack of more detailed observations within the local planetary boundary layer and high-resolution simulations prevents us from fully confirming this hypothesis.

Strong surface heating and daytime winds are drivers of micro-scale dust emission such as dust devils and non-rotating plumes (Koch & Renno 2005; Sinclair 1965; Sinclair 1969) and are important on a regional scale (Gillette & Sinclair 1990; Jemmett-Smith et al. 2015; Klose & Shao 2016; Tang et al. 2018). In the SYNOP dataset, less than 4% of recorded dust are dust devils as most observations are recorded not in the uninhabited desert or overwritten by other codes. However, Kurgansky et al. (2011) and Metzger et al. (2010) performed a survey for 12 days at a place outside Huara, 80 km inland from Iquique and detected 3622

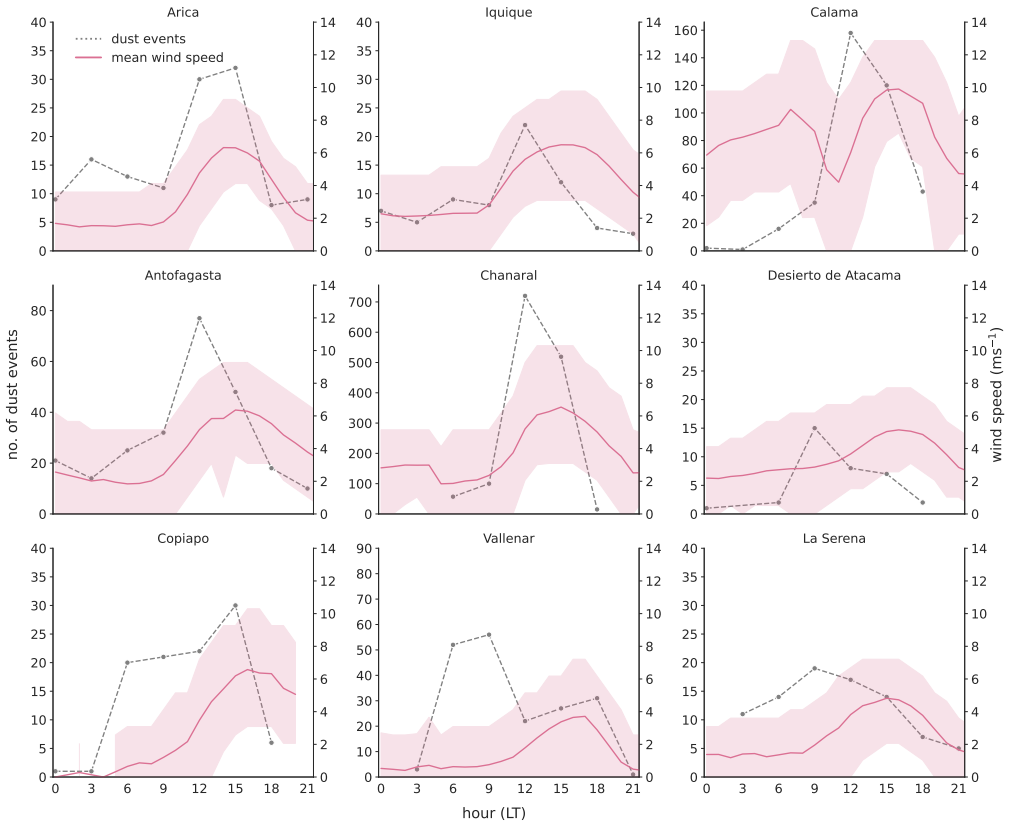

FIGURE 5.4: Total diurnal dust activity (1950–2021) with the hourly mean wind speed from all observations. The 5^{th}-95^{th} percentile interval of the wind speed at each station for hourly periods is shown with pink bands. Note the different number of dust events on the primary y-axis.

devils with activity beginning at 1130–1200 LT until 1600-1630 LT, at wind speeds ranging 1.5–8 ms^{-1}, highlighting the need for more observations in the Atacama for robust estimates.

5.3.2 *Seasonal Cycle*

The surface winds in the Atacama reach maximum velocities along the coast in the prevailing south, the southwest direction in spring (SON) and early summer (DJF) as seen in Figure 5.5 and modulated mainly by the intensity and position of the SEPA. The intensity of the anticyclone is strongest in spring and early summer when the skies are the clearest (Vincent 1998; Rahn & Garreaud 2014). This maximum wind velocity coincides with the summer and spring maxima in dust activity in Chañaral (Figure 5.6). At the other stations except La Serena, the dust activity has a winter (JJA) maximum, with some stations such as Arica, Antofagasta, Calama, Desierto de Atacama and Copiapó also exhibiting increased activity in spring and, Iquique and Vallenar exhibiting increased activity in autumn (MAM). In La Serena, the observations are too sparse to ensure the seasonality, but there is a minimum in June.

The seasonal variability of dust activity is smaller at Calama, Antofagasta, Vallenar and Chañaral compared to the rest of the stations. One possible explanation is the large number of dust activities reported in these four stations, which account for 81% of the total dust activity in the dataset (Chañaral accounts for almost 50%). The sparse reports in Arica, Iquique, Desierto de Atacama, Copiapó, and La Serena do not allow us to confirm the seasonality of dust activity. Furthermore, the strong interannual variability in monthly dust activity must be considered. As seen in Figure 5.7, there are periods of higher dust activity in the dataset, which may be related to human activities in the vicinity of the reporting stations and, therefore, not entirely due to changes in weather patterns. Nevertheless, the seasonality

in dust activity varies across the stations, with Chañaral exhibiting a minimum frequency in late autumn and winter. In contrast, other stations show maximum frequency in the winter.

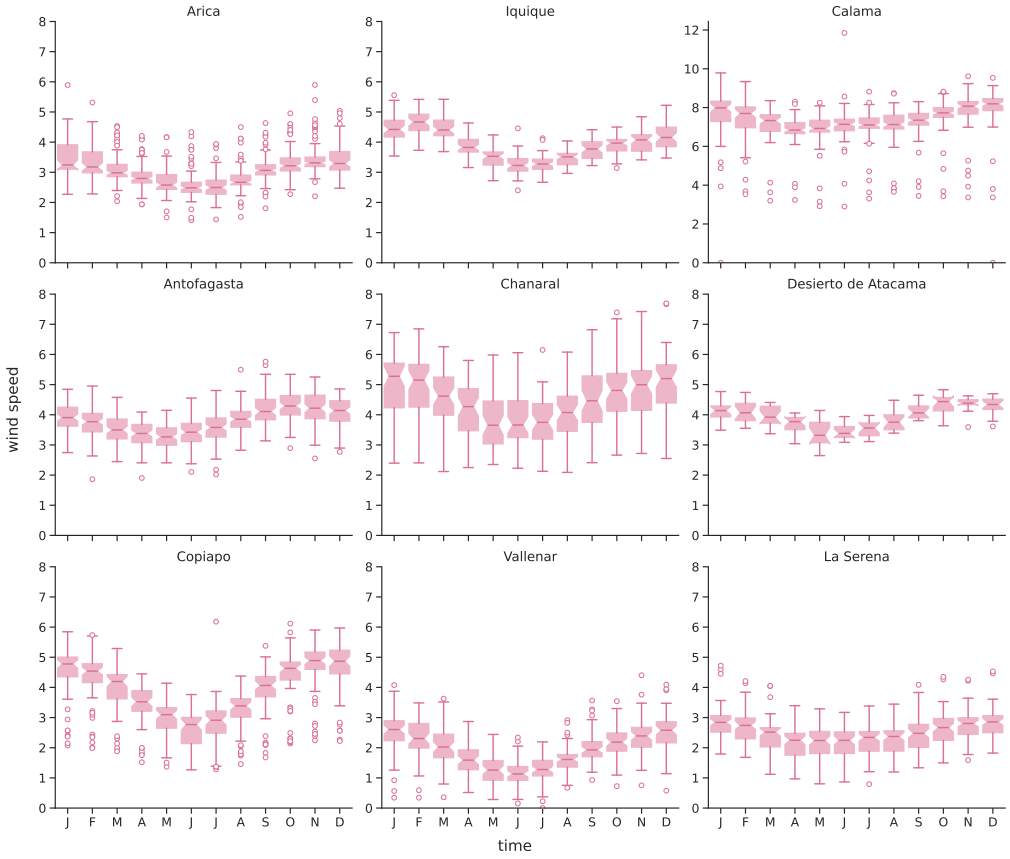

FIGURE 5.5: Seasonal distribution of 3-hourly mean wind speed for all observations in the period 1950–2021. Note the different y-axes for Calama.

Additionally, the seasonality of the different dust types was analysed. The dominant dust type recorded is suspended dust, with 63.5% of all dust events belonging to this group. Transported dust events are 17.6%, dust devils are 3.3%, and dust storms and severe dust storms are 4% and 0.8% of the total dust events, respectively. Other dust events include thunderstorms combined with dust storms at the time of observation (none present in the dataset) and the past weather code for dust. This represents 10.8% of all the dust events. 93% of the suspended dust is recorded in Chañaral. In Chañaral, the suspended dust activity has a clear seasonality with a minimum in winter while peaking in late spring and early summer (Figure 5.8). Transported dust activity shows variability from month to month and station to station with Chañaral and Vallenar (stations with most transported dust activity) exhibiting a maximum in late autumn and early winter and diminishing records through spring and summer. The frequency of dust storms and severe dust storms is the least in the dataset, but their impact is the most severe (Dirección Meteorológica de Chile - Servicios Climáticos 2016). In Figure 5.9, a seasonality is seen with a preference for winter and spring. This seasonality of dust storms is explored in detail in the next section.

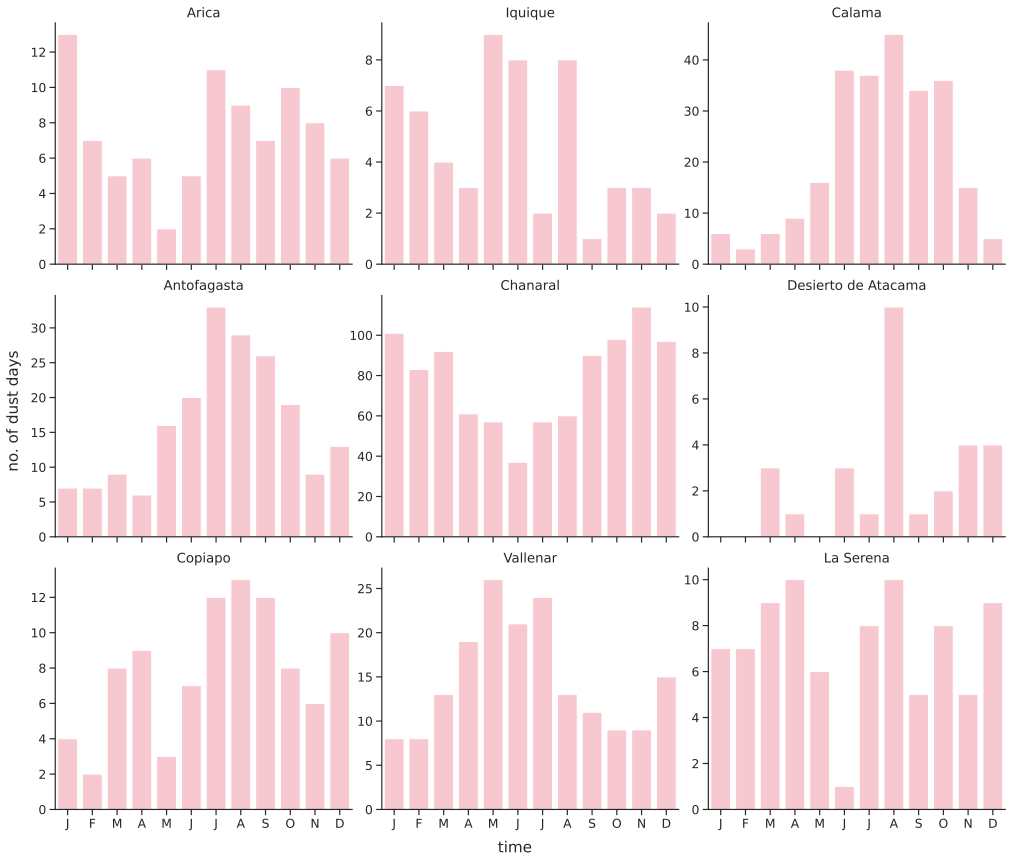

FIGURE 5.6: Total monthly dust days (1950–2021) at each station. Note the different y-axes.

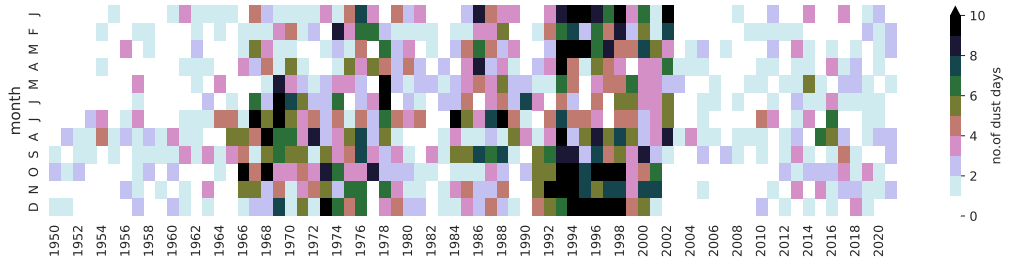

FIGURE 5.7: Heatmap showing the total number of dust days across the entire period for each month.

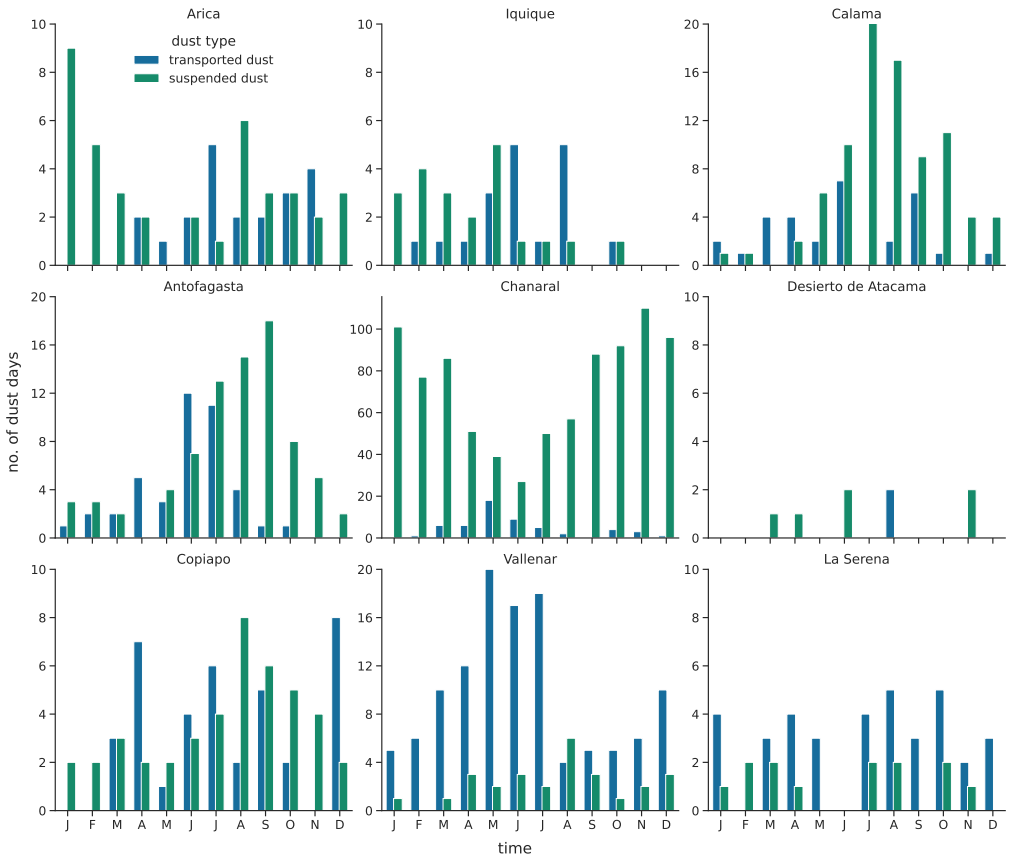

FIGURE 5.8: Monthly total number of suspended and transported dust days between 1950 and 2021 at each station. Note the different y-axes.

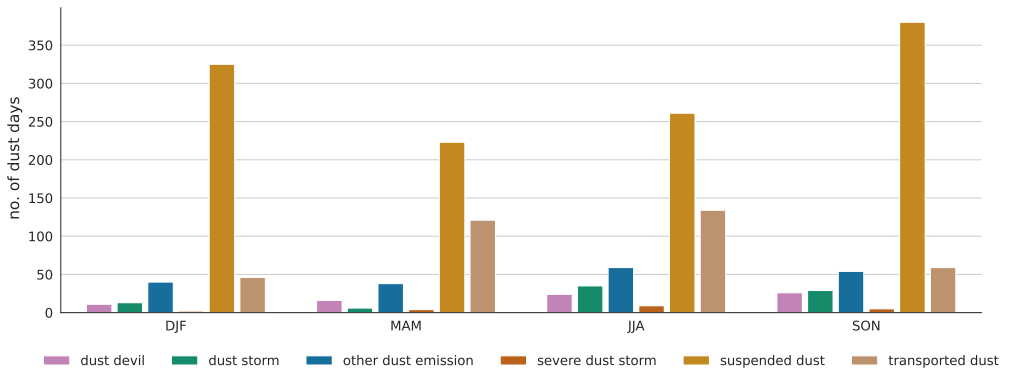

FIGURE 5.9: Total number of dust days between 1950 and 2021 for different seasons and dust types.

5.4 WEATHER PATTERNS AND DUST STORMS

There are 130 recorded dust storms in the entire period, with 36% and 34% recorded in winter and spring, respectively (Figure 5.10). Calama, a city on the outskirts of Chuquicamata, one of the world's largest open-pit copper mines in the world, recorded 42% of all dust storms. During the dust storms, the winds blew from the westerly, southwesterly and southerly directions and northwesterly directions (Figure 5.11). Although there is a preferential wind direction during dust storms, the low scatter from other directions hints at the possibility that several weather patterns may lead to dust activity. The mode of the wind speed distribution lies between 10–13 ms^{-1}. However, dust storms are recorded for lower and higher wind speeds than the mode. This range of wind speed distribution can be attributed to two instances: the threshold for dust emission and transport differs depending on the station where the dust storm was recorded. As stated in Chapter 3, these differences depend on soil properties. The dust storm may also be visible at a distance from the station, but the instruments capture only the wind speed at the station.

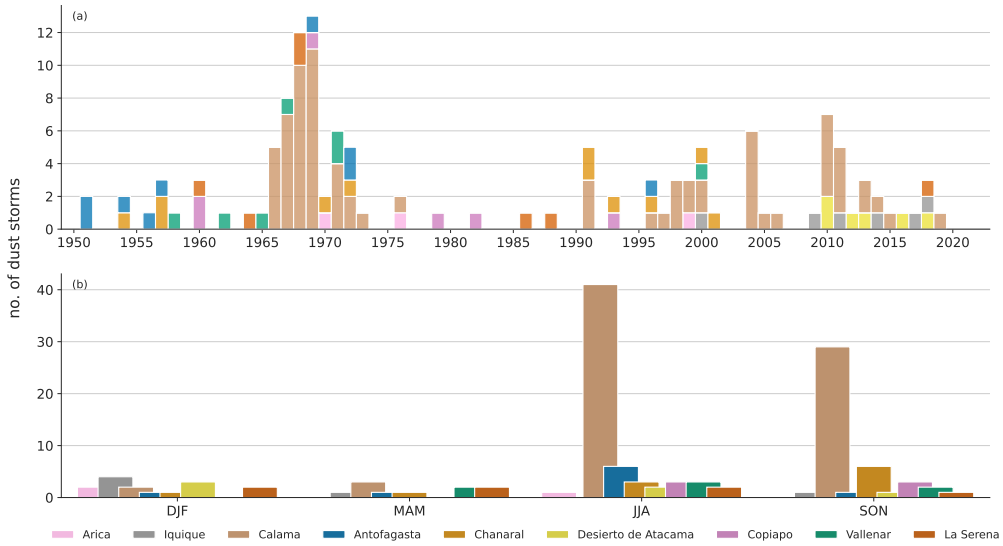

FIGURE 5.10: (a) Annual and (b) the seasonal total number of dust storms between 1950 and 2021 for the colour-coded stations, using the present weather codes, ww = [09,30–35].

The weather patterns for each dust storm based on visual inspection (Section Section 5.2.2) are classified and seven weather patterns associated with the dust storm reports are found. Most dust storms are driven by mid-tropospheric troughs (35.4%) and cut-off lows (22.3%) approaching the Atacama Desert from the west. 6.9% are surface lows and 12.3% UL troughs or mid-tropospheric troughs without surface projections. The remaining are driven by intense anticyclones (8.5%), coastal lows (8.5%) and ridges (6.1%) as seen in Figure 5.12.

The frequency of troughs connected to dust storms peaked during 1966–69, and since then, few have been related to dust storms. This increase is mainly recorded in Calama, but no corresponding increase in above-threshold winds was measured (see Figure 3.8 on page 38). Coincidentally, the exploration and development of the South Mine (Exotica) began in the 1960s and 1971, Chuquicamata was nationalised (Ossandón et al. 2001; Calderón-Seguel et al. 2021). There has been an increase in dust storms connected to CoLs since 1991. This increasing trend in CoLs in South America is also confirmed by other studies (Fuenzalida et al. 2005; Favre et al. 2012; Pinheiro et al. 2017; Ndarana et al. 2012), which attribute the increase in CoLs to either the increase in Rossby wave-breaking events which in turn might be linked to the depletion of the stratospheric ozone (Ndarana et al. 2012) or suggest that the increase in CoLs could be spurious trends as assimilation of observations and satellites in

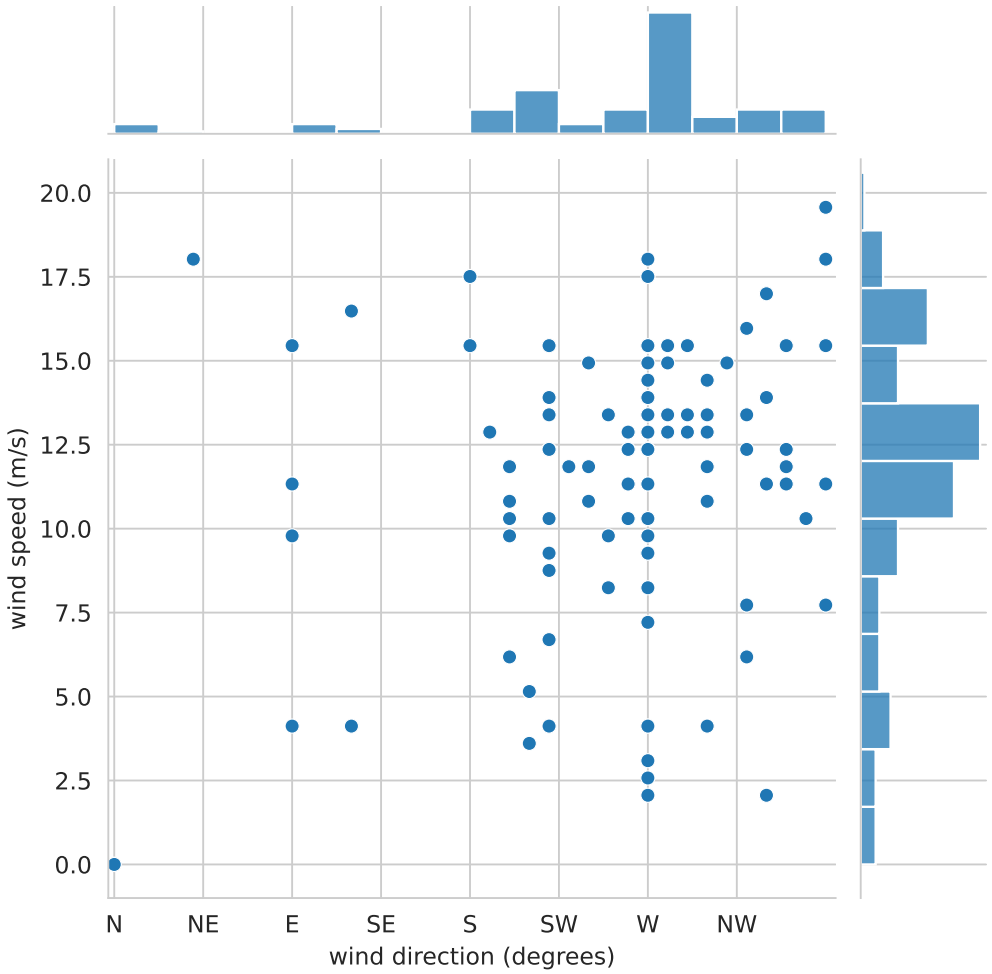

FIGURE 5.11: Distribution of 10 min mean wind speed and direction during records of dust storms. Note that the SYNOP code is recorded every 3 hours.

the recent years have contributed to the better quality of reanalysis data for the southern hemisphere (Pinheiro et al. 2017).

Troughs are vital to precipitation in the southern fringes of the Atacama (28°S), central and south Chile (Garreaud 2009; Falvey & Garreaud 2007; Barrett et al. 2011). CoLs are also vital as they are responsible for significant precipitation in northern and central Chile (Aceituno et al. 2021; Pizarro & Montecinos 2000; Fuenzalida et al. 2005). They can generate extreme rainfall events like that in March 2015, which resulted in the loss of life and damage to infrastructure (Bozkurt et al. 2016; Rondanelli et al. 2019; Barrett et al. 2016). Concerning dust activity, precipitation plays a dual role as it increases soil moisture and fosters aggregation of clay minerals, thereby inhibiting the emission potential of surfaces. In contrast, above-average rainfall in certain regions can increase the supply of erodible materials through river runoff and flash floods (Haug et al. 2010; Walk et al. 2020; Houston 2006b; Sepúlveda et al. 2006; Aguilar et al. 2021). Therefore, daily rainfall data were analysed to find rain events in three-day time windows ahead and behind dust storms. Non-zero precipitation around dust storms was found except for one record (on 11 Aug. 1993) of 1.3 mm rainfall in Chañaral, a day before a dust storm was recorded. This suggests that most troughs, cyclones and CoLs coincident with dust storms are mainly 'dry' in the Atacama and, do not produce any precipitation at the same station as the recorded dust storm.

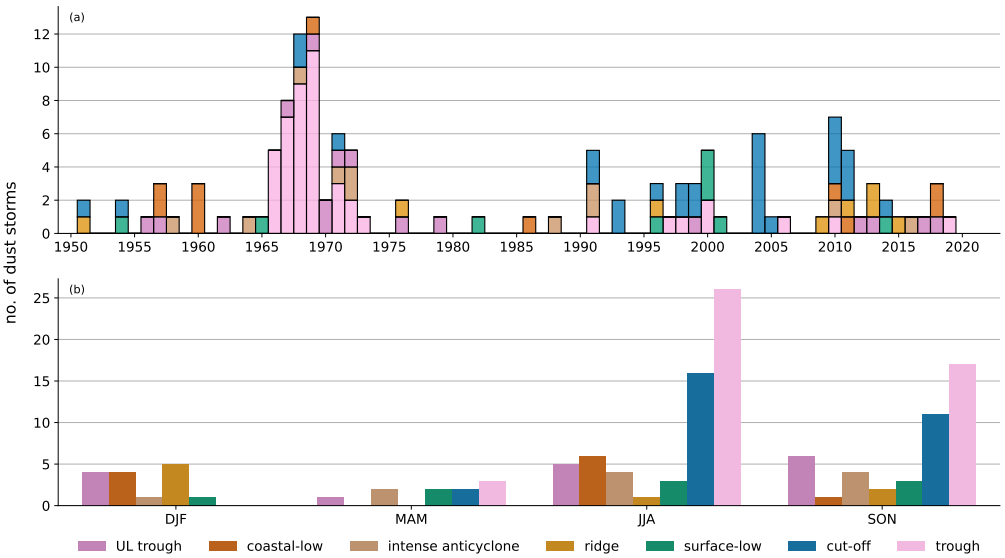

FIGURE 5.12: a) Annual and (b) seasonal total number of synoptic weather patterns associated with the recorded dust storms shown in Fig. Figure 5.10.

5.4.1 *Troughs and Surface Lows*

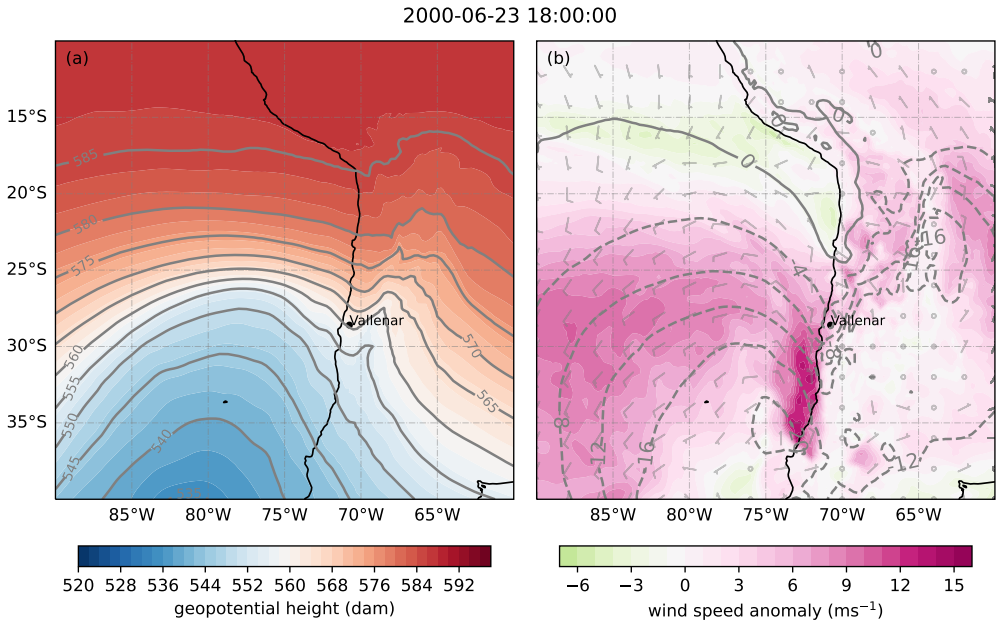

FIGURE 5.13: Winter dust storm in Vallenar. (a) Mid-tropospheric 500 hPa geopotential heights show a trough over the southeastern Pacific and continental Chile. (b) Surface cyclone associated with the mid-tropospheric trough driving northerly, northwesterly winds towards Vallenar, as shown with anomalies in the MSLP in hPa and in the 10 m wind speed in ms^{-1}.

Of the 130 dust storms detected at all stations, more than half the cases (55%) are connected to mid-tropospheric troughs, with 65% recorded in Calama and 35% at coastal stations, except La Serena where no dust storms associated with troughs have been identified. Surface signatures of mid-tropospheric troughs are rarely seen. In fact, of all the mid-tropospheric troughs related to dust storms at coastal stations, only 36% cyclonic disturbances or 'surface-lows' were observed at the surface level (Figure 5.13a & b). The mid-tropospheric troughs over Calama have a strong seasonality with 57% in winter, 37% in spring and 6% in autumn. This seasonality is present for 'UL troughs' and the surface lows with 32% in winter and 36% in spring. The winter maximum of the dust storms associated with troughs is possibly connected to the displacement of the SEPA to its northernmost position allowing the expansion of the region under the influence of the storm track from 35°S in summer to

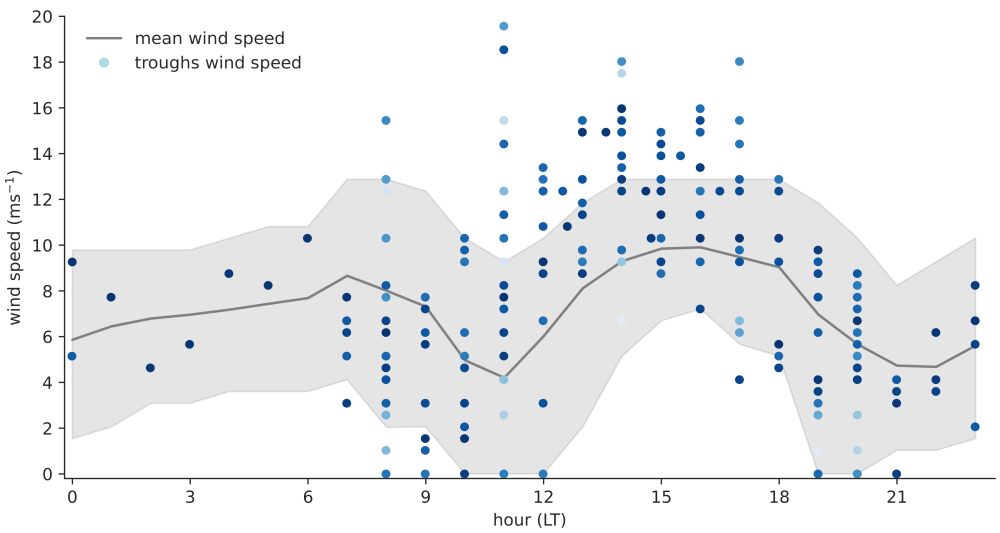

FIGURE 5.14: Wind speed composite for dust storms associated with troughs in Calama. The grey represents climatological mean wind speed in Calama, and the 5^{th}-95^{th} percentile interval of the wind speed at each station for hourly periods is shown with grey bands. The blue dots represent diurnal wind speeds during days with dust storms.

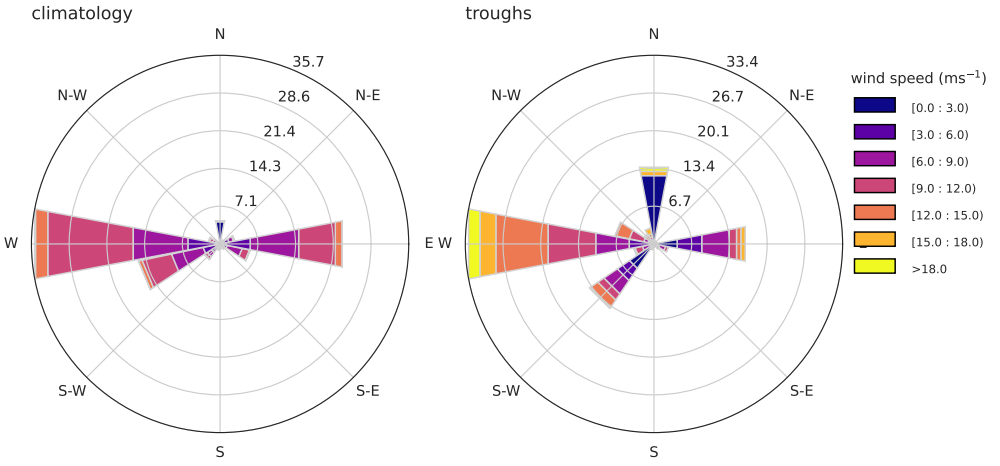

FIGURE 5.15: Composite analysis of wind direction during dust storms associated with troughs in Calama. The wind direction remains similar to the climatology except that they are strong. Strong winds from the north are also observed during troughs.

28°S in winter (Vuille & Ammann 1997; Rutllant & Ulriksen 1979; Hoskins & Hodges 2005; Garreaud 2013; Garreaud 2009).

Intense baroclinicity and, thus, strong winds related to the passage of frontal systems and their associated mid-tropospheric troughs lead to dust emission and transport. Along the Chilean coast, positively titled troughs (northwest-southeast) induce near-surface northwesterly winds, reinforcing the westerlies (Jacques-Coper et al. 2015) while weakening the characteristic southwesterly winds driven by the SEPA over the region. This is the case of the dust storm observed in Vallenar on 23-06-2000 (Figure 5.13a & b). Intensified northerly winds along the coast are observed in the reanalysis chart as the low-pressure approaches from the east. However, the cold Pacific waters, the presence of the SEPA, and the subsidence over the region usually inhibit cyclogenesis offshore Atacama, which can be seen with the few surface lows projected from troughs. Nevertheless, some fronts reach southern Atacama during winter and spring, inducing stronger winds along the coast.

The maximum number of dust storms associated with troughs is observed over Calama. This is because of its high altitude. As the mid-tropospheric troughs move over the region, near-surface winds intensify. However, the direction of the wind remains the same in most instances. This intensification of winds follows from the diurnal wind cycle, where during the day, westerly winds blow inland, but as the trough passes, the winds from the troughs couple with the climatological daytime westerly winds (Figure 5.14). For example, in Figure 5.15,

westerly winds up to 18 ms^{-1}, which is twice the maximum wind climatology can be observed. Therefore, the troughs can exceed the expected threshold wind speeds required for dust emission and induce dust storms. From Figure 5.14, it is evident that not all wind speeds are above the climatological mean. In certain cases, they are even below the mean. These instances could be due to non-local dust storms recorded by observation at the stations where the wind speed does not necessarily correspond to the dust storm at a distance that is receding or approaching. Using the horizontal visibility at the stations can help us identify such instances.

5.4.2 *Cut-off Lows*

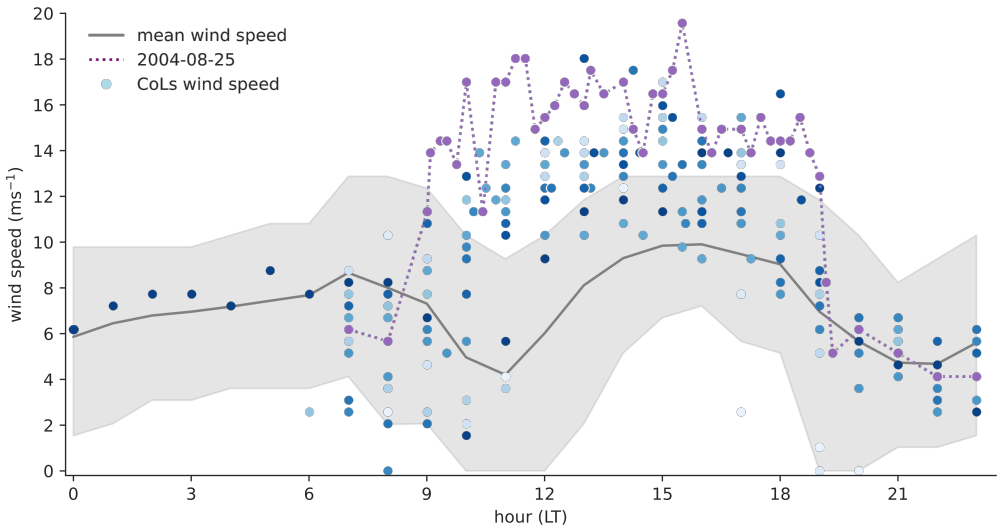

FIGURE 5.16: Wind speed composite for dust storms associated with CoLs in Calama. The grey represents climatological mean wind speed in Calama, and the 5^{th}-95^{th} percentile interval of the wind speed at each station for hourly periods is shown with grey bands. The blue dots represent diurnal wind speeds during days with dust storms. The purple line shows the wind speeds recorded in Calama during the dust storms on 25-08-2004 (Figure 5.18)

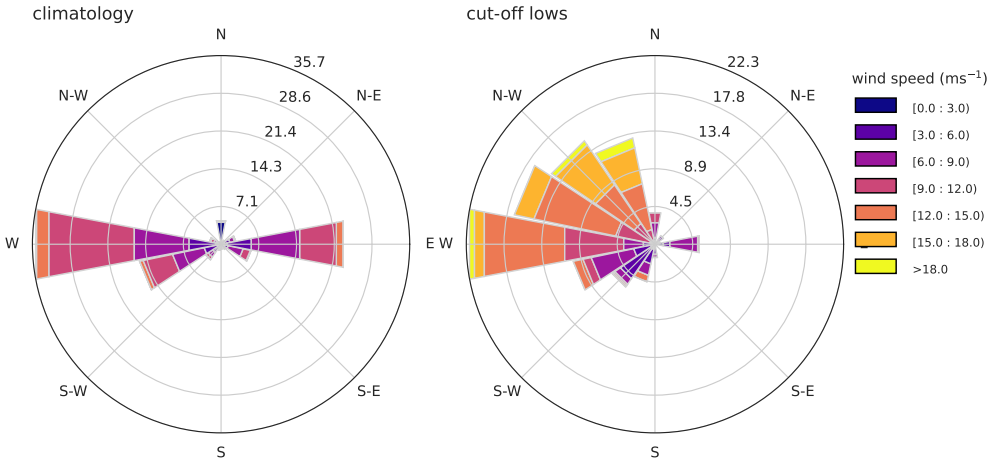

FIGURE 5.17: Composite analysis of wind direction during dust storms associated with CoLs in Calama.

Of all the dust storms recorded, 22.3% were associated with CoLs, with 83% recorded in Calama and nearly all in winter (55%) and spring (38%), which is consistent with the CoL seasonality (Muñoz et al. 2020; Fuenzalida et al. 2005; Reyers & Shao 2019). The remaining few CoLs (17% CoLs) producing dust storms were recorded in Chañaral, Antofagasta, La Serena and Copiapó. The CoLs are also projected to the surface (surface cyclones) in these cases. In Calama, where most of the CoLs are observed, the composite analysis reveals that the wind speeds during dust storms are significantly higher than the climatological mean and the

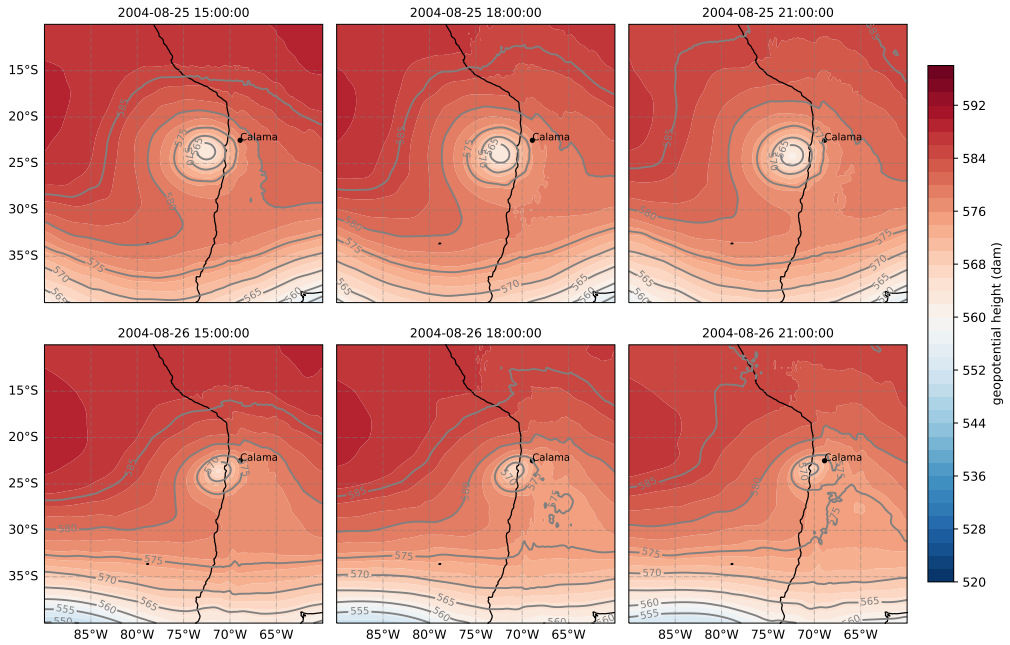

FIGURE 5.18: The geopotential heights at 500 hPa show a cut-off low over northern Chile, during which six dust storms over two days were recorded in Calama.

95^{th} percentile. A CoL west of Calama induces a similar effect as a trough approaching, with the CoL winds superimposing on the general westerly flow. However, as seen in Figure 5.17, the winds during CoL blow not just from the west but also the northwesterly directions depending on the position and shape of the CoL. For example, in Figure 5.18, the CoL induces northwesterly winds over Calama, which deviates from the climatology. The persistence of this CoL (CoLs usually last 2–3 days, Fuenzalida et al. (2005)) triggered six dust storms over two days (25-08-2004 to 26-08-2004).

As CoLs are cold air mass pockets in the mid-upper troposphere, they can induce instability in the lower troposphere and trigger local thunderstorms. This was the case of the CoL observed on 18 March 2023 (time not covered in the dataset), 100 km east of Chañaral, where a substantial dust outbreak was recorded. This CoL induced a dust storm, accompanied by high humidity on the preceding days and was followed by a thunderstorm. Dust storms associated with CoLs are infrequent at the coastal stations. This is perhaps because not all CoLs project onto the surface, a prerequisite for triggering dust storms in the coastal regions to enhance the surface winds. For example, Campetella and Possia (2007) analysed the 250 hPa geopotential height data for the period 1979–1988 over the southern South American region and reported that out of 171 CoLs detected, only 25% had a surface cyclonic circulation with high-frequency of occurrence south of 40°S. Given that only 29 CoLs over 72 years are associated with dust storms, it is evident that not all CoLs drive dust storm-emitting winds, making these rare events. The CoL projection towards the surface is probably more efficient for Calama as the station is at a higher altitude than other stations. Therefore, it is more influenced by mid-upper troposphere disturbances.

5.4.3 *Intense Anticyclones and Ridges*

In the Atacama, 8.5% of dust storms were found to be coincident with intense (anomalously high) anticyclones over the Southeast Pacific. They were recorded at all stations except the inland station Calama, the northernmost stations of Arica and Iquique, and, in Copiapó. Of the 11, four dust storms were in winter, four in spring, two in autumn, and one in summer. The effect on the surface of the strong anticyclone is the enhanced zonal pressure gradient

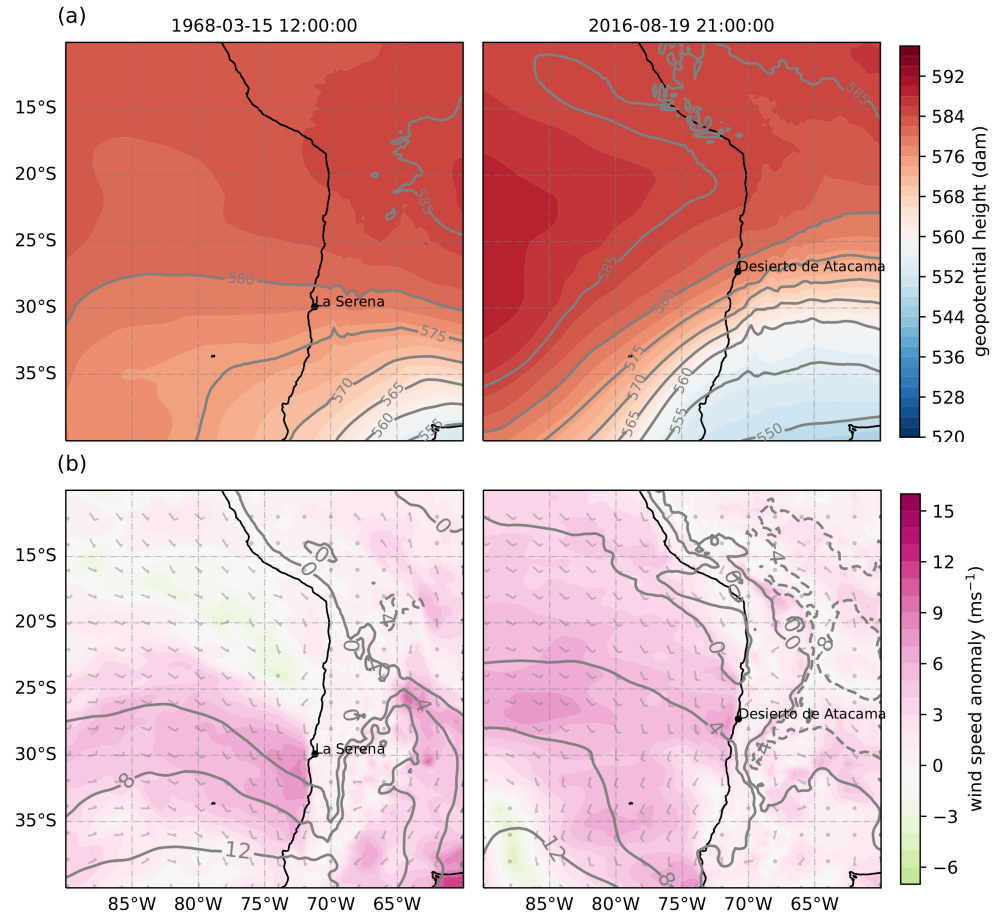

FIGURE 5.19: Two dust storms were recorded at different times in La Serena and Desierto de Atacama. (a) Mid-tropospheric charts show geopotential heights at 500 hPa with (b) the mean sea level pressure (hPa) and 10 m wind speed anomalies at the surface. At both stations, an anomalously high anticyclone and correspondingly high anomalous wind speeds can be seen.

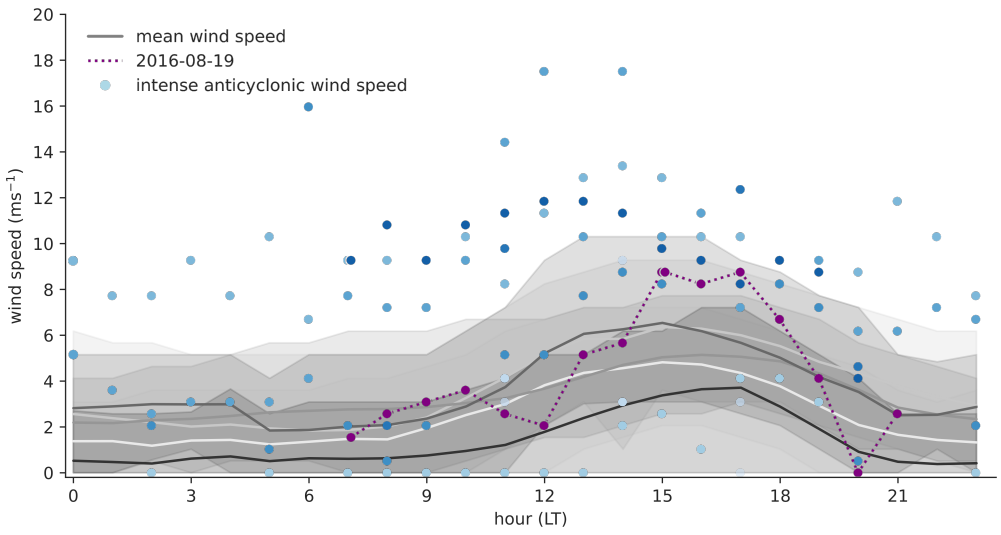

FIGURE 5.20: Diurnal wind speed composite for days with dust storms associated with intense anticyclones in Antofagasta, Desierto de Atacama, Vallenar, La Serena and Chañaral. The grey lines represent climatological mean wind speeds at each of these stations, and the 5^{th}-95^{th} percentile interval of the wind speed at each station for hourly periods is shown with grey bands. The blue dots represent diurnal wind speeds during days with dust storms. The purple line shows the recorded wind speeds during the 19-08-2016 dust storm in Desierto de Atacama (Figure 5.19b).

between the ocean and the coast, driving stronger than average southerly winds, which are more intense during winter and early spring around the region 28–30°S (Aguirre et al. 2021; Garreaud & Muñoz 2005). This agrees with the seasonality of dust storms driven by intense anticyclones, but several more instances are required for a robust estimation. The intense

anticyclone requires a ridge approaching from the west, intensifying the surface pressure. The enhanced anticyclone, connected with the migratory ridge, mainly affects the stations located in central and southern Atacama, which experience stronger than average coastal winds.

Two examples are presented in Figure 5.19, with two dust storms observed in La Serena and Desierto de Atacama on 15-03-1968 and 19-08-2016, respectively. The ridge approaching from the west and trough moving to Argentina are conducive to intensified coastal winds from the south, expressing an enhanced coastal jet with intensity up to 6 ms^{-1} in the reanalysis. A similar effect is observed in the diurnal cycle of the dust storms associated with intense anticyclones, where the observed winds exceed the climatological median and 95th percentile, even during the night (Figure 5.20), although maintaining similar wind direction compared to the climatology.

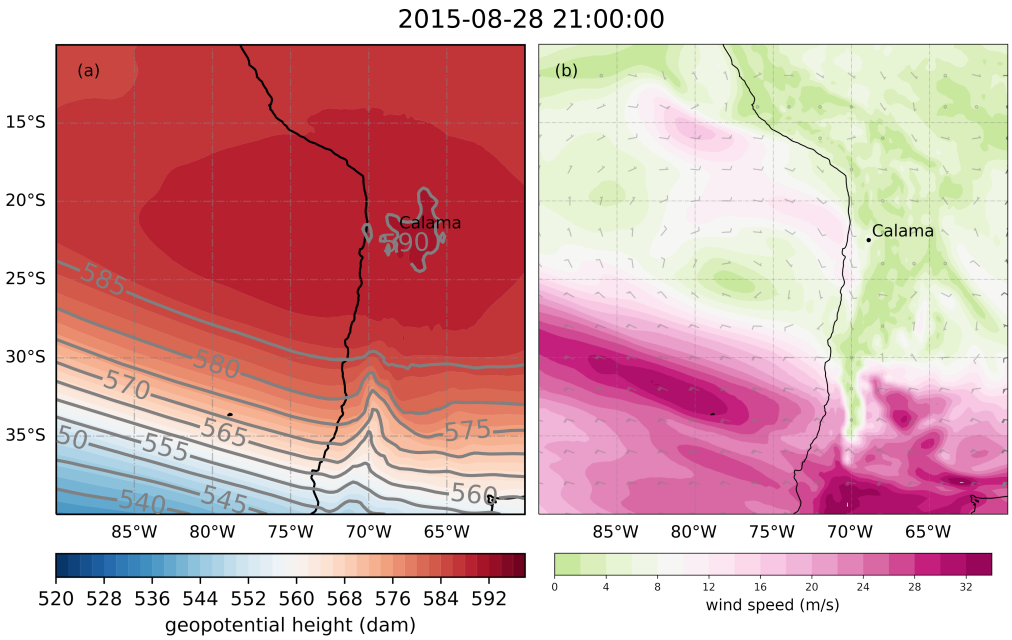

FIGURE 5.21: (a) Mid-tropospheric chart shows the geopotential heights at 500 hPa with a ridge over Calama (b) wind speed and direction at 700 hPa geopotential height

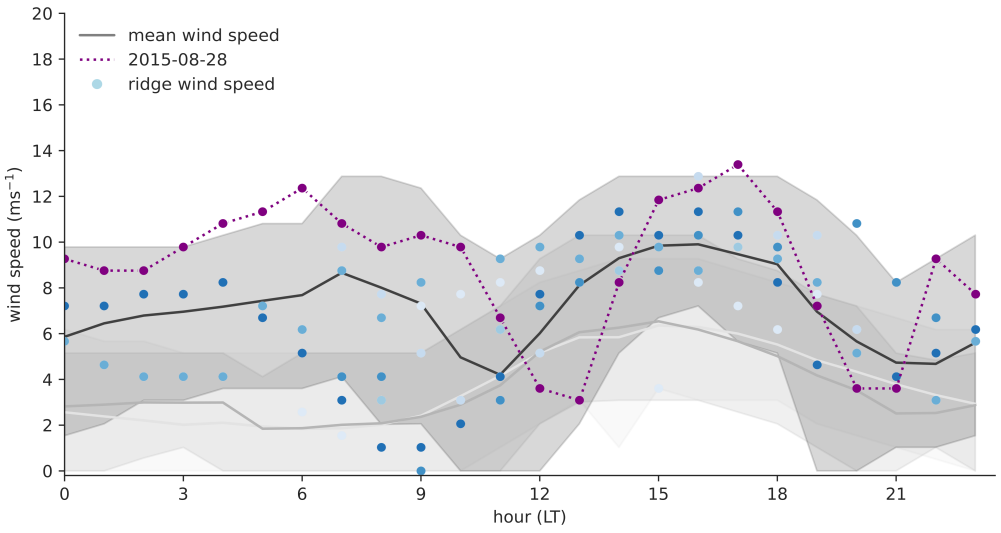

FIGURE 5.22: Diurnal wind speed composite for days with dust storms associated with ridges in Calama, Antofagasta, Iquique and Chañaral. The grey lines represent climatological mean wind speeds at each of these stations, with the black line representing Calama, and the 5th-95th percentile interval of the wind speed at each station for hourly periods is shown with grey bands. The blue dots represent diurnal wind speeds during days with dust storms. The purple line shows the wind speed in Calama during the 28-08-2015 dust storm (Figure 5.21).

Mid-tropospheric ridges (6.1%), albeit a few, are also associated with dust storms. Of the

eight instances of dust storms associated with mid-tropospheric ridging, these were primarily recorded in Calama and, one each in Antofagasta, Chañaral and Iquique, and five were in summer, one in winter, and two in spring. These ridges do not produce a strong anticyclone on the surface. However, the location of the centre of the ridge to the southeast of the station that recorded a dust storm indicates an easterly flux over the Atacama Desert in almost all cases. An example of this particular location of the centre of the ridge is presented in Figure 5.21 on 28-08-2015, in which a dust storm observed in Calama shows enhanced easterly winds (as recorded in SYNOP data) in the lower free troposphere (700 hPa) from 22 LT on 27-08-2015 to 10 LT on 28-08-2015, reaching a maximum of 12.4 ms^{-1} which is infrequent during the night. These winds remain strong until the wind changes direction at noon and, from 13 LT, the wind blows from the west with it increasing from 14 LT and the second maxima occurring at 17 LT, reaching 13.4 ms^{-1} (Figure 5.22). In the reanalysis data, there is some evidence of intensified winds close to Antofagasta but restricted to the coast. It is suspected that ERA5 is unsuitable for resolving near-surface changes in wind intensity and direction due to the complex topography and coarse resolution. For all the cases identified as ridges in the SYNOP dataset, there is an increase in the anomalous wind speed (1–3 ms^{-1}). However, it is difficult to assess the mechanism for dust emission in these instances as the number of cases is reduced.

5.4.4 *Coastal Lows*

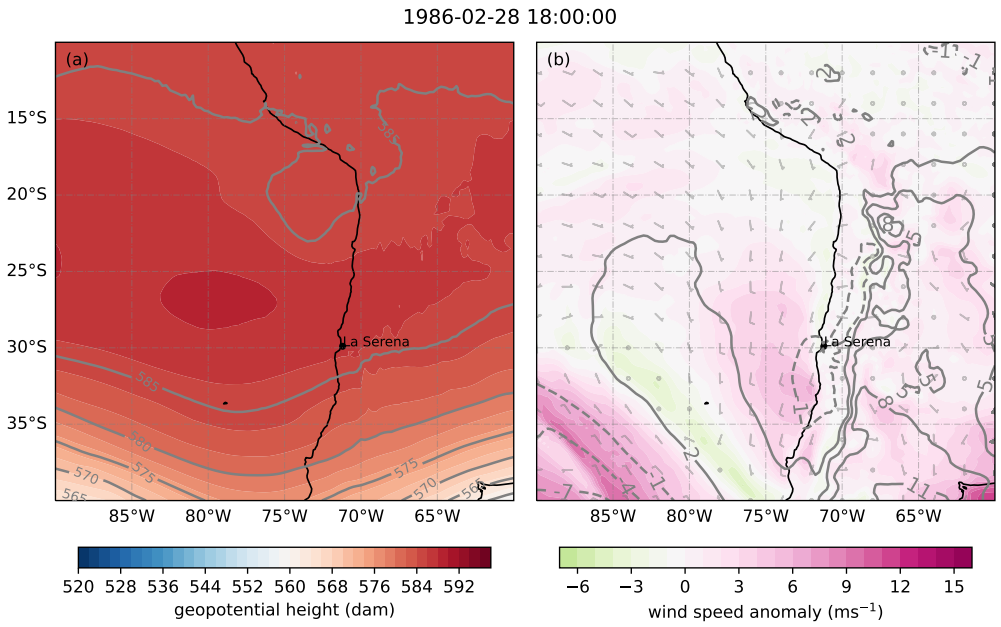

FIGURE 5.23: A coastal low at the time of a summer dust storm recorded at the station in La Serena. (a) A mid-tropospheric chart showing geopotential heights at 500 hPa. A ridge is seen extending over the station and the Andes, and (b) the mean sea level pressure (in hPa) and wind speed anomalies chart shows a westward displaced SEPA and a negative pressure anomaly (dotted contour line) along the north-central Chilean coast.

The last category of weather patterns responsible for 8.5% of dust storms is associated with coastal lows in Copiapó, La Serena, Desierto de Atacama, Chañaral and Iquique. Four of the eleven coastal lows were recorded in summer, six in winter and one in spring. The coastal lows form when a migratory anticyclone at around 40°S crosses the Andes (Garreaud et al. 2002). It develops at around 30° S and moves poleward, reversing the alongshore pressure gradient. This enhances easterly winds along the valleys leading to down-slope winds, named as *Terral* by local communities in north-central Chile (30°S, also La Serena) (Rutllant & Garreaud 2004; Montes et al. 2016), which do not always reach the coast. The hourly surface wind speed can reach intensities up to 14 ms^{-1} at any moment of the day as

the coastal low moves southward (Pinto 2019), leading to strong wind gusts, which may allow the lifting of dust. An example of this pattern is presented in (Figure 5.23), in which La Serena recorded a dust storm when a ridge at 500 hPa approached the coastal Atacama from the west, leading to an anomalous surface-low pressure in Central Chile.

Coastal lows are relatively frequent in Central Chile (roughly 1 per week) but are related to only a few cases of dust storms. This is probably because the southern edge of the Atacama, where coastal lows are prevalent, has soil conditions less conducive to dust emission (e.g., more vegetation). The coastal lows may also influence other stations north of La Serena as the surface pressure decreases towards the south, inducing stronger than average northerly winds, uncommon at the coastal stations (Figure 5.24). These winds need not necessarily be stronger than the climatological mean as the wind direction seems crucial (Figure 5.25). However, it is hard to explain the one case of dust storm at Iquique in connection with the coastal low as this station is far too north to be affected by changes in wind intensity and direction in the southern Atacama. Therefore, it is highly likely that other factors might play a role.

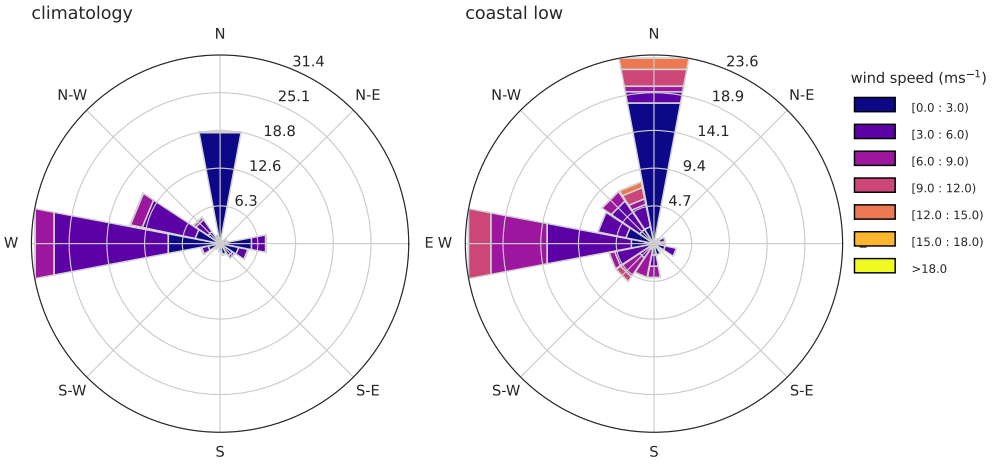

FIGURE 5.24: Composite analysis of wind direction during dust storms associated with coastal lows in Copiapó, La Serena, Desierto de Atacama, Chañaral and Iquique. The climatological wind rose is from La Serena, which is used as a reference station as coastal lows most influence it compared to other stations in the dataset.

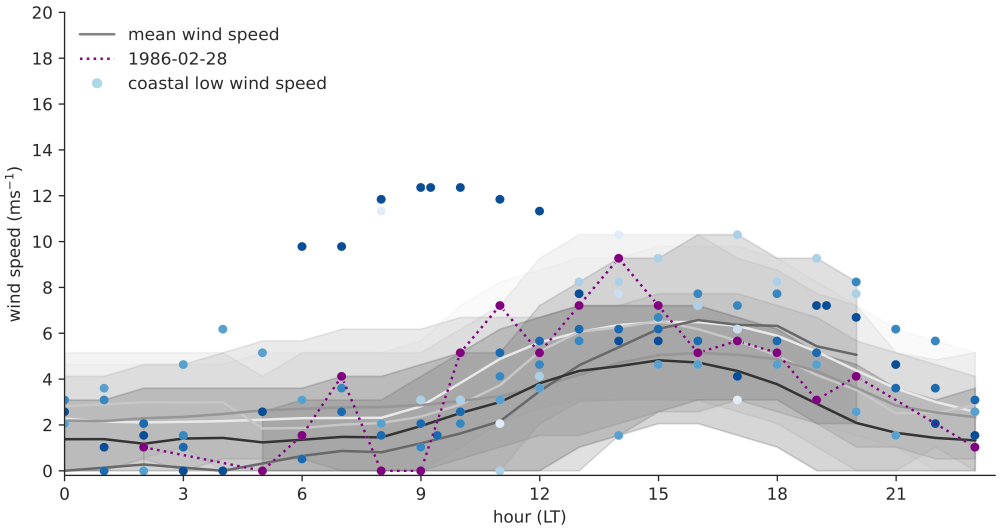

FIGURE 5.25: Diurnal wind speed composite for days with dust storms associated with coastal lows in Copiapó, La Serena, Desierto de Atacama, Chañaral and Iquique. The grey lines represent climatological mean wind speeds at each of these stations, with the black line representing La Serena, and the 5^{th}-95^{th} percentile interval of the wind speed at each station for hourly periods is shown with grey bands. The blue dots represent diurnal wind speeds during days with dust storms. The purple line shows the recorded wind speeds during the 28-02-1986 dust storm in La Serena (Figure 5.23).

5.5 DISCUSSION

Meteorological processes from the micro-scale influence dust emission and transport to the global scale. Both suspended dust and dust storms can be driven by several meteorological processes, such as the passage of fronts, convective systems like thunderstorms, and cyclogenesis; in addition, suspended dust can also be driven by diurnal winds and downslope winds from mountains like Chinook or Katabatic winds (Orgill & Sehmel 1976). The diurnal cycle of dust activity in the Atacama closely follows the wind speeds, which are maximum during the daytime. During the day, the strong solar insolation and thermal instability promote dry convection within the different levels of the atmosphere with the downward transport of high-momentum winds from the upper levels to the surface, thereby resulting in increased wind speeds at the surface (Stout 2010). The particles are suspended if this wind speed exceeds the dust emission threshold.

Dry convection is most likely the driver of the diurnal dust activity, given the link between thermal wind circulation and the diurnal cycle of dust activity. However, a supporting analysis from radiosonde measurements looking into the temperature and humidity profiles is necessary. It is hard to assess the natural seasonality of dust in the Atacama. The station-wise differences in seasonality point towards different meteorological drivers and varying soil conditions influencing dust activity. In Chañaral, where the seasonality in dust activity deviates from that of other stations, the dust activity follows the seasonality of the wind speed modulated by the SEPA. But it is important to note that 200–300 Mt mine tailings were deposited at the Chañaral Bay, north of the town, between 1930–1990 (Ramirez et al. 2005; Dold 2006; Castilla 1983; Martínez et al. 2016; Lee & Correa 2005; Neary & Garcia-Chevesich 2008) which means that more erodible material is available close to the station. This is further supported by the high count of suspended and transported dust events recorded at the station. At other stations, a maximum frequency of dust activity in winter closely follows the seasonality of dust storms associated with mid-tropospheric troughs and cut-off lows. But, dust records are too low, unlike that in Chañaral, to be specific.

The synoptic weather patterns were classified based on visually identifying the dominant weather pattern during which a dust storm is recorded. While most studies look at either surface features or upper-level features and not both, for the Atacama, this is simply insufficient because of the influence of the SEPA, the strong thermal inversion at 800–1000 m, and the location and elevation of the stations in the study. Implementing objective classification methods like principal component analysis, k-means, or machine learning techniques such as hierarchical clustering or self-organising maps would benefit a station like Calama, which has sufficient dust storm records. However, a simple visual classification for the coastal stations saves time and resources. Nevertheless, it is to be acknowledged that this method does come with a host of issues typified by the domain size and static time, such as the difficulty in identifying weather conditions when the feature used for the classification has a different position in the study domain and, the lack of information on the evolution of a weather condition (e.g., coastal low) from using only one-time instance. There also exists the issue with 'mixed' cases where more than one dominant feature is present in the domain (the category ridges contain three 'mixed trough-ridge' systems) and that the categories need to be defined a priori to the classification, which challenges the accuracy of visual identification.

In addition to the visual identification, the insufficient grid resolution of ERA5 might make it unable to capture the steep change in topographic features in northern Chile. The SYNOP data also suffers from various limitations (O'Loingsigh et al. 2010), including missing observations and incorrect assignments. For example, the dust storm on 8 July 2019 over Arica and Iquique, which was triggered by the presence of a mid-tropospheric trough (Reyers

et al. 2019), had weather codes 06 (transported dust) and 07 (suspended dust) at both stations despite the measurements in Iquique measuring wind speed 17 ms^{-1} and visibility zero at 12 UTC.

In 2023 alone, three dust storms were reported over social and news media and by Chilean authorities. Upon a quick analysis, it was found that on 14 June, a mid-tropospheric trough coincided with a dust storm in Antofagasta. On 3 September, another dust storm was driven by a mid-tropospheric trough. This highlights the need for further investigation of the mechanisms involved in intense dust activity through case studies and regional dust modelling to better understand what differentiates the synoptic weather patterns that trigger these events and those that do not. Furthermore, social media could be a strong tool for identifying dust storms in Atacama, partially overcoming the sparse network of airports and measurement stations.

5.6 CONCLUSION

Using SYNOP data, it is shown that the diurnal cycle of dust activity is connected to the thermal wind circulation in the Atacama, with dust activity peaking just before the wind speed maxima, driven most probably by dry convection. The dust-emitting winds blow from the south, southwest and westerly directions. The seasonality in dust activity varies across the stations, with Chañaral exhibiting a minimum frequency in the late autumn and winter. In contrast, other stations show maximum frequency in the winter. Dust storms, too, show a strong winter seasonality.

42% of the 130 dust storms were recorded in Calama, with 70% of the dust storms in the austral winter and spring were found. Using ERA5 data, five synoptic weather patterns associated with dust storms in the Atacama Desert were found. The mean sea level pressure, 10 m wind speed and direction and the geopotential heights at 500 hPa and 700 hPa pressure levels were used. Upon visual inspection, it was found that more than half of the dust storms were associated with mid-tropospheric troughs and their surface lows (54.6%), 22.3% with cut-off lows, 8.5% each with intense anticyclones and coastal lows and 6.1% with ridges. Composite analyses of wind speed and direction from station observations revealed that these weather patterns induce strong winds above the climatological mean and blow differently from the characteristic wind direction. Either of these criteria is often sufficient to trigger dust storms.

The visual analysis of ERA5 data showed that this reanalysis data is unsuitable for understanding surface winds in the interior of the Atacama. However, it proved sufficient for identifying large-scale patterns from 1950 to 2023. However, an in-depth analysis of the dust-triggering mechanisms should be conducted. In that case, more observations and high-resolution simulations that take into account the complex topography of the Atacama are required. Satellite data should also be investigated to compensate for the spare network coverage in the desert.

Part IV

CONCLUSION

6

Discussion and Summary

6.1 OUTLOOK

6.1.1 *Anthropogenic dust activity*

"Water, water, water.... There is no shortage of water in the desert but exactly the right amount, a perfect ratio of water to rock, water to sand, ensuring that wide free open, generous spacing among plants and animals, homes and towns and cities, which makes the arid West so different from any other part of the nation. There is no lack of water here unless you try to establish a city where no city should be."

—Desert Solitare, Edward Abbey

This work aimed to understand natural dust activity in the Atacama Desert. However, in the process of analysing the data and making sense of the irregularities surfacing from the results, I realised that, unlike other deserts in the world where human activity is sparse, the Atacama is teeming with industrial activity given the rich abundance of valuable minerals in the desert. The Atacama Desert is a hotbed of mineral extraction, especially for metals such as copper and lithium. Mining activities not only contribute to dramatic land and water degradation but also to anthropogenic dust-aerosols in the atmosphere (Jung et al. 2020a; Li et al. 2019; Zanetta-Colombo et al. 2022; Carkovic et al. 2016). This, no doubt, has had some influence on the dust activity recorded in the SYNOP dataset. Although it is hard to disentangle the natural from the anthropogenically triggered dust activity, the spatiotemporal distribution of dust activity in Chañaral and reports of severe mining pollution in the region (Ramirez et al. 2005; Dold 2006; Castilla 1983; Martínez et al. 2016; Lee & Correa 2005; Neary & Garcia-Chevesich 2008; Wisskirchen & Dold 2006), combined with the analysis of the wind speeds across the Atacama from this thesis, strongly suggests that dust records driven by anthropogenic activities are inextricably linked in the SYNOP dataset.

Similar findings have been reported in Oyarzún (2021) for regions close to Calama and the Antofagasta region, where the $PM_{2.5}$ measurements exceeded the WHO guidelines for safe air quality and, Li et al. (2019) found that the dust traps near open-pit mines recorded higher dust flux than other regions. While the anthropogenic influence might be evident in the dust records of Chañaral, in Copiapó, it is more conspicuous (see Figure 3.8). Silver mining has flourished around the region since the early nineteenth century, with copper now at the forefront. Agriculture and industries have expanded in a region with a mean annual precipitation of $20\,\mathrm{mm\,yr^{-1}}$. Consequently, the water consumption has increased, leaving behind a dry river bed (Carkovic et al. 2016; Greenfield 2022). With the global demand for lithium and other rare earth metals poised to skyrocket in the future (Kaunda 2020; Gajardo & Redón 2019; Greenfield 2022; Sengupta 2021; Riofrancos 2021), land-use change [8] and groundwater supply will become important drivers of dust activity in the Atacama.

[8] Mining companies are vying for the Maricunga salt flat, 160 km north-east of Copiapó (Greenfield 2022)

The difference in global dust cycle between model simulations and reanalysis and satellite data can potentially stem from the lack of or underestimation of anthropogenic dust (Kok et al. 2021) and its contribution to the global dust cycle (Ginoux et al. 2012a; Tegen et al. 2004). The extent to which human activities influence dust emissions directly via changes in land cover or indirectly via climate change is poorly quantified (Boucher et al. 2013; Zender

et al. 2004). Studies have concluded that global annual dust emissions have increased by 25% between the late nineteenth century and today, with both climate change and anthropogenic land cover change being essential drivers of dust emission changes, with 56% and 40% contributions respectively (Stanelle et al. 2014). Other estimates of dust emission driven by direct human activity vary from 10% to over 60% of the global dust emissions (Ginoux et al. 2012b; Xi & Sokolik 2016; Mahowald et al. 2010; Tegen et al. 2004; Mahowald & Luo 2003). This uncertainty may only worsen given that the global extraction of raw materials is expected to increase by 60% by 2060 (Neslen 2024).

The adequate way to quantify the anthropogenic dust activity in the Atacama Desert would be to measure the dust concentration at mining sites [9] via air quality monitors. Continuous air quality monitoring will help ascertain the frequency and emission rates of anthropogenically induced dust activity such as mining. However, in a real world where installation and access to such data might be complicated, quantifying the threshold wind speed needed to entrain dust from disturbed land surfaces is perhaps enough to approximate the dust emission potential from mining areas. From this work (see Section 4.3), we know that the threshold wind speeds for dust emission are lower for disturbed surfaces (5–9.5 ms^{-1}) than the naturally crusted surfaces in the Atacama (8–15 ms^{-1}). While the disturbed surface in the in-situ measurements is not precisely comparable to mining-related surfaces and the soil properties differ (Chane Kon & Korre 2007), it is valuable for differentiating natural and anthropogenic dust activity in the Atacama.

[9] Dust emitted from mining-related activities is called fugitive dust.

6.1.2 *Solar energy*

The dry conditions and high solar irradiance (Rondanelli et al. 2015; Molina et al. 2017; Cordero et al. 2018a), make the Atacama Desert a viable source for producing solar power. Photovoltaic power (PV) already represents 92.9% of the total installed capacity in Chile (Bayo-Besteiro et al. 2023) with PV power slated to cover 30% of all its energy supply by 2030 (Bayo-Besteiro et al. 2023). However, only some studies have explored the impact of dust aerosols on the efficiency of PV panels in the Atacama (Oyarzún 2021; Cordero et al. 2018a). In semi-arid and arid regions, dust aerosols can significantly accumulate on PV panels, reducing efficiency. For example, one study found that infrequent precipitation and high dust deposition led to significant annual energy losses in Arica and Iquique (39% and 18%, respectively). However, annual energy losses of 3% and less were estimated for high-altitude sites like Calama and southern coastal Atacama sites like Copiapó and La Serena (Cordero et al. 2018a). For perspective, the values calculated for Arica are on par with annual energy losses in North Africa and the Middle East, while elsewhere, it is typically within 1–7% (Cordero et al. 2018a).

The locally varying threshold wind speeds calculated in this thesis from ground-based observations and in-situ measurements reveal that the threshold wind speed for dust emission differs locally. Furthermore, we have the spatiotemporal distribution of dust storms for the Atacama. These results can help determine the best locations for future PV power projects in the Atacama. Interestingly, the low soiling rates obtained in (Cordero et al. 2018a) for Calama, Copiapó, and La Serena fit with the high thresholds computed for these sites. The high soiling rates estimated for Arica and Iquique suggest that the PV panels require more maintenance on these sites. However, this contrasts with this study, which shows that high thresholds are necessary for dust emission in Arica and Iquique, suggesting that they are ideal for PV panels. The results from this thesis also show that contrary to the peak dust activity simulated in models (Ginoux et al. 2012b) and satellite data (Oyarzún 2021), a higher soiling rate and possibly lower power production (aerosol extinction) is to be expected in winter and

spring given the seasonality of dust storms in the region (especially in Calama). However, the average daily soiling rate in Calama was nearly three times greater in summer and autumn than in winter and spring. This underlines the need for satellite-based and ground-based AOD validation (AERONET, for example) of results from this thesis.

6.1.3 *Modelling dust emissions*

Dust aerosols are lifted off the surface when the surface winds reach a threshold (Gillette 1978; Morales 1979; Helgren & Prospero 1987). This threshold depends on several soil characteristics, such as particle size distribution and surface roughness elements, such as vegetation and soil moisture, to name a few (Gillette et al. 1980a; Gillette & Passi 1988; Zender & Kwon 2005; Mahowald et al. 2005; Mahowald et al. 2003; Ginoux et al. 2012b; Shao et al. 2020; Fécan et al. 1998; Raupach et al. 1993). Given this dependence on soil properties, the threshold varies spatiotemporally (Helgren & Prospero 1987). As this high-resolution data is not available, especially for arid regions, climate models, global and regional, employ a static threshold wind speed of usually $6\,\mathrm{ms}^{-1}$ over arid regions (Donner et al. 2011; Tegen & Fung 1994; Takemura et al. 2000; Zhao et al. 2018). Some models do, however, parameterise the threshold wind speed as a function of soil moisture, surface roughness and vegetation cover (Shao 2001; Ginoux et al. 2001; Zender et al. 2003a). However, these dependencies themselves are not well resolved.

The threshold wind speeds calculated in this work suggest that the constant threshold value of $6\,\mathrm{ms}^{-1}$ is very low for the Atacama, and models need to increase this value to at least $10.9 \pm 1.6\,\mathrm{ms}^{-1}$. If models account for this new threshold combined with soil properties, then dust emission in the Atacama Desert might be better captured. Furthermore, using this study, it is found that mesoscale systems like coastal lows generate wind speeds sufficient to trigger dust storms in the region. However, global climate models do not accurately capture mesoscale dust activity (Schepanski et al. 2009; Klose & Shao 2013) such as dust devils (Klose & Shao 2016; Jemmett-Smith et al. 2015; Koch & Renno 2005; Klose & Shao 2013) and dust emitted via downdrafts from advancing thunderstorms [10] (Ridley et al. 2013) which possibly contributes to the uncertainties in the dust loading in this region. Additionally, the analyses (Section 3.4 & Section 5.6) suggest that reanalysis datasets are unsuitable for capturing the near-surface winds in the Atacama probably owing to the complex topography of the region. Improved representation of mesoscale processes in climate models and high-resolution reanalysis data might reduce some of the uncertainties in dust emissions from the region.

[10] Dust storms driven by moist convection are rare in the Atacama but one such event did occur on 17 March 2022 in Diego de Almagro, Southern Atacama.

6.1.4 *Desert dust in a changing climate*

With the changing climate, studies have found that there is a negative trend in precipitation in central and southern Chile, a poleward shift of the storm track and the expansion of the subtropical dry regime under the influence of the Hadley cell (Schulz et al. 2012b; Fyfe 2003; Kushner et al. 2001; Quintana 2012; Montecinos & Aceituno 2003). Several studies have looked into the alongshore winds or wind stress off the coast of Atacama. Some have found the weakening of mean upwelling-favourable winds for regions below 30° S due to the poleward shift of the SEPA (Aguirre et al. 2021; Belmadani et al. 2014) and some show an intensification of the maximum alongshore pressure gradient (Falvey & Garreaud 2009) and hence intensification of alongshore winds equatorward of 30° S in spring (Weidberg et al. 2020) and in winter (Schneider et al. 2017).

To my knowledge, there has been no study on the future changes in near-surface winds in the Atacama to hypothesise the future of dust activity in the region. However, the results from

analysing ground-based observations of wind speeds, using stations with at least 40 years of data, show that the frequency of wind speeds above the threshold required for dust emission (threshold computed at each station) increases in Iquique and decreases at almost all other stations (see Figure 3.7 and Figure 3.8). Additionally, the poleward shift of the storm track and the SEPA could mean lesser mid-tropospheric disturbances, such as mid-tropospheric troughs and cut-off lows reaching the Atacama. This could imply that there may be fewer dust storms in the future. Nevertheless, changing wind speeds and precipitation trends due to changing weather patterns will affect dust emission and transport in the region.

Quantifying the dust activity in the past will be crucial to understanding landscape evolution in the Atacama. The weather patterns identified in this study, coupled with information on changes in surface types, might yield clues as to the dust emission rates not just in the future but also in the past. Identifying the drivers for dust emission in paleo global climate models combined with sediment cores (Prospero & Bonatti 1969; Saukel et al. 2011; Martínez 2013; Stuut & Lamy 2004; Flores-Aqueveque et al. 2015) might provide hints as to whether the winds and the soil surface were favourable for dust emission in the past.

6.1.5 *Surface crusts*

The surface texture and crust in the Atacama are influenced by fog, precipitation and soil moisture (Houston 2006a; Davis et al. 2010; Jung et al. 2020b; Sun et al. 2024). Increased soil moisture leads to increased thresholds as it strengthens the inter-particle cohesion force between them (McKenna-Neuman & Nickling 1989; Neuman 2004). However, in arid regions, relative humidity and, consequently, soil moisture can change soil surface properties, contributing to the local variation in threshold wind speed and dust emission potential (Yang et al. 2019; Leeuwen et al. 2021). In field experiments and laboratories, changes in near-surface humidity are shown to affect the threshold friction velocity of surfaces, only under arid conditions, as it changes the soil moisture content (Gregory & Darwish 1990; Munkhtsetseg et al. 2016) via adhesion (Ravi et al. 2004; Ravi et al. 2006; Shao 2024). The increase in soil moisture due to humidity depends strongly on the soil content and the duration of humid periods (Fécan et al. 1999; Selah & Fryrear 1995). However, relative humidity is notoriously tricky to use as a predictor for dust emission estimates as it depends on the soil's microscopic properties (Shao 2024). This can also be extended to the potential role of fog in indirectly changing the threshold wind speed through changes in soil moisture. Quantifying to what extent fog in the Atacama increases soil moisture will be valuable to understanding how fog and the surface crust control the dust emission potential of soil surfaces.

Laboratory studies have shown that depending on the soil content (fraction of sand, silt and clay), saltating particles can either easily break the crust (when the silt and clay fraction is less than 12%) or barely make a dent (silt-clay fraction greater than 60%) as fine particles can form a firm, stable surface (Rice et al. 1999; Rice & McEwan 2001). This is also true of biological crusts susceptible to cracks by impacting particles (McKenna Neuman et al. 1996; Neuman & Maxwell 2002). From the fieldwork, the crusts and the amount of gypsum nodules at both test sites are different was established. However, without information on soil content, mineralogy and crust strength, it is difficult to prove that the repeated bombardment of particles on the crust driven by sufficient friction velocity weakens the crust. Soil samples from the sites with and without the crust were collected to determine the grain size distribution, the soil content, mineralogy, and solubility of minerals in the soil. These samples were prepared for analysis in January 2023 along with L. Weber at the Institute for Geology and Mineralogy, University of Cologne. Only preliminary results are in and further verification

is required for accuracy and confidence in lab results. These results will complement the PI-SWERL data and station observations and help locate the point dust sources (locally higher dust emission potential) within the Atacama Desert.

6.2 SUMMARY

When the wind stress acting on soil particles is higher than a threshold value, dust is emitted (Gillette 1978; Morales 1979; Helgren & Prospero 1987). This threshold wind speed depends on the soil properties, surface roughness and vegetation (Shao 2001; Okin 2008; King et al. 2005; Menut et al. 2013). Soil moisture increases the threshold due to the strengthening of soil cohesion (Fécan et al. 1998) while surface roughness elements such as vegetation and gravel absorb a fraction of the wind momentum, which also increases the threshold for dust emission (Raupach et al. 1993). This implies that arid and semi-arid regions are potential sources of mineral-dust aerosols (Kohfeld & Tegen 2007). However, global climate models and reanalysis data show that the dust emission in the Atacama Desert is low (Kok et al. 2021; Schepanski 2018). This leads us to the central questions in this thesis:

Given the limited moisture supply and barren landscape,
the Atacama Desert should be a region prone to dust emission.

Why, then, is the dust activity low in the Atacama Desert?

If the dust activity is low,
then, what drives the rare yet intense dust storms in the Atacama?

Little is known about the dust activity in the Atacama Desert. In investigating the central questions, the spatiotemporal dust activity in the Atacama Desert was quantified. The threshold wind speeds required for dust emission using long-term ground-based observations and in situ measurements were estimated. The synoptic-scale weather patterns driving dust storms in the region were investigated. It was also found that surface crusts influence the threshold wind speed and, consequently, the dust emission potential in the Atacama Desert. The short answer to the above questions is that high wind speeds (significantly higher than the climatological mean) are required for dust emission in the Atacama. This is due to surface crusts that fixate erodible soil particles. However, synoptic-scale weather patterns, modulated by the southeast Pacific anticyclone, can generate the threshold wind speeds that trigger dust storms. The dominant weather patterns in the Atacama that are associated with dust storms are mid-tropospheric troughs and their surface lows and cut-off lows. Other significant findings of this work are summarised below.

- WHY IS THE DUST ACTIVITY IN THE ATACAMA DESERT LOW DESPITE ITS ARIDITY?

  The first study provides the first-ever assessment of dust events using dust and meteorological observations from nine stations in the Atacama. Between 1950 and 2021, 1920 dust days were recorded. Of these dust events, less than 10% are recorded as dust storms. This supports model-based results that point towards the Atacama being a non-prolific dust region compared to deserts such as the Sahara. Most dust activity was recorded in Chañaral with 19.6 dust days per year and other stations with 2.7 days per year. The 1990s was the dustiest

decade in the dataset. There is no trend in dust activity, but several periods of increased activity in 1966–1978, 1984–1988, and 1992–2002. This enhanced activity cannot alone be explained by increasing threshold wind speeds or changes in precipitation.

Threshold wind speeds required for dust emission were computed for each station. The mean annual threshold wind speed at 10 m height for 5, 25 and 50% dust event occurrences were 10.9 ±1.6 ms^{-1}, 13.2 ±1.9 ms^{-1} and 15.6 ±2.3 ms^{-1} respectively. This is significantly higher than the thresholds used in global climate models that employ a constant threshold wind speed for arid regions (Donner et al. 2011; Tegen & Fung 1994; Takemura et al. 2000; Zhao et al. 2018) and studies that estimated the thresholds for the Atacama using satellite and reanalysis datasets (Pu & Ginoux 2019; Pu et al. 2020). The thresholds in this thesis are also higher than the thresholds found for dust emission in the Sahara and Sahel (Cowie et al. 2014) and the Gobi and Taklamakan deserts, also computed using ground-based observations (SYNOP). This suggests that despite the region's aridity and lack of vegetation, high wind speeds are required for dust emission in the desert and that the mean wind speeds are insufficient for dust activity. This study hypothesised that the surface in the Atacama has a crucial role in influencing the threshold wind speeds, leading us to the next study.

The soil surface of the Atacama Desert: A control for dust emission

To understand why a region with minimal precipitation and vegetation requires threshold wind speeds higher than other arid regions, the second study in this thesis investigated the in-situ threshold wind speeds using the Portable in situ Wind Erosion Lab (PI-SWERL). The measurements were conducted in two sites, Chuculay Faults and Pisagua, over undisturbed and disturbed surfaces, where the crust was removed. The near-surface threshold wind speeds are higher for crusted surfaces in Chuculay with 0.37–0.62 ms^{-1} and for disturbed surfaces with 0.19–0.37 ms^{-1}. Similarly, in Pisagua, undisturbed surfaces have thresholds ranging from 0.27–0.39 ms^{-1} while the disturbed surfaces range from 0.21–0.29 ms^{-1}. Therefore, the mean threshold wind speed on surface crusts is at least twice that on disturbed surfaces. This confirms that the presence of surface crusts increases the threshold wind speed despite the aridity.

The threshold wind speeds at 10 m height of 9.5–15 ms^{-1} from crusted surfaces in Chuculay are consistent with the estimates for threshold wind speeds of 9.5–13 ms^{-1} from ground-based observations excluding Chañaral. However, the threshold for crusted surfaces (7–10 ms^{-1}) in Pisagua is lower than the estimates from the observations. High local variability between the surfaces makes it difficult to constrain the thresholds without more field measurements.

What drives the rare dust activity in the Atacama Desert?

Given the surface crust and high threshold wind speeds for dust emission, which meteorological processes are responsible for triggering intense dust activity in the Atacama Desert? The third study in this thesis addresses this question by analysing the diurnal and seasonal cycle of dust activity and identifying the synoptic weather patterns concurring with dust storms. Using the surface observations, it was found that the dust activity follows a diurnal cycle, with most activity recorded between 9–15 local time, with peak activity around noon local time, just before the wind speed maxima. The connection between the daily dust cycle and the thermal wind speed suggests that the diurnal cycle of dust activity is probably driven by dry convection. On the other hand, the seasonality is hard to deduce, with Chañaral exhibiting a minimum frequency in the late autumn and winter, in contrast with a winter maximum at other stations. Winter seasonality is also seen in dust storms.

Between 1950 and 2021, 130 dust storms were recorded in the Atacama Desert. Of these, 42% were recorded in Calama, with 70% occurring in austral winter and spring. To identify the meteorological processes generating winds higher than the thresholds, the mean sea level pressure, 10 m wind speed and direction and the geopotential heights at 500 hPa and 700 hPa pressure levels from the ECMWF ERA5 reanalysis datasets were visually analysed. Five synoptic weather patterns associated with the recorded dust storms were found. Nearly 54.6% of dust storms were related to mid-tropospheric troughs and their surface lows, 22.3% with cut-off lows, 8.5% each with intense anticyclones and coastal lows and 6.1% with ridges. The results show that these synoptic weather patterns generate wind speeds well above the climatological mean of the station where the dust storm was recorded. At times, the direction of the dust-emitting winds differs from their characteristic wind direction, which also triggers dust storms.

6.3 LIMITATIONS AND FUTURE WORK

This thesis is only the beginning of extensive research that hopefully will follow and is required to support the results found in this work. Some of the issues with the results stem from the datasets used. The ground-based observations, while being much needed to validate model-based results, are sparse. And this is even more so for the Atacama Desert. Only nine stations are available for a latitudinal extent that spans 18° S to 28° S. Of these nine stations, most are along the inhabited coast, albeit the stations where measurements are recorded are away from cities. These stations are not in Central Atacama, the hyper-arid core. This would not be an issue if we were only interested in understanding the potential damage of intense dust activity to the health and socio-economic sectors. However, the stations' location poses an issue precisely because most cities are built around mines. The dust codes recorded in the SYNOP dataset, thus, not only comprise naturally triggered dust events but also events induced by human activity. Therefore, it is difficult to ascertain the meteorological mechanisms that drive natural desert dust activity in the region, especially the seasonality of dust activity and long-term trends. Hence, it is essential to validate the threshold winds and the frequency of dust activity with satellite data and ground-based AOD measurements (of which only one AERONET site exists in the Atacama).

The thresholds estimated via ground-based observations were validated against in-situ measurements, but these measurements were not near the stations. In Chapter 4, it was found that the soil surfaces in the Atacama are heterogeneous, affecting the thresholds of wind speed and the dust concentration measured by the PI-SWERL. So, while the ground-based and in-situ thresholds are in the same range, the spread can be constrained further by testing more sites in the Atacama Desert. Unfortunately, despite having soil samples, this work could not use detailed information on soil properties such as particle size distribution, soil texture, and composition. This information would have helped us understand the differences between the test sites and, in general, added more value to the analysis.

Therefore, future work should combine the information on soil properties with the PI-SWERL measurements to better understand how the surface crusts' characteristics contribute to the local variability in the threshold wind speeds measured in this work. Furthermore, verifying dust storms recorded in the dataset with satellite images will help establish some quality control on the ground-based observations. Analysing radiosonde data from Antofagasta and the vertical profiles of temperature and humidity from WRF simulations can help confirm if dry convection drives the diurnal dust cycle. This can be followed up with case studies using regional models and reanalysis data of dust storms to pinpoint the exact meteorological mechanisms responsible for rare yet intense dust activity in the Atacama Desert.

Bibliography

Aceituno, P., J. P. Boisier, R. Garreaud, R. Rondanelli, & J. A. Rutllant (2021). "Climate and Weather in Chile". *Water Resources of Chile*. Ed. by B. Fernández & J. Gironás. Cham: Springer International Publishing, pp. 7–29. ISBN: 978-3-030-56901-3. DOI: 10.1007/978-3-030-56901-3_2. URL: https://doi.org/10.1007/978-3-030-56901-3_2 (cit. on pp. 13, 14, 70).

Ackerman, A. S., O. B. Toon, D. E. Stevens, A. J. Heymsfield, V. Ramanathan, & E. J. Welton (2000). "Reduction of Tropical Cloudiness by Soot". *Science* 288.5468, pp. 1042–1047. DOI: 10.1126/science.288.5468.1042. eprint: https://www.science.org/doi/pdf/10.1126/science.288.5468.1042. URL: https://www.science.org/doi/abs/10.1126/science.288.5468.1042 (cit. on p. 9).

Ackerman, S. A. & S. K. Cox (1989). "Surface weather observations of atmospheric dust over the southwest summer monsoon region". *Meteorology and Atmospheric Physics* 41.1, pp. 19–34. ISSN: 1436-5065. DOI: 10.1007/BF01032587. URL: https://doi.org/10.1007/BF01032587 (cit. on p. 29).

Aguilar, G., A. Valdés, A. Cabré, & F. Galdames (2021). "Flash floods controlling Cu, Pb, As and Hg variations in fluvial sediments of a river impacted by metal mining in the Atacama Desert". *Journal of South American Earth Sciences* 109, p. 103290. ISSN: 0895-9811. DOI: https://doi.org/10.1016/j.jsames.2021.103290. URL: https://www.sciencedirect.com/science/article/pii/S0895981121001371 (cit. on pp. 19, 70).

Aguirre, C., V. Flores-Aqueveque, P. Vilches, A. Vásquez, J. A. Rutllant, & R. Garreaud (2021). "Recent Changes in the Low-Level Jet along the Subtropical West Coast of South America". *Atmosphere* 12.4. ISSN: 2073-4433. DOI: 10.3390/atmos12040465. URL: https://www.mdpi.com/2073-4433/12/4/465 (cit. on pp. 15, 75, 85).

Albani, S. et al. (2015). "Twelve thousand years of dust: the Holocene global dust cycle constrained by natural archives". *Climate of the Past* 11.6, pp. 869–903. DOI: 10.5194/cp-11-869-2015. URL: https://cp.copernicus.org/articles/11/869/2015/ (cit. on p. 7).

Alfaro, S. C., V. Flores-Aqueveque, G. Foret, S. Caquineau, G. Vargas, & J. A. Rutllant (2011). "A simple model accounting for the uptake, transport, and deposition of wind-eroded mineral particles in the hyperarid coastal Atacama Desert of northern Chile". *Earth Surface Processes and Landforms* 36.7, pp. 923–932. DOI: https://doi.org/10.1002/esp.2122. eprint: https://onlinelibrary.wiley.com/doi/pdf/10.1002/esp.2122. URL: https://onlinelibrary.wiley.com/doi/abs/10.1002/esp.2122 (cit. on p. 21).

Araya, N., A. Kraslawski, & L. A. Cisternas (2020). "Towards mine tailings valorization: Recovery of critical materials from Chilean mine tailings". *Journal of Cleaner Production* 263, p. 121555. ISSN: 0959-6526. DOI: https://doi.org/10.1016/j.jclepro.2020.121555. URL: https://www.sciencedirect.com/science/article/pii/S0959652620316024 (cit. on pp. 17, 19, 41).

Arenas-Díaz, F., B. Fuentes, M. Reyers, S. Fiedler, C. Böhm, E. Campos, Y. Shao, & R. Bol (2022). "Dust and aerosols in the Atacama Desert". *Earth-Science Reviews* 226, p. 103925. ISSN: 0012-8252. DOI: https://doi.org/10.1016/j.earscirev.2022.103925. URL: https://www.sciencedirect.com/science/article/pii/S0012825222000095 (cit. on pp. 16, 22).

Babidge, S. (2019). "Sustaining ignorance: the uncertainties of groundwater and its extraction in the Salar de Atacama, northern Chile". *Journal of the Royal Anthropological Institute* 25.1, pp. 83–102. DOI: https://doi.org/10.1111/1467-9655.12965. eprint: https://rai.onlinelibrary.wiley.com/doi/pdf/10.1111/1467-9655.12965. URL: https://rai.onlinelibrary.wiley.com/doi/abs/10.1111/1467-9655.12965 (cit. on p. 40).

Bacon, S. N., E. V. McDonald, R. Amit, Y. Enzel, & O. Crouvi (2011). "Total suspended particulate matter emissions at high friction velocities from desert landforms". *Journal of Geophysical Research: Earth Surface* 116.F3. DOI: https://doi.org/10.1029/2011JF001965. eprint: https://agupubs.onlinelibrary.wiley.com/doi/pdf/10.1029/2011JF001965. URL: https://agupubs.onlinelibrary.wiley.com/doi/abs/10.1029/2011JF001965 (cit. on p. 52).

Bagnold, R. (1974). "The Physics of Blown Sand and Desert Dunes" (cit. on pp. 10, 11, 43).

Barnes, M. A., T. Ndarana, & W. A. Landman (2021). "Cut-off lows in the Southern Hemisphere and their extension to the surface". *Climate Dynamics* 56.11, pp. 3709–3732. ISSN: 1432-0894. DOI: 10.1007/s00382-021-05662-7. URL: https://doi.org/10.1007/s00382-021-05662-7 (cit. on p. 14).

Barrett, B. S., D. A. Campos, J. V. Veloso, & R. Rondanelli (2016). "Extreme temperature and precipitation events in March 2015 in central and northern Chile". *Journal of Geophysical Research: Atmospheres* 121.9, pp. 4563–4580. DOI: https://doi.org/10.1002/2016JD024835. eprint: https://agupubs.onlinelibrary.wiley.com/doi/pdf/10.1002/2016JD024835. URL: https://agupubs.onlinelibrary.wiley.com/doi/abs/10.1002/2016JD024835 (cit. on p. 70).

Barrett, B. S., D. B. Krieger, & C. P. Barlow (2011). "Multiday Circulation and Precipitation Climatology during Winter Rain Events of Differing Intensities in Central Chile". *Journal of Hydrometeorology* 12.5, pp. 1071–1085. DOI: https:

//doi.org/10.1175/2011JHM1377.1. URL: https://journals.ametsoc.org/view/journals/hydr/12/5/2011jhm1377_1.xml (cit. on p. 70).

Bayo-Besteiro, S., L. de la Torre, X. Costoya, M. Gómez-Gesteira, A. Pérez-Alarcón, M. deCastro, & J. Añel (2023). "Photovoltaic power resource at the Atacama Desert under climate change". *Renewable Energy* 216, p. 118999. ISSN: 0960-1481. DOI: https://doi.org/10.1016/j.renene.2023.118999. URL: https://www.sciencedirect.com/science/article/pii/S0960148123009059 (cit. on p. 84).

Bell, G. D. & L. F. Bosart (1989). "A 15-year climatology of Northern Hemisphere 500 mb closed cyclone and anticyclone centers". *Monthly Weather Review* 117.10, pp. 2142–2164 (cit. on p. 63).

Belmadani, A., V. Echevin, F. Codron, K. Takahashi, & C. Junquas (Oct. 2014). "What dynamics drive future wind scenarios for coastal upwelling off Peru and Chile?" *Climate Dynamics* 43.7, pp. 1893–1914. ISSN: 1432-0894. DOI: 10.1007/s00382-013-2015-2. URL: https://doi.org/10.1007/s00382-013-2015-2 (cit. on p. 85).

Böhm, C., M. Reyers, L. Knarr, & S. Crewell (2021a). "The Role of Moisture Conveyor Belts for Precipitation in the Atacama Desert". *Geophysical Research Letters* 48.24. e2021GL094372 2021GL094372, e2021GL094372. DOI: https://doi.org/10.1029/2021GL094372. eprint: https://agupubs.onlinelibrary.wiley.com/doi/pdf/10.1029/2021GL094372. URL: https://agupubs.onlinelibrary.wiley.com/doi/abs/10.1029/2021GL094372 (cit. on p. 13).

Böhm, C., J. H. Schween, M. Reyers, B. Maier, U. Löhnert, & S. Crewell (2021b). "Toward a Climatology of Fog Frequency in the Atacama Desert via Multispectral Satellite Data and Machine Learning Techniques". *Journal of Applied Meteorology and Climatology* 60.8, pp. 1149–1169. DOI: https://doi.org/10.1175/JAMC-D-20-0208.1. URL: https://journals.ametsoc.org/view/journals/apme/60/8/JAMC-D-20-0208.1.xml (cit. on p. 13).

Boucher, O., D. Randall, P. Artaxo, C. Bretherton, G. Feingold, P. Forster, V. Kerminen, Y. Kondo, H. Liao, U. Lohmann, et al. (2013). "Climate change 2013: the physical science basis. Contribution of Working Group I to the Fifth Assessment Report of the Intergovernmental Panel on Climate Change". *K., Tignor, M., Allen, SK, Boschung, J., Nauels, A., Xia, Y., Bex, V., and Midgley, PM, Cambridge University Press, Cambridge, UK* (cit. on p. 83).

Bozkurt, D., R. Rondanelli, R. Garreaud, & A. Arriagada (2016). "Impact of Warmer Eastern Tropical Pacific SST on the March 2015 Atacama Floods". *Monthly Weather Review* 144.11, pp. 4441–4460. DOI: https://doi.org/10.1175/MWR-D-16-0041.1. URL: https://journals.ametsoc.org/view/journals/mwre/144/11/mwr-d-16-0041.1.xml (cit. on pp. 14, 63, 70).

Briceño-Zuluaga, F., A. Castagna, J. Rutllant, V. Flores-Aqueveque, S. Caquineau, A. Sifeddine, F. Velazco, D. Gutierrez, & J. Cardich (2017). "Paracas dust storms: Sources, trajectories and associated meteorological conditions". *Atmospheric Environment* 165, pp. 99–110. ISSN: 1352-2310. DOI: https://doi.org/10.1016/j.atmosenv.2017.06.019. URL: https://www.sciencedirect.com/science/article/pii/S1352231017304004 (cit. on p. 14).

Brown, L. J. (2007). "Wind erosion in sparsely vegetated rangelands". PhD thesis. University of Guelph. URL: https://atrium.lib.uoguelph.ca/items/615974ce-3d71-4e0f-9beb-f2bec4115158 (cit. on p. 52).

Buck, B. J., J. King, & V. Etyemezian (2011). "Effects of Salt Mineralogy on Dust Emissions, Salton Sea, California". *Soil Science Society of America Journal* 75.5, pp. 1971–1985. DOI: https://doi.org/10.2136/sssaj2011.0049. eprint: https://acsess.onlinelibrary.wiley.com/doi/pdf/10.2136/sssaj2011.0049. URL: https://acsess.onlinelibrary.wiley.com/doi/abs/10.2136/sssaj2011.0049 (cit. on p. 53).

Cacciuttolo, C. & F. Valenzuela (2022). "Efficient Use of Water in Tailings Management: New Technologies and Environmental Strategies for the Future of Mining". *Water* 14.11. ISSN: 2073-4441. DOI: 10.3390/w14111741. URL: https://www.mdpi.com/2073-4441/14/11/1741 (cit. on p. 19).

Cáceres, L., B. Gómez-Silva, X. Garró, V. Rodríguez, V. Monardes, & C. P. McKay (2007). "Relative humidity patterns and fog water precipitation in the Atacama Desert and biological implications". *Journal of Geophysical Research: Biogeosciences* 112.G4. DOI: https://doi.org/10.1029/2006JG000344. eprint: https://agupubs.onlinelibrary.wiley.com/doi/pdf/10.1029/2006JG000344. URL: https://agupubs.onlinelibrary.wiley.com/doi/abs/10.1029/2006JG000344 (cit. on p. 13).

Cakmur, R. V., R. L. Miller, J. Perlwitz, I. V. Geogdzhayev, P. Ginoux, D. Koch, K. E. Kohfeld, I. Tegen, & C. S. Zender (2006). "Constraining the magnitude of the global dust cycle by minimizing the difference between a model and observations". *Journal of Geophysical Research: Atmospheres* 111.D6. DOI: https://doi.org/10.1029/2005JD005791. eprint: https://agupubs.onlinelibrary.wiley.com/doi/pdf/10.1029/2005JD005791. URL: https://agupubs.onlinelibrary.wiley.com/doi/abs/10.1029/2005JD005791 (cit. on p. 9).

Cakmur, R. V., R. L. Miller, & O. Torres (2004). "Incorporating the effect of small-scale circulations upon dust emission in an atmospheric general circulation model". *Journal of Geophysical Research: Atmospheres* 109.D7. DOI: https://doi.org/10.1029/2003JD004067. eprint: https://agupubs.onlinelibrary.wiley.com/doi/pdf/10.1029/2003JD004067. URL: https://agupubs.onlinelibrary.wiley.com/doi/abs/10.1029/2003JD004067 (cit. on p. 6).

Calderón-Seguel, M., M. Prieto, O. Meseguer-Ruiz, F. Viñales, P. Hidalgo, & E. Esper (2021). "Mining, Urban Growth, and Agrarian Changes in the Atacama Desert: The Case of the Calama Oasis in Northern Chile". *Land* 10.11. ISSN: 2073-445X. DOI: 10.3390/land10111262. URL: https://www.mdpi.com/2073-445X/10/11/1262 (cit. on p. 69).

Campetella, C. M. & N. E. Possia (Apr. 2007). "Upper-level cut-off lows in southern South America". *Meteorology and Atmospheric Physics* 96.1, pp. 181–191. ISSN: 1436-5065. DOI: 10.1007/s00703-006-0227-2. URL: https://doi.org/10.1007/s00703-006-0227-2 (cit. on pp. 14, 15, 74).

Carkovic, A. B., M. S. Calcagni, A. S. Vega, M. Coquery, P. M. Moya, C. A. Bonilla, & P. A. Pastén (Aug. 2016). "Active and legacy mining in an arid urban environment: challenges and perspectives for Copiapó, Northern Chile". *Environmental Geochemistry and Health* 38.4, pp. 1001–1014. ISSN: 1573-2983. DOI: 10.1007/s10653-016-9793-5. URL: https://doi.org/10.1007/s10653-016-9793-5 (cit. on pp. 41, 83).

Castilla, J. C. (1983). "Environmental impact in sandy beaches of copper mine tailings at Chañaral, Chile". *Marine Pollution Bulletin* 14.12, pp. 459–464. ISSN: 0025-326X. DOI: https://doi.org/10.1016/0025-326X(83)90046-2. URL: https://www.sciencedirect.com/science/article/pii/0025326X83900462 (cit. on pp. 39, 79, 83).

Castro, S. H. & M. Sánchez (2003). "Environmental viewpoint on small-scale copper, gold and silver mining in Chile". *Journal of Cleaner Production* 11.2. Environmental management, pp. 207–213. ISSN: 0959-6526. DOI: https://doi.org/10.1016/S0959-6526(02)00040-9. URL: https://www.sciencedirect.com/science/article/pii/S0959652602000409 (cit. on p. 19).

Cereceda, P., H. Larrain, P. Osses, M. Farías, & I. Egaña (2008). "The spatial and temporal variability of fog and its relation to fog oases in the Atacama Desert, Chile". *Atmospheric Research* 87.3. Third International Conference on Fog, Fog Collection and Dew, pp. 312–323. ISSN: 0169-8095. DOI: https://doi.org/10.1016/j.atmosres.2007.11.012. URL: https://www.sciencedirect.com/science/article/pii/S0169809507002104 (cit. on p. 13).

Chand, D., D. A. Hegg, R. Wood, G. E. Shaw, D. Wallace, & D. S. Covert (2010). "Source attribution of climatically important aerosol properties measured at Paposo (Chile) during VOCALS". *Atmospheric Chemistry and Physics* 10.22, pp. 10789–10801. DOI: 10.5194/acp-10-10789-2010. URL: https://acp.copernicus.org/articles/10/10789/2010/ (cit. on p. 4).

Chane Kon, S. D. & A. Korre (2007). "The development and application of a wind erosion model for the assessment of fugitive dust emissions from mine tailings dumps". *International Journal of Mining, Reclamation and Environment* 21.3, pp. 198–218. DOI: 10.1080/17480930701365547. eprint: https://doi.org/10.1080/17480930701365547. URL: https://doi.org/10.1080/17480930701365547 (cit. on p. 84).

Chaulya, S. (2003). "Assessment and management of air quality in a mining area". *Environmental Quality Management* 12.4, pp. 45–59. DOI: https://doi.org/10.1002/tqem.10085. eprint: https://onlinelibrary.wiley.com/doi/pdf/10.1002/tqem.10085. URL: https://onlinelibrary.wiley.com/doi/abs/10.1002/tqem.10085 (cit. on p. 19).

Chen, Y.-S., P.-C. Sheen, E.-R. Chen, Y.-K. Liu, T.-N. Wu, & C.-Y. Yang (2004). "Effects of Asian dust storm events on daily mortality in Taipei, Taiwan". *Environmental Research* 95.2, pp. 151–155. ISSN: 0013-9351. DOI: https://doi.org/10.1016/j.envres.2003.08.008. URL: https://www.sciencedirect.com/science/article/pii/S0013935103001695 (cit. on pp. 4, 9).

Chepil, W. S. (1956). "Influence of Moisture on Erodibility of Soil by Wind". *Soil Science Society of America Journal* 20.2, pp. 288–292. DOI: https://doi.org/10.2136/sssaj1956.03615995002000020033x. eprint: https://acsess.onlinelibrary.wiley.com/doi/pdf/10.2136/sssaj1956.03615995002000020033x. URL: https://acsess.onlinelibrary.wiley.com/doi/abs/10.2136/sssaj1956.03615995002000020033x (cit. on p. 11).

Chung, Y. S., H.-S. Kim, & Y. Chun (2014). "On large-scale transport of dust storms and anthropogenic dust-falls over east Asia observed in central Korea in 2009". *Asia-Pacific Journal of Atmospheric Sciences* 50.3, pp. 345–354. ISSN: 1976-7951. DOI: 10.1007/s13143-014-0021-x. URL: https://doi.org/10.1007/s13143-014-0021-x (cit. on p. 14).

Claquin, T., M. Schulz, Y. Balkanski, & O. Boucher (Jan. 1998). "Uncertainties in assessing radiative forcing by mineral dust". *Tellus B: Chemical and Physical Meteorology*. DOI: 10.3402/tellusb.v50i5.16233 (cit. on p. 9).

Clemens, S. C. (1998). "Dust response to seasonal atmospheric forcing: Proxy evaluation and calibration". *Paleoceanography* 13.5, pp. 471–490. DOI: https://doi.org/10.1029/98PA02131. eprint: https://agupubs.onlinelibrary.wiley.com/doi/pdf/10.1029/98PA02131. URL: https://agupubs.onlinelibrary.wiley.com/doi/abs/10.1029/98PA02131 (cit. on p. 7).

Cordero, R. R., A. Damiani, J. Jorquera, E. Sepúlveda, M. Caballero, S. Fernandez, S. Feron, P. J. Llanillo, J. Carrasco, D. Laroze, & F. Labbe (Aug. 2018a). "Ultraviolet radiation in the Atacama Desert". *Antonie van Leeuwenhoek* 111.8, pp. 1301–1313. ISSN: 1572-9699. DOI: 10.1007/s10482-018-1075-z. URL: https://doi.org/10.1007/s10482-018-1075-z (cit. on pp. 22, 84).

Cordero, R. R., A. Damiani, D. Laroze, S. MacDonell, J. Jorquera, E. Sepúlveda, S. Feron, P. Llanillo, F. Labbe, J. Carrasco, J. Ferrer, & G. Torres (2018b). "Effects of soiling on photovoltaic (PV) modules in the Atacama Desert". *Scientific Reports* 8.1, p. 13943. ISSN: 2045-2322. DOI: 10.1038/s41598-018-32291-8. URL: https://doi.org/10.1038/s41598-018-32291-8 (cit. on p. 22).

Cowie, S. M., P. Knippertz, & J. H. Marsham (2014). "A climatology of dust emission events from northern Africa using long-term surface observations". *Atmospheric Chemistry and Physics* 14.16, pp. 8579–8597. DOI: 10.5194/acp-14-8579-2014. URL: https://acp.copernicus.org/articles/14/8579/2014/ (cit. on pp. 23, 29, 30, 40, 41, 61, 88).

CRC1211-Proposal (2020). *Proposal for the Second Funding Period of the Collaborative Research Centre 1211*. Proposal (cit. on p. 7).

— (2024). *Proposal for the Third Funding Period of the Collaborative Research Centre 1211*. Proposal (cit. on pp. 7, 42, 43).

Cui, M., H. Lu, G. F. Wiggs, V. Etyemezian, M. R. Sweeney, & Z. Xu (2019). "Quantifying the effect of geomorphology on aeolian dust emission potential in northern China". *Earth Surface Processes and Landforms* 44.14, pp. 2872–2884. DOI:

https://doi.org/10.1002/esp.4714. eprint: https://onlinelibrary.wiley.com/doi/pdf/10.1002/esp.4714. URL: https://onlinelibrary.wiley.com/doi/abs/10.1002/esp.4714 (cit. on pp. 46, 52, 53).

Dagsson-Waldhauserova, P., O. Arnalds, & H. Olafsson (2014). "Long-term variability of dust events in Iceland (1949–2011)". *Atmospheric Chemistry and Physics* 14.24, pp. 13411–13422. DOI: 10.5194/acp-14-13411-2014. URL: https://acp.copernicus.org/articles/14/13411/2014/ (cit. on p. 29).

Davis, W. L., I. de Pater, & C. P. McKay (2010). "Rain infiltration and crust formation in the extreme arid zone of the Atacama Desert, Chile". *Planetary and Space Science* 58.4. Exploring other worlds by exploring our own: The role of terrestrial analogue studies in planetary exploration, pp. 616–622. ISSN: 0032-0633. DOI: https://doi.org/10.1016/j.pss.2009.08.011. URL: https://www.sciencedirect.com/science/article/pii/S0032063309002505 (cit. on p. 86).

de Silva, S., J. Bailey, K. Mandt, & J. Viramonte (2010). "Yardangs in terrestrial ignimbrites: Synergistic remote and field observations on Earth with applications to Mars". *Planetary and Space Science* 58.4. Exploring other worlds by exploring our own: The role of terrestrial analogue studies in planetary exploration, pp. 459–471. ISSN: 0032-0633. DOI: https://doi.org/10.1016/j.pss.2009.10.002. URL: https://www.sciencedirect.com/science/article/pii/S0032063309003018 (cit. on p. 17).

Demortier, A., D. Bozkurt, & M. Jacques-Coper (2021). "Identifying key driving mechanisms of heat waves in central Chile". *Climate Dynamics* 57.9, pp. 2415–2432. ISSN: 1432-0894. DOI: 10.1007/s00382-021-05810-z. URL: https://doi.org/10.1007/s00382-021-05810-z (cit. on p. 15).

Dickey, H., M. Schreuder, B. Schmid, & Y. T. Yimam (2023). "Quantifying dust emission potential of playa and desert surfaces in the Salton Sea Air Basin, California, United States". *Aeolian Research* 60, p. 100850. ISSN: 1875-9637. DOI: https://doi.org/10.1016/j.aeolia.2022.100850. URL: https://www.sciencedirect.com/science/article/pii/S1875963722000805 (cit. on p. 44).

Dirección Meteorológica de Chile - Servicios Climáticos (2016). *Eventos Extremos en Chile 2016*. Tech. rep. Dirección Meteorológica de Chile - Servicios Climáticos. URL: https://climatologia.meteochile.gob.cl/application/publicaciones/documentoPdf/boletinEventosExtremos/boletinEventosExtremos-2016.pdf (cit. on pp. 3, 66).

— (2019). *Servicios Climáticos*. dataset. URL: https://climatologia.meteochile.gob.cl/ (cit. on pp. 23, 29, 61, 113).

Dold, B. (Feb. 2006). "Element flows associated with marine shore mine tailings deposits". en. *Environ Sci Technol* 40.3, pp. 752–758 (cit. on pp. 19, 39, 79, 83).

Donner, L. J. et al. (2011). "The Dynamical Core, Physical Parameterizations, and Basic Simulation Characteristics of the Atmospheric Component AM3 of the GFDL Global Coupled Model CM3". *Journal of Climate* 24.13, pp. 3484–3519. DOI: 10.1175/2011JCLI3955.1. URL: https://journals.ametsoc.org/view/journals/clim/24/13/2011jcli3955.1.xml (cit. on pp. 85, 88).

Dubovik, O., B. Holben, T. F. Eck, A. Smirnov, Y. J. Kaufman, M. D. King, D. Tanré, & I. Slutsker (2002). "Variability of Absorption and Optical Properties of Key Aerosol Types Observed in Worldwide Locations". *Journal of the Atmospheric Sciences* 59.3, pp. 590–608. DOI: 10.1175/1520-0469(2002)059<0590:VOAAOP>2.0.CO;2. URL: https://journals.ametsoc.org/view/journals/atsc/59/3/1520-0469_2002_059_0590_voaaop_2.0.co_2.xml (cit. on p. 21).

Ekström, M., G. H. McTainsh, & A. Chappell (2004). "Australian dust storms: temporal trends and relationships with synoptic pressure distributions (1960–99)". *International Journal of Climatology* 24.12, pp. 1581–1599. DOI: https://doi.org/10.1002/joc.1072. eprint: https://rmets.onlinelibrary.wiley.com/doi/pdf/10.1002/joc.1072. URL: https://rmets.onlinelibrary.wiley.com/doi/abs/10.1002/joc.1072 (cit. on p. 14).

Engelstaedter, S., K. E. Kohfeld, I. Tegen, & S. P. Harrison (2003). "Controls of dust emissions by vegetation and topographic depressions: An evaluation using dust storm frequency data". *Geophysical Research Letters* 30.6. DOI: https://doi.org/10.1029/2002GL016471. eprint: https://agupubs.onlinelibrary.wiley.com/doi/pdf/10.1029/2002GL016471. URL: https://agupubs.onlinelibrary.wiley.com/doi/abs/10.1029/2002GL016471 (cit. on pp. 32, 39).

Ericksen, G. E. (1981). *Geology and origin of the Chilean nitrate deposits*. ENGLISH. Tech. rep. Report. DOI: 10.3133/pp1188. URL: http://pubs.er.usgs.gov/publication/pp1188 (cit. on pp. 13, 17, 42).

Esfandiari, G. & M. Zarghami (Dec. 18, 2023). *Iran's Climate Migration Crisis Could Turn Into National 'Disaster'*. Accessed on 29.02.2024. URL: https://www.rferl.org/a/iran-climate-migrants-crisis/32729538.html (cit. on p. 9).

Etyemezian, V., J. Gillies, M. Shinoda, G. Nikolich, J. King, & A. Bardis (2014). "Accounting for surface roughness on measurements conducted with PI-SWERL: Evaluation of a subjective visual approach and a photogrammetric technique". *Aeolian Research* 13, pp. 35–50. ISSN: 1875-9637. DOI: https://doi.org/10.1016/j.aeolia.2014.03.002. URL: https://www.sciencedirect.com/science/article/pii/S1875963714000214 (cit. on p. 46).

Etyemezian, V., G. Nikolich, S. Ahonen, M. Pitchford, M. Sweeney, R. Purcell, J. Gillies, & H. Kuhns (2007). "The Portable In Situ Wind Erosion Laboratory (PI-SWERL): A new method to measure PM10 windblown dust properties and potential for emissions". *Atmospheric Environment* 41.18, pp. 3789–3796. ISSN: 1352-2310. DOI: https://doi.org/10.1016/j.atmosenv.2007.01.018. URL: https://www.sciencedirect.com/science/article/pii/S1352231007000647 (cit. on pp. 41, 43, 47, 48).

Ewing, S. A., B. Sutter, J. Owen, K. Nishiizumi, W. Sharp, S. S. Cliff, K. Perry, W. Dietrich, C. P. McKay, & R. Amundson (2006). "A threshold in soil formation at Earth's arid–hyperarid transition". *Geochimica et Cosmochimica Acta* 70.21,

pp. 5293–5322. ISSN: 0016-7037. DOI: https://doi.org/10.1016/j.gca.2006.08.020. URL: https://www.sciencedirect.com/science/article/pii/S0016703706020023 (cit. on pp. 7, 16, 42).

Falvey, M. & R. Garreaud (2007). "Wintertime precipitation episodes in central Chile: Associated meteorological conditions and orographic influences". *Journal of Hydrometeorology* 8.2, pp. 171–193 (cit. on p. 70).

— (2009). "Regional cooling in a warming world: Recent temperature trends in the southeast Pacific and along the west coast of subtropical South America (1979–2006)". *Journal of Geophysical Research: Atmospheres* 114.D4. DOI: https://doi.org/10.1029/2008JD010519. eprint: https://agupubs.onlinelibrary.wiley.com/doi/pdf/10.1029/2008JD010519. URL: https://agupubs.onlinelibrary.wiley.com/doi/abs/10.1029/2008JD010519 (cit. on p. 85).

Favre, A., B. Hewitson, M. Tadross, C. Lennard, & R. Cerezo-Mota (2012). "Relationships between cut-off lows and the semiannual and southern oscillations". *Climate Dynamics* 38.7, pp. 1473–1487. ISSN: 1432-0894. DOI: 10.1007/s00382-011-1030-4. URL: https://doi.org/10.1007/s00382-011-1030-4 (cit. on pp. 63, 69).

Fécan, F., B. Marticorena, & G. Bergametti (1998). "Parametrization of the increase of the aeolian erosion threshold wind friction velocity due to soil moisture for arid and semi-arid areas". *Annales Geophysicae* 17.1, pp. 149–157. ISSN: 1432-0576. DOI: 10.1007/s00585-999-0149-7. URL: https://doi.org/10.1007/s00585-999-0149-7 (cit. on pp. 11, 85, 87).

— (1999). "Parametrization of the increase of the aeolian erosion threshold wind friction velocity due to soil moisture for arid and semi-arid areas". *Annales Geophysicae* 17.1, pp. 149–157. DOI: 10.1007/s00585-999-0149-7. URL: https://angeo.copernicus.org/articles/17/149/1999/ (cit. on p. 86).

Finstad, K., M. Pfeiffer, & R. Amundson (2014). "Hyperarid Soils and the Soil Taxonomy". *Soil Science Society of America Journal* 78.6, pp. 1845–1851. DOI: https://doi.org/10.2136/sssaj2014.06.0247. eprint: https://acsess.onlinelibrary.wiley.com/doi/pdf/10.2136/sssaj2014.06.0247. URL: https://acsess.onlinelibrary.wiley.com/doi/abs/10.2136/sssaj2014.06.0247 (cit. on pp. 16, 33).

Fletcher, B. (Apr. 1976). "The erosion of dust by an airflow". *Journal of Physics D: Applied Physics* 9.6, p. 913. DOI: 10.1088/0022-3727/9/6/005. URL: https://dx.doi.org/10.1088/0022-3727/9/6/005 (cit. on p. 12).

Flores-Aqueveque, V., S. Alfaro, S. Caquineau, G. Foret, G. Vargas, & J. A. Rutllant (2012). "Inter-annual variability of southerly winds in a coastal area of the Atacama Desert: implications for the export of aeolian sediments to the adjacent marine environment". *Sedimentology* 59.3, pp. 990–1000. DOI: https://doi.org/10.1111/j.1365-3091.2011.01288.x. eprint: https://onlinelibrary.wiley.com/doi/pdf/10.1111/j.1365-3091.2011.01288.x. URL: https://onlinelibrary.wiley.com/doi/abs/10.1111/j.1365-3091.2011.01288.x (cit. on pp. 6, 21, 39, 54).

Flores-Aqueveque, V., S. Alfaro, R. C. Muñoz, J. A. Rutllant, S. Caquineau, J. P. Le Roux, & G. Vargas (2010). "Aeolian erosion and sand transport over the Mejillones Pampa in the coastal Atacama Desert of northern Chile". *Geomorphology* 120.3, pp. 312–325. ISSN: 0169-555X. DOI: https://doi.org/10.1016/j.geomorph.2010.04.003. URL: https://www.sciencedirect.com/science/article/pii/S0169555X1000173X (cit. on pp. 6, 17, 21, 39, 48, 52, 54).

Flores-Aqueveque, V., S. Alfaro, G. Vargas, J. A. Rutllant, & S. Caquineau (2015). "Aeolian particles in marine cores as a tool for quantitative high-resolution reconstruction of upwelling favorable winds along coastal Atacama Desert, Northern Chile". *Progress in Oceanography* 134, pp. 244–255. ISSN: 0079-6611. DOI: https://doi.org/10.1016/j.pocean.2015.02.003. URL: https://www.sciencedirect.com/science/article/pii/S0079661115000373 (cit. on pp. 7, 86).

Francis, D., R. Fonseca, N. Nelli, D. Bozkurt, J. Cuesta, & E. Bosc (2023). "On the Middle East's severe dust storms in spring 2022: Triggers and impacts". *Atmospheric Environment* 296, p. 119539. ISSN: 1352-2310. DOI: https://doi.org/10.1016/j.atmosenv.2022.119539. URL: https://www.sciencedirect.com/science/article/pii/S1352231022006045 (cit. on p. 14).

Fuenzalida, H. A. (1996). "Daily cycle of sea-level atmospheric pressure around 30 S over the Chilean coast". *Contributions to atmospheric physics* 69 (cit. on p. 62).

Fuenzalida, H. A., R. Sánchez, & R. Garreaud (2005). "A climatology of cutoff lows in the Southern Hemisphere". *Journal of Geophysical Research: Atmospheres* 110.D18. DOI: https://doi.org/10.1029/2005JD005934. eprint: https://agupubs.onlinelibrary.wiley.com/doi/pdf/10.1029/2005JD005934. URL: https://agupubs.onlinelibrary.wiley.com/doi/abs/10.1029/2005JD005934 (cit. on pp. 14, 15, 63, 69, 70, 73, 74).

Fyfe, J. C. (2003). "Extratropical Southern Hemisphere Cyclones: Harbingers of Climate Change?" *Journal of Climate* 16.17, pp. 2802–2805. DOI: https://doi.org/10.1175/1520-0442(2003)016<2802:ESHCHO>2.0.CO;2. URL: https://journals.ametsoc.org/view/journals/clim/16/17/1520-0442_2003_016_2802_eshcho_2.0.co_2.xml (cit. on p. 85).

Gajardo, G. & S. Redón (2019). "Andean hypersaline lakes in the Atacama Desert, northern Chile: Between lithium exploitation and unique biodiversity conservation". *Conservation Science and Practice* 1.9, e94. DOI: https://doi.org/10.1111/csp2.94. eprint: https://conbio.onlinelibrary.wiley.com/doi/pdf/10.1111/csp2.94. URL: https://conbio.onlinelibrary.wiley.com/doi/abs/10.1111/csp2.94 (cit. on p. 83).

Gallardo, L., G. Olivares, J. Langner, & B. Aarhus (2002). "Coastal lows and sulfur air pollution in Central Chile". *Atmospheric Environment* 36.23, pp. 3829–3841. ISSN: 1352-2310. DOI: https://doi.org/10.1016/S1352-

2310(02)00285-6. URL: https://www.sciencedirect.com/science/article/pii/S1352231002002856 (cit. on p. 15).

Garreaud, R. (2009). "The Andes climate and weather". *Advances in Geosciences* 22, pp. 3–11. DOI: 10.5194/adgeo-22-3-2009. URL: https://adgeo.copernicus.org/articles/22/3/2009/ (cit. on pp. 70, 72).

— (2013). "Warm Winter Storms in Central Chile". *Journal of Hydrometeorology* 14.5, pp. 1515–1534. DOI: https://doi.org/10.1175/JHM-D-12-0135.1. URL: https://journals.ametsoc.org/view/journals/hydr/14/5/jhm-d-12-0135_1.xml (cit. on p. 72).

Garreaud, R., A. Molina, & M. Farias (2010). "Andean uplift, ocean cooling and Atacama hyperaridity: A climate modeling perspective". *Earth and Planetary Science Letters* 292.1, pp. 39–50. ISSN: 0012-821X. DOI: https://doi.org/10.1016/j.epsl.2010.01.017. URL: https://www.sciencedirect.com/science/article/pii/S0012821X10000464 (cit. on p. 13).

Garreaud, R. & H. A. Fuenzalida (2007). "The Influence of the Andes on Cutoff Lows: A Modeling Study". *Monthly Weather Review* 135.4, pp. 1596–1613. DOI: https://doi.org/10.1175/MWR3350.1. URL: https://journals.ametsoc.org/view/journals/mwre/135/4/mwr3350.1.xml (cit. on p. 14).

Garreaud, R. & R. C. Muñoz (2005). "The Low-Level Jet off the West Coast of Subtropical South America: Structure and Variability". *Monthly Weather Review* 133.8, pp. 2246–2261. DOI: https://doi.org/10.1175/MWR2972.1. URL: https://journals.ametsoc.org/view/journals/mwre/133/8/mwr2972.1.xml (cit. on pp. 15, 75).

Garreaud, R., J. Rutllant, & H. Fuenzalida (2002). "Coastal Lows along the Subtropical West Coast of South America: Mean Structure and Evolution". *Monthly Weather Review* 130.1, pp. 75–88. DOI: https://doi.org/10.1175/1520-0493(2002)130<0075:CLATSW>2.0.CO;2. URL: https://journals.ametsoc.org/view/journals/mwre/130/1/1520-0493_2002_130_0075_clatsw_2.0.co_2.xml (cit. on pp. 15, 16, 63, 77).

Gillette, D. A. (1978). "Tests with a portable wind tunnel for determining wind erosion threshold velocities". *Atmospheric Environment (1967)* 12.12, pp. 2309–2313. ISSN: 0004-6981. DOI: https://doi.org/10.1016/0004-6981(78)90271-8. URL: https://www.sciencedirect.com/science/article/pii/0004698178902718 (cit. on pp. 6, 10, 85, 87).

— (1999). "A qualitative geophysical explanation for hot spot dust emitting source regions". *Contributions to atmospheric physics* 72, pp. 67–77 (cit. on p. 11).

Gillette, D. A., J. Adams, A. Endo, D. Smith, & R. Kihl (1980a). "Threshold velocities for input of soil particles into the air by desert soils". *Journal of Geophysical Research: Oceans* 85.C10, pp. 5621–5630. DOI: https://doi.org/10.1029/JC085iC10p05621. eprint: https://agupubs.onlinelibrary.wiley.com/doi/pdf/10.1029/JC085iC10p05621. URL: https://agupubs.onlinelibrary.wiley.com/doi/abs/10.1029/JC085iC10p05621 (cit. on pp. 11, 85).

— (1980b). "Threshold velocities for input of soil particles into the air by desert soils". *Journal of Geophysical Research: Oceans* 85.C10, pp. 5621–5630. DOI: https://doi.org/10.1029/JC085iC10p05621. eprint: https://agupubs.onlinelibrary.wiley.com/doi/pdf/10.1029/JC085iC10p05621. URL: https://agupubs.onlinelibrary.wiley.com/doi/abs/10.1029/JC085iC10p05621 (cit. on p. 53).

Gillette, D. A., J. Adams, D. Muhs, & R. Kihl (1982). "Threshold friction velocities and rupture moduli for crusted desert soils for the input of soil particles into the air". *Journal of Geophysical Research: Oceans* 87.C11, pp. 9003–9015. DOI: https://doi.org/10.1029/JC087iC11p09003. eprint: https://agupubs.onlinelibrary.wiley.com/doi/pdf/10.1029/JC087iC11p09003. URL: https://agupubs.onlinelibrary.wiley.com/doi/abs/10.1029/JC087iC11p09003 (cit. on pp. 7, 11, 42, 53).

Gillette, D. A., T. C. Niemeyer, & P. J. Helm (2001). "Supply-limited horizontal sand drift at an ephemerally crusted, unvegetated saline playa". *Journal of Geophysical Research: Atmospheres* 106.D16, pp. 18085–18098. DOI: https://doi.org/10.1029/2000JD900324. eprint: https://agupubs.onlinelibrary.wiley.com/doi/pdf/10.1029/2000JD900324. URL: https://agupubs.onlinelibrary.wiley.com/doi/abs/10.1029/2000JD900324 (cit. on p. 12).

Gillette, D. A. & R. Passi (1988). "Modeling dust emission caused by wind erosion". *Journal of Geophysical Research: Atmospheres* 93.D11, pp. 14233–14242. DOI: https://doi.org/10.1029/JD093iD11p14233. eprint: https://agupubs.onlinelibrary.wiley.com/doi/pdf/10.1029/JD093iD11p14233. URL: https://agupubs.onlinelibrary.wiley.com/doi/abs/10.1029/JD093iD11p14233 (cit. on pp. 11, 85).

Gillette, D. A. & P. C. Sinclair (1990). "Estimation of suspension of alkaline material by dust devils in the United States". *Atmospheric Environment. Part A. General Topics* 24.5, pp. 1135–1142. ISSN: 0960-1686. DOI: https://doi.org/10.1016/0960-1686(90)90078-2. URL: https://www.sciencedirect.com/science/article/pii/0960168690900782 (cit. on p. 64).

Ginoux, P., M. Chin, I. Tegen, J. M. Prospero, B. Holben, O. Dubovik, & S.-J. Lin (2001). "Sources and distributions of dust aerosols simulated with the GOCART model". *Journal of Geophysical Research: Atmospheres* 106.D17, pp. 20255–20273. DOI: https://doi.org/10.1029/2000JD000053. eprint: https://agupubs.onlinelibrary.wiley.com/doi/pdf/10.1029/2000JD000053. URL: https://agupubs.onlinelibrary.wiley.com/doi/abs/10.1029/2000JD000053 (cit. on pp. 6, 85).

Ginoux, P., J. M. Prospero, T. E. Gill, N. C. Hsu, & M. Zhao (2012a). "Global-scale attribution of anthropogenic and natural dust sources and their emission rates based on MODIS Deep Blue aerosol products". *Reviews of Geophysics* 50.3. DOI: https://doi.org/10.1029/2012RG000388. eprint: https://agupubs.onlinelibrary.wiley.com/doi/pdf/

10.1029/2012RG000388. URL: https://agupubs.onlinelibrary.wiley.com/doi/abs/10.1029/2012RG000388 (cit. on pp. 4, 83).
— (2012b). "Global-scale attribution of anthropogenic and natural dust sources and their emission rates based on MODIS Deep Blue aerosol products". *Reviews of Geophysics* 50.3. DOI: https://doi.org/10.1029/2012RG000388. eprint: https://agupubs.onlinelibrary.wiley.com/doi/pdf/10.1029/2012RG000388. URL: https://agupubs.onlinelibrary.wiley.com/doi/abs/10.1029/2012RG000388 (cit. on pp. 5, 11, 84, 85).
Glotter, M. & J. Elliott (Dec. 2016). "Simulating US agriculture in a modern Dust Bowl drought". *Nature Plants* 3.1, p. 16193. ISSN: 2055-0278. DOI: 10.1038/nplants.2016.193. URL: https://doi.org/10.1038/nplants.2016.193 (cit. on pp. 4, 9).
Goossens, D. (2004). "Effect of soil crusting on the emission and transport of wind-eroded sediment: field measurements on loamy sandy soil". *Geomorphology* 58.1, pp. 145–160. ISSN: 0169-555X. DOI: https://doi.org/10.1016/S0169-555X(03)00229-0. URL: https://www.sciencedirect.com/science/article/pii/S0169555X03002290 (cit. on pp. 11, 12, 42).
Goudie, A. S. (2013a). "Aeolian Geomorphology". *Arid and Semi-Arid Geomorphology*. Cambridge University Press, pp. 114–159. DOI: 10.1017/CBO9780511794261.004 (cit. on p. 17).
— (2013b). "Regional Variety". *Arid and Semi-Arid Geomorphology*. Cambridge University Press, pp. 303–324. DOI: 10.1017/CBO9780511794261.008 (cit. on p. 5).
— (2014). "Desert dust and human health disorders". *Environment International* 63, pp. 101–113. ISSN: 0160-4120. DOI: https://doi.org/10.1016/j.envint.2013.10.011. URL: https://www.sciencedirect.com/science/article/pii/S0160412013002262 (cit. on pp. 4, 9).
Graffam, G., M. Rivera, & A. Carevič (1996). "Ancient Metallurgy in the Atacama: Evidence for Copper Smelting during Chile's Early Ceramic Period". *Latin American Antiquity* 7.2, pp. 101–113. DOI: 10.2307/971612 (cit. on p. 41).
Grange, G. (1973). "The control of dust from mine dumps". *Journal of the Southern African Institute of Mining and Metallurgy* 74.2, pp. 67–73. DOI: 10.10520/AJA0038223X_325. eprint: https://journals.co.za/doi/pdf/10.10520/AJA0038223X_325. URL: https://journals.co.za/doi/abs/10.10520/AJA0038223X_325 (cit. on p. 19).
Greeley, R. & J. D. Iversen (1985). *Wind as a Geological Process: On Earth, Mars, Venus and Titan*. Cambridge Planetary Science Old. Cambridge University Press (cit. on p. 12).
Greenfield, N. (Apr. 26, 2022). *Lithium Mining Is Leaving Chile's Indigenous Communities High and Dry (Literally)*. Accessed on 22.09.2023. URL: https://www.nrdc.org/stories/lithium-mining-leaving-chiles-indigenous-communities-high-and-dry-literally (cit. on p. 83).
Gregory, J. & M. Darwish (1990). "Threshold friction velocity prediction considering water content". *Paper-American Society of Agricultural Engineers (USA)* (cit. on p. 86).
Gross, D. A. (June 2, 2014). *Caliche: the conflict mineral that fuelled the first world war*. Accessed on 18.02.2024. URL: https://www.theguardian.com/science/the-h-word/2014/jun/02/caliche-great-war-first-world-war-conflict-mineral (cit. on p. 17).
Grotjahn, R. (2004). "Remote weather associated with South Pacific subtropical sea-level high properties". *International Journal of Climatology: A Journal of the Royal Meteorological Society* 24.7, pp. 823–839 (cit. on p. 14).
Hartshorn, E., B. Sion, M. Sweeney, & E. McDonald (2023). *Visual Surface Roughness Look-up Table for PI-SWERL Measurements*. database. URL: https://www.dri.edu/itap/PI-SWERL-Roughness (cit. on p. 46).
Haug, E. W., E. R. Kraal, J. O. Sewall, M. Van Dijk, & G. C. Diaz (2010). "Climatic and geomorphic interactions on alluvial fans in the Atacama Desert, Chile". *Geomorphology* 121.3, pp. 184–196. ISSN: 0169-555X. DOI: https://doi.org/10.1016/j.geomorph.2010.04.005. URL: https://www.sciencedirect.com/science/article/pii/S0169555X10001844 (cit. on pp. 36, 70).
Heinold, B., P. Knippertz, J. H. Marsham, S. Fiedler, N. S. Dixon, K. Schepanski, B. Laurent, & I. Tegen (2013). "The role of deep convection and nocturnal low-level jets for dust emission in summertime West Africa: Estimates from convection-permitting simulations". *Journal of Geophysical Research: Atmospheres* 118.10, pp. 4385–4400. DOI: https://doi.org/10.1002/jgrd.50402. eprint: https://agupubs.onlinelibrary.wiley.com/doi/pdf/10.1002/jgrd.50402. URL: https://agupubs.onlinelibrary.wiley.com/doi/abs/10.1002/jgrd.50402 (cit. on p. 14).
Helgren, D. M. & J. M. Prospero (1987). "Wind Velocities Associated with Dust Deflation Events in the Western Sahara". *Journal of Applied Meteorology and Climatology* 26.9, pp. 1147–1151. DOI: 10.1175/1520-0450(1987)026<1147:WVAWDD>2.0.CO;2. URL: https://journals.ametsoc.org/view/journals/apme/26/9/1520-0450_1987_026_1147_wvawdd_2_0_co_2.xml (cit. on pp. 6, 10, 23, 30, 31, 85, 87).
Hersbach, H. (2023). *ECMWF reanalysis activities: from research to operations* (cit. on p. 62).
Hersbach, H. et al. (2020). "The ERA5 global reanalysis". *Quarterly Journal of the Royal Meteorological Society* 146.730, pp. 1999–2049. DOI: https://doi.org/10.1002/qj.3803. eprint: https://rmets.onlinelibrary.wiley.com/doi/pdf/10.1002/qj.3803. URL: https://rmets.onlinelibrary.wiley.com/doi/abs/10.1002/qj.3803 (cit. on p. 61).
Highwood, E. J. & C. L. Ryder (2014). "Radiative Effects of Dust". *Mineral Dust: A Key Player in the Earth System*. Ed. by P. Knippertz & J.-B. W. Stuut. Dordrecht: Springer Netherlands, pp. 267–286. ISBN: 978-94-017-8978-3. DOI: 10.1007/978-94-017-8978-3_11. URL: https://doi.org/10.1007/978-94-017-8978-3_11 (cit. on pp. 4, 9).

Hoffmeister, D. (2018). *Meteorological and soil measurements of the permanent weather stations in the Atacama desert, Chile*. en. DOI: 10.5880/CRC1211DB.1. URL: https://www.crc1211db.uni-koeln.de//DOI/doi.php?doiID=1 (cit. on p. 43).

Holben, B., T. Eck, I. Slutsker, D. Tanré, J. Buis, A. Setzer, E. Vermote, J. Reagan, Y. Kaufman, T. Nakajima, F. Lavenu, I. Jankowiak, & A. Smirnov (1998). "AERONET—A Federated Instrument Network and Data Archive for Aerosol Characterization". *Remote Sensing of Environment* 66.1, pp. 1–16. ISSN: 0034-4257. DOI: https://doi.org/10.1016/S0034-4257(98)00031-5. URL: https://www.sciencedirect.com/science/article/pii/S0034425798000315 (cit. on p. 21).

Hoskins, B. J. & K. I. Hodges (2005). "A New Perspective on Southern Hemisphere Storm Tracks". *Journal of Climate* 18.20, pp. 4108–4129. DOI: https://doi.org/10.1175/JCLI3570.1. URL: https://journals.ametsoc.org/view/journals/clim/18/20/jcli3570.1.xml (cit. on p. 72).

Hoskins, B. J., M. E. McIntyre, & A. W. Robertson (1985). "On the use and significance of isentropic potential vorticity maps". *Quarterly Journal of the Royal Meteorological Society* 111.470, pp. 877–946. DOI: https://doi.org/10.1002/qj.49711147002. eprint: https://rmets.onlinelibrary.wiley.com/doi/pdf/10.1002/qj.49711147002. URL: https://rmets.onlinelibrary.wiley.com/doi/abs/10.1002/qj.49711147002 (cit. on p. 14).

Houser, C. A. & W. G. Nickling (2001). "The emission and vertical flux of particulate matter <10μm from a disturbed clay-crusted surface". *Sedimentology* 48.2, pp. 255–267. DOI: https://doi.org/10.1046/j.1365-3091.2001.00359.x. eprint: https://onlinelibrary.wiley.com/doi/pdf/10.1046/j.1365-3091.2001.00359.x. URL: https://onlinelibrary.wiley.com/doi/abs/10.1046/j.1365-3091.2001.00359.x (cit. on p. 12).

Houston, J. (2006a). "Evaporation in the Atacama Desert: An empirical study of spatio-temporal variations and their causes". *Journal of Hydrology* 330.3, pp. 402–412. ISSN: 0022-1694. DOI: https://doi.org/10.1016/j.jhydrol.2006.03.036. URL: https://www.sciencedirect.com/science/article/pii/S0022169406001855 (cit. on p. 86).

— (2006b). "The great Atacama flood of 2001 and its implications for Andean hydrology". *Hydrological Processes* 20.3, pp. 591–610. DOI: https://doi.org/10.1002/hyp.5926. eprint: https://onlinelibrary.wiley.com/doi/pdf/10.1002/hyp.5926. URL: https://onlinelibrary.wiley.com/doi/abs/10.1002/hyp.5926 (cit. on pp. 36, 70).

— (2006c). "Variability of precipitation in the Atacama Desert: its causes and hydrological impact". *International Journal of Climatology* 26.15, pp. 2181–2198. DOI: https://doi.org/10.1002/joc.1359. eprint: https://rmets.onlinelibrary.wiley.com/doi/pdf/10.1002/joc.1359. URL: https://rmets.onlinelibrary.wiley.com/doi/abs/10.1002/joc.1359 (cit. on pp. 4, 13, 63).

Houston, J. & A. J. Hartley (2003). "The central Andean west-slope rainshadow and its potential contribution to the origin of hyper-aridity in the Atacama Desert". *International Journal of Climatology* 23.12, pp. 1453–1464. DOI: https://doi.org/10.1002/joc.938. eprint: https://rmets.onlinelibrary.wiley.com/doi/pdf/10.1002/joc.938. URL: https://rmets.onlinelibrary.wiley.com/doi/abs/10.1002/joc.938 (cit. on pp. 4, 12, 13).

Huang, J., P. Minnis, B. Chen, Z. Huang, Z. Liu, Q. Zhao, Y. Yi, & J. K. Ayers (2008). "Long-range transport and vertical structure of Asian dust from CALIPSO and surface measurements during PACDEX". *Journal of Geophysical Research: Atmospheres* 113.D23 (cit. on p. 14).

Huneeus, N., L. Gallardo, & J. A. Rutllant (2006). "Offshore transport episodes of anthropogenic sulfur in northern Chile: Potential impact on the stratocumulus cloud deck". *Geophysical Research Letters* 33.19. DOI: https://doi.org/10.1029/2006GL026921. eprint: https://agupubs.onlinelibrary.wiley.com/doi/pdf/10.1029/2006GL026921. URL: https://agupubs.onlinelibrary.wiley.com/doi/abs/10.1029/2006GL026921 (cit. on p. 15).

Huneeus, N. et al. (2011). "Global dust model intercomparison in AeroCom phase I". *Atmospheric Chemistry and Physics* 11.15, pp. 7781–7816. DOI: 10.5194/acp-11-7781-2011. URL: https://acp.copernicus.org/articles/11/7781/2011/ (cit. on pp. 5, 6).

IVERSEN, J. D. & B. R. WHITE (1982). "Saltation threshold on Earth, Mars and Venus". *Sedimentology* 29.1, pp. 111–119. DOI: https://doi.org/10.1111/j.1365-3091.1982.tb01713.x. eprint: https://onlinelibrary.wiley.com/doi/pdf/10.1111/j.1365-3091.1982.tb01713.x. URL: https://onlinelibrary.wiley.com/doi/abs/10.1111/j.1365-3091.1982.tb01713.x (cit. on p. 12).

Jacques-Coper, M., M. Falvey, & R. C. Muñoz (2015). "Inter-daily variability of a strong thermally-driven wind system over the Atacama Desert of South America: synoptic forcing and short-term predictability using the GFS global model". *Theoretical and Applied Climatology* 121.1, pp. 211–223. ISSN: 1434-4483. DOI: 10.1007/s00704-014-1231-y. URL: https://doi.org/10.1007/s00704-014-1231-y (cit. on pp. 14, 16, 72).

Jemmett-Smith, B. C., J. H. Marsham, P. Knippertz, & C. A. Gilkeson (2015). "Quantifying global dust devil occurrence from meteorological analyses". *Geophysical Research Letters* 42.4, pp. 1275–1282. DOI: https://doi.org/10.1002/2015GL063078. eprint: https://agupubs.onlinelibrary.wiley.com/doi/pdf/10.1002/2015GL063078. URL: https://agupubs.onlinelibrary.wiley.com/doi/abs/10.1002/2015GL063078 (cit. on pp. 64, 85).

Jerolmack, D. J., M. D. Reitz, & R. L. Martin (2011). "Sorting out abrasion in a gypsum dune field". *Journal of Geophysical Research: Earth Surface* 116.F2. DOI: https://doi.org/10.1029/2010JF001821. eprint: https://agupubs.onlinelibrary.wiley.com/doi/pdf/10.1029/2010JF001821. URL: https://agupubs.onlinelibrary.wiley.com/doi/abs/10.1029/2010JF001821 (cit. on p. 53).

Jickells, T. D., Z. S. An, K. K. Andersen, A. R. Baker, G. Bergametti, N. Brooks, J. J. Cao, P. W. Boyd, R. A. Duce, K. A. Hunter, H. Kawahata, N. Kubilay, J. laRoche, P. S. Liss, N. Mahowald, J. M. Prospero, A. J. Ridgwell, I. Tegen, & R. Torres (2005).

"Global Iron Connections Between Desert Dust, Ocean Biogeochemistry, and Climate". *Science* 308.5718, pp. 67–71. DOI: 10.1126/science.1105959. eprint: https://www.science.org/doi/pdf/10.1126/science.1105959. URL: https://www.science.org/doi/abs/10.1126/science.1105959 (cit. on p. 5).

Jickells, T., P. Boyd, & K. A. Hunter (2014). "Biogeochemical Impacts of Dust on the Global Carbon Cycle". *Mineral Dust: A Key Player in the Earth System*. Ed. by P. Knippertz & J.-B. W. Stuut. Dordrecht: Springer Netherlands, pp. 359–384. ISBN: 978-94-017-8978-3. DOI: 10.1007/978-94-017-8978-3_14. URL: https://doi.org/10.1007/978-94-017-8978-3_14 (cit. on p. 9).

Jorquera, H. (June 2009). "Source apportionment of PM10 and PM2.5 at Tocopilla, Chile (22°05'S, 70°12'W)". *Environmental Monitoring and Assessment* 153.1, pp. 235–251. ISSN: 1573-2959. DOI: 10.1007/s10661-008-0352-0. URL: https://doi.org/10.1007/s10661-008-0352-0 (cit. on p. 19).

Jung, P., K. Baumann, D. Emrich, A. Springer, V. J. Felde, S. Dultz, C. Baum, M. Frank, B. Büdel, & P. Leinweber (2020a). "Lichens Bite the Dust – A Bioweathering Scenario in the Atacama Desert". *iScience* 23.11, p. 101647. ISSN: 2589-0042. DOI: https://doi.org/10.1016/j.isci.2020.101647. URL: https://www.sciencedirect.com/science/article/pii/S2589004220308397 (cit. on pp. 41, 83).

Jung, P., K. Baumann, L. W. Lehnert, E. Samolov, S. Achilles, M. Schermer, L. M. Wraase, K.-U. Eckhardt, M. Y. Bader, P. Leinweber, U. Karsten, J. Bendix, & B. Büdel (2020b). "Desert breath—How fog promotes a novel type of soil biocenosis, forming the coastal Atacama Desert's living skin". *Geobiology* 18.1, pp. 113–124. DOI: https://doi.org/10.1111/gbi.12368. eprint: https://onlinelibrary.wiley.com/doi/pdf/10.1111/gbi.12368. URL: https://onlinelibrary.wiley.com/doi/abs/10.1111/gbi.12368 (cit. on p. 86).

Kahraman, M. M. & M. Erkayaoglu (Feb. 2021). "A Data-Driven Approach to Control Fugitive Dust in Mine Operations". *Mining, Metallurgy & Exploration* 38.1, pp. 549–558. ISSN: 2524-3470. DOI: 10.1007/s42461-020-00318-2. URL: https://doi.org/10.1007/s42461-020-00318-2 (cit. on p. 19).

Kaskaoutis, D. G., A. Rashki, E. E. Houssos, A. Mofidi, D. Goto, A. Bartzokas, P. Francois, & M. Legrand (July 2015). "Meteorological aspects associated with dust storms in the Sistan region, southeastern Iran". *Climate Dynamics* 45.1, pp. 407–424. ISSN: 1432-0894. DOI: 10.1007/s00382-014-2208-3. URL: https://doi.org/10.1007/s00382-014-2208-3 (cit. on p. 14).

Kaunda, R. B. (2020). "Potential environmental impacts of lithium mining". *Journal of Energy & Natural Resources Law* 38.3, pp. 237–244. DOI: 10.1080/02646811.2020.1754596. eprint: https://doi.org/10.1080/02646811.2020.1754596. URL: https://doi.org/10.1080/02646811.2020.1754596 (cit. on p. 83).

Kidder, J., M. Leybourne, D. Layton-Matthews, R. Bowell, & C. Rissmann (2020). "A review of hydrogeochemical mineral exploration in the Atacama Desert, Chile". *Ore Geology Reviews* 124, p. 103562. ISSN: 0169-1368. DOI: https://doi.org/10.1016/j.oregeorev.2020.103562. URL: https://www.sciencedirect.com/science/article/pii/S0169136820300767 (cit. on p. 19).

King, J., V. Etyemezian, M. Sweeney, B. J. Buck, & G. Nikolich (2011). "Dust emission variability at the Salton Sea, California, USA". *Aeolian Research* 3.1. AGU Fall Meeting session on Aeolian Dust: Transport Processes, Anthropogenic Forces and Biogeochemical Cycling, pp. 67–79. ISSN: 1875-9637. DOI: https://doi.org/10.1016/j.aeolia.2011.03.005. URL: https://www.sciencedirect.com/science/article/pii/S1875963711000164 (cit. on p. 44).

King, J., W. G. Nickling, & J. A. Gillies (2005). "Representation of vegetation and other nonerodible elements in aeolian shear stress partitioning models for predicting transport threshold". *Journal of Geophysical Research: Earth Surface* 110.F4. DOI: https://doi.org/10.1029/2004JF000281. eprint: https://agupubs.onlinelibrary.wiley.com/doi/pdf/10.1029/2004JF000281. URL: https://agupubs.onlinelibrary.wiley.com/doi/abs/10.1029/2004JF000281 (cit. on pp. 6, 87).

Kinne, S. et al. (2006). "An AeroCom initial assessment – optical properties in aerosol component modules of global models". *Atmospheric Chemistry and Physics* 6.7, pp. 1815–1834. DOI: 10.5194/acp-6-1815-2006. URL: https://acp.copernicus.org/articles/6/1815/2006/ (cit. on p. 9).

Klein, S. A. & D. L. Hartmann (1993). "The Seasonal Cycle of Low Stratiform Clouds". *Journal of Climate* 6.8, pp. 1587–1606. DOI: 10.1175/1520-0442(1993)006<1587:TSCOLS>2.0.CO;2. URL: https://journals.ametsoc.org/view/journals/clim/6/8/1520-0442_1993_006_1587_tscols_2_0_co_2.xml (cit. on pp. 12, 14).

Klose, M., T. E. Gill, V. Etyemezian, G. Nikolich, Z. Ghodsi Zadeh, N. P. Webb, & R. S. Van Pelt (2019). "Dust emission from crusted surfaces: Insights from field measurements and modelling". *Aeolian Research* 40, pp. 1–14. ISSN: 1875-9637. DOI: https://doi.org/10.1016/j.aeolia.2019.05.001. URL: https://www.sciencedirect.com/science/article/pii/S1875963719300709 (cit. on pp. 11, 42).

Klose, M. & Y. Shao (2013). "Large-eddy simulation of turbulent dust emission". *Aeolian Research* 8, pp. 49–58. ISSN: 1875-9637. DOI: https://doi.org/10.1016/j.aeolia.2012.10.010. URL: https://www.sciencedirect.com/science/article/pii/S1875963712000705 (cit. on p. 85).

— (2016). "A numerical study on dust devils with implications to global dust budget estimates". *Aeolian Research* 22, pp. 47–58. ISSN: 1875-9637. DOI: https://doi.org/10.1016/j.aeolia.2016.05.003. URL: https://www.sciencedirect.com/science/article/pii/S187596371630012X (cit. on pp. 64, 85).

Klose, M., Y. Shao, M. K. Karremann, & A. H. Fink (2010). "Sahel dust zone and synoptic background". *Geophysical Research Letters* 37.9. DOI: https://doi.org/10.1029/2010GL042816. eprint: https://agupubs.onlinelibrary.

wiley.com/doi/pdf/10.1029/2010GL042816. URL: https://agupubs.onlinelibrary.wiley.com/doi/abs/10.1029/2010GL042816 (cit. on p. 29).

Koch, J. & N. O. Renno (2005). "The role of convective plumes and vortices on the global aerosol budget". *Geophysical Research Letters* 32.18. DOI: https://doi.org/10.1029/2005GL023420. eprint: https://agupubs.onlinelibrary.wiley.com/doi/pdf/10.1029/2005GL023420. URL: https://agupubs.onlinelibrary.wiley.com/doi/abs/10.1029/2005GL023420 (cit. on pp. 64, 85).

Kohfeld, K. E., R. L. Reynolds, J. D. Pelletier, & B. Nickling (2005). "Linking the scales of observation, process, and modeling of dust emissions". *Eos, Transactions American Geophysical Union* 86.11, pp. 113–113. DOI: https://doi.org/10.1029/2005EO110005. eprint: https://agupubs.onlinelibrary.wiley.com/doi/pdf/10.1029/2005EO110005. URL: https://agupubs.onlinelibrary.wiley.com/doi/abs/10.1029/2005EO110005 (cit. on p. 6).

Kohfeld, K. & I. Tegen (2007). "4.13 - Record of Mineral Aerosols and Their Role in the Earth System". *Treatise on Geochemistry*. Ed. by H. D. Holland & K. K. Turekian. Oxford: Pergamon, pp. 1–26. ISBN: 978-0-08-043751-4. DOI: https://doi.org/10.1016/B978-008043751-4/00236-4. URL: https://www.sciencedirect.com/science/article/pii/B9780080437514002364 (cit. on pp. 7, 9, 40, 87).

Kok, J. F., A. A. Adebiyi, S. Albani, Y. Balkanski, R. Checa-Garcia, M. Chin, P. R. Colarco, D. S. Hamilton, Y. Huang, A. Ito, M. Klose, L. Li, N. M. Mahowald, R. L. Miller, V. Obiso, C. Pérez García-Pando, A. Rocha-Lima, & J. S. Wan (2021). "Contribution of the world's main dust source regions to the global cycle of desert dust". *Atmospheric Chemistry and Physics* 21.10, pp. 8169–8193. DOI: 10.5194/acp-21-8169-2021. URL: https://acp.copernicus.org/articles/21/8169/2021/ (cit. on pp. 5, 6, 83, 87).

Kok, J. F., D. A. Ridley, Q. Zhou, R. L. Miller, C. Zhao, C. L. Heald, D. S. Ward, S. Albani, & K. Haustein (Apr. 2017). "Smaller desert dust cooling effect estimated from analysis of dust size and abundance". *Nature Geoscience* 10.4, pp. 274–278. ISSN: 1752-0908. DOI: 10.1038/ngeo2912. URL: https://doi.org/10.1038/ngeo2912 (cit. on p. 9).

Kok, J. F., T. Storelvmo, V. A. Karydis, A. A. Adebiyi, N. M. Mahowald, A. T. Evan, C. He, & D. M. Leung (Feb. 2023). "Mineral dust aerosol impacts on global climate and climate change". *Nature Reviews Earth & Environment* 4.2, pp. 71–86. ISSN: 2662-138X. DOI: 10.1038/s43017-022-00379-5. URL: https://doi.org/10.1038/s43017-022-00379-5 (cit. on pp. 4, 6).

Kurgansky, M. V., A. Montecinos, V. Villagran, & S. M. Metzger (Feb. 2011). "Micrometeorological Conditions for Dust-Devil Occurrence in the Atacama Desert". *Boundary-Layer Meteorology* 138.2, pp. 285–298. ISSN: 1573-1472. DOI: 10.1007/s10546-010-9549-1. URL: https://doi.org/10.1007/s10546-010-9549-1 (cit. on pp. 6, 21, 64).

Kurosaki, Y. & M. Mikami (2007). "Threshold wind speed for dust emission in east Asia and its seasonal variations". *Journal of Geophysical Research: Atmospheres* 112.D17. DOI: https://doi.org/10.1029/2006JD007988. eprint: https://agupubs.onlinelibrary.wiley.com/doi/pdf/10.1029/2006JD007988. URL: https://agupubs.onlinelibrary.wiley.com/doi/abs/10.1029/2006JD007988 (cit. on pp. 23, 29, 30, 35, 40, 41).

Kushner, P. J., I. M. Held, & T. L. Delworth (2001). "Southern Hemisphere Atmospheric Circulation Response to Global Warming". *Journal of Climate* 14.10, pp. 2238–2249. DOI: https://doi.org/10.1175/1520-0442(2001)014<0001:SHACRT>2.0.CO;2. URL: https://journals.ametsoc.org/view/journals/clim/14/10/1520-0442_2001_014_0001_shacrt_2.0.co_2.xml (cit. on p. 85).

Kwon, H.-J., S.-H. Cho, Y. Chun, F. Lagarde, & G. Pershagen (2002). "Effects of the Asian Dust Events on Daily Mortality in Seoul, Korea". *Environmental Research* 90.1, pp. 1–5. ISSN: 0013-9351. DOI: https://doi.org/10.1006/enrs.2002.4377. URL: https://www.sciencedirect.com/science/article/pii/S001393510294377X (cit. on pp. 4, 9).

Latorre, C., A. L. González, J. Quade, J. M. Fariña, R. Pinto, & P. A. Marquet (2011). "Establishment and formation of fog-dependent Tillandsia landbeckii dunes in the Atacama Desert: Evidence from radiocarbon and stable isotopes". *Journal of Geophysical Research: Biogeosciences* 116.G3. DOI: https://doi.org/10.1029/2010JG001521. eprint: https://agupubs.onlinelibrary.wiley.com/doi/pdf/10.1029/2010JG001521. URL: https://agupubs.onlinelibrary.wiley.com/doi/abs/10.1029/2010JG001521 (cit. on p. 13).

Lee, M. R. & J. A. Correa (2005). "Effects of copper mine tailings disposal on littoral meiofaunal assemblages in the Atacama region of northern Chile". *Marine Environmental Research* 59.1, pp. 1–18. ISSN: 0141-1136. DOI: https://doi.org/10.1016/j.marenvres.2004.01.002. URL: https://www.sciencedirect.com/science/article/pii/S0141113604000236 (cit. on pp. 39, 79, 83).

Lee, V. (June 22, 2023). *In Iran, Some Are Chasing the Last Drops of Water*. Accessed on 29.02.2024. URL: https://www.nytimes.com/2023/06/21/world/middleeast/iran-drought-water-climate.html (cit. on p. 9).

Leeuwen, C. C. E. van, W. Fister, H. C. Vos, L. H. Cammeraat, & N. J. Kuhn (Feb. 2021). "A cross-comparison of threshold friction velocities for PM10 emissions between a traditional portable straight-line wind tunnel and PI-SWERL". *Aeolian Research* 49, p. 100661. ISSN: 1875-9637. URL: https://www.sciencedirect.com/science/article/pii/S1875963720301130 (cit. on pp. 52, 86).

Leslie, L. M. & M. S. Speer (2006). "Modelling dust transport over central eastern Australia". *Meteorological Applications* 13.2, pp. 141–167 (cit. on p. 14).

Levin, Z., E. Ganor, & V. Gladstein (1996). "The Effects of Desert Particles Coated with Sulfate on Rain Formation in the Eastern Mediterranean". *Journal of Applied Meteorology and Climatology* 35.9, pp. 1511–1523. DOI: 10.1175/1520-0450(1996)035<1511:TEODPC>2.0.CO;2. URL: https://journals.ametsoc.org/view/journals/apme/35/9/1520-0450_1996_035_1511_teodpc_2_0_co_2.xml (cit. on p. 9).

Li, F., P. Ginoux, & V. Ramaswamy (2008). "Distribution, transport, and deposition of mineral dust in the Southern Ocean and Antarctica: Contribution of major sources". *Journal of Geophysical Research: Atmospheres* 113.D10. DOI: https://doi.org/10.1029/2007JD009190. eprint: https://agupubs.onlinelibrary.wiley.com/doi/pdf/10.1029/2007JD009190. URL: https://agupubs.onlinelibrary.wiley.com/doi/abs/10.1029/2007JD009190 (cit. on p. 5).

Li, J., F. Wang, G. Michalski, & B. Wilkins (2019). "Atmospheric deposition across the Atacama Desert, Chile: Compositions, source distributions, and interannual comparisons". *Chemical Geology* 525, pp. 435–446. ISSN: 0009-2541. DOI: https://doi.org/10.1016/j.chemgeo.2019.07.037. URL: https://www.sciencedirect.com/science/article/pii/S0009254119303638 (cit. on pp. 7, 16, 23, 41, 42, 83).

Liao, H. & J. H. Seinfeld (1998). "Radiative forcing by mineral dust aerosols: Sensitivity to key variables". *Journal of Geophysical Research: Atmospheres* 103.D24, pp. 31637–31645. DOI: https://doi.org/10.1029/1998JD200036. eprint: https://agupubs.onlinelibrary.wiley.com/doi/pdf/10.1029/1998JD200036. URL: https://agupubs.onlinelibrary.wiley.com/doi/abs/10.1029/1998JD200036 (cit. on p. 9).

López-Berenguer, G., J. M. Pérez-García, A. J. García-Fernández, & E. Martínez-López (Aug. 2021). "High Levels of Heavy Metals detected in Feathers of an Avian Scavenger Warn of a High Pollution Risk in the Atacama Desert (Chile)". *Archives of Environmental Contamination and Toxicology* 81.2, pp. 227–235. ISSN: 1432-0703. DOI: 10.1007/s00244-021-00862-y. URL: https://doi.org/10.1007/s00244-021-00862-y (cit. on pp. 17, 19).

Lunt, D. J. & P. J. Valdes (2002). "The modern dust cycle: Comparison of model results with observations and study of sensitivities". *Journal of Geophysical Research: Atmospheres* 107.D23, AAC 1-1-AAC 1–16. DOI: https://doi.org/10.1029/2002JD002316. eprint: https://agupubs.onlinelibrary.wiley.com/doi/pdf/10.1029/2002JD002316. URL: https://agupubs.onlinelibrary.wiley.com/doi/abs/10.1029/2002JD002316 (cit. on p. 6).

Luo, C., N. Mahowald, & C. Jones (2004). "Temporal variability of dust mobilization and concentration in source regions". *Journal of Geophysical Research: Atmospheres* 109.D20. DOI: https://doi.org/10.1029/2004JD004861. eprint: https://agupubs.onlinelibrary.wiley.com/doi/pdf/10.1029/2004JD004861. URL: https://agupubs.onlinelibrary.wiley.com/doi/abs/10.1029/2004JD004861 (cit. on p. 59).

Ma, C.-C., C. R. Mechoso, A. W. Robertson, & A. Arakawa (1996). "Peruvian stratus clouds and the tropical Pacific circulation: A coupled ocean-atmosphere GCM study". *Journal of Climate* 9.7, pp. 1635–1645 (cit. on p. 14).

Macpherson, T., W. G. Nickling, J. A. Gillies, & V. Etyemezian (2008). "Dust emissions from undisturbed and disturbed supply-limited desert surfaces". *Journal of Geophysical Research: Earth Surface* 113.F2. DOI: https://doi.org/10.1029/2007JF000800. eprint: https://agupubs.onlinelibrary.wiley.com/doi/pdf/10.1029/2007JF000800. URL: https://agupubs.onlinelibrary.wiley.com/doi/abs/10.1029/2007JF000800 (cit. on pp. 44, 52, 53).

Maher, B., J. Prospero, D. Mackie, D. Gaiero, P. Hesse, & Y. Balkanski (2010). "Global connections between aeolian dust, climate and ocean biogeochemistry at the present day and at the last glacial maximum". *Earth-Science Reviews* 99.1, pp. 61–97. ISSN: 0012-8252. DOI: https://doi.org/10.1016/j.earscirev.2009.12.001. URL: https://www.sciencedirect.com/science/article/pii/S0012825210000024 (cit. on p. 7).

Mahowald, N. M., S. Kloster, S. Engelstaedter, J. K. Moore, S. Mukhopadhyay, J. R. McConnell, S. Albani, S. C. Doney, A. Bhattacharya, M. A. J. Curran, M. G. Flanner, F. M. Hoffman, D. M. Lawrence, K. Lindsay, P. A. Mayewski, J. Neff, D. Rothenberg, E. Thomas, P. E. Thornton, & C. S. Zender (2010). "Observed 20th century desert dust variability: impact on climate and biogeochemistry". *Atmospheric Chemistry and Physics* 10.22, pp. 10875–10893. DOI: 10.5194/acp-10-10875-2010. URL: https://acp.copernicus.org/articles/10/10875/2010/ (cit. on p. 84).

Mahowald, N., K. Kohfeld, M. Hansson, Y. Balkanski, S. P. Harrison, I. C. Prentice, M. Schulz, & H. Rodhe (1999). "Dust sources and deposition during the last glacial maximum and current climate: A comparison of model results with paleodata from ice cores and marine sediments". *Journal of Geophysical Research: Atmospheres* 104.D13, pp. 15895–15916. DOI: https://doi.org/10.1029/1999JD900084. eprint: https://agupubs.onlinelibrary.wiley.com/doi/pdf/10.1029/1999JD900084. URL: https://agupubs.onlinelibrary.wiley.com/doi/abs/10.1029/1999JD900084 (cit. on p. 7).

Mahowald, N. M., A. R. Baker, G. Bergametti, N. Brooks, R. A. Duce, T. D. Jickells, N. Kubilay, J. M. Prospero, & I. Tegen (2005). "Atmospheric global dust cycle and iron inputs to the ocean". *Global Biogeochemical Cycles* 19.4. DOI: https://doi.org/10.1029/2004GB002402. eprint: https://agupubs.onlinelibrary.wiley.com/doi/pdf/10.1029/2004GB002402. URL: https://agupubs.onlinelibrary.wiley.com/doi/abs/10.1029/2004GB002402 (cit. on pp. 11, 85).

Mahowald, N. M., J. A. Ballantine, J. Feddema, & N. Ramankutty (2007). "Global trends in visibility: implications for dust sources". *Atmospheric Chemistry and Physics* 7.12, pp. 3309–3339. DOI: 10.5194/acp-7-3309-2007. URL: https://acp.copernicus.org/articles/7/3309/2007/ (cit. on pp. 23, 39).

Mahowald, N. M., R. G. Bryant, J. del Corral, & L. Steinberger (2003). "Ephemeral lakes and desert dust sources". *Geophysical Research Letters* 30.2. DOI: https://doi.org/10.1029/2002GL016041. eprint: https://agupubs.onlinelibrary.wiley.com/doi/pdf/10.1029/2002GL016041. URL: https://agupubs.onlinelibrary.wiley.com/doi/abs/10.1029/2002GL016041 (cit. on pp. 11, 85).

Mahowald, N. M. & C. Luo (2003). "A less dusty future?" *Geophysical Research Letters* 30.17. DOI: https://doi.org/10.1029/2003GL017880. eprint: https://agupubs.onlinelibrary.wiley.com/doi/pdf/10.1029/2003GL017880. URL: https://agupubs.onlinelibrary.wiley.com/doi/abs/10.1029/2003GL017880 (cit. on p. 84).

Maisel, D. (2019). *Desolation desert*. Accessed on 18.02.2024. URL: https://davidmaisel.com/works/desolation-desert/ (cit. on p. 20).

Marticorena, B. & G. Bergametti (1995). "Modeling the atmospheric dust cycle: 1. Design of a soil-derived dust emission scheme". *Journal of Geophysical Research: Atmospheres* 100.D8, pp. 16415–16430. DOI: https://doi.org/10.1029/95JD00690. eprint: https://agupubs.onlinelibrary.wiley.com/doi/pdf/10.1029/95JD00690. URL: https://agupubs.onlinelibrary.wiley.com/doi/abs/10.1029/95JD00690 (cit. on pp. 21, 39, 54).

Marticorena, B. (2014). "Dust Production Mechanisms". *Mineral Dust: A Key Player in the Earth System*. Ed. by P. Knippertz & J.-B. W. Stuut. Dordrecht: Springer Netherlands, pp. 93–120. ISBN: 978-94-017-8978-3. DOI: 10.1007/978-94-017-8978-3_5. URL: https://doi.org/10.1007/978-94-017-8978-3_5 (cit. on pp. 10–12).

Martínez, D. (2013). "Eastern Pacific background state and tropical South American climate history during the last 3 million years". PhD dissertation. University of Bremen, pp. 143–157 (cit. on pp. 7, 86).

Martínez, L., S. M. Monsalve, K. Y. Vásquez, S. A. Orellana, J. K. Vergara, M. M. Mateo, R. C. Salazar, M. F. Alburquenque, A. M. Alcaíno, R. Torres, & D. D. C. Lillo (2016). "Indoor-outdoor concentrations of fine particulate matter in school building microenvironments near a mine tailing deposit". *AIMS Environmental Science* 3.4, pp. 752–764. ISSN: 2372-0352. DOI: 10.3934/environsci.2016.4.752. URL: https://www.aimspress.com/article/doi/10.3934/environsci.2016.4.752 (cit. on pp. 39, 79, 83).

May, S. M., L. Meine, D. Hoffmeister, D. Brill, A. Medialdea, V. Wennrich, M. Gröbner, P. Schulte, F. Steininger, M. Deprez, T. de Kock, & O. Bubenzer (2020). "Origin and timing of past hillslope activity in the hyper-arid core of the Atacama Desert – The formation of fine sediment lobes along the Chuculay Fault System, Northern Chile". *Global and Planetary Change* 184, p. 103057. ISSN: 0921-8181. DOI: https://doi.org/10.1016/j.gloplacha.2019.103057. URL: https://www.sciencedirect.com/science/article/pii/S0921818119305429 (cit. on pp. 42, 43).

McInnes, K. L., L. M. Leslie, & J. L. McBride (1992). "Numerical simulation of cut-off lows on the Australian east coast: Sensitivity to sea-surface temperature". *International Journal of Climatology* 12.8, pp. 783–795. DOI: https://doi.org/10.1002/joc.3370120803. eprint: https://rmets.onlinelibrary.wiley.com/doi/pdf/10.1002/joc.3370120803. URL: https://rmets.onlinelibrary.wiley.com/doi/abs/10.1002/joc.3370120803 (cit. on p. 14).

McKay, C. P., E. I. Friedmann, B. Gómez-Silva, L. Cáceres-Villanueva, D. T. Andersen, & R. Landheim (2003). "Temperature and Moisture Conditions for Life in the Extreme Arid Region of the Atacama Desert: Four Years of Observations Including the El Niño of 1997–1998". *Astrobiology* 3.2. PMID: 14577886, pp. 393–406. DOI: 10.1089/153110703769016460. eprint: https://doi.org/10.1089/153110703769016460. URL: https://doi.org/10.1089/153110703769016460 (cit. on pp. 4, 12).

McKenna Neuman, C., C. D. Maxwell, & J. W. Boulton (1996). "Wind transport of sand surfaces crusted with photoautotrophic microorganisms". *CATENA* 27.3, pp. 229–247. ISSN: 0341-8162. DOI: https://doi.org/10.1016/0341-8162(96)00023-9. URL: https://www.sciencedirect.com/science/article/pii/0341816296000239 (cit. on pp. 7, 86).

McKenna-Neuman, C. & W. G. Nickling (1989). "A theoretical and wind tunnel experiment of the effect of capillary water on the entrainment of sediment by wind". *Canadian Journal of Soil Science* 69.1, pp. 79–96. DOI: 10.4141/cjss89-008. eprint: https://doi.org/10.4141/cjss89-008. URL: https://doi.org/10.4141/cjss89-008 (cit. on pp. 11, 86).

McTainsh, G. H. & J. R. Pitblado (1987). "Dust storms and related phenomena measured from meteorological records in Australia". *Earth Surface Processes and Landforms* 12.4, pp. 415–424. DOI: https://doi.org/10.1002/esp.3290120407. eprint: https://onlinelibrary.wiley.com/doi/pdf/10.1002/esp.3290120407. URL: https://onlinelibrary.wiley.com/doi/abs/10.1002/esp.3290120407 (cit. on p. 29).

Mechoso, C., R. Wood, R. Weller, C. Bretherton, A. Clarke, H. Coe, C. Fairall, J. Farrar, G. Feingold, R. Garreaud, et al. (2014). "Ocean–cloud–atmosphere–land interactions in the southeastern Pacific: The VOCALS program". *Bulletin of the American Meteorological Society* 95.3, pp. 357–375 (cit. on p. 14).

Méndez, M. (2021). "Genealogy of mining territories in the Atacama Desert: The production of modern waterscapes in Tarapacá region, northern Chile (1853–1924)". *The Extractive Industries and Society* 8.1, pp. 111–122. ISSN: 2214-790X. DOI: https://doi.org/10.1016/j.exis.2020.05.003. URL: https://www.sciencedirect.com/science/article/pii/S2214790X20301453 (cit. on p. 41).

Menut, L., C. Pérez, K. Haustein, B. Bessagnet, C. Prigent, & S. Alfaro (2013). "Impact of surface roughness and soil texture on mineral dust emission fluxes modeling". *Journal of Geophysical Research: Atmospheres* 118.12, pp. 6505–6520. DOI: https://doi.org/10.1002/jgrd.50313. eprint: https://agupubs.onlinelibrary.wiley.com/doi/pdf/10.1002/jgrd.50313. URL: https://agupubs.onlinelibrary.wiley.com/doi/abs/10.1002/jgrd.50313 (cit. on pp. 6, 87).

Mesías Monsalve, S., L. Martínez, K. Yohannessen Vásquez, S. Alvarado Orellana, J. Klarián Vergara, M. Martín Mateo, R. Costilla Salazar, M. Fuentes Alburquenque, & D. D. Cáceres Lillo (June 2018). "Trace element contents in fine particulate matter (PM2.5) in urban school microenvironments near a contaminated beach with mine tailings, Chañaral, Chile". *Environmental Geochemistry and Health* 40.3, pp. 1077–1091. ISSN: 1573-2983. DOI: 10.1007/s10653-017-9980-z. URL: https://doi.org/10.1007/s10653-017-9980-z (cit. on p. 17).

Metzger, S., M. Kurgansky, A. Montecinos, V. Villagran, & H. Verdejo (Mar. 2010). "Chasing Dust Devils in Chile's Atacama Desert". *41st Annual Lunar and Planetary Science Conference*. Lunar and Planetary Science Conference, p. 2564 (cit. on pp. 21, 64).

Michalski, G., J. Böhlke, & M. Thiemens (2004). "Long term atmospheric deposition as the source of nitrate and other salts in the Atacama Desert, Chile: New evidence from mass-independent oxygen isotopic compositions". *Geochimica et Cosmochimica Acta* 68.20, pp. 4023–4038. ISSN: 0016-7037. DOI: https://doi.org/10.1016/j.gca.2004.04.009. URL: https://www.sciencedirect.com/science/article/pii/S0016703704003084 (cit. on pp. 7, 16, 42).

Middleton, N., S. S. Kashani, S. Attarchi, M. Rahnama, & S. T. Mosalman (2021). "Synoptic Causes and Socio-Economic Consequences of a Severe Dust Storm in the Middle East". *Atmosphere* 12.11. ISSN: 2073-4433. DOI: 10.3390/atmos12111435. URL: https://www.mdpi.com/2073-4433/12/11/1435 (cit. on pp. 4, 59).

MODIS Science Team (2017). *MOD02HKM MODIS/Terra Calibrated Radiances 5-Min L1B Swath 500m*. DOI: 10.5067/MODIS/MOD02HKM.061. URL: https://ladsweb.modaps.eosdis.nasa.gov/missions-and-measurements/products/MOD02HKM (cit. on p. 3).

Molina, A., M. Falvey, & R. Rondanelli (Nov. 2017). "A solar radiation database for Chile". *Scientific Reports* 7.1, p. 14823. ISSN: 2045-2322. DOI: 10.1038/s41598-017-13761-x. URL: https://doi.org/10.1038/s41598-017-13761-x (cit. on p. 84).

Montecino, V. & C. B. Lange (2009). "The Humboldt Current System: Ecosystem components and processes, fisheries, and sediment studies". *Progress in Oceanography* 83.1. Eastern Boundary Upwelling Ecosystems: Integrative and Comparative Approaches, pp. 65–79. ISSN: 0079-6611. DOI: https://doi.org/10.1016/j.pocean.2009.07.041. URL: https://www.sciencedirect.com/science/article/pii/S0079661109001049 (cit. on p. 12).

Montecinos, A. & P. Aceituno (2003). "Seasonality of the ENSO-Related Rainfall Variability in Central Chile and Associated Circulation Anomalies". *Journal of Climate* 16.2, pp. 281–296. DOI: https://doi.org/10.1175/1520-0442(2003)016<0281:SOTERR>2.0.CO;2. URL: https://journals.ametsoc.org/view/journals/clim/16/2/1520-0442_2003_016_0281_soterr_2.0.co_2.xml (cit. on p. 85).

Montes, C., J. A. Rutllant, A. Aguirre, L. Bascuñán-Godoy, & C. Juliá (2016). "Terral de Vicuña, a Foehnlike Wind in Semiarid Northern Chile: Meteorological Aspects and Implications for the Fulfillment of Chill Requirements in Deciduous Fruit Trees". *Journal of Applied Meteorology and Climatology* 55.5, pp. 1183–1196. DOI: https://doi.org/10.1175/JAMC-D-15-0275.1. URL: https://journals.ametsoc.org/view/journals/apme/55/5/jamc-d-15-0275.1.xml (cit. on pp. 15, 16, 77).

Morales, C. (1979). "The Use of Meteorological Observations for Studies of the Mobilization, Transport, and Deposition of Saharan Soil Dust". *SAHARAN DUST Mobilization, Transport, Deposition*. John Wiley & Sons. Chap. 6, pp. 119–131 (cit. on pp. 6, 10, 23, 30, 85, 87).

Munkhtsetseg, E., M. Shinoda, J. A. Gillies, R. Kimura, J. King, & G. Nikolich (2016). "Relationships between soil moisture and dust emissions in a bare sandy soil of Mongolia". *Particuology* 28, pp. 131–137. ISSN: 1674-2001. DOI: https://doi.org/10.1016/j.partic.2016.03.001. URL: https://www.sciencedirect.com/science/article/pii/S167420011630027X (cit. on p. 86).

Muñoz, R. C., M. J. Falvey, M. Arancibia, V. I. Astudillo, J. Elgueta, M. Ibarra, C. Santana, & C. Vásquez (2018). "Wind Energy Exploration over the Atacama Desert: A Numerical Model?Guided Observational Program". *Bulletin of the American Meteorological Society* 99.10, pp. 2079–2092. DOI: 10.1175/BAMS-D-17-0019.1. URL: https://journals.ametsoc.org/view/journals/bams/99/10/bams-d-17-0019.1.xml (cit. on pp. 16, 64).

Muñoz, R. C., M. J. Falvey, M. Araya, & M. Jacques-Coper (2013). "Strong Down-Valley Low-Level Jets over the Atacama Desert: Observational Characterization". *Journal of Applied Meteorology and Climatology* 52.12, pp. 2735–2752. DOI: https://doi.org/10.1175/JAMC-D-13-063.1. URL: https://journals.ametsoc.org/view/journals/apme/52/12/jamc-d-13-063.1.xml (cit. on pp. 16, 64).

Muñoz, R. C. & R. Garreaud (2005). "Dynamics of the Low-Level Jet off the West Coast of Subtropical South America". *Monthly Weather Review* 133.12, pp. 3661–3677. DOI: https://doi.org/10.1175/MWR3074.1. URL: https://journals.ametsoc.org/view/journals/mwre/133/12/mwr3074.1.xml (cit. on pp. 14, 15).

Muñoz, R. C., D. Schultz, & G. Vaughan (2020). "A Midlatitude Climatology and Interannual Variability of 200- and 500-hPa Cut-Off Lows". *Journal of Climate* 33.6, pp. 2201–2222. DOI: https://doi.org/10.1175/JCLI-D-19-0497.1. URL: https://journals.ametsoc.org/view/journals/clim/33/6/jcli-d-19-0497.1.xml (cit. on pp. 14, 15, 63, 73).

Muñoz, R. C., R. A. Zamora, & J. A. Rutllant (2011). "The Coastal Boundary Layer at the Eastern Margin of the Southeast Pacific (23.4°S, 70.4°W): Cloudiness-Conditioned Climatology". *Journal of Climate* 24.4, pp. 1013–1033. DOI: https://doi.org/10.1175/2010JCLI3714.1. URL: https://journals.ametsoc.org/view/journals/clim/24/4/2010jcli3714.1.xml (cit. on p. 62).

Ndarana, T., D. W. Waugh, L. M. Polvani, G. J. P. Correa, & E. P. Gerber (2012). "Antarctic ozone depletion and trends in tropopause Rossby wave breaking". *Atmospheric Science Letters* 13.3, pp. 164–168. DOI: https://doi.org/10.1002/asl.384. eprint: https://rmets.onlinelibrary.wiley.com/doi/pdf/10.1002/asl.384. URL: https://rmets.onlinelibrary.wiley.com/doi/abs/10.1002/asl.384 (cit. on pp. 15, 69).

Ndarana, T. & D. W. Waugh (2010). "The link between cut-off lows and Rossby wave breaking in the Southern Hemisphere". *Quarterly Journal of the Royal Meteorological Society* 136.649, pp. 869–885. DOI: https://doi.org/10.1002/qj.

627. eprint: https://rmets.onlinelibrary.wiley.com/doi/pdf/10.1002/qj.627. URL: https://rmets.onlinelibrary.wiley.com/doi/abs/10.1002/qj.627 (cit. on p. 14).

Neary, D. G. & P. Garcia-Chevesich (2008). *Hydrology and erosion impacts of mining derived coastal sand dunes, Chanaral Bay, Chile* (cit. on pp. 39, 79, 83).

Nenes, A., B. Murray, & A. Bougiatioti (2014). "Mineral Dust and its Microphysical Interactions with Clouds". *Mineral Dust: A Key Player in the Earth System*. Ed. by P. Knippertz & J.-B. W. Stuut. Springer Netherlands, pp. 287–325. ISBN: 978-94-017-8978-3. DOI: 10.1007/978-94-017-8978-3_12. URL: https://doi.org/10.1007/978-94-017-8978-3_12 (cit. on pp. 4, 9).

Neslen, A. (Jan. 31, 2024). *Extraction of raw materials to rise by 60% by 2060, says UN report*. Accessed on 21.02.2024. URL: https://www.theguardian.com/environment/2024/jan/31/raw-materials-extraction-2060-un-report (cit. on p. 84).

Neuman, C. M. (2004). "Effects of temperature and humidity upon the transport of sedimentary particles by wind". *Sedimentology* 51.1, pp. 1–17. DOI: https://doi.org/10.1046/j.1365-3091.2003.00604.x. eprint: https://onlinelibrary.wiley.com/doi/pdf/10.1046/j.1365-3091.2003.00604.x. URL: https://onlinelibrary.wiley.com/doi/abs/10.1046/j.1365-3091.2003.00604.x (cit. on p. 86).

Neuman, C. M. & C. Maxwell (2002). "Temporal aspects of the abrasion of microphytic crusts under grain impact". *Earth Surface Processes and Landforms* 27.8, pp. 891–908. DOI: https://doi.org/10.1002/esp.360. eprint: https://onlinelibrary.wiley.com/doi/pdf/10.1002/esp.360. URL: https://onlinelibrary.wiley.com/doi/abs/10.1002/esp.360 (cit. on p. 86).

O'Loingsigh, T., G. McTainsh, N. Tapper, & P. Shinkfield (2010). "Lost in code: A critical analysis of using meteorological data for wind erosion monitoring". *Aeolian Research* 2.1, pp. 49–57. ISSN: 1875-9637. DOI: https://doi.org/10.1016/j.aeolia.2010.03.002. URL: https://www.sciencedirect.com/science/article/pii/S1875963710000054 (cit. on pp. 29, 30, 79).

Okin, G. S. (2008). "A new model of wind erosion in the presence of vegetation". *Journal of Geophysical Research: Earth Surface* 113.F2. DOI: https://doi.org/10.1029/2007JF000758. eprint: https://agupubs.onlinelibrary.wiley.com/doi/pdf/10.1029/2007JF000758. URL: https://agupubs.onlinelibrary.wiley.com/doi/abs/10.1029/2007JF000758 (cit. on pp. 6, 87).

Orgill, M. & G. Sehmel (1976). "Frequency and diurnal variation of dust storms in the contiguous U.S.A." *Atmospheric Environment (1967)* 10.10, pp. 813–825. ISSN: 0004-6981. DOI: https://doi.org/10.1016/0004-6981(76)90136-0. URL: https://www.sciencedirect.com/science/article/pii/0004698176901360 (cit. on p. 79).

Orihuela, J. C. (2014). "The Environmental Rules of Economic Development: Governing Air Pollution from Smelters in Chuquicamata and La Oroya". *Journal of Latin American Studies* 46.1, pp. 151–183. DOI: 10.1017/S0022216X13001545 (cit. on p. 19).

Ortega, C., G. Vargas, M. Rojas, J. A. Rutllant, P. Muñoz, C. B. Lange, S. Pantoja, L. Dezileau, & L. Ortlieb (2019). "Extreme ENSO-driven torrential rainfalls at the southern edge of the Atacama Desert during the Late Holocene and their projection into the 21th century". *Global and Planetary Change* 175, pp. 226–237. ISSN: 0921-8181. DOI: https://doi.org/10.1016/j.gloplacha.2019.02.011. URL: https://www.sciencedirect.com/science/article/pii/S0921818118304995 (cit. on p. 63).

Ossandón, G., R. Fréraut C., L. B. Gustafson, D. D. Lindsay, & M. Zentilli (Mar. 2001). "Geology of the Chuquicamata Mine: A Progress Report". *Economic Geology* 96.2, pp. 249–270. ISSN: 0361-0128. DOI: 10.2113/gsecongeo.96.2.249. eprint: https://pubs.geoscienceworld.org/segweb/economicgeology/article-pdf/96/2/249/3493351/249.pdf. URL: https://doi.org/10.2113/gsecongeo.96.2.249 (cit. on p. 69).

Oyarzún, D. V. (2021). "Climate Change and Air Pollution Relationships. Lessons from a Subtropical Desert Region". PhD dissertation. University College London (cit. on pp. 6, 21, 83, 84).

Palmén, E. (1949). "Origin and Structure of High-Level Cyclones South of the: Maximum Westerlies". *Tellus* 1.1, pp. 22–31 (cit. on p. 14).

Palmén, E. & C. Newton (1969). "10 Three-Dimensional Flow Patterns in Extratropical Disturbances". *Atmospheric Circulation Systems*. Vol. 13. International Geophysics. Academic Press, pp. 273–314. DOI: https://doi.org/10.1016/S0074-6142(08)62802-8. URL: https://www.sciencedirect.com/science/article/pii/S0074614208628028 (cit. on p. 14).

Paskoff, R. P. (2005). "A Unique Coastal Dune in the Atacama Desert: The Cerro El Dragón, Iquique, Chile". *Journal of Coastal Research*, pp. 63–67. ISSN: 07490208, 15515036. URL: http://www.jstor.org/stable/25736974 (visited on 04/12/2023) (cit. on p. 16).

Pinheiro, H., M. Gan, & K. Hodges (2021). "Structure and evolution of intense austral cut-off lows". *Quarterly Journal of the Royal Meteorological Society* 147.734, pp. 1–20. DOI: https://doi.org/10.1002/qj.3900. eprint: https://rmets.onlinelibrary.wiley.com/doi/pdf/10.1002/qj.3900. URL: https://rmets.onlinelibrary.wiley.com/doi/abs/10.1002/qj.3900 (cit. on p. 63).

Pinheiro, H., K. I. Hodges, M. A. Gan, & N. J. Ferreira (2017). "A new perspective of the climatological features of upper-level cut-off lows in the Southern Hemisphere". *Climate Dynamics* 48.1, pp. 541–559. ISSN: 1432-0894. DOI: 10.1007/s00382-016-3093-8. URL: https://doi.org/10.1007/s00382-016-3093-8 (cit. on pp. 14, 69, 70).

Pinto, A. (2019). *Caracterización observacional de eventos de Terral en el valle del Río Pelambres*. Master Thesis. URL: https://repositorio.uchile.cl/handle/2250/172670 (cit. on pp. 15, 78).

Pizarro, J. & A. Montecinos (2000). "Cutoff cyclones off the subtropical coast of Chile". *Proc. Sixth Int. Conf. on Southern Hemisphere Meteorology and Oceanography*, pp. 278–279 (cit. on pp. 14, 15, 70).

Pozo, D., J. C. Marín, G. B. Raga, J. Arévalo, D. Baumgardner, A. M. Córdova, & J. Mora (2019). "Synoptic and local circulations associated with events of high particulate pollution in Valparaiso, Chile". *Atmospheric Environment* 196, pp. 164–178. ISSN: 1352-2310. DOI: https://doi.org/10.1016/j.atmosenv.2018.10.006. URL: https://www.sciencedirect.com/science/article/pii/S1352231018306952 (cit. on p. 15).

Prospero, J. M. (1996). "Saharan Dust Transport Over the North Atlantic Ocean and Mediterranean: An Overview". *The Impact of Desert Dust Across the Mediterranean*. Ed. by S. Guerzoni & R. Chester. Dordrecht: Springer Netherlands, pp. 133–151. ISBN: 978-94-017-3354-0. DOI: 10.1007/978-94-017-3354-0_13. URL: https://doi.org/10.1007/978-94-017-3354-0_13 (cit. on pp. 13, 59).

Prospero, J. M. & E. Bonatti (1969). "Continental dust in the atmosphere of the Eastern Equatorial Pacific". *Journal of Geophysical Research (1896-1977)* 74.13, pp. 3362–3371. DOI: https://doi.org/10.1029/JC074i013p03362. eprint: https://agupubs.onlinelibrary.wiley.com/doi/pdf/10.1029/JC074i013p03362. URL: https://agupubs.onlinelibrary.wiley.com/doi/abs/10.1029/JC074i013p03362 (cit. on pp. 7, 86).

Pu, B., P. Ginoux, H. Guo, N. C. Hsu, J. Kimball, B. Marticorena, S. Malyshev, V. Naik, N. T. O'Neill, C. Pérez García-Pando, J. Paireau, J. M. Prospero, E. Shevliakova, & M. Zhao (2020). "Retrieving the global distribution of the threshold of wind erosion from satellite data and implementing it into the Geophysical Fluid Dynamics Laboratory land–atmosphere model (GFDL AM4.0/LM4.0)". *Atmospheric Chemistry and Physics* 20.1, pp. 55–81. DOI: 10.5194/acp-20-55-2020. URL: https://acp.copernicus.org/articles/20/55/2020/ (cit. on pp. 40, 53, 88).

Pu, B. & P. Ginoux (2019). *Monthly and annual mean threshold of wind erosion dataset*. URL: https://www.gfdl.noaa.gov/pag-homepage/ (visited on 12/15/2022) (cit. on pp. 40, 88).

Qian, W., L. Quan, & S. Shi (2002). "Variations of the Dust Storm in China and its Climatic Control". *Journal of Climate* 15.10, pp. 1216–1229. DOI: https://doi.org/10.1175/1520-0442(2002)015<1216:VOTDSI>2.0.CO;2. URL: https://journals.ametsoc.org/view/journals/clim/15/10/1520-0442_2002_015_1216_votdsi_2.0.co_2.xml (cit. on p. 14).

Quintana, J. (2012). "Changes in the rainfall regime along the extratropical west coast of South America (Chile): 30-43º S". *Atmósfera* 25.1, pp. 1–22 (cit. on p. 85).

Rahn, D. A. (2012). "Influence of large scale oscillations on upwelling-favorable coastal wind off central Chile". *Journal of Geophysical Research: Atmospheres* 117.D19. DOI: https://doi.org/10.1029/2012JD018016. eprint: https://agupubs.onlinelibrary.wiley.com/doi/pdf/10.1029/2012JD018016. URL: https://agupubs.onlinelibrary.wiley.com/doi/abs/10.1029/2012JD018016 (cit. on pp. 14, 63).

Rahn, D. A. & R. Garreaud (2014). "A synoptic climatology of the near-surface wind along the west coast of South America". *International Journal of Climatology* 34.3, pp. 780–792. DOI: https://doi.org/10.1002/joc.3724. eprint: https://rmets.onlinelibrary.wiley.com/doi/pdf/10.1002/joc.3724. URL: https://rmets.onlinelibrary.wiley.com/doi/abs/10.1002/joc.3724 (cit. on pp. 63, 65).

Ramirez, M., S. Massolo, R. Frache, & J. A. Correa (2005). "Metal speciation and environmental impact on sandy beaches due to El Salvador copper mine, Chile". *Marine Pollution Bulletin* 50.1, pp. 62–72. ISSN: 0025-326X. DOI: https://doi.org/10.1016/j.marpolbul.2004.08.010. URL: https://www.sciencedirect.com/science/article/pii/S0025326X04003066 (cit. on pp. 39, 79, 83).

Ramon, J., L. Lledó, V. Torralba, A. Soret, & F. J. Doblas-Reyes (2019). "What global reanalysis best represents near-surface winds?" *Quarterly Journal of the Royal Meteorological Society* 145.724, pp. 3236–3251. DOI: https://doi.org/10.1002/qj.3616. eprint: https://rmets.onlinelibrary.wiley.com/doi/pdf/10.1002/qj.3616. URL: https://rmets.onlinelibrary.wiley.com/doi/abs/10.1002/qj.3616 (cit. on p. 40).

Raupach, M. R., D. A. Gillette, & J. F. Leys (1993). "The effect of roughness elements on wind erosion threshold". *Journal of Geophysical Research: Atmospheres* 98.D2, pp. 3023–3029. DOI: https://doi.org/10.1029/92JD01922. eprint: https://agupubs.onlinelibrary.wiley.com/doi/pdf/10.1029/92JD01922. URL: https://agupubs.onlinelibrary.wiley.com/doi/abs/10.1029/92JD01922 (cit. on pp. 11, 85, 87).

Ravi, S., P. D'Odorico, D. D. Breshears, J. P. Field, A. S. Goudie, T. E. Huxman, J. Li, G. S. Okin, R. J. Swap, A. D. Thomas, S. Van Pelt, J. J. Whicker, & T. M. Zobeck (2011). "AEOLIAN PROCESSES AND THE BIOSPHERE". *Reviews of Geophysics* 49.3. DOI: https://doi.org/10.1029/2010RG000328. eprint: https://agupubs.onlinelibrary.wiley.com/doi/pdf/10.1029/2010RG000328. URL: https://agupubs.onlinelibrary.wiley.com/doi/abs/10.1029/2010RG000328 (cit. on pp. 4, 9).

Ravi, S., P. D'Odorico, T. M. Over, & T. M. Zobeck (2004). "On the effect of air humidity on soil susceptibility to wind erosion: The case of air-dry soils". *Geophysical Research Letters* 31.9. DOI: https://doi.org/10.1029/2004GL019485. eprint: https://agupubs.onlinelibrary.wiley.com/doi/pdf/10.1029/2004GL019485. URL: https://agupubs.onlinelibrary.wiley.com/doi/abs/10.1029/2004GL019485 (cit. on p. 86).

Ravi, S., T. M. Zobeck, T. M. Over, G. S. Okin, & P. D'Odorico (2006). "On the effect of moisture bonding forces in air-dry soils on threshold friction velocity of wind erosion". *Sedimentology* 53.3, pp. 597–609. DOI: https://doi.org/10.1111/j.1365-3091.2006.00775.x. eprint: https://onlinelibrary.wiley.com/doi/pdf/10.1111/j.1365-

3091.2006.00775.x. URL: https://onlinelibrary.wiley.com/doi/abs/10.1111/j.1365-3091.2006.00775.x (cit. on p. 86).

Reboita, M. S., R. Nieto, L. Gimeno, R. P. da Rocha, T. Ambrizzi, R. Garreaud, & L. F. Krüger (2010). "Climatological features of cutoff low systems in the Southern Hemisphere". *Journal of Geophysical Research: Atmospheres* 115.D17. DOI: https://doi.org/10.1029/2009JD013251. eprint: https://agupubs.onlinelibrary.wiley.com/doi/pdf/10.1029/2009JD013251. URL: https://agupubs.onlinelibrary.wiley.com/doi/abs/10.1029/2009JD013251 (cit. on pp. 14, 15).

Reyers, M., C. Böhm, L. Knarr, Y. Shao, & S. Crewell (2021). "Synoptic-to-Regional-Scale Analysis of Rainfall in the Atacama Desert (18°–26°S) Using a Long-Term Simulation with WRF". *Monthly Weather Review* 149.1, pp. 91–112. DOI: https://doi.org/10.1175/MWR-D-20-0038.1. URL: https://journals.ametsoc.org/view/journals/mwre/149/1/mwr-d-20-0038.1.xml (cit. on p. 63).

Reyers, M., M. Hamidi, & Y. Shao (2019). "Synoptic analysis and simulation of an unusual dust event over the Atacama Desert". *Atmospheric Science Letters* 20.6, e899. DOI: https://doi.org/10.1002/asl.899. eprint: https://rmets.onlinelibrary.wiley.com/doi/pdf/10.1002/asl.899. URL: https://rmets.onlinelibrary.wiley.com/doi/abs/10.1002/asl.899 (cit. on pp. 3, 6, 21, 79).

Reyers, M. & Y. Shao (2019). "Cutoff lows off the coast of the Atacama Desert under present day conditions and in the Last Glacial Maximum". *Global and Planetary Change* 181, p. 102983. ISSN: 0921-8181. DOI: https://doi.org/10.1016/j.gloplacha.2019.102983. URL: https://www.sciencedirect.com/science/article/pii/S0921818119300050 (cit. on pp. 14, 15, 59, 63, 73).

Reynolds, R. L., J. C. Yount, M. Reheis, H. Goldstein, P. Chavez Jr., R. Fulton, J. Whitney, C. Fuller, & R. M. Forester (2007). "Dust emission from wet and dry playas in the Mojave Desert, USA". *Earth Surface Processes and Landforms* 32.12, pp. 1811–1827. DOI: https://doi.org/10.1002/esp.1515. eprint: https://onlinelibrary.wiley.com/doi/pdf/10.1002/esp.1515. URL: https://onlinelibrary.wiley.com/doi/abs/10.1002/esp.1515 (cit. on p. 53).

Rice, M. A. & I. K. McEwan (2001). "Crust strength: a wind tunnel study of the effect of impact by saltating particles on cohesive soil surfaces". *Earth Surface Processes and Landforms* 26.7, pp. 721–733. DOI: https://doi.org/10.1002/esp.217. eprint: https://onlinelibrary.wiley.com/doi/pdf/10.1002/esp.217. URL: https://onlinelibrary.wiley.com/doi/abs/10.1002/esp.217 (cit. on pp. 7, 12, 86).

Rice, M. A., I. K. McEwan, & C. E. Mullins (1999). "A conceptual model of wind erosion of soil surfaces by saltating particles". *Earth Surface Processes and Landforms* 24.5, pp. 383–392. DOI: https://doi.org/10.1002/(SICI)1096-9837(199905)24:5<383::AID-ESP995>3.0.CO;2-K. eprint: https://onlinelibrary.wiley.com/doi/pdf/10.1002/%28SICI%291096-9837%28199905%2924%3A5%3C383%3A%3AAID-ESP995%3E3.0.CO%3B2-K. URL: https://onlinelibrary.wiley.com/doi/abs/10.1002/%28SICI%291096-9837%28199905%2924%3A5%3C383%3A%3AAID-ESP995%3E3.0.CO%3B2-K (cit. on pp. 12, 86).

Ridley, D. A., C. L. Heald, J. F. Kok, & C. Zhao (2016). "An observationally constrained estimate of global dust aerosol optical depth". *Atmospheric Chemistry and Physics* 16.23, pp. 15097–15117. DOI: 10.5194/acp-16-15097-2016. URL: https://acp.copernicus.org/articles/16/15097/2016/ (cit. on p. 22).

Ridley, D. A., C. L. Heald, J. R. Pierce, & M. J. Evans (2013). "Toward resolution-independent dust emissions in global models: Impacts on the seasonal and spatial distribution of dust". *Geophysical Research Letters* 40.11, pp. 2873–2877. DOI: https://doi.org/10.1002/grl.50409. eprint: https://agupubs.onlinelibrary.wiley.com/doi/pdf/10.1002/grl.50409. URL: https://agupubs.onlinelibrary.wiley.com/doi/abs/10.1002/grl.50409 (cit. on pp. 6, 85).

Riofrancos, T. (June 14, 2021). *The rush to 'go electric' comes with a hidden cost: destructive lithium mining*. Accessed on 22.09.2023. URL: https://www.theguardian.com/commentisfree/2021/jun/14/electric-cost-lithium-mining-decarbonasation-salt-flats-chile (cit. on p. 83).

Rodwell, M. J. & B. J. Hoskins (2001). "Subtropical Anticyclones and Summer Monsoons". *Journal of Climate* 14.15, pp. 3192–3211. DOI: https://doi.org/10.1175/1520-0442(2001)014<3192:SAASM>2.0.CO;2. URL: https://journals.ametsoc.org/view/journals/clim/14/15/1520-0442_2001_014_3192_saasm_2.0.co_2.xml (cit. on pp. 12, 14).

Rondanelli, R., B. Hatchett, J. Rutllant, D. Bozkurt, & R. Garreaud (2019). "Strongest MJO on Record Triggers Extreme Atacama Rainfall and Warmth in Antarctica". *Geophysical Research Letters* 46.6, pp. 3482–3491. DOI: https://doi.org/10.1029/2018GL081475. eprint: https://agupubs.onlinelibrary.wiley.com/doi/pdf/10.1029/2018GL081475. URL: https://agupubs.onlinelibrary.wiley.com/doi/abs/10.1029/2018GL081475 (cit. on p. 70).

Rondanelli, R., A. Molina, & M. Falvey (2015). "The Atacama Surface Solar Maximum". *Bulletin of the American Meteorological Society* 96.3, pp. 405–418. DOI: 10.1175/BAMS-D-13-00175.1. URL: https://journals.ametsoc.org/view/journals/bams/96/3/bams-d-13-00175.1.xml (cit. on p. 84).

Rundel, P. W., M. Dillon, B. Palma, H. Mooney, S. L. Gulmon, & J. R. Ehleringer (1991). "The phytogeography and ecology of the coastal Atacama and Peruvian deserts". *Aliso* 13, pp. 1–49. URL: https://api.semanticscholar.org/CorpusID:3220622 (cit. on p. 13).

Rutllant, J. (1994). *On the generation of coastal lows in central Chile* (cit. on pp. 15, 16, 63).

Rutllant, J., R. C. Muñoz, & R. D. Garreaud (2013). "Meteorological observations on the northern Chilean coast during VOCALS-REx". *Atmospheric Chemistry and Physics* 13.6, pp. 3409–3422. DOI: 10.5194/acp-13-3409-2013. URL: https://acp.copernicus.org/articles/13/3409/2013/ (cit. on pp. 16, 59).

Rutllant, J. & P. Ulriksen (Aug. 1979). "Boundary-layer dynamics of the extremely arid northern part of Chile". *Boundary-Layer Meteorology* 17.1, pp. 41–55. ISSN: 1573-1472. DOI: 10.1007/BF00121936. URL: https://doi.org/10.1007/BF00121936 (cit. on p. 72).

Rutllant, J., H. Fuenzalida, & P. Aceituno (2003). "Climate dynamics along the arid northern coast of Chile: The 1997–1998 Dinámica del Clima de la Región de Antofagasta (DICLIMA) experiment". *Journal of Geophysical Research: Atmospheres* 108.D17. DOI: https://doi.org/10.1029/2002JD003357. eprint: https://agupubs.onlinelibrary.wiley.com/doi/pdf/10.1029/2002JD003357. URL: https://agupubs.onlinelibrary.wiley.com/doi/abs/10.1029/2002JD003357 (cit. on pp. 12, 13, 16, 59).

Rutllant, J. & R. Garreaud (1995). "Meteorological air pollution potential for Santiago, Chile: Towards an objective episode forecasting". *Environmental Monitoring and Assessment* 34.3, pp. 223–244. ISSN: 1573-2959. DOI: 10.1007/BF00554796. URL: https://doi.org/10.1007/BF00554796 (cit. on pp. 15, 63).

Rutllant, J. & V. Montecino (2002). "Multiscale upwelling forcing cycles and biological response off north-central Chile". *Revista Chilena de Historia Natural* 75.217, e231 (cit. on p. 12).

Rutllant, J. & R. Garreaud (2004). "Episodes of Strong Flow down the Western Slope of the Subtropical Andes". *Monthly Weather Review* 132.2, pp. 611–622. DOI: https://doi.org/10.1175/1520-0493(2004)132<0611:EOSFDT>2.0.CO;2. URL: https://journals.ametsoc.org/view/journals/mwre/132/2/1520-0493_2004_132_0611_eosfdt_2.0.co_2.xml (cit. on pp. 15, 77).

Ryder, C. L., F. Marenco, J. K. Brooke, V. Estelles, R. Cotton, P. Formenti, J. B. McQuaid, H. C. Price, D. Liu, P. Ausset, P. D. Rosenberg, J. W. Taylor, T. Choularton, K. Bower, H. Coe, M. Gallagher, J. Crosier, G. Lloyd, E. J. Highwood, & B. J. Murray (2018). "Coarse-mode mineral dust size distributions, composition and optical properties from AER-D aircraft measurements over the tropical eastern Atlantic". *Atmospheric Chemistry and Physics* 18.23, pp. 17225–17257. DOI: 10.5194/acp-18-17225-2018. URL: https://acp.copernicus.org/articles/18/17225/2018/ (cit. on p. 9).

Salazar, D., D. Jackson, J. L. Guendon, H. Salinas, D. Morata, V. Figueroa, G. Manríquez, & V. Castro (2011). "Early Evidence (ca. 12,000 BP) for Iron Oxide Mining on the Pacific Coast of South America". *Current Anthropology* 52.3, pp. 463–475. DOI: 10.1086/659426. eprint: https://doi.org/10.1086/659426. URL: https://doi.org/10.1086/659426 (cit. on p. 41).

Saukel, C., F. Lamy, J.-B. W. Stuut, R. Tiedemann, & C. Vogt (2011). "Distribution and provenance of wind-blown SE Pacific surface sediments". *Marine Geology* 280.1, pp. 130–142. ISSN: 0025-3227. DOI: https://doi.org/10.1016/j.margeo.2010.12.006. URL: https://www.sciencedirect.com/science/article/pii/S0025322710003178 (cit. on pp. 7, 23, 86).

Schepanski, K., I. Tegen, M. C. Todd, B. Heinold, G. Bönisch, B. Laurent, & A. Macke (2009). "Meteorological processes forcing Saharan dust emission inferred from MSG-SEVIRI observations of subdaily dust source activation and numerical models". *Journal of Geophysical Research: Atmospheres* 114.D10. DOI: https://doi.org/10.1029/2008JD010325. eprint: https://agupubs.onlinelibrary.wiley.com/doi/pdf/10.1029/2008JD010325. URL: https://agupubs.onlinelibrary.wiley.com/doi/abs/10.1029/2008JD010325 (cit. on p. 85).

Schepanski, K. (2018). "Transport of Mineral Dust and Its Impact on Climate". *Geosciences* 8.5. ISSN: 2076-3263. DOI: 10.3390/geosciences8050151. URL: https://www.mdpi.com/2076-3263/8/5/151 (cit. on pp. 5, 13, 59, 87).

Schneider, W., D. Donoso, J. Garcés-Vargas, & R. Escribano (2017). "Water-column cooling and sea surface salinity increase in the upwelling region off central-south Chile driven by a poleward displacement of the South Pacific High". *Progress in Oceanography* 151, pp. 38–48. ISSN: 0079-6611. DOI: https://doi.org/10.1016/j.pocean.2016.11.004. URL: https://www.sciencedirect.com/science/article/pii/S0079661116300325 (cit. on p. 85).

Schulz, M., J. M. Prospero, A. R. Baker, F. Dentener, L. Ickes, P. S. Liss, N. M. Mahowald, S. Nickovic, C. P. García-Pando, S. Rodríguez, M. Sarin, I. Tegen, & R. A. Duce (2012a). "Atmospheric Transport and Deposition of Mineral Dust to the Ocean: Implications for Research Needs". *Environmental Science & Technology* 46.19. PMID: 22994868, pp. 10390–10404. DOI: 10.1021/es300073u. eprint: https://doi.org/10.1021/es300073u. URL: https://doi.org/10.1021/es300073u (cit. on pp. 4, 9).

Schulz, N., J. P. Boisier, & P. Aceituno (2012b). "Climate change along the arid coast of northern Chile". *International Journal of Climatology* 32.12, pp. 1803–1814. DOI: https://doi.org/10.1002/joc.2395. eprint: https://rmets.onlinelibrary.wiley.com/doi/pdf/10.1002/joc.2395. URL: https://rmets.onlinelibrary.wiley.com/doi/abs/10.1002/joc.2395 (cit. on pp. 62, 85).

Schulz, N. (2009). "Loma-Formationen der Küsten-Atacama/Nordchile unter besonderer Berücksichtigung rezenter Vegetations- und Klimaveränderungen". doctoralthesis. Friedrich-Alexander-Universität Erlangen-Nürnberg (FAU) (cit. on p. 14).

Schwartzstein, P. (Jan. 25, 2019). *Drought turns part of Iran into a new dust bowl*. Accessed on 29.02.2024. URL: https://www.nationalgeographic.com/environment/article/drought-climate-change-turn-iran-sistan-and-baluchestan-into-dust-bowl (cit. on p. 9).

Schween, J. H., D. Hoffmeister, & U. Löhnert (2020). "Filling the observational gap in the Atacama Desert with a new network of climate stations". *Global and Planetary Change* 184, p. 103034. ISSN: 0921-8181. DOI: https://doi.org/10.1016/j.gloplacha.2019.103034. URL: https://www.sciencedirect.com/science/article/pii/S0921818119305193 (cit. on pp. 16, 43).

Seinfeld, J. H. et al. (2016). "Improving our fundamental understanding of the role of aerosol–cloud interactions in the climate system". *Proceedings of the National Academy of Sciences* 113.21, pp. 5781–5790. DOI: 10.1073/pnas.1514043113. eprint: https://www.pnas.org/doi/pdf/10.1073/pnas.1514043113. URL: https://www.pnas.org/doi/abs/10.1073/pnas.1514043113 (cit. on p. 4).

Selah, A. & D. W. Fryrear (1995). "Threshold wind velocities of wet soils as affected by wind blown sand". *Soil Science* 160.4. ISSN: 0038-075X. URL: https://journals.lww.com/soilsci/fulltext/1995/10000/threshold_wind_velocities_of_wet_soils_as_affected.9.aspx (cit. on p. 86).

Sengupta, S. (Dec. 28, 2021). *Chile Writes a New Constitution, Confronting Climate Change Head On*. Accessed on 22.09.2023. URL: https://www.nytimes.com/2021/12/28/climate/chile-constitution-climate-change.html (cit. on p. 83).

Sepúlveda, S. A., S. Rebolledo, & G. Vargas (2006). "Recent catastrophic debris flows in Chile: Geological hazard, climatic relationships and human response". *Quaternary International* 158.1. Holocene environmental catastrophes in South America: from the lowlands to the Andes, pp. 83–95. ISSN: 1040-6182. DOI: https://doi.org/10.1016/j.quaint.2006.05.031. URL: https://www.sciencedirect.com/science/article/pii/S104061820600156X (cit. on pp. 36, 70).

Shaffer, G., S. Hormazabal, O. Pizarro, & S. Salinas (1999). "Seasonal and interannual variability of currents and temperature off central Chile". *Journal of Geophysical Research: Oceans* 104.C12, pp. 29951–29961 (cit. on p. 12).

Shao, Y., M. R. Raupach, & P. A. Findlater (1993). "Effect of saltation bombardment on the entrainment of dust by wind". *Journal of Geophysical Research: Atmospheres* 98.D7, pp. 12719–12726. DOI: https://doi.org/10.1029/93JD00396. eprint: https://agupubs.onlinelibrary.wiley.com/doi/pdf/10.1029/93JD00396. URL: https://agupubs.onlinelibrary.wiley.com/doi/abs/10.1029/93JD00396 (cit. on p. 11).

Shao, Y., J. Zhang, M. Ishizuka, M. Mikami, J. Leys, & N. Huang (2020). "Dependency of particle size distribution at dust emission on friction velocity and atmospheric boundary-layer stability". *Atmospheric Chemistry and Physics* 20.21, pp. 12939–12953. DOI: 10.5194/acp-20-12939-2020. URL: https://acp.copernicus.org/articles/20/12939/2020/ (cit. on pp. 11, 85).

Shao, Y. (2001). "A model for mineral dust emission". *Journal of Geophysical Research: Atmospheres* 106.D17, pp. 20239–20254. DOI: https://doi.org/10.1029/2001JD900171. eprint: https://agupubs.onlinelibrary.wiley.com/doi/pdf/10.1029/2001JD900171. URL: https://agupubs.onlinelibrary.wiley.com/doi/abs/10.1029/2001JD900171 (cit. on pp. 6, 85, 87).

— (2008). *Physics and modelling of wind erosion*. Springer (cit. on pp. 4, 9–13, 59).

— (2024). "Adhesion theory and model for air humidity impact on dust emission". *Aeolian Research* 66, p. 100898. ISSN: 1875-9637. DOI: https://doi.org/10.1016/j.aeolia.2024.100898. URL: https://www.sciencedirect.com/science/article/pii/S1875963724000090 (cit. on p. 86).

Shao, Y., M. Klose, & K.-H. Wyrwoll (2013). "Recent global dust trend and connections to climate forcing". *Journal of Geophysical Research: Atmospheres* 118.19, pp. 11, 107–11, 118. DOI: https://doi.org/10.1002/jgrd.50836. eprint: https://agupubs.onlinelibrary.wiley.com/doi/pdf/10.1002/jgrd.50836. URL: https://agupubs.onlinelibrary.wiley.com/doi/abs/10.1002/jgrd.50836 (cit. on pp. 23, 29, 30, 61).

Shao, Y. & H. Lu (2000). "A simple expression for wind erosion threshold friction velocity". *Journal of Geophysical Research: Atmospheres* 105.D17, pp. 22437–22443. DOI: https://doi.org/10.1029/2000JD900304. eprint: https://agupubs.onlinelibrary.wiley.com/doi/pdf/10.1029/2000JD900304. URL: https://agupubs.onlinelibrary.wiley.com/doi/abs/10.1029/2000JD900304 (cit. on pp. 11, 12).

Sinclair, P. C. (1965). "on the rotation of dust devils". *Bulletin of the American Meteorological Society* 46.7, pp. 388–391. DOI: https://doi.org/10.1175/1520-0477-46.7.388. URL: https://journals.ametsoc.org/view/journals/bams/46/7/1520-0477-46_7_388.xml (cit. on p. 64).

— (1969). "General Characteristics of Dust Devils". *Journal of Applied Meteorology and Climatology* 8.1, pp. 32–45. DOI: https://doi.org/10.1175/1520-0450(1969)008<0032:GCODD>2.0.CO;2. URL: https://journals.ametsoc.org/view/journals/apme/8/1/1520-0450_1969_008_0032_gcodd_2_0_co_2.xml (cit. on p. 64).

Sokolik, I. N. & O. B. Toon (June 1996). "Direct radiative forcing by anthropogenic airborne mineral aerosols". *Nature* 381.6584, pp. 681–683. ISSN: 1476-4687. DOI: 10.1038/381681a0. URL: https://doi.org/10.1038/381681a0 (cit. on p. 9).

Stanelle, T., I. Bey, T. Raddatz, C. Reick, & I. Tegen (2014). "Anthropogenically induced changes in twentieth century mineral dust burden and the associated impact on radiative forcing". *Journal of Geophysical Research: Atmospheres* 119.23, pp. 13, 526–13, 546. DOI: https://doi.org/10.1002/2014JD022062. eprint: https://agupubs.onlinelibrary.wiley.com/doi/pdf/10.1002/2014JD022062. URL: https://agupubs.onlinelibrary.wiley.com/doi/abs/10.1002/2014JD022062 (cit. on p. 84).

Stout, J. E. (2010). "Diurnal patterns of blowing sand". *Earth Surface Processes and Landforms* 35.3, pp. 314–318. DOI: https://doi.org/10.1002/esp.1919. eprint: https://onlinelibrary.wiley.com/doi/pdf/10.1002/esp.1919. URL: https://onlinelibrary.wiley.com/doi/abs/10.1002/esp.1919 (cit. on p. 79).

Strub, P. T. (1998). "Coastal ocean circulation off western South America". *The global coastal ocean. Regional studies and syntheses*, pp. 273–315 (cit. on p. 12).

Stuut, J.-B. W. & F. Lamy (2004). "Climate variability at the southern boundaries of the Namib (southwestern Africa) and Atacama (northern Chile) coastal deserts during the last 120,000 yr". *Quaternary Research* 62.3, pp. 301–309. ISSN: 0033-5894. DOI: https://doi.org/10.1016/j.yqres.2004.08.001. URL: https://www.sciencedirect.com/science/article/pii/S0033589404000948 (cit. on pp. 7, 86).

Stuut, J.-B. W., M. A. Prins, R. R. Schneider, G. J. Weltje, J. Jansen, & G. Postma (2002). "A 300-kyr record of aridity and wind strength in southwestern Africa: inferences from grain-size distributions of sediments on Walvis Ridge, SE Atlantic". *Marine Geology* 180.1, pp. 221–233. ISSN: 0025-3227. DOI: https://doi.org/10.1016/S0025-3227(01)00215-8. URL: https://www.sciencedirect.com/science/article/pii/S0025322701002158 (cit. on p. 7).

Sun, X., W. Amelung, E. Klumpp, J. Walk, R. Mörchen, C. Böhm, G. Moradi, S. M. May, F. Tamburini, Y. Wang, & R. Bol (2024). "Fog controls biological cycling of soil phosphorus in the Coastal Cordillera of the Atacama Desert". *Global Change Biology* 30.1. e17068 GCB-23-2344, e17068. DOI: https://doi.org/10.1111/gcb.17068. eprint: https://onlinelibrary.wiley.com/doi/pdf/10.1111/gcb.17068. URL: https://onlinelibrary.wiley.com/doi/abs/10.1111/gcb.17068 (cit. on p. 86).

Swap, R., M. Garstang, S. Greco, R. Talbot, & P. Kållberg (1992). "Saharan dust in the Amazon Basin". *Tellus B* 44.2, pp. 133–149. DOI: https://doi.org/10.1034/j.1600-0889.1992.t01-1-00005.x. eprint: https://onlinelibrary.wiley.com/doi/pdf/10.1034/j.1600-0889.1992.t01-1-00005.x. URL: https://onlinelibrary.wiley.com/doi/abs/10.1034/j.1600-0889.1992.t01-1-00005.x (cit. on pp. 4, 9).

Sweeney, M., V. Etyemezian, T. Macpherson, W. Nickling, J. Gillies, G. Nikolich, & E. McDonald (2008). "Comparison of PI-SWERL with dust emission measurements from a straight-line field wind tunnel". *Journal of Geophysical Research: Earth Surface* 113.F1. DOI: https://doi.org/10.1029/2007JF000830. eprint: https://agupubs.onlinelibrary.wiley.com/doi/pdf/10.1029/2007JF000830. URL: https://agupubs.onlinelibrary.wiley.com/doi/abs/10.1029/2007JF000830 (cit. on pp. 43, 52).

Sweeney, M. & J. A. Mason (2013). "Mechanisms of dust emission from Pleistocene loess deposits, Nebraska, USA". *Journal of Geophysical Research: Earth Surface* 118.3, pp. 1460–1471. DOI: https://doi.org/10.1002/jgrf.20101. eprint: https://agupubs.onlinelibrary.wiley.com/doi/pdf/10.1002/jgrf.20101. URL: https://agupubs.onlinelibrary.wiley.com/doi/abs/10.1002/jgrf.20101 (cit. on pp. 44, 48, 53).

Sweeney, M. R., S. L. Forman, & E. V. McDonald (Dec. 2021). "Contemporary and future dust sources and emission fluxes from gypsum- and quartz-dominated eolian systems, New Mexico and Texas, USA". *Geology* 50.3, pp. 356–360. ISSN: 0091-7613. DOI: 10.1130/G49488.1. eprint: https://pubs.geoscienceworld.org/gsa/geology/article-pdf/50/3/356/5547388/g49488.1.pdf. URL: https://doi.org/10.1130/G49488.1 (cit. on p. 53).

Sweeney, M. R., E. V. McDonald, & V. Etyemezian (2011). "Quantifying dust emissions from desert landforms, eastern Mojave Desert, USA". *Geomorphology* 135.1, pp. 21–34. ISSN: 0169-555X. DOI: https://doi.org/10.1016/j.geomorph.2011.07.022. URL: https://www.sciencedirect.com/science/article/pii/S0169555X1100376X (cit. on pp. 44, 52, 53).

Takemi, T. & N. Seino (2005). "Dust storms and cyclone tracks over the arid regions in east Asia in spring". *Journal of Geophysical Research: Atmospheres* 110.D18. DOI: https://doi.org/10.1029/2004JD004698. eprint: https://agupubs.onlinelibrary.wiley.com/doi/pdf/10.1029/2004JD004698. URL: https://agupubs.onlinelibrary.wiley.com/doi/abs/10.1029/2004JD004698 (cit. on p. 14).

Takemura, T., H. Okamoto, Y. Maruyama, A. Numaguti, A. Higurashi, & T. Nakajima (2000). "Global three-dimensional simulation of aerosol optical thickness distribution of various origins". *Journal of Geophysical Research: Atmospheres* 105.D14, pp. 17853–17873. DOI: https://doi.org/10.1029/2000JD900265. eprint: https://agupubs.onlinelibrary.wiley.com/doi/pdf/10.1029/2000JD900265. URL: https://agupubs.onlinelibrary.wiley.com/doi/abs/10.1029/2000JD900265 (cit. on pp. 85, 88).

Tang, Y., Y. Han, & Z. Liu (2018). "Temporal and spatial characteristics of dust devils and their contribution to the aerosol budget in East Asia—An analysis using a new parameterization scheme for dust devils". *Atmospheric Environment* 182, pp. 225–233. ISSN: 1352-2310. DOI: https://doi.org/10.1016/j.atmosenv.2018.03.050. URL: https://www.sciencedirect.com/science/article/pii/S1352231018302048 (cit. on p. 64).

Tapia, J., R. González, B. Townley, V. Oliveros, F. Álvarez, G. Aguilar, A. Menzies, & M. Calderón (Aug. 2018). "Geology and geochemistry of the Atacama Desert". *Antonie van Leeuwenhoek* 111.8, pp. 1273–1291. ISSN: 1572-9699. DOI: 10.1007/s10482-018-1024-x. URL: https://doi.org/10.1007/s10482-018-1024-x (cit. on pp. 17, 18).

Targino, A. C., R. Krejci, K. J. Noone, & P. Glantz (2006). "Single particle analysis of ice crystal residuals observed in orographic wave clouds over Scandinavia during INTACC experiment". *Atmospheric Chemistry and Physics* 6.7, pp. 1977–1990. DOI: 10.5194/acp-6-1977-2006. URL: https://acp.copernicus.org/articles/6/1977/2006/ (cit. on p. 9).

Tegen, I., A. A. Lacis, & I. Fung (1996). "The influence of mineral aerosols from disturbed soils on the global radiation budget". *Nature* 380, pp. 419–422. DOI: 10.1038/380419a0 (cit. on p. 9).

Tegen, I., M. Werner, S. P. Harrison, & K. E. Kohfeld (2004). "Relative importance of climate and land use in determining present and future global soil dust emission". *Geophysical Research Letters* 31.5. DOI: https://doi.org/10.1029/2003GL019216. eprint: https://agupubs.onlinelibrary.wiley.com/doi/pdf/10.1029/2003GL019216. URL: https://agupubs.onlinelibrary.wiley.com/doi/abs/10.1029/2003GL019216 (cit. on pp. 83, 84).

Tegen, I. (2003). "Modeling the mineral dust aerosol cycle in the climate system". *Quaternary Science Reviews* 22.18. Loess and the Dust Indicators and Records of Terrestrial and Mari ne Palaeoenvironments (DIRTMAP) database, pp. 1821–1834. ISSN: 0277-3791. DOI: https://doi.org/10.1016/S0277-3791(03)00163-X. URL: https://www.sciencedirect.com/science/article/pii/S027737910300163X (cit. on p. 9).

Tegen, I. & I. Fung (1994). "Modeling of mineral dust in the atmosphere: Sources, transport, and optical thickness". *Journal of Geophysical Research: Atmospheres* 99.D11, pp. 22897–22914. DOI: https://doi.org/10.1029/94JD01928. eprint: https://agupubs.onlinelibrary.wiley.com/doi/pdf/10.1029/94JD01928. URL: https://agupubs.onlinelibrary.wiley.com/doi/abs/10.1029/94JD01928 (cit. on pp. 85, 88).

UNEP (2011). *Global Drylands: A UN system-wide response*. https://resources.unep-wcmc.org/products/WCMC_RT134. Tech report. [Accessed 11-03-2024] (cit. on p. 12).

USGS (2018). *The Mineral Industry of Chile*. Report. Accessed on 18.02.2024. URL: https://pubs.usgs.gov/myb/vol3/2017-18/myb3-2017-18-chile.pdf (cit. on p. 17).

— (2024a). *Copper: World Mine and Refinery Production and Reserves*. Report. Accessed on 18.02.2024. URL: https://pubs.usgs.gov/periodicals/mcs2024/mcs2024-copper.pdf (cit. on p. 17).

— (2024b). *Lithium: World Mine and Refinery Production and Reserves*. Report. Accessed on 18.02.2024. URL: https://pubs.usgs.gov/periodicals/mcs2024/mcs2024-lithium.pdf (cit. on p. 17).

— (2024c). *Molybdenum: World Mine and Refinery Production and Reserves*. Report. Accessed on 18.02.2024. URL: https://pubs.usgs.gov/periodicals/mcs2024/mcs2024-molybdenum.pdf (cit. on p. 17).

Vargas, G., J. Rutllant, & L. Ortlieb (2006). "ENSO tropical–extratropical climate teleconnections and mechanisms for Holocene debris flows along the hyperarid coast of western South America (17°–24°S)". *Earth and Planetary Science Letters* 249.3, pp. 467–483. ISSN: 0012-821X. DOI: https://doi.org/10.1016/j.epsl.2006.07.022. URL: https://www.sciencedirect.com/science/article/pii/S0012821X06005140 (cit. on pp. 13, 14, 63).

Vincent, D. G. (1998). "Pacific Ocean". *Meteorology of the Southern Hemisphere*. Ed. by D. J. Karoly & D. G. Vincent. Boston, MA: American Meteorological Society, pp. 101–117. ISBN: 978-1-935704-10-2. DOI: 10.1007/978-1-935704-10-2_4. URL: https://doi.org/10.1007/978-1-935704-10-2_4 (cit. on p. 65).

Vos, H. C., W. Fister, J. R. von Holdt, F. D. Eckardt, A. R. Palmer, & N. J. Kuhn (2021). "Assessing the PM10 emission potential of sandy, dryland soils in South Africa using the PI-SWERL". *Aeolian Research* 53, p. 100747. ISSN: 1875-9637. DOI: https://doi.org/10.1016/j.aeolia.2021.100747. URL: https://www.sciencedirect.com/science/article/pii/S1875963721000847 (cit. on pp. 44, 53).

Vuille, M. & C. Ammann (July 1997). "Regional Snowfall Patterns In The High, Arid Andes". *Climatic Change* 36.3, pp. 413–423. ISSN: 1573-1480. DOI: 10.1023/A:1005330802974. URL: https://doi.org/10.1023/A:1005330802974 (cit. on pp. 13, 14, 72).

Walk, J., G. Stauch, M. Reyers, P. Vásquez, F. A. Sepúlveda, M. Bartz, D. Hoffmeister, H. Brückner, & F. Lehmkuhl (2020). "Gradients in climate, geology, and topography affecting coastal alluvial fan morphodynamics in hyperarid regions – The Atacama perspective". *Global and Planetary Change* 185, p. 102994. ISSN: 0921-8181. DOI: https://doi.org/10.1016/j.gloplacha.2019.102994. URL: https://www.sciencedirect.com/science/article/pii/S0921818119301419 (cit. on pp. 36, 70).

Wang, F., G. Michalski, H. Luo, & M. Caffee (2017). "Role of biological soil crusts in affecting soil evolution and salt geochemistry in hyper-arid Atacama Desert, Chile". *Geoderma* 307, pp. 54–64. ISSN: 0016-7061. DOI: https://doi.org/10.1016/j.geoderma.2017.07.035. URL: https://www.sciencedirect.com/science/article/pii/S0016706116305766 (cit. on pp. 7, 16, 23).

Wang, F., G. Michalski, J.-h. Seo, & W. Ge (2014). "Geochemical, isotopic, and mineralogical constraints on atmospheric deposition in the hyper-arid Atacama Desert, Chile". *Geochimica et Cosmochimica Acta* 135, pp. 29–48. ISSN: 0016-7037. DOI: https://doi.org/10.1016/j.gca.2014.03.017. URL: https://www.sciencedirect.com/science/article/pii/S0016703714001811 (cit. on pp. 7, 16, 23, 42).

Wang, F., G. Michalski, J.-H. Seo, D. E. Granger, N. Lifton, & M. Caffee (2015). "Beryllium-10 concentrations in the hyper-arid soils in the Atacama Desert, Chile: Implications for arid soil formation rates and El Niño driven changes in Pliocene precipitation". *Geochimica et Cosmochimica Acta* 160, pp. 227–242. ISSN: 0016-7037. DOI: https://doi.org/10.1016/j.gca.2015.03.008. URL: https://www.sciencedirect.com/science/article/pii/S0016703715001404 (cit. on p. 23).

Weidberg, N., A. Ospina-Alvarez, J. Bonicelli, M. Barahona, C. M. Aiken, B. R. Broitman, & S. A. Navarrete (2020). "Spatial shifts in productivity of the coastal ocean over the past two decades induced by migration of the Pacific Anticyclone and Bakun's effect in the Humboldt Upwelling Ecosystem". *Global and Planetary Change* 193, p. 103259. ISSN: 0921-8181. DOI: https://doi.org/10.1016/j.gloplacha.2020.103259. URL: https://www.sciencedirect.com/science/article/pii/S0921818120301508 (cit. on p. 85).

White, B. R. (1979). "soil transport by winds on Mars". *Journal of Geophysical Research: Solid Earth* 84.B9, pp. 4643–4651. DOI: https://doi.org/10.1029/JB084iB09p04643. eprint: https://agupubs.onlinelibrary.wiley.com/

doi/pdf/10.1029/JB084iB09p04643. URL: https://agupubs.onlinelibrary.wiley.com/doi/abs/10.1029/JB084iB09p04643 (cit. on p. 54).

Wisskirchen, C. & B. Dold (2006). "THE MARINE SHORE PORPHYRY COPPER MINE TAILINGS DEPOSIT AT CHAÑARAL, NORTHERN CHILE 1". *Journal of the American Society of Mining and Reclamation* 2006, pp. 2480–2489. URL: https://api.semanticscholar.org/CorpusID:53349133 (cit. on pp. 39, 83).

Wolfe, S. A. & W. G. Nickling (1993). "The protective role of sparse vegetation in wind erosion". *Progress in Physical Geography: Earth and Environment* 17.1, pp. 50–68. DOI: 10.1177/030913339301700104. eprint: https://doi.org/10.1177/030913339301700104. URL: https://doi.org/10.1177/030913339301700104 (cit. on p. 11).

World Meteorological Organization (1995). *Manual on Codes, International Codes, vol. I.1 (Annex II to WMO Technical Regulations), part A, Alphanumeric Codes*. Geneva, Switzerland (cit. on pp. 23, 30, 61).

Worster, D. (2004). *Dust Bowl-The Southern Plains in the 1930s*. USA: Oxford University Press (cit. on p. 9).

Wu, C., Z. Lin, & X. Liu (2020). "The global dust cycle and uncertainty in CMIP5 (Coupled Model Intercomparison Project phase 5) models". *Atmospheric Chemistry and Physics* 20.17, pp. 10401–10425. DOI: 10.5194/acp-20-10401-2020. URL: https://acp.copernicus.org/articles/20/10401/2020/ (cit. on p. 6).

Wurzler, S., T. G. Reisin, & Z. Levin (2000). "Modification of mineral dust particles by cloud processing and subsequent effects on drop size distributions". *Journal of Geophysical Research: Atmospheres* 105.D4, pp. 4501–4512. DOI: https://doi.org/10.1029/1999JD900980. eprint: https://agupubs.onlinelibrary.wiley.com/doi/pdf/10.1029/1999JD900980. URL: https://agupubs.onlinelibrary.wiley.com/doi/abs/10.1029/1999JD900980 (cit. on p. 9).

Xi, X. & I. N. Sokolik (2016). "Quantifying the anthropogenic dust emission from agricultural land use and desiccation of the Aral Sea in Central Asia". *Journal of Geophysical Research: Atmospheres* 121.20, pp. 12, 270–12, 281. DOI: https://doi.org/10.1002/2016JD025556. eprint: https://agupubs.onlinelibrary.wiley.com/doi/pdf/10.1002/2016JD025556. URL: https://agupubs.onlinelibrary.wiley.com/doi/abs/10.1002/2016JD025556 (cit. on p. 84).

Yang, X., C. Zhou, W. Huo, F. Yang, X. Liu, & A. Mamtimin (July 2019). "A study on the effects of soil moisture, air humidity, and air temperature on wind speed threshold for dust emissions in the Taklimakan Desert". *Natural Hazards* 97.3, pp. 1069–1081. ISSN: 1573-0840. DOI: 10.1007/s11069-019-03686-1. URL: https://doi.org/10.1007/s11069-019-03686-1 (cit. on p. 86).

Yu, H., M. Chin, T. Yuan, H. Bian, L. A. Remer, J. M. Prospero, A. Omar, D. Winker, Y. Yang, Y. Zhang, Z. Zhang, & C. Zhao (2015). "The fertilizing role of African dust in the Amazon rainforest: A first multiyear assessment based on data from Cloud-Aerosol Lidar and Infrared Pathfinder Satellite Observations". *Geophysical Research Letters* 42.6, pp. 1984–1991. DOI: https://doi.org/10.1002/2015GL063040. eprint: https://agupubs.onlinelibrary.wiley.com/doi/pdf/10.1002/2015GL063040. URL: https://agupubs.onlinelibrary.wiley.com/doi/abs/10.1002/2015GL063040 (cit. on pp. 4, 9).

Zanetta-Colombo, N. C., Z. L. Fleming, E. M. Gayo, C. A. Manzano, M. Panagi, J. Valdés, & A. Siegmund (2022). "Impact of mining on the metal content of dust in indigenous villages of northern Chile". *Environment International* 169, p. 107490. ISSN: 0160-4120. DOI: https://doi.org/10.1016/j.envint.2022.107490. URL: https://www.sciencedirect.com/science/article/pii/S0160412022004172 (cit. on pp. 41, 83).

Zender, C. S., R. L. L. Miller, & I. Tegen (2004). "Quantifying mineral dust mass budgets:Terminology, constraints, and current estimates". *Eos, Transactions American Geophysical Union* 85.48, pp. 509–512. DOI: https://doi.org/10.1029/2004EO480002. eprint: https://agupubs.onlinelibrary.wiley.com/doi/pdf/10.1029/2004EO480002. URL: https://agupubs.onlinelibrary.wiley.com/doi/abs/10.1029/2004EO480002 (cit. on pp. 9, 83).

Zender, C. S., H. Bian, & D. Newman (2003a). "Mineral Dust Entrainment and Deposition (DEAD) model: Description and 1990s dust climatology". *Journal of Geophysical Research: Atmospheres* 108.D14. DOI: https://doi.org/10.1029/2002JD002775. eprint: https://agupubs.onlinelibrary.wiley.com/doi/pdf/10.1029/2002JD002775. URL: https://agupubs.onlinelibrary.wiley.com/doi/abs/10.1029/2002JD002775 (cit. on p. 85).

Zender, C. S. & E. Y. Kwon (2005). "Regional contrasts in dust emission responses to climate". *Journal of Geophysical Research: Atmospheres* 110.D13. DOI: https://doi.org/10.1029/2004JD005501. eprint: https://agupubs.onlinelibrary.wiley.com/doi/pdf/10.1029/2004JD005501. URL: https://agupubs.onlinelibrary.wiley.com/doi/abs/10.1029/2004JD005501 (cit. on pp. 11, 85).

Zender, C. S., D. Newman, & O. Torres (2003b). "Spatial heterogeneity in aeolian erodibility: Uniform, topographic, geomorphic, and hydrologic hypotheses". *Journal of Geophysical Research: Atmospheres* 108.D17. DOI: https://doi.org/10.1029/2002JD003039. eprint: https://agupubs.onlinelibrary.wiley.com/doi/pdf/10.1029/2002JD003039. URL: https://agupubs.onlinelibrary.wiley.com/doi/abs/10.1029/2002JD003039 (cit. on p. 6).

Zhao, A., C. L. Ryder, & L. J. Wilcox (2022). "How well do the CMIP6 models simulate dust aerosols?" *Atmospheric Chemistry and Physics* 22.3, pp. 2095–2119. DOI: 10.5194/acp-22-2095-2022. URL: https://acp.copernicus.org/articles/22/2095/2022/ (cit. on p. 6).

Zhao, M. et al. (2018). "The GFDL Global Atmosphere and Land Model AM4.0/LM4.0: 2. Model Description, Sensitivity Studies, and Tuning Strategies". *Journal of Advances in Modeling Earth Systems* 10.3, pp. 735–769. DOI: https://doi.org/10.1002/2017MS001209. eprint: https://agupubs.onlinelibrary.wiley.com/doi/pdf/10.1002/

2017MS001209. URL: https://agupubs.onlinelibrary.wiley.com/doi/abs/10.1002/2017MS001209 (cit. on pp. 85, 88).

Zimon, A. D. (2012). *Adhesion of dust and powder*. Springer Science & Business Media (cit. on p. 11).

Zobeck, T. M. (1991). "Soil properties affecting wind erosion". *Journal of Soil and Water Conservation* 46.2, pp. 112–118. ISSN: 0022-4561. eprint: https://www.jswconline.org/content/46/2/112.full.pdf. URL: https://www.jswconline.org/content/46/2/112 (cit. on p. 7).

Data Availability

The data used for dust events in Chapter 3 and dust storms in Chapter 5 can be downloaded with the following instructions:

Surface synoptic observations from the Dirección Meteorológica de Chile (Dirección Meteorológica de Chile- Servicios Climáticos 2019) were used in this dataset. The dataset is available upon registration at https://climatologia.meteochile.gob.cl/application/requerimiento/producto/RE7002. The WMO station IDs or the " código de la estación" for the stations are: 180005 (Arica), 200006 (Iquique), 220002 (Calama), 230001 (Antofagasta), 260002 (Chañaral), 270008 (Desierto de Atacama), 270002 (Copiapó), 280003 (Vallenar) and 290004 (La Serena). For example, the data for Arica (https://climatologia.meteochile.gob.cl/application/informacion/fichaDeEstacion/180005) can be accessed under "10. Elementos Asignados a la Estación e Inventario de Datos" or Station Assigned Elements and Data Inventory. Here, the information on different meteorological variables with the total number of records (Registros), the beginning of the observation period (Año Desde) and the end of the observation period (Año Hasta) is available. The meteorological data used in this study are present weather code (Tiempo Presente Sinóptico, ID: 34), past weather code (Tiempo Pasado Sinóptico, ID: 33), wind speed and direction (Viento a 10 m. de Altura, ID: 28), horizontal visibility (Visibilidad Horizontal Sinóptica, ID: 32) and accumulated precipitation (Agua Caida, Acumulada 6 Horas, ID: 57).

The ECMWF ERA5 reanalysis data was used in Chapter 5 to identify synoptic weather patterns. This data is available in the Climate Data Store. More specifically, the 500 hPa and 700 hPa geopotential heights were downloaded from https://cds.climate.copernicus.eu/cdsapp#!/dataset/reanalysis-era5-pressure-levels?tab=overview and the mean sea level pressure and 10 m winds from https://cds.climate.copernicus.eu/cdsapp#!/dataset/reanalysis-era5-single-levels?tab=overview.

The PI-SWERL raw data files used to compute the threshold wind speeds (from Chapter 4) in Pisagua and Chuculay Faults between Sep–Oct 2022 can be downloaded on the CRC1211 database: https://www.crc1211db.uni-koeln.de/site/index.php.

Declaration

Hiermit versichere ich an Eides statt, dass ich die vorliegende Dissertation selbstständig und ohne die Benutzung anderer als der angegebenen Hilfsmittel und Literatur angefertigt habe. Alle Stellen, die wörtlich oder sinngemäß aus veröffentlichten und nicht veröffentlichten Werken dem Wortlaut oder dem Sinn nach entnommen wurden, sind als solche kenntlich gemacht. Ich versichere an Eides statt, dass diese Dissertation noch keiner anderen Fakultät oder Universität zur Prüfung vorgelegen wurde; dass sie - abgesehen von unten angegebenen Teilpublikationen und eingebundenen Artikeln und Manuskripten - noch nicht veröffentlicht worden ist sowie, dass ich eine Veröffentlichung der Dissertation vor Abschluss der Promotion nicht ohne Genehmigung des Promotionsausschusses vornehmen werde. Die Bestimmungen dieser Ordnung sind mir bekannt. Darüber hinaus erkläre ich hiermit, dass ich die Ordnung zur Sicherung guter wissenschaftlicher Praxis und zum Umgang mit wissenschaftlichem Fehlverhalten der Universität zu Köln gelesen und sie bei der Durchführung der der Dissertation zugrundeliegenden Arbeiten und der schriftlich verfassten Dissertation beachtet habe und verpflichte mich hiermit, die dort genannten Vorgaben bei allen wissenschaftlichen Tätigkeiten zu beachten und umzusetzen. Ich versichere, dass die eingereichte elektronische Fassung der eingereichten Druckfassung vollständig entspricht.

Teilpublikationen:

Pinto, R. & Fiedler, S. (2024). **Why is the dust activity in the Atacama Desert low despite its aridity?**. JGR: Atmospheres

11. März 2024, Köln Rovina Janis Pinto